Molecular Address Tags for Vaccines

Rebecca Winsbury

This thesis is submitted in fulfilment of the requirements of the
degree of Doctor of Philosophy at the University of East Anglia

Department of Biological Chemistry
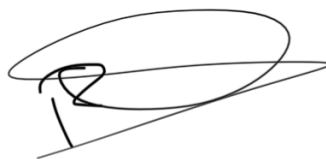
John Innes Centre

Norwich

January 2019

Date

22/01/2019

I declare that the work contained in this thesis, submitted by me for the degree of Doctor of Philosophy, is to the best of my knowledge my own original work, except where due reference is made.

Signed

Rebecca Winsbury

This PhD thesis is dedicated to Colin Webster, whose good examples taught me to work hard for what I aspire to achieve.

The gentlest of men.

Thank you, Grandad.

1934 - 2018

Acknowledgements

First and foremost, I would like to thank Rob for his continued support throughout the course of this PhD project. Thank you for your unrelenting optimism towards a persistent pessimist, without which this tough journey would have been even tougher. A special thank you to my secondary supervisors, Norihito and Nathalie, your supervision and support throughout this process were truly invaluable. To Sergey and Martin, thank you for your advice and guidance on all aspect of chemistry.

The Field group was a fantastic place to conduct the research for this PhD, not only due to the outstanding scientific facilities available, but for the family atmosphere created by all members of the research group which made the good times more enjoyable, and the tough times more bearable. In one way or another they have all contributed to the success for this project, be it through an extra pair of hands in the lab, guidance on scientific knowledge, or simply through the consumption of cake when the moment calls, usually 3pm. A special thank you to Alex, Brydie, Lily and Irina, whose friendship and support made this rollercoaster journey so special. Thank you to Ben, Ed, Giulia and Mike for guiding me through this process with stories of your own experiences. Your friendship and knowledge were truly valuable to the success of this project. To the past members who have since embarked on new adventures around the world; Ana, Lucky, Meng and Phoebe, thank you for sharing this experience with me, I hope our paths will cross again soon.

Thank you to Mologic Ltd, the industrial sponsors of this BBSRC iCASE studentship. A special thank you to Mark and Paul Davis for their support and enthusiasm for science, the annual Science Day was always a delight to attend. Thank you to Lucy Beales of Mologic York, and the rest of the York team who welcomed me into the lab and provided invaluable guidance on all aspects of immunoassays. Thank you to everyone at the Royal Society of Chemistry, particularly Fiona and Aurora for your support during the writing of this thesis.

I am extremely fortunate in that this PhD project has allowed me to travel around the world and present my scientific knowledge across the globe, including in Barcelona, Teipei, Bangor, Wageningen, and not forgetting the infamous ventures in St. Andrews.

The unconditional support of my entire family over the entire course of my scientific career was ever more appreciated during these past 4 years. Thank you to Mumsie and Dad, your support and encouragement got me through the ups and downs of this journey. Thank you to all of my grandparents, Nanna, Mema and Grandad. Nanna, although you are not around to see it, you always said I would be a Doctor one day. Thank you to Mema and Grandad, even though time was against us on certain aspects of this journey.

And last, but by no means least, Jack. Simply put, the best thing about my time in Norwich.

Acknowledgement of Contributions

I would like to thank the following individuals for their contributions to this PhD thesis:

- Dr Irina Ivanova of the John Innes Centre, for chemically synthesising the virenose antigens used in this PhD thesis,
- Dr Simone Dedola of Iceni Diagnostics for generation of virenose-VLP vaccine conjugates used in the immunisation trials of this PhD thesis,
- Dr Lucy Beales of Mologic for conducting the immunisation trials in this PhD thesis.

List of Abbreviations

Ab	Antibody
Ac$_2$O	Acetic anhydride
AcOH	Acetic acid
Ag	Antigen
An	Analyte
ANOVA	Analysis of variance
APC	Antigen presenting cell
BCA assay	Bicinchoninic acid assay
Bcl-10	B cell lymphoma-10
BCN-NHS	(1R,8S,9S)-bicyclo[6.1.0]non-4-yn-9-ylmethyl N-succinimidyl carbonate
BDCA-2	Blood dendritic cell antigen 2
BSA	Bovine serum albumin
CARD9	Caspase-associated recruitment domain
CD	Cluster of differentiation
CDC	Centre for disease control
CDCl$_3$	Deuterated chloroform
CHO cells	Chinese hamster ovary cells
CLEC-1	C-type lectin receptor 1
CLR	C-type lectin receptor
CPRG	Chlorophenol red β-D-galactopyranoside
CPS	Capsular polysaccharide
CRD	Carbohydrate recognition domain
CuAAC	Copper(I)-catalyzed azide-alkyne cycloaddition
CuSO$_4$	Copper sulfate
D$_2$O	Deuterated water
Da	Daltons
DC-SIGN	Dendritic cell-specific intercellular adhesion molecule-3-grabbing non-integrin
DCIR	Dendritic cell immunoreceptor
DCM	Dichloromethane
DCs	Dendritic cells

DHB	2,5-Dihydroxybenzoic acid
DIPEA	Diisopropylethylamine
DLEC	Dendritic cell lectin
DMC	2-Chloro-1,3-dimethylimidazolinium chloride
DMF	Dimethylformamide
DMSO	Dimethyl sulfoxide
DP	Degree of polymerisation
ELISA	Enzyme-linked immunosorbent assay
EPS	Exopolysaccharide
eq	Equivalents
ESI-MS	Electrospray Ionisation Mass Spectrometry
EtOAc	Ethyl acetate
FTIR	Fourier-transform infrared spectroscopy
Glc	Glucose
GlcNAc	*N*-Acetyl glucosamine
GPC	Gel permeation chromatography
H$_2$SO$_4$	Sulfuric acid
HCl	Hydrochloric acid
Hep	Heptose
His	Histadine
HIV	Human immunodeficiency virus
HMOs	Human milk oligosaccharides
HPAEC-PAD	High performance anion exchange chromatography with pulsed amperometric detection
HRP	Horse radish peroxidase
HSQCed	Heteronuclear single quantum coherence spectroscopy
IL	Interleukine
IPTG	Isopropyl β-D-1-thiogalactopyranoside
ITAM	Immunoreceptor tyrosine-based activation motif
ITIM	Immunoreceptor tyrosine-based inhibition motif
K$_2$CO$_3$	Potassium carbonate
kDa	Kilodaltons
Kdo	3-Deoxy-D-Manno-Octulosonic Acid
KLH	Keyhole limpet haemocyanin

LCs	Langerhans cells
LLIR	Lectin-like immunoreceptor
LPS	Lipopolysaccharide
Lys	Lysine
M	Molar
m/z	Mass to charge ratio
M1P	Mannose-1-phosphate
mAb	Monoclonal antibody
MALDI-TOF/MS	Matrix assisted desorption ionisation mass spectrometry time of flight
MALT-1	Mucosa-associated lymphoid tissue lymphoma gene-1
Man	Mannose
MAT	Molecular address tag
MeCN	Acetonitrile
MeI	Methyl iodide
MeOH	Methanol
MHC	Major Histocompatibility complex
MHz	Megahertz
MR	Mannose receptor
NaAsc	Sodium ascorbate
NaN$_3$	Sodium azide
NaOAc	Sodium acetate
NaOH	Sodium hydroxide
NaOMe	Sodium methoxide
NFκB	Nuclear factor kappa-light-chain-enhancer of activated B cells
NHS	*N*-hydroxy succinimide
NK cells	Natural Killer cells
NMR	Nuclear magnetic resonance
OVA	Ovalbumin
pAb	Polyclonal antibody
PAMP	Pathogen associated molecular pattern
PBS	Phosphate buffer saline
ppm	Parts per million
RT	Room temperature

SA	Sinapinic acd
SDS	Sodium dodecyl sulfate
SDS-PAGE	Sodium dodecyl sulfate polyacrylamide gel electrophoresis
SNP	Single nucleotide polymorphism
Strep	Streptose
TEA	Triethylamine
TetHc	Tetanus toxoid heavy chain
TFA	Trifluoroacetic acid
THPTA	Tris(3-hydroxypropyltriazolylmethyl)amine
TLC	Thin layer chromatography
TNF-α	Tumour necrosis factor alpha
Trp	Tryptophan
TT	Tetanus toxoid
Vir	Virenose
VLP	Virus-like particle

Table of Contents

1. Chapter 1: Introduction

Carbohydrates are one of the most abundant and structurally diverse organic molecules in nature[1]. With a wide variety of monosaccharide building blocks occurring both naturally and synthetically, a diverse range of possible chain lengths and the possibility of multiple configurations, the number of possible carbohydrates is infinite[2]. Unlike proteins and nucleic acid structures, the blueprints for carbohydrates are not directly outlined in the sequence of DNA, resulting in difficulties identifying carbohydrate sequences. However, unlike proteins and nucleic acids, carbohydrates are not susceptible to mutations, making their stability an appealing attribute in the medical field.

The use of carbohydrates in medicine is a very broad field, with their characteristics exploited in a number of areas, including therapeutics[3] and diagnostics[4]. This thesis set out to develop a glycoconjugate vaccine technology which utilises the interaction of carbohydrates with the immune system.

This chapter will give an introduction into β-glucans and how they interact with receptors of the immune system. A focus on Dectin-1, a C-type lectin receptor with a specificity for β-(1-3)-glucans[5], will provide an insight into how this interaction can be utilised in targeted vaccination therapies. The latter half of this chapter will focus on fungal β-(1-2)-mannan antigens and their use in vaccines, along with the need for Q fever specific antibodies.

1.1. The structural properties of β-glucans

Beta-glucans are naturally occurring polysaccharides which are abundant in nature, from the cell walls of higher plant species and the storage granules in algal species, to surface polysaccharides on microorganisms, such as fungi, moulds and yeasts[6]. They are formed from repeating units of D-glucose in a beta-configuration. The relative molecular weight of β-glucans is extremely varied, ranging from a disaccharide of 342 Da to several thousands of kilodaltons for storage polysaccharides.

The linear backbone of β-glucans exists in a number of linkage configurations depending on the origin of the polysaccharides, including the unusual cyclic β-(1-2)-glucans excreted by *Rhizobium spp.*[7], β-(1-3)-glucans in the form of paramylon and curdlan, β-(1-4)-glucans found within cellulose and β-(1-6)-glucans such as pustulan[6] (**Figure 1. 1**). As well as linear structures, β-glucans also exist in a number of branched forms, primarily of β-(1-6) linkage[6]. These varying structures have contributed to the use of β-glucans in a number of industrial applications, including use as a bulking agent in the food industry due to their unique gelling properties[8].

β-(1-3)-glucan β-(1-4)-glucan β-(1-6)-glucan

β-(1-3)-glucan with β-(1-6)-branching

β-(1-3)-glucan with β-(1-4)-branching
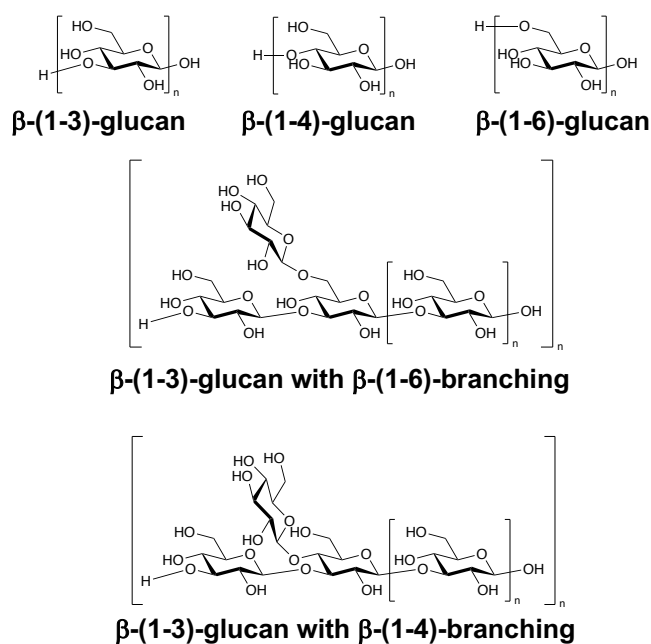
Figure 1. 1 – The chemical structures of β-glucans. Beta-glucans can exist as linear chains of repeating D-glucose units in β-(1-3), β-(1-6) or β-(1-4) linkage configuration. Linear β-glucan backbones may also be decorated with branching in β-(1-6) or β-(1-4) configuration.

Beta-(1-3)-glucans exist in both soluble and insoluble forms. In solution, the number of hydrogen bonds present in the polysaccharide structure allows the molecule to take on particular 3D structures, which can be presented as a triple helices, single helices or random coil (**Figure 1. 2**), as determined by x-ray fiber diffraction[9], solid state ^{13}C NMR spectroscopy[10], multiangle laser light scattering[11], fluorescence resonance energy transfer spectroscopy[12], and molecular dynamics simulation[13]. Due to the ability of these large molecules to form triple helical structures[14], it has often been difficult to determine the molecular weight and degree of polymerisation (DP)[15].
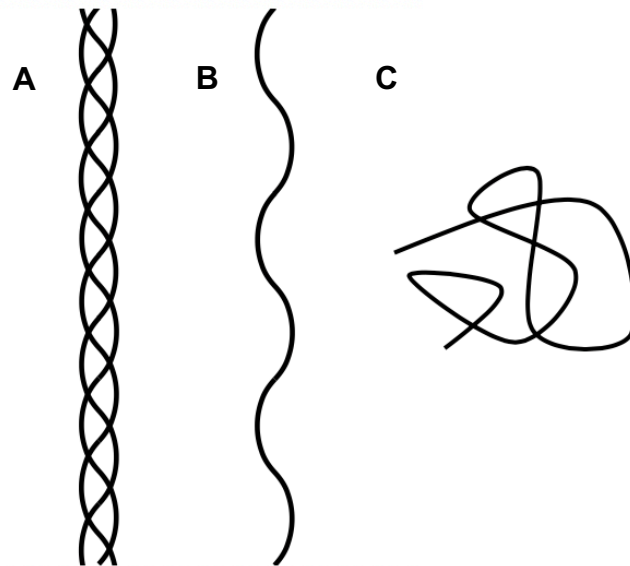
Figure 1. 2 – The physical properties of soluble β-(1-3)-glucans. In solution, β-(1-3)-glucans take on a helical conformation, allowing them to take on triple helical (A), single helical (B), and random coil (C) structures.

Beta-glucans have long been exploited for their health benefits. For thousands of years, ancient civilisations have used edible fungi, such as the Shitaki mushroom, *Lentinula edodes*, for their healing powers demonstrated by their anticarcinogenic activity and stimulation of Th1 lymophocytes[16,17]. More recently, traditional Chinese medicines have been explored for their extensive knowledge of β-(1,3)-glucan polysaccharides[18], and their uses as anti-

inflammatory, anticancer and antimicrobial agents[19,20]. This knowledge has been utilised in advancing immunotherapies, by the use of β-glucans as adjuvants[21], drug delivery systems[22], and even in aquaculture as an immune stimulant in farmed fish[23]. Whilst it is evident that these naturally occurring moleculars have clear health benefits, the mechanisms by which these effects are stimulated remains unclear, with the chain length/branching requirments yet to be defined.

1.1.1. Origins and diversity of naturally occurring β-glucans

β-Glucans from different sources have been demonstrated to not only have different structures, but also different biological properties[24], as outlined in **Table 1. 1**. A number of β-glucan polysaccharides comprise of a linear structure with β-(1-3)-linkages, including paramylon – the storage polysaccharide of *Euglena gracilis* which has been shown to have a pro-inflammatory effect[25], curdlan – a particulate β-(1-3)-glucan produced by *Agrobacterium spp.* shown to have anti-tumour and wound repair traits[26], whole glucan partical (WGP) – comprised of hollow yeast cell wall with functions in wound repair and as a pro-inflammatory agent[27], zymosan – a pro-inflammatory agent found on the surface of yeast[28], pachyman – a fungal polysaccharide with antitumour activities[29], and callose – a plant polysaccharide located within the cell wall[30].

Linear β-(1-3)-glucans also exist with occasional β-(1-6)-branching. Laminarin, produced as a storage polysaccharide within *Laminaria digitata*, contains β-(1-6)-glucan sidechains approximately every 3 residues along a linear β-(1-3)-glucan backbone[31], although the overall structure of laminarin varies depending on location of the source, season of harvest, extraction method, and a number of other environmental factors[32]. Scleroglucan also contains β-(1-6)-branch points approximately every 3-4 residues along the linear backbone[33]. This soluble polysaccharide has shown antitumour and antiviral properties[34]. Schizophyllan has also demonstrated antitumour properties[35], with β-(1-6)-branch points located every 3 residues along the backbone[35]. β-

Glucans with a mixture of β-(1-4) and β-(1-6)-branch points are also present in the form of lentinan, a polysaccharide with antitumour and pro-inflammatory properties[25].

Linear β-glucans are also present in a number of other linkages, such as β-(1-6)-glucan polysaccharides - as is the case of pustulan[36], β-(1-4)-glucan polysaccharides such as cellulose - one of the most abundant β-glucans in nature[6], and cyclic β-(1-2)-glucans. Whilst many of these polysaccharides occur abundantly in nature, their immunological function remains unknown.

Table 1. 1 – The physical, chemical and biological properties of β-glucans.

Origin	Source	Name	Linkage	MW (kDa)	DP$_n$	Soluble	Biological Activity
Algae	*Laminaria digitata*	Laminarin	β-(1-3)-glucan main chain, β-(1-6)-glucan side chains (3:1)[31]	~5.3[31]	25-35[31]	Yes	Dectin-1 inhibitor, inhibits myeloid leukaemia proliferation[31]
	Euglena gracilis	Paramylon	β-(1-3)-glucan[15]	>500[15]	3000[15]	No	Pro-inflammatory[25]
Bacteria	*Alcaligenes faecalis*	Curdlan	β-(1-3)-glucan[15]	~800[15]	540-5500[15]	No	Antitumor, wound repair, anti-HIV[26]
	Agrobacterium spp.[37], *Rhizobium spp.*[38]	Cyclic β-(1-2)-glucan	β-(1-2)-glucan (cyclic)	Low molecular weight	ND	Yes	ND
Fungi and lichens	*Lasallia pustulata*	Pustulan	β-(1-6)-glucan[36]	~20[36]	320[36]	No	ND
	Sclerotium rolfsii	Scleroglucan	β-(1-3)-glucan main chain, β-(1-6)-glucan side chains (3-4:1)[33]	~1650[33]	2400-2500[33]	Yes	Antitumor, antiviral[34]
Fungi (edible)	*Schizophyllum commune*	Schizophyllan	β-(1-3)-glucan main chain, β-(1-6)-glucan side chains (3:1)[35]	~450[35]	ND*	Yes	Antitumor[35]
	Lentinula edodes (Shitaki)	Lentinan	β-(1-3)-glucan main chain, β-(1-6) or β-(1-4)-glucan side chains (3:1)[11]	~570[11]	ND*	Yes	Antitumor, pro-inflammatory[39]
	Poria cocos	Pachyman	β-(1-3)-glucan[40]	~40[40]	700[40]	No	Antitumor[29]
Plant	Various	Cellulose	β-(1-4)-glucan[6]	Var[41]	Var[41]	No	ND
	Various	Callose	β-(1-3)-glucan[6]	Var[30]	Var[30]	No	ND
Yeast	*Saccharomyces cerevisiae*	Whole glucan particle (WGP) dispersible	β-(1-3)-glucan[6]	Hollow yeast cell wall	ND	No	Activates Dectin-1, pro-inflammatory, wound repair[27]
	S. cerevisiae	Zymosan	β-(1-3)-glucan[6]	ND	ND	No	Pro-inflammatory[28]

*ND – not determined; * - may form triple helices; Var - variable across species*

1.2. Carbohydrates and the immune system

Carbohydrates play a central role in immunity[4], with the fields of glycomics and proteomics exploring the interaction carbohydrates have with the immune system[39]. The importance of carbohydrates in immunity is demonstrated by the ability of sugars to modulate the immune reaction during microbe-host interactions[40]. The cell surface of microorganisms reveals an abundance of carbohydrates in the form of lipopolysaccharides (LPSs), exopolysaccharides (EPSs), capsular polysaccharides (CPSs), glycoproteins and cell wall carbohydrates. These carbohydrates have a range of functions, including preventing desiccation, enabling biofilm formation and evading the hosts immune system to allow invasion and infection of the host[44]. As well as mimicking host carbohydrates to aid invasion, carbohydrates found on pathogens can also inhibit key pathways of the hosts immune system. Invading pathogens take advantage of the hosts immune system, with some using receptors to gain entry and infect the host. For instance, the ManLAM ligand on the surface of *Mycobacterium tuberculosis* is able to interact with mannose receptor (MR), present on the surface of macrophages, immature DCs, and liver sinusoidal endothelial cells, to stimulate internalisation of the pathogen where it resides within lysosomes, but is able to inhibit phagosome-lysosome fusion to evade the immune system[45].

However, the human immune system is well adapted to recognising carbohydrate epitopes on pathogens to initiate an immune response. The ability of our immune system to recognise carbohydrates on pathogens helps to develop our immune system from a young age. Many microbial species need to bind to the surface lectins on host immune cells to colonise[46]. Carbohydrates found within human milk mimic those found on the surface of pathogens, providing a decoy for invading pathogens and protecting the host from infection, as outlined in **Figure 1. 3**. Analysis of human milk oligosaccharides (HMOs) has revealed the presence of lacto-*N*-biose, a known pathogen associated molecular pattern (PAMP) located on the surface of *Bifidus spp.* In the presence of HMOs, *Biffidus spp* binds to lacto-*N*-biose, which acts as a decoy to the invading microbe[47].
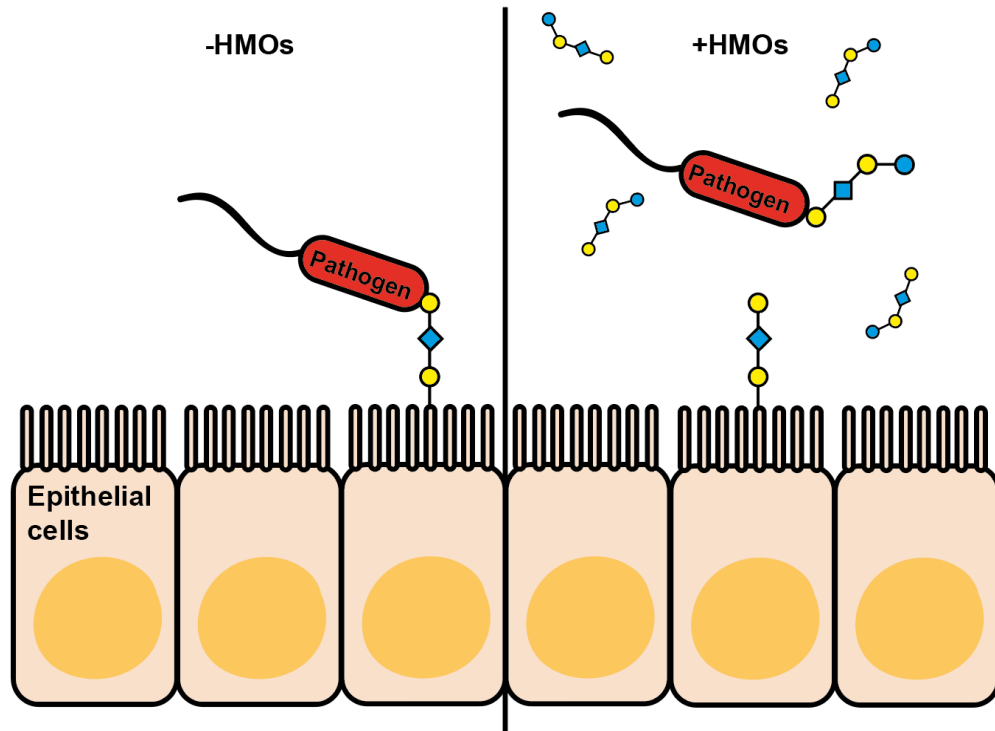
Figure 1. 3 – Schematic representation of human milk oligosaccharides (HMOs) acting as decoys to invading pathogens. *HMOs mimic carbohydrate structures which are present on the epithelial surface. Receptors on invading pathogens bind to the decoy carbohydrates, allowing the host to evade infection. Image adapted from Bode 2012[47].*

1.2.1. The innate (primary) immune system

Epithelial surfaces of the innate immune system form the first line of defence against invading pathogens[48] (**Figure 1. 4**). Physical and chemical barriers, such as the skin and mucus membranes, prevent microbes and foreign matter from entering the host. If these barriers are breached, the invading body encounters a series of primary immune cells which work together to coordinate the destruction of the invading material.
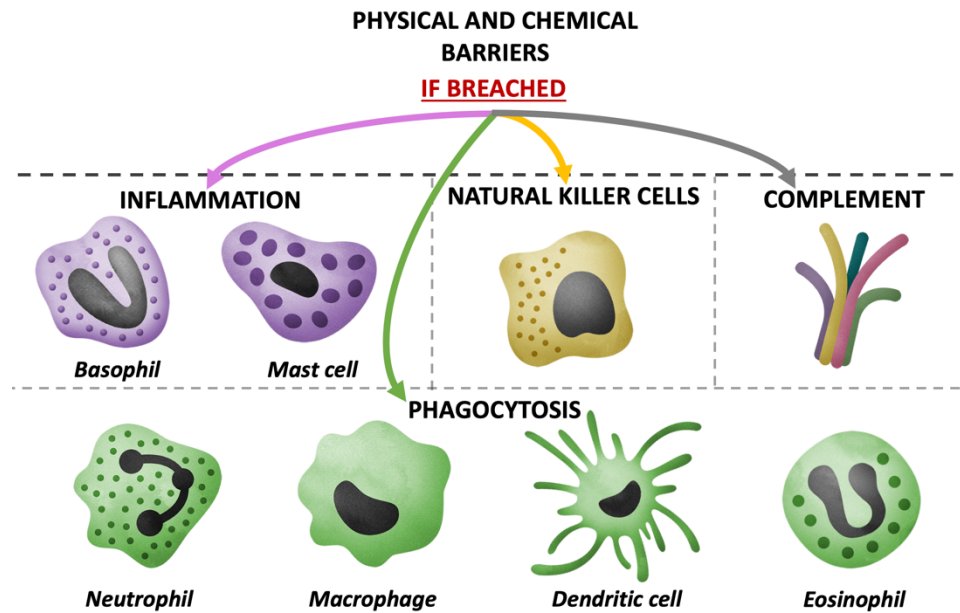
Figure 1. 4 – The innate immune system defences. *Physical and chemical barriers form the first line of defence against invading pathogens. If these barriers are breached, pathogens encounter a series of immune cells, such as: inflammatory cells (basophil and mast cells), natural killer cells, complement, and phagocytic cells (neutrophil, macrophage, dendritic cell, and eosinophil).*

Basophil and mast cells play a central role in inflammation and allergic reactions by releasing potent mediators, such as histamine. Natural killer (NK) cells play a major role in host-rejection of tumours and pathogen infected cells. They are cytotoxic cells capable of inducing apoptosis through the release of perforin and proteases. Complement consists of a series of >20 proteins found in the blood plasma which are capable of opsonisation and killing of bacteria[49]. The complement system also attracts macrophages and neutrophils, and also activates mast cells.

Phagocytic cells are able to engulf and process foreign materials and microorganisms. The phagocytic cell family consists of four major cells types; neutrophils – specialising in the destruction of bacteria, macrophages – capable of engulfing and digesting apoptotic cells, eosinophils – specialising in the destruction of multicellular parasites, allergic reactions and cancer, and dendritic cells – antigen presenting cells which process foreign materials and microbes and present fragments on major histocompatibility complex II (MHCII) to T cells. Dendritic cells form the link between the innate immune system and the adaptive immune system.

1.2.2. The adaptive (secondary) immune system

Microbes which breach these barriers encounter the more complex adaptive immune system. Subsets of antigen presenting cells (APCs), such as macrophages and dendritic cells (DCs) lay beneath epithelial cells where dendrites can extend and reach between cells to sample foreign materials (**Figure 1. 5**). Surface lectins on APCs allow for recognition of ligands displayed by pathogens and therapeutics which stimulate signalling cascades leading to phagocytosis of foreign matter.
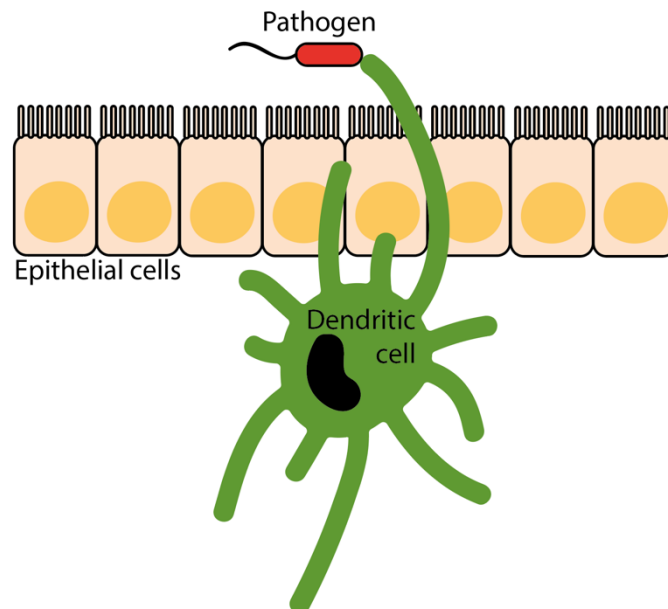
Figure 1. 5 – Schematic representation of Dendritic cells sampling for foreign material. Dendrites extend between epithelial cells to sample for foreign material and invading pathogens.

After processing this material, fragments are presented to B cells and T cells for cytotoxic (CD8$^+$ T cells) and antibody (CD4$^+$ T cells) responses through major histocompatibility complex I (MHCI) and MHCII, respectively[50], a process known as antigen presentation[51] (**Figure 1. 6**). Cells expressing receptors which are able to recognise the antigen fragments being presented are selected through clonal selection[52]. This process initiates clonal expansion[53], whereby the cells replicate to produce multiple identical copies. At this stage, helper T cells begin to release cytokines which causes B cells to

mature into antibody producing plasma cells. Also, cytotoxic T cells begin to release perforins, which destroy invading pathogens through cell lysis. Memory cells of B cells, helper T cells and cytotoxic T cells are also produced[54], which allows a rapid immune response to be initiated upon future infection of pathogens expressing the same epitope.
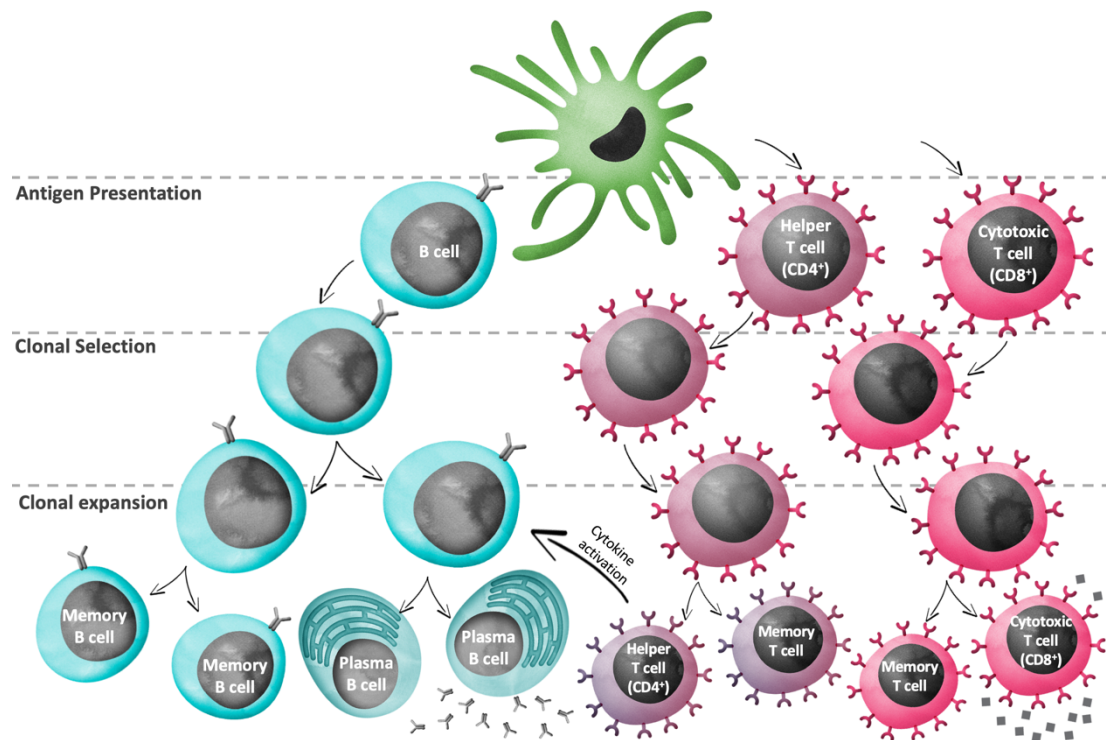
Figure 1. 6 – A schematic representation showing the adaptive immune system.

1.3. The C-type lectin receptor family

The interaction between host and pathogen forms the molecular basis for determining the appropriate immune response. Receptors present on the surface of APCs recognise a range of antigenic moieties, including lipids, proteins and carbohydrates, which are recognise by a immune receptors, such as the NOD-like[55] and Toll-like[56] families of receptors. Invasive and opportunistic pathogens display carbohydrate epitopes on their surface which interact with a family of receptors known as the C-type lectin receptors [(CLRs) **Figure 1. 7**][57]. The CLRs comprise a large family of receptors, the majority of

which bind carbohydrates in a calcium (Ca^{2+})-dependent manner. Carbohydrate binding by these receptors is mediated by at least 1 conserved carbohydrate recognition domain (CRD), which coordinates ligand binding through key amino acid residues.
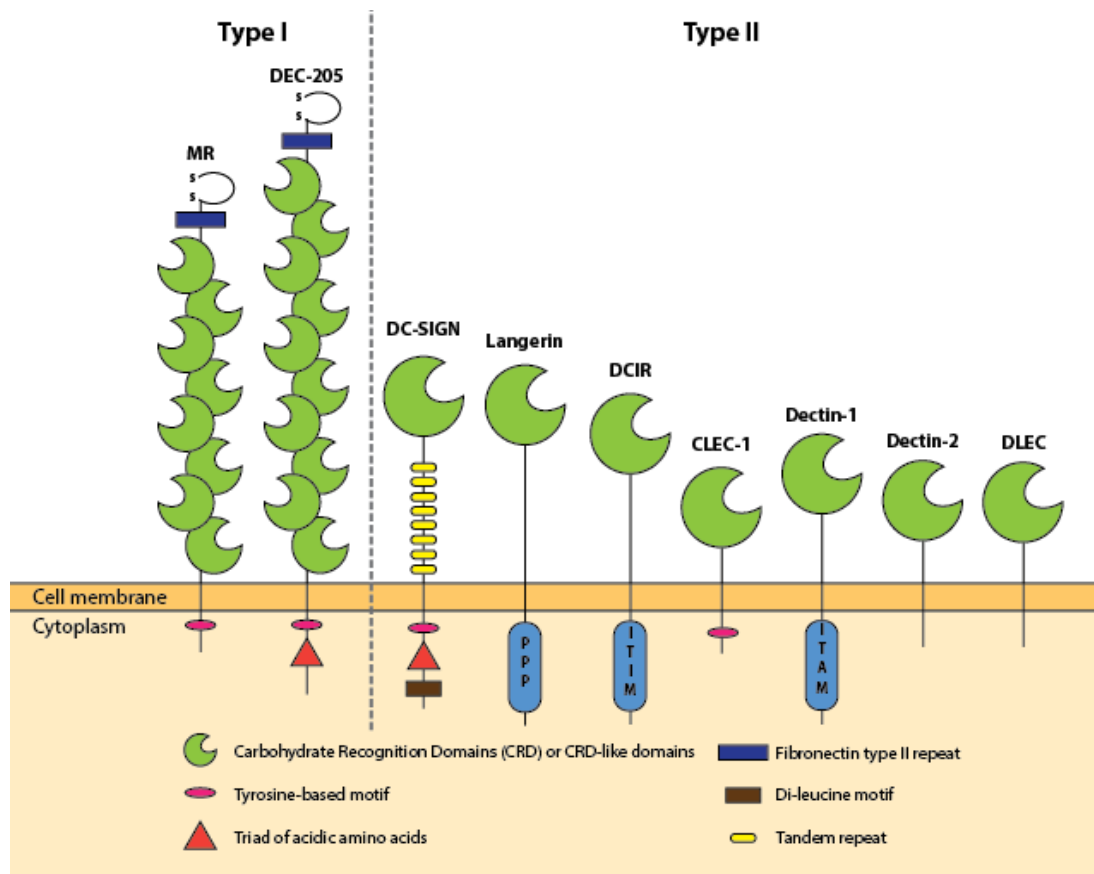
Figure 1. 7 - Schematic representation of C-type lectin receptors expressed on antigen presenting cells. *Type I C-type lectin family consists of MR and Dec-205, both of which bind carbohydrates through multiple CRDs in a Ca2+-dependent manner. The type II C-type lectin family consists of DC-SIGN, Langerin, DCIR, CLEC-1, Dectin-1, Dectin-2 and DLEC, all of which contain a single CRD at their C-terminus. Image adapted from Figdor et al[57].*

1.3.1. Type I C-type lectins

The Type I C-type lectins are defined as having their N-termini oriented outside of the cell. Receptors within this family, such as mannose receptor (MR) and Dec-205, contain 8-10 carbohydrate recognition domains, a fibronectin type II repeat and a cysteine-rich repeat (S-S) at the N-terminal[57]. As outlined in

Table 1. 2, MR is able to recognise mannose, fucose and sialyl-Lewis X ligands[58] through CRD4 and CRD5 in a Ca^{2+}-dependent manner[59], whereas Dec-205 is able to recognise ligands containing α-galactosylceramide. Both lectins have been utilised in targeted vaccination therapies due to their wide spread expression across immune cells and their roles in antigen uptake[60–63]. Whilst their abundant expression makes them an appealing target, this also poses potential risks as the desired immune response is more difficult to control.

1.3.2. Type II C-type lectins

The Type II C-type lectins are defined as having their N-termini oriented into the cytoplasm. Receptors within this family contain a single CRD at the extracellular C-terminal and a diverse range of conserved signalling motifs located within the cytoplasm.

The dendritic-cell-specific ICAM-3 grabbing non-integrin (DC-SIGN) receptor has been of great interest recently as it has been identified as the entry point for HIV-1 infection[64,65]. It is expressed solely on DCs and comprises a CRD, seven complete and one incomplete tandem repeat motifs, cytoplasmic tyrosine-based motif, triad of acidic amino acids and di-leucine motif[66]. Homologues of DC-SIGN have been identified, DC-SIGNR[67] or L-SIGN[68], and show the same ligand specificity[68,69], but they are not expressed by DCs or Langerhan cells (LCs).

Langerin, originally thought to be expressed exclusively on LCs in the epidermis and localised with Birbeck granules, is expressed on a range of DC subsets[70–72]. The ligand comprises a CRD with an affinity for mannose, GlcNAc and fucose, a stalk region, and a cytoplasmic PPP putative signalling domain[73].

DC immunoreceptor (DCIR), also known as lectin-like immunoreceptor – LLIR[74]) is expressed on a wide range of immune cells. The ligand comprises of a CRD with an affinity for sialyl-Lewis A (sLeA), a stalk region, and a

conserved cytoplasmic immunoreceptor tyrosine-based inhibitory motif (ITIM)[75]. Little is known about this receptor, but it is thought to play a role in antigen handling[76].

C-type lectin receptor 1 (CLEC-1) is a membrane spanning receptor comprising of a extracellular CRD and cytoplasmic tyrosine-based motif[77]. Ligands for the CRD, as well as the downstream signalling pathway, have yet to be determined. It has been proposed that signalling may be mediated through the tyrosine-based motif, comprising of amino acids tyrosine-serine-serine-theonine (YSST), in a similar way to tyrosine-independent signalling stimulated by Dectin-1[77], although there is currently no evidence to support this.

Dectin-1 is an extensively researched C-type lectin-like receptor. The CRD domain has been shown to have an exclusive affinity for β-(1-3)-glucans of at least 12 degrees of polymerisation (DP12)[5]. Coupled to the CRD is a linker region which spans the membrane to an immunoreceptor tyrosine-based activation motif (ITAM)[78]. This receptor is expressed primarily on DCs and macrophages[79], and is discussed more extensively in **Chapter 1.4**.

Dectin-2 shares 27 % and 33 % sequence homology with Dectin-1 in human and mouse, respectively. The CRD of Dectin-1 is able to bind α-mannan and high-mannose structures, but does not contain a cytoplasmic signalling motif so is unable to induce an independent signalling cascade[80]. This receptor is essential for protective immunity[81,82].

Previously thought to be a novel C-type lectin, DC lectin (DLEC) has since been shown to be identical to blood DC antigen 2 (BDCA-2)[83,84]. Ligands for the CRD of this receptor have not yet been determined, and similarly to Dectin-2, DLEC does not have a conserved signalling domain.

Table 1. 2 – Table of C-type lectin receptors

Family	Lectin	Ligand	Pathogen	Expression	Function
Type 1	MR	Mannose, fucose, sLeX	*M. tuberculosis*[85], *C. albicans*, *Leishmania spp*[86]	DCs, LCs, Mo, Mφ, DMECs	Antigen uptake[53]
	DEC-205	α-galactosylceramide[87]	*Yersinia pestis*[88]	DCs, LCs, high on actDCs, thymic ECs	Antigen uptake[89]
Type 2	Dectin-1	β-glucans[5]	*M. tuberculosis*[90], *C. albicans*[91], *A. fumigatus*[92]	DCs, LCs	T-cell interaction[93]
	Dectin-2	α-mannans, high mannose[94]	*M. tuberculosis*[95]	DCs, LCs	Antigen uptake[96]
	Langerin	Mannose, GlcNAc, fucose	HIV-1[97], *M. leprae*[98]	DCs, LCs	Formation of Birbeck granules[99]
	DCIR[74,75]	sLeA	HIV-1[76]	DCs, Mo, Mφ, PMN, B cells	?
	CLEC-1	?	?	DCs[100]	?
	DC-SIGN	HIV (gp120)[68], SIV, mannan, ICAM-2, ICAM-3	HIV-1, BCG, *C. albicans*, *M. tuberculosis, ebola virus*	DCs	T-cell interaction[101], HIV-1 pathology[68], migration[102], antigen uptake

Abbreviations: MR, mannose receptor; DEC-205, dendritic and epithelial cell 205; DCIR, dendritic cell immunoreceptor; CLEC-1, c-type lectin receptor 1; BDCA-2, blood DC antigen 2; DC-SIGN, DC-specific intercellular adhesion molecule-3-grabbing non-integrin; sLeX, sialyl Lewis X; Mo, monocyte; Mφ, macrophage; DMECs, dermal microvascular endothelial cells; DCs, dendritic cells; LCs, Langerhans cells; actDCs, active DCs; GlcNAc, N-acetylglucosamine; sLeA, sialyl Lewis A; PMN, polymorphic nuclear cells; HCV, hepatitis C virus.

1.4. Dectin-1: A β-(1-3)-glucan receptor

Dectin-1, a member of the CLR family, has been of major interest in recent years as a target for therapeutics against fungal pathogens. The 28 kDa membrane-associated protein consists of a conserved CRD coupled via a linker region to a transmembrane domain containing an immunoreceptor tyrosine-based activation motif (ITAM), characterised by the conserved tyrosine-x-x-leucine (YxxL) amino acid sequence (**Figure 1. 8**). Although it lacks key amino acid residues required to coordinate calcium ligation, typical of other members of the CLR family, it can bind particles rich in β-(1,3)-glucans. The results of a microarray, in which over 100 different carbohydrate moieties were tested, revealed the CRD specificity of soluble monomeric Dectin-1Fc fusion as being highly preferential for β-(1,3)-glucans with a minimum degree of polymerisation (DP) of 12 glucose units[103], although the ability of a molecule to bind to a receptor does not necessarily translate into a signalling response.
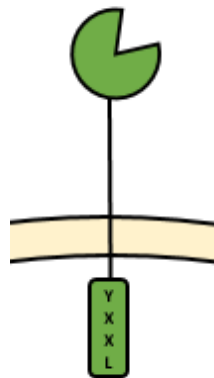
Figure 1. 8 – Schematic representation of Dectin-1. *The receptor consists of a conserved carbohydrate recognition domain which is coupled to a transmembrane domain via a linker region. The transmembrane domain contained a conserved signalling domain, immunoreceptor tyrosine-based activation motif (ITAM), characterised by the conserved YxxL amino acid sequence.*

Homologues of Dectin-1 have been found across many mammalian species, with conserved amino acid sequences located throughout the proteins (**Figure 1. 9**). Murine Dectin-1 shares 61 % sequence identity with human Dectin-1, with 62 % identity when comparing the CRDs alone. Homologues have also

been identified in rabbits and sheep, with 68 % and 72 % sequence homology to human Dectin-1, respectively. Interestingly, comparison of their CRDs with human Dectin-1 reveals 72 % and 74 % sequence homology for rabbits and sheep, respectively. Single nucleotide polymorphisms (SNPs) within CRD can lead to changes in ligand recognition, while a mutagenesis study revealed a single SNP within human langerin, where Lys-313 is converted to isoleucine, results in loss of binding to oligosaccharides with terminal $6SO_4$-Gal, but enhances recognition towards GlcNAc[104]. Therefore, it is possible that differences in the amino acid sequence for Dectin-1 CRD across species may result in altered ligand recognition.

Figure 1. 9 – Amino acid sequence alignment of Dectin-1 homologues. *Bold black – conserved hemITAM signalling domain, blue – possible Asn-Xaa-Ser/Thr glycosylation site, blue underlined – predicted asparagine glycosylation, red and orange – conserved Trp and His residues required for binding β-glucans.*

Multiple splicing variants have also been identified within species (**Figure 1. 10**). Murine Dectin-1 has been well characterised, and has been shown to consist of 2 variants, A1 and A2, with the latter being truncated due to the lack of a stalk region[105]. Alternative splicing of human Dectin-1 results in 2 major isoforms (A and B) and 6 minor isoforms (C-H)[106]. Isoforms A and B are the

major receptors for β-(1-3)-glucans, however, the functions of isoforms C-H are yet to be elucidated. Interestingly, isoform E contains a full CRD and ITAM signalling domain but has been shown to reside within the cytoplasm and is not secreted, the reason for this remains unclear[107].
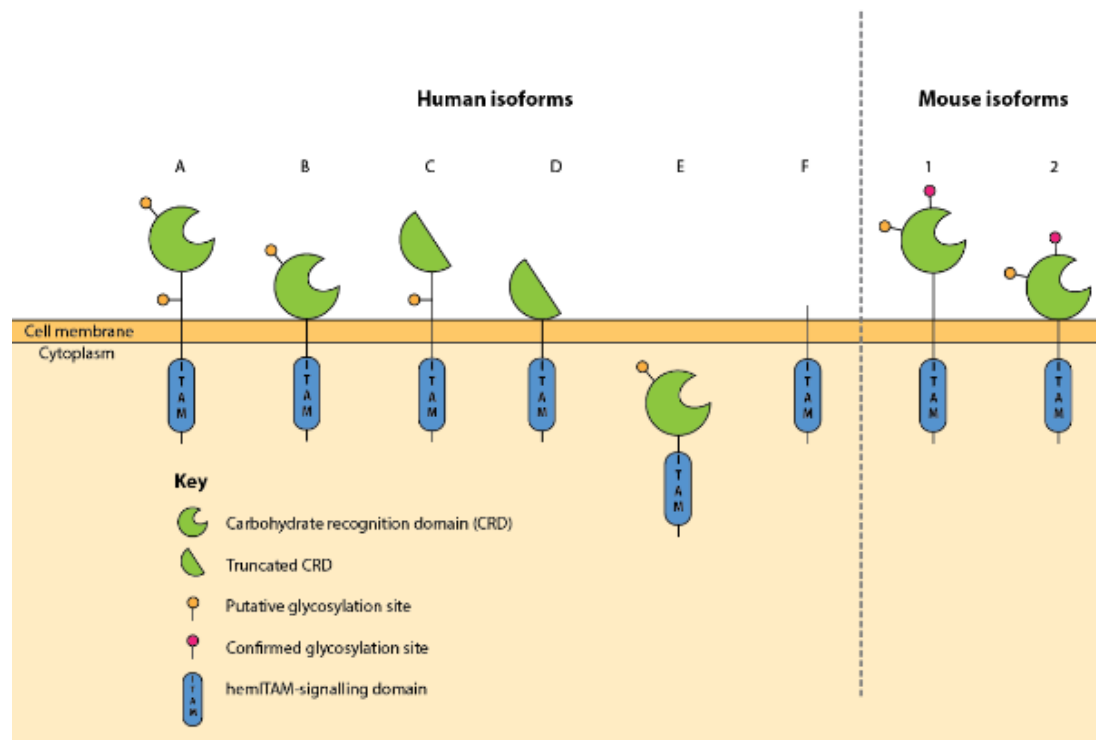
Figure 1. 10 – Schematic representation of Dectin-1 receptor orthologues. *Dectin-1 consists of a C-terminal carbohydrate recognition domain which contains conserved amino acids required for binding carbohydrates, although it lacks key amino acid residues required for Ca²⁺ ligation. A stalk region links the CRD to the transmembrane domain, which links to a cytoplasmic hemITAM-domain containing the conserved 'YxxL'-motif for phosphorylation.*

Sequence similarity between human and mouse Dectin-1 CRD orthologues is high between the two species, with 61 % sequence identity between the hDectin-1_A (**Figure 1. 11 yellow**) and mDectin-1_1 (**Figure 1. 11 light blue**) CRD receptors. The crystal structure of murine Dectin-1 CRD has been solved, and two amino acids, Trp221 (**Figure 1. 11 red residue**) and His223 (**Figure 1. 11 orange residue**), have been identified as being instrumental in coordinating β-glucan binding[108]. Despite this finding, these amino acids are located on the side of the CRD, away from the main groove where the trisaccharide is shown to be bound. Although crystals of Dectin-1 with a

decasaccharide ligand bound have been attempted[108], failure to identify the carbohydrate ligand within these crystals means that key information is missing with regards to β-glucan binding. Referring to the Dectin-1 microarray where DP12 was shown to be the minimum chain length required for binding, it may be that the carbohydrate chain loops around the protein to also coordinate with Trp221 and His223. Interestingly a glycosylation site within mDectin-1 (**Figure 1. 11 dark blue residue**) is located close to these key amino acids[109], and it is reasonable to speculate that this may affect the coordination of the carbohydrates bound, as well as the configuration of carbohydrates which bind to this receptor. As the Dectin-1 crystals used within the crystal structure study lack glycosylation, producing crystals of Dectin-1 from cells able to carry out glycosylation would be advantageous for studying the effect of murine glycosylation on β-glucan binding. However, as exact copies of the protein are required for crystals to form, introducing glycosylation to the protein would increase the difficulty of producing viable protein crystals.
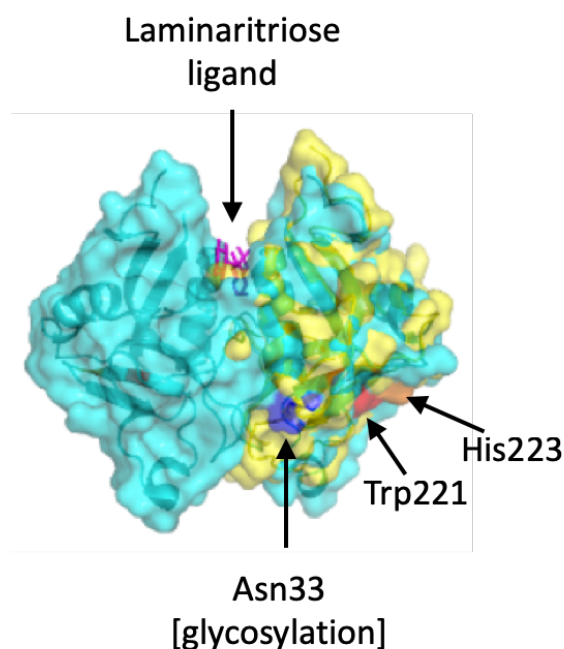
Figure 1. 11 – The crystal structure of murine Dectin-1 (blue) with human Dectin-1 overlayed (yellow) and laminaritriose bound. *Dark blue represents the site of glycosylation, and red and orange represent conserved Trp and His residues, respectively, required for β-(1-3)-glucan binding.*

1.4.1. The Dectin-1 signalling pathway

Receptor activation on immune cells, such as DCs, induces signalling cascades which modulate cellular responses. Dectin-1-mediated signalling responses occur as a result of ligand binding to the CRD (**Figure 1. 12**). Ligand engagement leads to the clustering of receptors and the phosphorylation of the hemITAM motif by Src kinases, creating a docking site for Syk, a tyrosine protein kinase[78]. Syk docks to two phosphorylation sites and stimulates caspase-associated recruitment domain (CARD9), which exists as a complex with B cell lymphoma-10 (Bcl-10) and mucosa-associated lymphoid tissue lymphoma gene-1 (MALT-1)[110], which in turn leads to the activation of IKK kinase complex, activating NFκB and leading to the induction of pro-inflammatory cytokines and the differentiation of CD4+ T cells into Th1 and Th17 T cells[111–113].
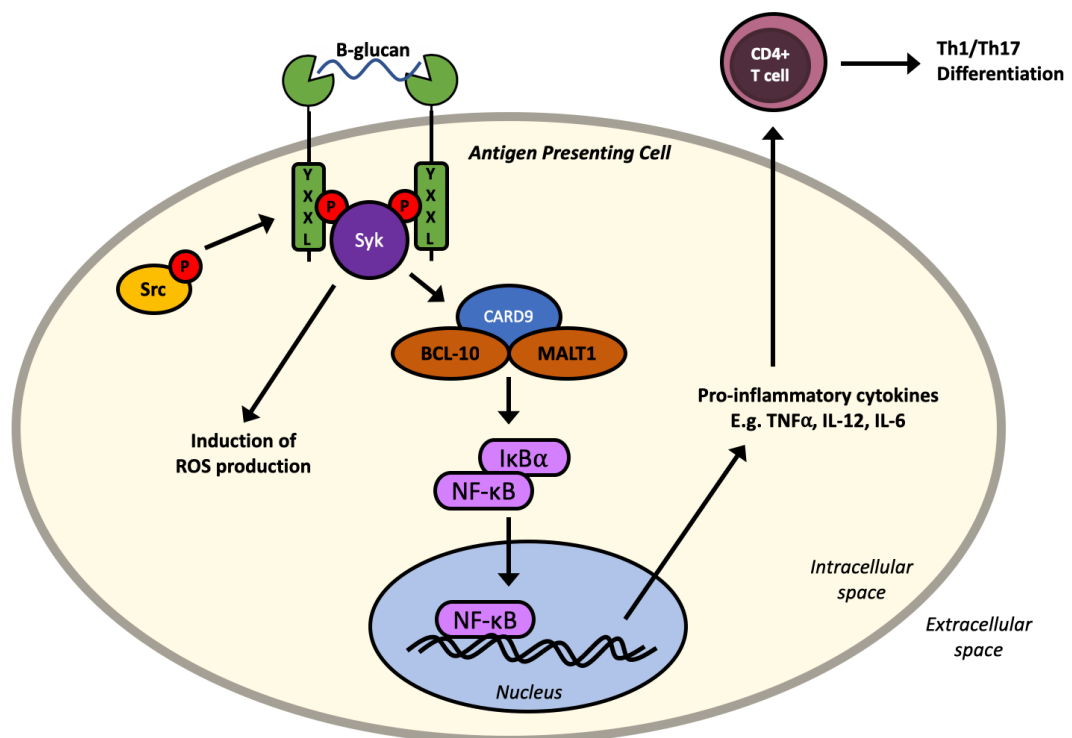
Figure 1. 12 – The Dectin-1 signalling pathway. *Following binding of β-glucans to the CRD, the YxxL motif in the cytoplasm is phosphorylated by Src, providing a docking site for Syk. Upon Syk docking to two phosphorylated YxxL motifs, ROS production is induced and the CARD9 signalling cascade initiated. CARD9 exists in complex with BCL-10 and MALT-1 which activate the IKK kinase complex leading to induction of pro-inflammatory cytokines and the differentiation of CD4+ T cells into Th1 and Th17 cells.*

1.4.2. Activation of Dectin-1-mediated signalling

As mentioned previously, binding to Dectin-1 requires β-(1-3)-glucans of at least DP12[5], however, it is not yet clear if this translates into a Dectin-1-mediated signalling response. Laminarin is often used as a Dectin-1 antagonist due to its high binding capacity[114], but it is not able to trigger a Dectin-1-mediated signalling response in its free form[115]. Goodridge *et al*[116] have proposed that short β-(1-3)-glucans are indeed able to bind to Dectin-1, but the close proximity of hemITAM to dephosphorylation motifs of CD45 and CD148 on the cell membrane quickly remove the phosphorylation on hemITAM, preventing a signalling cascade from taking place (**Figure 1. 13**).
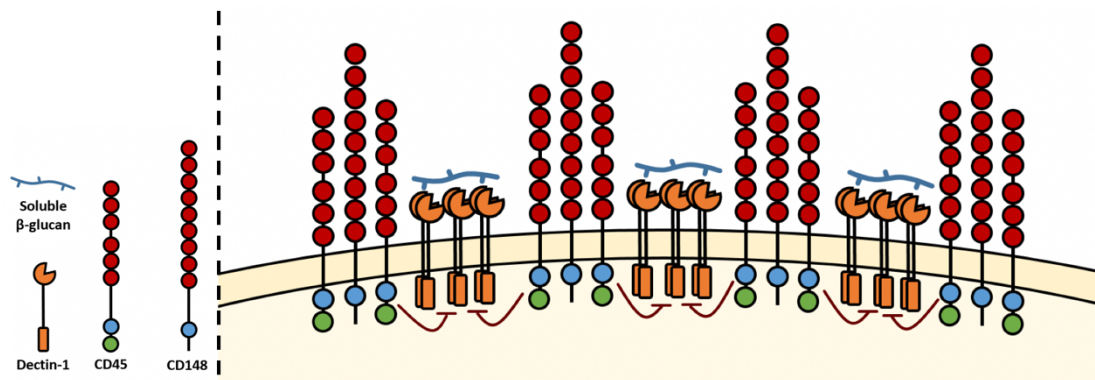
Figure 1. 13 – Schematic representation of short β-(1-3)-glucans preventing a Dectin-1-mediated signalling response. Binding of short β-glucans to CRD does not result in a Dectin-1-mediated signalling response due to inhibition of the signalling motif by CD45 and CD148. Adapted from Goodridge et al[116].

For a signalling cascade to be initiated, Goodridge *et al* propose the formation of a 'phagocytic synapse' (**Figure 1. 14**)[116]. Unlike short β-(1-3)-glucans, large particulate β-(1-3)-glucans are able to produce a larger Dectin-1 cluster[117], forcing CD45 and CD148 aside and thus creating a 'phagocytic synapse' which allows hemITAM to remain phosphorylated and Dectin-1-mediated signalling to occur.
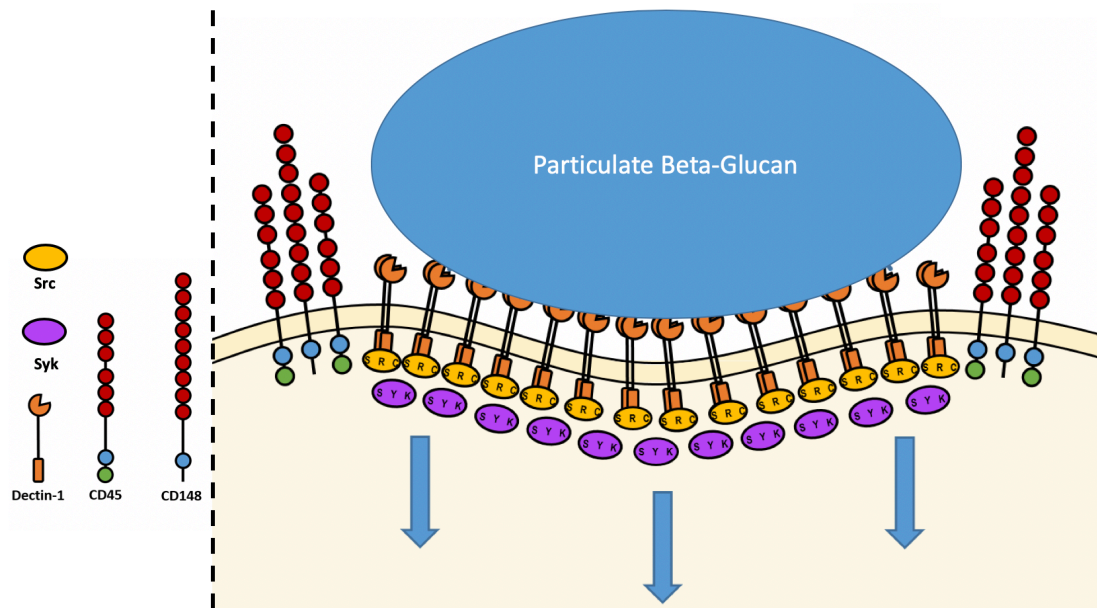
Figure 1. 14 – Schematic representation showing formation of a 'phagocytic synapse' resulting in Dectin-1-mediated signalling. *Binding of Dectin-1 to particulate β-(1-3)-glucans results in the formation of a 'phagocytic synapse'. The clustering of multiple Dectin-1 receptors forces CD45 and CD148 aside, allowing the phosphorylation of YxxL by Src, and a signalling cascade to be initiated. Adapted from Goodridge et al[116].*

1.5. Carbohydrate vaccination therapies

In an era of widespread antibiotic resistance, microbial infection rates are on the rise. As well as many bacterial species becoming resistant to second-line antimicrobials, many fungal species are no longer responding to antifungal treatments[118]. It is estimated that 7 % of all infections caused by *Candida glabrate* are resistant to fluconazole (**Figure 1. 15 A**), a second-line antifungal medication which inhibits 14α-demethylase, a fungal cytochrome P450 enzyme, preventing the conversion of lamosterol to ergosterol, an essential component of the fungal cytoplasmic membrane. It is also estimated that 8% of infections are resistant to echinocandin (**Figure 1. 15 B**), an antifungal agent which inhibits β-(1-3)-glucan synthase, preventing synthesis of β-(1-3)-glucan – a major component of the fungal cell wall[119]. Antifungal resistance is not limited to *Candida* species, with 3-6 % of *Aspergillus* species, the causative agent of aspergillosis, also showing signs of azole resistance (antifungal medicines containing azole rings)[120]. Although the full extent of antimicrobial resistance is still not known, it is clear that preventative measures need to be taken, with targeted therapeutics becoming an attractive option[121].
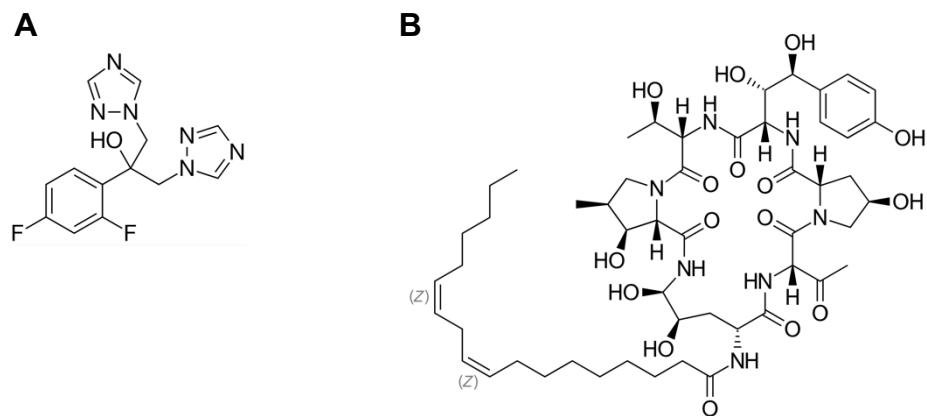
Figure 1. 15 – Chemical structure of fluconazole (A), and echinocandin (B).

As mentioned in **Chapter 1.2**, carbohydrates play a pivotal role in generating immune responses towards invading pathogens. Polysaccharides located on the surface of pathogens are ideal candidate antigens due to their stability and exposure on the cell surface. On their own, carbohydrates are poorly immunogenic, however, conjugation to a protein carrier vastly enhances their immunogenicity, as discovered by Avery and Goebel in late 1929[122]. Since then, many glycoconjugate vaccines have been generated and have successfully made it through clinal trials to market[123]. One particular success story is the elimination of *Meningococcus* C from the UK following a substantial vaccination programme in 1999 using the MenC vaccine, a conjugate vaccine of *Meningococcus* C capsular polysaccharide conjugated to Tetanus Toxoid carrier protein[124].

The ability of DCs to activate CD8+ T cells makes them an ideal target for vaccination therapies. Studies have explored the possibility of preloading *ex vivo* generated DCs with antigens in order to enhance the immune response, however this approach did not provide conclusive results, and proved to be very labour intensive[125]. The possibility of inducing a strong immune response by targeting receptors expressed on immune cells is proving to be a more promising and robust approach. Vaccines targeted towards receptors using monoclonal antibodies have proven to provide enhanced immune responses

when administered with an adjuvant[126], although the mechanism by which adjuvants stimulate the immune system is not well understood, leading to safety concerns over the use of adjuvants in vaccines[127].

Vaccines targeted towards DCs using carbohydrates provides a stable alternative to mAb targeting[126], and their ability to stimulate an immune response eliminates the need of adjuvants. The Dectin-1 antagonist, laminarin, has been investigated for its ability to target vaccines towards Dectin-1 by introducing the β-glucan tag onto glycoconjugates in a multivalent manner, thus eliminating the need to use adjuvants to stimulate a strong immune response[128]. Free laminarin is able to bind to Dectin-1 CRDs, but is unable to initiate a Dectin-1-mediated signalling response, however multimeric presentation of laminarin on carrier proteins is likely to induce a larger Dectin-1 clustering effect, thus enabling a signalling response. In a study performed by *Lipinski et al*[128], laminarin was incorporated into a tri-component glycoconjugate vaccine along with a β-(1-2)-mannotriose antigen, and tetanus toxoid as a carrier protein, as shown in **Figure 1. 16**. The addition of laminarin to the vaccine conjugate resulted in a 5- to 10- fold increased antibody titre, with IgG showing an increase in protective β-mannan mAbs from immunisation in mice. Such results reveal promising prospects for the use of β-(1,3)-glucan address tags in vaccination therapies.
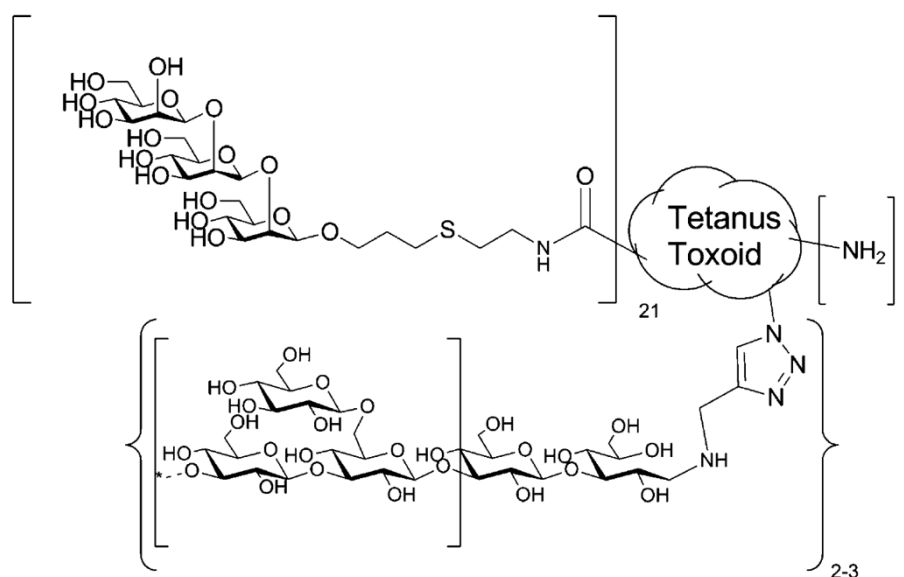
Figure 1. 16 – Structure of β-(1-2)-mannotriose-Tetanus Toxoid-laminarin vaccine conjugate. Image taken from Lipinski et al[128].

The studies in this thesis focused on fungal β-(1-2)-mannan antigens, and *Coxiella* LPS, both of which are introduced in the next two sections.

1.5.1. β-(1-2)-Mannans as antigens

The surface carbohydrates of pathogens play an important role in immunity, as mentioned in **Chapter 1.2**, with carbohydrate epitopes being key markers for pathogen recognition. *Candida albicans*, the causative agent of candidiasis, is a major cause of disease amongst immunocompromised patients[129]. Two infective strains of *C. albicans*, serotype A and serotype B, contain antigenic mannose regions within their CPS, comprising of both α-(1-2) and β-(1-2) oligomannosyl residues[130]. These oligomannans comprise an acid-stable region which is coupled to asparagine residues (Asn) via an inner core and two GlcNAc residues (**Figure 1. 17**). The composition of mannans within this region vary between the serotypes, with mannans specific to serotype A shown in bold in **Figure 1. 17**. Both serotypes also comprise of acid-label β-(1-2)-mannans which are thought to be responsible for inducing an immune response in infected patients[131].
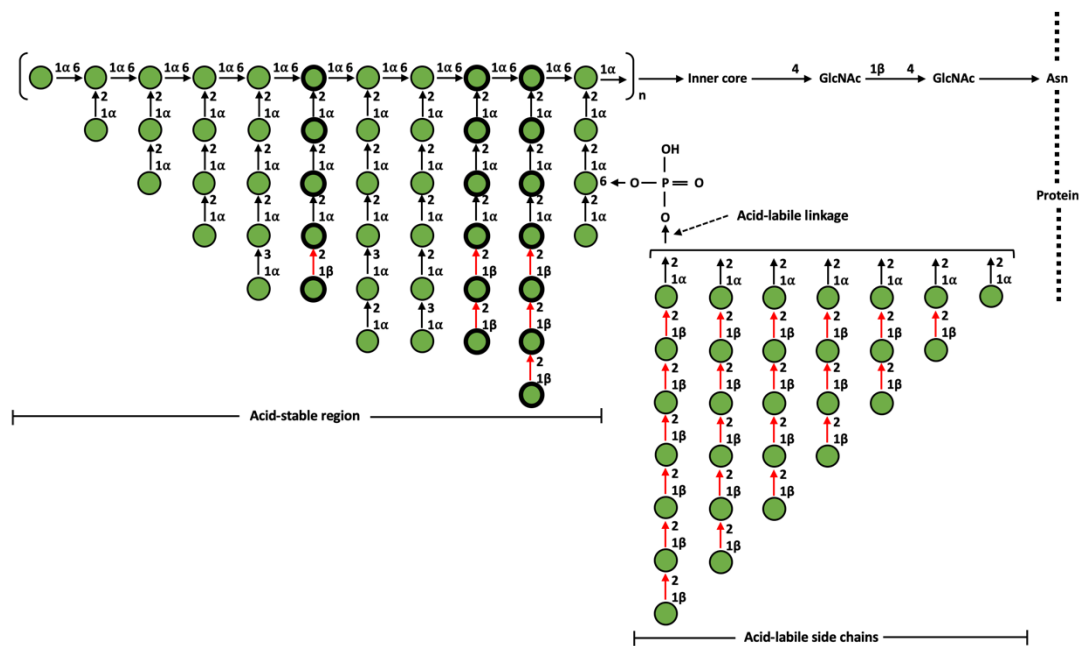
Figure 1. 17 – The representative structure of C. albicans mannan. *Bold circles represent serotype A-specific antigenic mannose regions. Red arrows represent β-(1-2)-linkages. Figure adapted from Shibata et al[132].*

β-(1-2)-Mannan antigens have been incorporated into vaccines for immunisation studies, and it has been shown that antibodies raised against β-(1-2)-mannotriose antigens are able to protect against disseminated candidiasis and vaginal infection in mouse models[133]. Until recently, β-(1-2)-mannans could only be obtained by extraction from microbial cultures[134], or chemical synthesis[135], requiring category 2 containment facilities or complex protecting group chemistry, respectively. The recent identification of two enzymes, Teth514_1788 and Teth514_1789[136], both able to synthesis β-(1-2)-mannans, allows the potential production of linkage specific β-(1-2)-oligomannans. In this thesis, Teth514_1788, was utilised to generate β-(1-2)-mannan antigens for incorporation into targeted vaccination therapies.

1.5.2. Q Fever: A potential Biowarfare Agent

Coxiella burnetii, the causative agent of Q fever, is widespread amongst livestock worldwide[137]. The zoonotic bacteria are able to survive within the bodily fluids of domesticated livestock and are released into the environment through their natural waste cycles, such as urination, defecation and waste birth products. Wind can carry dust particles containing *C. burnetii* for long distances, allowing the infection to spread. People in direct contact with infected animals, particularly during birthing such as farmers and veterinarians, are at greater risk of contracting the disease. Characteristics such as strong environmental persistence and high infectivity rates have resulted in this bacterium being categorised as a potential biowarfare agent by the Centre for Disease Control (CDC)[138,139].

Only two commercial vaccines are licenced for protection against Q fever, Q-Vax for use in humans[140], and Coxevac for livestock use[141]. Both vaccines comprise of whole-killed *C. burnetii* cells which results in a broad range antibody response. Lack of antibodies specific to Q fever means diagnosis of the disease is slow, with current methods relying on timely polymerase chain reaction (PCR) analysis, where detection is confirmed by successful amplification of key marker genes.[142]. In this thesis, an attempt was made to produce antibodies specific for *C. burnetii* to provide human protection against Q fever, but also for use in diagnostic kits to allow rapid and precise detection of the disease.

Coxiella burnetii is a Gram-negative bacterium, displaying a complex array of carbohydrates on its cell surface (**Figure 1. 18**). The lipopolysaccharide (LPS) of *C. burnetii* has been shown to contain components unique to this organism. Linked to the membrane bound lipid A component is the core region, which is divided into the inner and outer regions. The inner core is proposed to contain a combination of mannose, heptose and kdo carbohydrates, whilst the outer core is proposed to contain mannose and heptose residues. Together, the lipid A and core region comprise the phase II (avirulent) form of LPS. The virulent form LPS is known as phase I, and comprises of phase II LPS with an additional *O* antigen domain attached to the outer core.
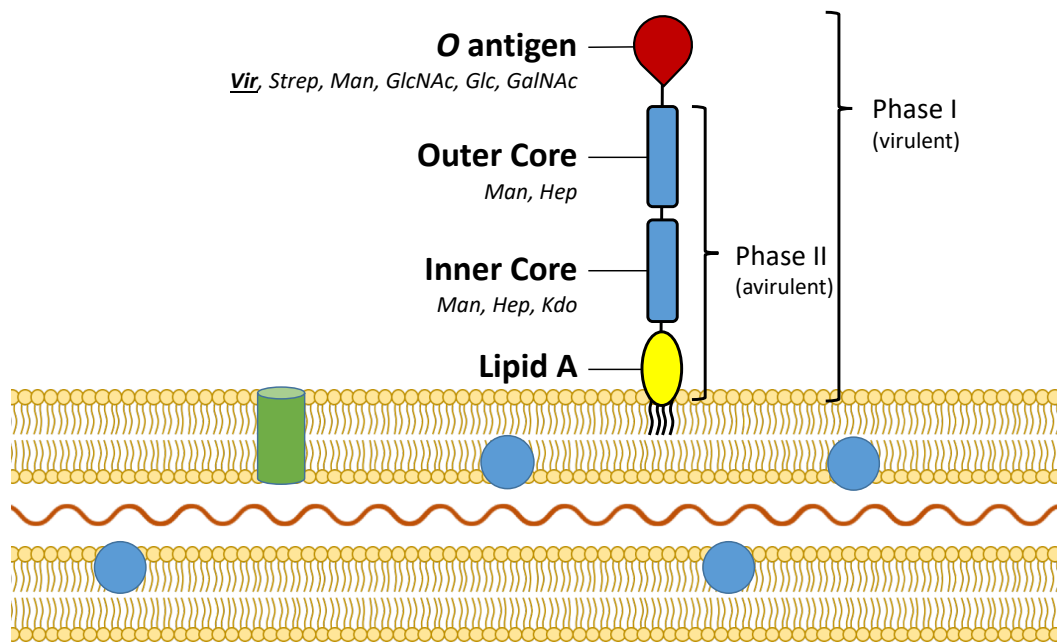
Figure 1. 18 – Proposed structure of C. burnetii LPS. *The putative LPS structure is comprised of an avirulent phase (phase II) and a virulent phase (phase I). Phase II comprises of a membrane-bound lipid A domain coupled to an inner core which comprises of Man, Hep and Kdo. Linked to the inner core is the outer core, which consists of Man and Hep carbohydrates. Together these domains form Phase II LPS. Phase I LPS contains all the components of phase II with the addition of an O antigen domain in which Vir, DHHS, Man, GlcNAc, Glc and GalNAc have been identified.*

Within the *O* antigen of *C. burnetii* LPS, the composition of sugars has been identified, although the sequence and linkage of many have yet to be elucidated. The structural composition of LPS I has been proposed as follows (mol %); Man (32.6), Vir (32.3), Hep (14.4), GlcN (12.2), dihydrohydroxystreptose [DHHS (6.7)], Glc (1.8) and Gal (trace)[143]. The unique characteristics of virenose and DHHS (**Figure 1. 19**) make them appealing target antigens for both vaccination and diagnostic therapies. Streptose, a component of the antibiotic streptomycin, is found in *Streptomyces spp.* Virenose has been identified in only a few species of bacteria, *C. burnetii*[144]*, Streptomyces spp.*[145] and *Bacillus cereus*[146] (where it is referred to as cillose). It has been proposed that virenose exists at the terminal end of *C. burnetii O* antigen in a (1,4)-linkage, with the linkage configuration yet to be determined[147].
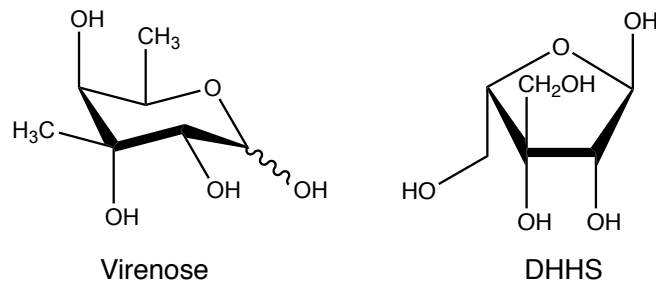
Figure 1. 19 – The chemical structure of virenose and dihydrohydroxystreptose (DHHS).

Although a vaccine against Q fever exists for each humans and livestock, they are produced from whole killed *Coxiella burnetii* cells and require a 7 days skin test before administration[141]. Using whole killed cells in vaccination therapies also poses a risk of cross-reactivity with other species due to the broad range of antibodies being produced. Engineering a vaccine to protect against unique components of *C. burnetii* LPS would not only allow immediate administration, but also generate a more potent antibody response specifically towards *C. burnetii* due to the selective specificity.

Generation of specific antibodies also holds scope for improved diagnostic tests against Q fever. Current methods of detection involve either nucleic acid amplification, which itself requires specialist laboratory safety procedures for handling and storage of a category 3 pathogen, or serological screens of antibody titers via immunosorbent assays which have been shown to have cross-reactivity[148]. Specific antibodies raised towards virenose would vastly improve the efficiency of diagnosis of the pathogen. Used in lateral flow devices, diagnosis would not only be specific for Q fever, but the time for accurate diagnosis would be reduced to a matter of minutes, allowing for fast and convenient diagnosis.

1.6.   General Aim

It is evident that binding to the Dectin-1 receptor requires β-(1-3)-glucans of at least DP12[5]. However, the requirements for β-glucan binding to translate into a Dectin-1-mediated signalling response are not clear. It is possible that this

response is dependent on β-glucan chains larger than DP12, physical size, branching and orientation of carbohydrates. Elucidating the requirements for such a response would have a profound effect on the development of vaccination therapies, by stimulating signalling cascades to result in better antigen presentation on dendritic cells, and therefore a more robust antibody response. The primary aim of this thesis was to investigate the minimum chain length required for inducing such an immune response and assess the use of these polysaccharides as 'molecular address tags' (MATs) for targeting to Dectin-1 (**Chapter 2**).

The latter part of this thesis focuses on the recent advances in the enzymatic synthesis of β-(1-2)-mannan antigens[136], and the application of β-(1-3)-glucans in targeted glycoconjugate vaccine candidates (**Chapter 3**). The initial aim was to generate a β-(1-2)-mannotriose and β-(1-2)-mannotetraose antigens to determine the immunogenic effect of these oligosaccharides, along with the addition of a β-(1-3)-glucan MAT to enhance antigen presentation.

β-(1-3)-Glucan targeted vaccination therapies would also be applied to a vaccine conjugate containing virenose antigens, in collaboration with JIC spin-out Iceni Diagnostics, in order to improve vaccination therapies towards *C. burnetii*, the causative agent of Q fever. The vaccine would comprise of comprise of chemically synthesised virenose antigens, a laminarin MAT, and a virus-like particle (VLP) proteinaceous carrier. The efficacy of the vaccine would be determined via immunisation trials in rabbits, in collaboration with Mologic. ELISA analysis of the resulting sera would determine the specificity of the antibody response generated. The ability to generate antibodies specific to unique antigens present within capsular polysaccharide of *C. burnetii*, would pave the way for an improved vaccination therapy for Q fever, and also specific and rapid diagnostics of the disease.

1.7. References

1. Varki, A., Cummings, R. D., Esko, J. D., Stanley, P., Hart, G. W., Aebi, M., Darvill, A. G., Kinoshita, T., Packer, N. H., Prestegard, J. H., Schnaar, R. L. & Seeberger, P. H. Essentials of glycobiology, third edition. *Cold Spring Harb. Lab. Press*, 1–57, (2017). doi:10.1016/S0962-8924(00)01855-9

2. Lee, Y. C. & Lee, R. T. Carbohydrate-Protein Interactions: Basis of Glycobiology. *Acc. Chem. Res.* **28,** 321–327 (1995).

3. Kuberan, B. & Lindhardt, R. J. Carbohydrate based vaccines. *Curr. Org. Chem.* **4,** 653–677 (2000).

4. Rabinovich, G. A., van Kooyk, Y. & Cobb, B. A. Glycobiology of immune responses. *Ann. N. Y. Acad. Sci.* **1253,** 1–15 (2012).

5. Palma, A. S., Feizi, T., Zhang, Y., Stoll, M. S., Lawson, A. M., Díaz-Rodríguez, E., Campanero-Rhodes, M. A., Costa, J., Gordon, S., Brown, G. D. & Chai, W. Ligands for the β-glucan receptor, dectin-1, assigned using 'designer' microarrays of oligosaccharide probes (neoglycolipids) generated from glucan polysaccharides. *J. Biol. Chem.* **281,** 5771–5779 (2006).

6. Stone, B. A. Chemistry, Biochemistry, and Biology of 1-3 Beta Glucans and Related Polysaccharides. *Academic Press*, 5–47 (2009). doi:10.1016/B978-0-12-373971-1.00002-9

7. Breedveld, M. W., Zevenhuizen, L. P. & Zehnder, A. J. Excessive excretion of cyclic beta-(1,2)-glucan by Rhizobium trifolii TA-1. *Appl. Environ. Microbiol.* **56,** 2080–6 (1990).

8. Zhu, F., Du, B. & Xu, B. A critical review on production and industrial applications of beta-glucans. *Food Hydrocoll.* **52,** 275–288 (2016).

9.   Chuah, C. T., Sarko, A., Deslandes, Y. & Marchessault, R. H. Packing analysis of carbohydrates and polysaccharides. Part 14. Triple-helical crystalline structure of curdlan and paramylon hydrates. *Macromolecules* (2005). doi:10.1021/ma00242a020

10.   Yoshioka, Y., Uehara, N. & Saitô, H. Conformation-dependent change in antitumor activity of linear and branched (1-3)-beta-D-glucans on the basis of conformational elucidation by carbon-13 nuclear magnetic resonance spectroscopy. *Chem. Pharm. Bull. (Tokyo).* **40,** 1221–6 (1992).

11.   Zhang, L., Li, X., Xu, X. & Zeng, F. Correlation between antitumor activity, molecular weight, and conformation of lentinan. *Carbohydr. Res.* **340,** 1515–1521 (2005).

12.   Young, S. H., Dong, W. J. & Jacobs, R. R. Observation of a partially opened triple-helix conformation in 1-3-beta-glucan by fluorescence resonance energy transfer spectroscopy. *J. Biol. Chem.* **275,** 11874–9 (2000).

13.   Okobira, T., Miyoshi, K., Uezu, K., Sakurai, K. & Shinkai, S. Molecular Dynamics Studies of Side Chain Effect on the β-1,3- d -Glucan Triple Helix in Aqueous Solution. *Biomacromolecules* **9,** 783–788 (2008).

14.   Kanagawa, M., Satoh, T., Ikeda, A., Adachi, Y., Ohno, N. & Yamaguchi, Y. Structural insights into recognition of triple-helical beta-glucans by an insect fungal receptor. *J. Biol. Chem.* **286,** 29158–29165 (2011).

15.   Marchessault, R. H. & Deslandes, Y. Fine structure of (1→3)-β-d-glucans: curdlan and paramylon. *Carbohydr. Res.* **75,** 231–242 (1979).

16.   Borchers, A. T., Keen, C. L. & Gershwini, M. E. Mushrooms, Tumors, and Immunity: An Update. *Exp. Biol. Med.* **229,** 393–406 (2004).

17.   Rop, O., Mlcek, J. & Jurikova, T. Beta-glucans in higher fungi and their health effects. *Nutr. Rev.* **67,** 624–631 (2009).

18. Chang, R. Bioactive Polysaccharides from Traditional Chinese Medicine Herbs as Anticancer Adjuvants. *J. Altern. Complement. Med.* **8,** 559–565 (2002).

19. Baldassano, S., Accardi, G. & Vasto, S. Beta-glucans and cancer: The influence of inflammation and gut peptide. *Eur. J. Med. Chem.* **142,** 486–492 (2017).

20. Du, B., Lin, C., Bian, Z. & Xu, B. An insight into anti-inflammatory effects of fungal beta-glucans. *Trends Food Sci. Technol.* **41,** 49–59 (2015).

21. Baran, J., Allendorf, D. J., Hong, F. & Ross, G. D. Oral beta-glucan adjuvant therapy converts nonprotective Th2 response to protective Th1 cell-mediated immune response in mammary tumor-bearing mice. *Folia Histochem. Cytobiol.* **45,** 107–114 (2007).

22. Bromuro, C., Romano, M., Chiani, P., Berti, F., Tontini, M., Proietti, D., Mori, E., Torosantucci, A., Costantino, P., Rappuoli, R. & Cassone, A. Beta-glucan-CRM197 conjugates as candidates antifungal vaccines. *Vaccine* **28,** 2615–2623 (2010).

23. Meena, D. K., Das, P., Kumar, S., Mandal, S. C., Prusty, A. K., Singh, S. K., Akhtar, M. S., Behera, B. K., Kumar, K., Pal, A. K. & Mukherjee, S. C. Beta-glucan: an ideal immunostimulant in aquaculture (a review). *Fish Physiol. Biochem.* **39,** 431–457 (2013).

24. Du, B. & Xu, B. Oxygen radical absorbance capacity (ORAC) and ferric reducing antioxidant power (FRAP) of β-glucans from different sources with various molecular weight. *Bioact. Carbohydrates Diet. Fibre* **3,** 11–16 (2014).

25. Russo, R., Barsanti, L., Evangelista, V., Frassanito, A. M., Longo, V., Pucci, L., Penno, G. & Gualtieri, P. Euglena gracilis paramylon activates human lymphocytes by upregulating pro-inflammatory factors. *Food Sci. Nutr.* **5,** 205–214 (2017).

26. Bohn, J. A. & BeMiller, J. N. (1→3)-β-D-Glucans as biological response modifiers: a review of structure-functional activity relationships. *Carbohydr. Polym.* **28,** 3–14 (1995).

27. Zhu, W., Ma, H., Miao, J., Huang, G., Tong, M. & Zou, S. β-Glucan modulates the lipopolysaccharide-induced innate immune response in rat mammary epithelial cells. *Int. Immunopharmacol.* **15,** 457–465 (2013).

28. Jawhara, S., Habib, K., Maggiotto, F., Pignede, G., Vandekerckove, P., Maes, E., Dubuquoy, L., Fontaine, T., Guerardel, Y. & Poulain, D. Modulation of Intestinal Inflammation by Yeasts and Cell Wall Extracts: Strain Dependence and Unexpected Anti-Inflammatory Role of Glucan Fractions. *PLoS One* **7,** e40648 (2012).

29. Chihara, G., Hamuro, J., Maeda, Y., Arai, Y. & Fukuoka, F. Antitumour Polysaccharide derived Chemically from Natural Glucan (Pachyman). *Nature* **225,** 943–944 (1970).

30. Chen, X.-Y. & Kim, J.-Y. Callose synthesis in higher plants. *Plant Signal. Behav.* **4,** 489–492 (2009).

31. Pang, Z., Otaka, K., Maoka, T., Hidaka, K., Ishijima, S., Oda, M. & Ohnishi, M. Structure of β-Glucan Oligomer from Laminarin and Its Effect on Human Monocytes to Inhibit the Proliferation of U937 Cells. *Biosci. Biotechnol. Biochem.* **69,** 553–558 (2005).

32. Read, S. M., Currie, G. & Bacic, A. Analysis of the structural heterogeneity of laminarin by electrospray-ionisation-mass spectrometry. *Carbohydr. Res.* **281,** 187–201 (1996).

33. Rinaudo, M. & Vincendon, M. 13C NMR structural investigation of scleroglucan. *Carbohydr. Polym.* **2,** 135–144 (1982).

34. Singh, P. P., Whistler, R. L., Tokuzen, R. & Nakahara, W. Scleroglucan, an antitumor polysaccharide from Sclerotium glucanicum. *Carbohydr. Res.* **37,** 245–247 (1974).

35. Komatsu, N., Okubo, S., Kikumoto, S., Kimura, K., Saito, G. & Sakai, S. Host-Mediated antitumor action of schizophyllan, a glucan produced by Schizophyllum commune. *GANN Japanese J. Cancer Res.* **60,** 137–144 (1969).

36. Kim, Y.-T., Kim, E.-H., Cheong, C., Williams, D. L., Kim, C.-W. & Lim, S.-T. Structural characterization of β-d-(1→3, 1→6)-linked glucans using NMR spectroscopy. *Carbohydr. Res.* **328,** 331–341 (2000).

37. Cangelosi, G. A., Martinetti, G., Leigh, J. A., Lee, C. C., Theines, C. & Nester, E. W. Role for Agrobacterium tumefaciens ChvA protein in export of beta-1,2-glucan. *J. Bacteriol.* **171**, 1609–1615 (1989).

38. Geremia, R. A., Cavaignac, S., Zorreguieta, A., Toro, N., Olivares, J. & Ugalde, R. A. A Rhizobium meliloti mutant that forms ineffective pseudonodules in alfalfa produces exopolysaccharide but fails to form β-(1→2) glucan. *J. Bacteriol.* **169**, 880–884 (1987).

39. Maeda, Y. Y. & Chihara, G. Lentinan, a New Immuno-accelerator of Cell-mediated Responses. *Nature* **229,** 634–634 (1971).

40. Hoffmann, G. C., Simson, B. W. & Timell, T. E. Structure and molecular size of pachyman. *Carbohydr. Res.* **20,** 185–188 (1971).

41. Hallac, B. B. & Ragauskas, A. J. Analyzing cellulose degree of polymerization and its relevancy to cellulosic ethanol. *Biofuels, Bioprod. Biorefining* **5,** 215–225 (2011).

42. Lloyd, D. H., Viac, J., Werling, D., Rème, C. A. & Gatto, H. Role of sugars in surface microbe-host interactions and immune reaction modulation. *Vet. Dermatol.* **18,** 197–204 (2007).

43. Kolarich, D., Lepenies, B. & Seeberger, P. H. Glycomics, glycoproteomics and the immune system. *Curr. Opin. Chem. Biol.* **16,** 214–220 (2012).

44. Mahla, R. S., Reddy, C. M., Prasad, D. & Kumar, H. Sweeten PAMPs: role of sugar complexed PAMPs in innate immunity and vaccine biology. *Front. Immunol.* **4,** 1–16 (2013).

45. Goyal, S., Klassert, T. E. & Slevogt, H. C-type lectin receptors in tuberculosis: what we know. *Med. Microbiol. Immunol.* **205,** 513–535 (2016).

46. Kaiko, G. E. & Stappenbeck, T. S. Host–microbe interactions shaping the gastrointestinal environment. *Trends Immunol.* **35,** 538–548 (2014).

47. Bode, L. Human milk oligosaccharides: Every baby needs a sugar mama. *Glycobiology* **22,** 1147–1162 (2012).

48. Peterson, L. W. & Artis, D. Intestinal epithelial cells: regulators of barrier function and immune homeostasis. *Nat. Rev. Immunol.* **14,** 141–153 (2014).

49. Sarma, J. V. & Ward, P. A. The complement system. *Cell Tissue Res.* **343,** 227–235 (2011).

50. Dudziak, D., Kamphorst, A. O., Heidkamp, G. F., Buchholz, V. R., Trumpfheller, C., Yamazaki, S., Cheong, C., Liu, K., Lee, H.-W., Park, C. G., Steinman, R. M. & Nussenzweig, M. C. Differential Antigen Processing by Dendritic Cell Subsets in Vivo. *Science (80-.).* **315,** 107–111 (2007).

51. Guermonprez, P., Valladeau, J., Zitvogel, L., Théry, C. & Amigorena, S. Antigen Presentation and T Cell Stimulation by Dendritic Cells. *Annu. Rev. Immunol.* **20,** 621–667 (2002).

52. Bean, W. B. The Clonal Selection Theory of Acquired Immunity. *AMA Arch Intern Med* **105,** 973–974 (1960).

53. Mueller, D. L., Jenkins, M. K. & Schwartz, R. H. Clonal Expansion Versus Functional Clonal Inactivation: A Costimulatory Signalling Pathway Determines the Outcome of T Cell Antigen Receptor Occupancy. *Annu. Rev. Immunol.* **7,** 445–480 (1989).

54. Sanders, M. E., Makgoba, M. W. & Shaw, S. Human naive and memory T cells: reinterpretation of helper-inducer and suppressor-inducer subsets. *Immunol. Today* **9,** 195–199 (1988).

55. Chen, G., Shaw, M. H., Kim, Y.-G. & Nuñez, G. NOD-like receptors: role in innate immunity and inflammatory disease. *Annu. Rev. Pathol. Mech. Dis.* **4,** 365–398 (2009).

56. Takeda, K., Kaisho, T. & Akira, S. Toll-like receptors. *Annu. Rev. Immunol.* **21,** 335–376 (2003).

57. Figdor, C. G., van Kooyk, Y. & Adema, G. J. C-type lectin receptors on dendritic cells and Langerhans cells. *Nat. Rev. Immunol.* **2,** 77–84 (2002).

58. Sallusto, F., Cella, M., Danieli, C. & Lanzavecchia, A. Dendritic cells use macropinocytosis and the mannose receptor to concentrate macromolecules in the major histocompatibility complex class II compartment: downregulation by cytokines and bacterial products. *J. Exp. Med.* **182,** 389–400 (1995).

59. Weidenmaier, C. & Peschel, A. Teichoic acids and related cell-wall glycopolymers in Gram-positive physiology and host interactions. *Nat. Rev. Microbiol.* **6,** 276–287 (2008).

60. Tan, M., Mommaas, A. M., Drijfhout, J. W., Jordens, R., Onderwater, J. J. M., Verwoerd, D., Mulder, A. A., vanderHeiden, A. N., Scheidegger, D., Oomen, L., Ottenhoff, T. H. M., Tulp, A., Neefjes, J. J. & Koning, F. Mannose receptor-mediated uptake of antigens strongly enhances HLA class II-restricted antigen presentation by cultured dendritic cells. *Eur. J. Immunol.* **27,** 2426–2435 (1997).

61. Bozzacco, L., Trumpfheller, C., Siegal, F. P., Mehandru, S., Markowitz, M., Carrington, M., Nussenzweig, M. C., Piperno, A. G. & Steinman, R. M. DEC-205 receptor on dendritic cells mediates presentation of HIV gag protein to CD8+ T cells in a spectrum of human MHC I haplotypes. *Proc. Natl. Acad. Sci. U. S. A.* **104,** 1289–1294 (2007).

62. Keler, T., Ramakrishna, V. & Fanger, M. W. Mannose receptor-targeted vaccines. *Expert Opin Biol Ther* **4,** 1953–1962 (2004).

63. Bonifaz, L., Bonnyay, D., Mahnke, K., Rivera, M., Nussenzweig, M. C. & Steinman, R. M. Efficient Targeting of Protein Antigen to the Dendritic Cell Receptor DEC-205 in the Steady State Leads to Antigen Presentation on Major Histocompatibility Complex Class I Products and Peripheral CD8+ T Cell Tolerance. *J. Exp. Med.* **196,** 1627–1638 (2002).

64. Curtis, B. M., Scharnowske, S. & Watson, A. J. Sequence and expression of a membrane-associated C-type lectin that exhibits CD4-independent binding of human immunodeficiency virus envelope glycoprotein gp120. *Proc. Natl. Acad. Sci. U. S. A.* **89,** 8356–8360 (1992).

65. Geijtenbeek, T. B. H., Kwon, D. S., Torensma, R., van Vliet, S. J., van Duijnhoven, G. C. F., Middel, J., Cornelissen, I., Nottet, H., KewalRamani, V. N., Littman, D. R., Figdor, C. G. & van Kooyk, Y. DC-SIGN, a dendritic cell-specific HIV-1-binding protein that enhances trans-infection of T cells. *Cell* **100,** 587–597 (2000).

66. Pederson, K., Mitchell, D. A. & Prestegard, J. H. Structural Characterization of the DC-SIGN-Lewis(X) Complex. *Biochemistry* **53,** 5700–5709 (2014).

67. Soilleux, E. J., Barten, R. & Trowsdale, J. DC-SIGN; a Related Gene, DC-SIGNR; and CD23 Form a Cluster on 19p13. *J. Immunol.* **165,** 2937–2942 (2000).

68. Bashirova, A. A., Geijtenbeek, T. B. H., Van Duijnhoven, G. C. F., Van Vliet, S. J., Eilering, J. B. G., Martin, M. P., Wu, L., Martin, T. D., Viebig, N., Knolle, P. A., Kewalramani, V. N., Van Kooyk, Y. & Carrington, M. A Dendritic Cell–specific Intercellular Adhesion Molecule 3–grabbing Nonintegrin (DC-SIGN)–related Protein Is Highly Expressed on Human Liver Sinusoidal Endothelial Cells and Promotes HIV-1 Infection. *J. Exp. Med.* **193,** 671–678 (2001).

69. Pohlmann, S., Soilleux, E. J., Baribaud, F., Leslie, G. J., Morris, L. S., Trowsdale, J., Lee, B., Coleman, N. & Doms, R. W. DC-SIGNR, a DC-SIGN homologue expressed in endothelial cells, binds to human and simian immunodeficiency viruses and activates infection in trans. *Proc. Natl. Acad. Sci. U. S. A.* **98,** 2670–2675 (2001).

70. Ginhoux, F., Collin, M. P., Bogunovic, M., Abel, M., Leboeuf, M., Helft, J., Ochando, J., Kissenpfennig, A., Malissen, B., Grisotto, M., Snoeck, H., Randolph, G. & Merad, M. Blood-derived dermal langerin(+) dendritic cells survey the skin in the steady state. *J. Exp. Med.* **204,** 3133–3146 (2007).

71. Poulin, L. F., Henri, S., de Bovis, B., Devilard, E., Kissenpfenning, A. & Malissen, B. The dermis contains langerin(+) dendritic cells that develop and function independently of epidermal Langerhans cells. *J. Exp. Med.* **204,** 3119–3131 (2007).

72. Romani, N., Clausen, B. E. & Stoitzner, P. Langerhans cells and more: langerin-expressing dendritic cell subsets in the skin. *Immunol. Rev.* **234,** 120–141 (2010).

73. Ren, R. B., Mayer, B. J., Cicchetti, P. & Baltimore, D. Identification of a 10-amino acid proline-rich SH3 binding-site. *Science (80-.).* **259,** 1157–1161 (1993).

74. Huang, X., Yuan, Z., Chen, G., Zhang, M., Zhang, W., Yu, Y. & Cao, X. Cloning and characterization of a novel ITIM containing lectin-like immunoreceptor LLIR and its two transmembrane region deletion variants. *Biochem. Biophys. Res. Commun.* **281,** 131–140 (2001).

75. Bates, E. E. M., Fournier, N., Garcia, E., Valladeau, J., Durand, I., Pin, J. J., Zurawski, S. M., Patel, S., Abrams, J. S., Lebecque, S., Garrone, P. & Saeland, S. APCs express DCIR, a novel C-type lectin surface receptor containing an immunoreceptor tyrosine-based inhibitory motif. *J. Immunol.* **163,** 1973–1983 (1999).

76. Bloem, K., Vuist, I. M., van den Berk, M., Klaver, E. J., van Die, I., Knippels, L. M., Garssen, J., Garcia-Vallejo, J. J., van Vliet, S. J. & van Kooyk, Y. DCIR interacts with ligands from both endogenous and pathogenic origin. *Immunol. Lett.* **158,** 33–41 (2014).

77. Colonna, M., Samaridis, J. & Angman, L. Molecular characterization of two novel C-type lectin-like receptors, one of which is selectively expressed in human dendritic cells. *Eur. J. Immunol.* **30,** 697–704 (2000).

78. Brown, G. D. Dectin-1: a signalling non-TLR pattern-recognition receptor. *Nat. Rev. Immunol.* **6,** 33–43 (2006).

79. Brown, G. D., Taylor, P. R., Reid, D. M., Willment, J. A., Williams, D. L., Martinez-Pomares, L., Wong, S. Y. C. & Gordon, S. Dectin-1 is a major beta-glucan receptor on macrophages. *J. Exp. Med.* **196,** 407–412 (2002).

80. Gorjestani, S., Yu, M., Tang, B., Zhang, D., Wang, D. & Lin, X. Phospholipase Cγ2 (PLCγ2) is key component in Dectin-2 signaling pathway, mediating anti-fungal innate immune responses. *J. Biol. Chem.* **286,** 43651–43659 (2011).

81. Robinson, M. J., Osorio, F., Rosas, M., Freitas, R. P., Schweighoffer, E., Gross, O., SjefVerbeek, J., Ruland, J., Tybulewicz, V., Brown, G. D., Moita, L. F., Taylor, P. R. & Reis e Sousa, C. Dectin-2 is a Syk-coupled pattern recognition receptor crucial for Th17 responses to fungal infection. *J. Exp. Med.* **206,** 2037–2051 (2009).

82. Saijo, S., Ikeda, S., Yamabe, K., Kakuta, S., Ishigame, H., Akitsu, A., Fujikado, N., Kusaka, T., Kubo, S., Chung, S. H., Komatsu, R., Miura, N., Adachi, Y., Ohno, N., Shibuya, K., Yamamoto, N., Kawakami, K., Yamasaki, S., Saito, T., Akira, S. & Iwakura, Y. Dectin-2 Recognition of alpha-Mannans and Induction of Th17 Cell Differentiation Is Essential for Host Defense against Candida albicans. *Immunity* **32,** 681–691 (2010).

83. Dzionek, A., Sohma, Y., Nagafune, J., Cella, M., Colonna, M., Facchetti, F., Gunther, G., Johnston, I., Lanzavecchia, A., Nagasaka, T., Okada, T., Vermi, W., Winkels, G., Yamamoto, T., Zysk, M., Yamaguchi, Y. & Schmitz, J. BDCA-2, a novel plasmacytoid dendritic cell-specific type IIC-type lectin, mediates antigen capture and is a potent inhibitor of interferon alpha/beta induction. *J. Exp. Med.* **194,** 1823–1834 (2001).

84. Eichler, W., Ruschpler, P., Wobus, M. & Drossler, K. Differentially induced expression of C-type lectins in activated lymphocytes. *J. Cell. Biochem. Suppl.* **Suppl 36,** 201–208 (2001).

85. Azad, A. K., Rajaram, M. V. S. & Schlesinger, L. S. Exploitation of the Macrophage Mannose Receptor (CD206) in Infectious Disease Diagnostics and Therapeutics. *J. Cytol. Mol. Biol.* **1,** 1000003 (2014).

86. Singodia, D., Verma, A., Verma, R. K. & Mishra, P. R. Investigations into an alternate approach to target mannose receptors on macrophages using 4-sulfated N-acetyl galactosamine more efficiently in comparison with mannose-decorated liposomes: an application in drug delivery. *Nanomedicine-Nanotechnology Biol. Med.* **8,** 468–477 (2012).

87. Kogo, H., Takahashi, H. & Uchida, E. Murine tumor growth suppression through CD8+ CTLs via activated DEC-205+ dendritic cells by sequential administration of α-galactosylceramide in vivo. *Cancer Res.* **78,** 4695–4695 (2018).

88. Zhang, S. S., Park, C. G., Zhang, P., Bartra, S. S., Plano, G. V, Klena, J. D., Skurnik, M., Hinnebusch, B. J. & Chen, T. Plasminogen Activator Pla of Yersinia pestis Utilizes Murine DEC-205 (CD205) as a Receptor to Promote Dissemination. *J. Biol. Chem.* **283,** 31511–31521 (2008).

89. Jiang, W. P., Swiggard, W. J., Heufler, C., Peng, M., Mirza, A., Steinman, R. M. & Nussenzweig, M. C. The receptor DEC-205 expressed by dendritic cells and thymic epithelial cells is involved in antigen processing. *Nature* **375,** 151–155 (1995).

90. Huang, H., Ostroff, G. R., Lee, C. K., Wang, J. P., Specht, C. A. & Levitz, S. M. Distinct patterns of dendritic cell cytokine release stimulated by fungal β-glucans and toll-like receptor agonists. *Infect. Immun.* **77,** 1774–1781 (2009).

91. Goodridge, H. S., Wolf, A. J. & Underhill, D. M. beta-glucan recognition by the innate immune system. *Immunol. Rev.* **230,** 38–50 (2009).

92. Steele, C., Rapaka, R. R., Metz, A., Pop, S. M., Williams, D. L., Gordon, S., Kolls, J. K. & Brown, G. D. The beta-glucan receptor dectin-1 recognizes specific morphologies of Aspergillus fumigatus. *PLoS Pathog.* **1,** 323–334 (2005).

93. Xie, J., Guo, L., Ruan, Y., Zhu, H., Wang, L., Zhou, L., Yun, X. & Gu, J. Laminarin-mediated targeting to Dectin-1 enhances antigen-specific immune responses. *Biochem. Biophys. Res. Commun.* **391,** 958–962 (2010).

94. McGreal, E. P., Rosas, M., Brown, G. D., Zamze, S., Wong, S. Y. C., Gordon, S., Martinez-Pomares, L. & Taylor, P. R. The carbohydrate-recognition domain of Dectin-2 is a C-type lectin with specificity for high mannose. *Glycobiology* **16,** 422–430 (2006).

95. Yonekawa, A., Saijo, S., Hoshino, Y., Miyake, Y., Ishikawa, E., Suzukawa, M., Inoue, H., Tanaka, M., Yoneyama, M., Oh-hora, M., Akashi, K. & Yamasaki, S. Dectin-2 Is a Direct Receptor for Mannose-Capped Lipoarabinomannan of Mycobacteria. *Immunity* **41,** 402–413 (2014).

96. Kimura, Y., Inoue, A., Hangai, S., Saijo, S., Negishi, H., Nishio, J., Yamasaki, S., Iwakura, Y., Yanai, H. & Taniguchi, T. The innate immune receptor Dectin-2 mediates the phagocytosis of cancer cells by Kupffer cells for the suppression of liver metastasis. *Proc. Natl. Acad. Sci. U. S. A.* **113,** 14097–14102 (2016).

97. de Witte, L., Nabatov, A., Pion, M., Fluitsma, D., de Jong, M. A. W. P., de Gruijl, T., Piguet, V., van Kooyk, Y. & Geijtenbeek, T. B. H. Langerin is a natural barrier to HIV-1 transmission by Langerhans cells. *Nat. Med.* **13,** 367–371 (2007).

98. Kim, H. J., Brennan, P. J., Heaslip, D., Udey, M. C., Modlin, R. L. & Belisle, J. T. Carbohydrate-Dependent Binding of Langerin to SodC, a Cell Wall Glycoprotein of Mycobacterium leprae. *J. Bacteriol.* **197,** 615–625 (2015).

99. Stambach, N. S. & Taylor, M. E. Characterization of carbohydrate recognition by langerin, a C-type lectin of Langerhans cells. *Glycobiology* **13,** 401–410 (2003).

100. Sattler, S., Reiche, D., Sturtzel, C., Karas, I., Richter, S., Kalb, M. L., Gregor, W. & Hofer, E. The Human C-Type Lectin-Like Receptor CLEC-1 is Upregulated by TGF-ss and Primarily Localized in the Endoplasmic Membrane Compartment. *Scand. J. Immunol.* **75,** 282–292 (2012).

101. Geijtenbeek, T. B. H., Torensma, R., van Vliet, S. J., van Duijnhoven, G. C. F., Adema, G. J., van Kooyk, Y. & Figdor, C. G. Identification of DC-SIGN, a novel dendritic cell-specific ICAM-3 receptor that supports primary immune responses. *Cell* **100,** 575–585 (2000).

102. Geijtenbeek, T. B. H., Krooshoop, D., Bleijs, D. A., van Vliet, S. J., van Duijnhoven, G. C. F., Grabovsky, V., Alon, R., Figdor, C. G. & van Kooyk, Y. DC-SIGN-ICAM-2 interaction mediates dendritic cell trafficking. *Nat. Immunol.* **1,** 353–357 (2000).

103. Palma, A. S., Zhang, Y., Childs, R. A., Campanero-Rhodes, M. A., Liu, Y., Feizi, T. & Chai, W. Neoglycolipid-based 'designer' oligosaccharide microarrays to define β-glucan ligands for dectin-1. *Methods Mol. Biol.* **808,** 337–359 (2012).

104. Feinberg, H., Rowntree, T. J. W., Tan, S. L. W., Drickamer, K., Weis, W. I. & Taylor, M. E. Common polymorphisms in human langerin change specificity for glycan ligands. *J. Biol. Chem.* **288,** 36762–36771 (2013).

105. Heinsbroek, S. E., Taylor, P. R., Rosas, M., Willment, J. A., Williams, D. L., Gordon, S. & Brown, G. D. Expression of functionally different dectin-1 isoforms by murine macrophages. *J. Immunol.* **176,** 5513–5518 (2006).

106. Willment, J. A., Gordon, S. & Brown, G. D. Characterisation of the human [beta]-glucan receptor and its alternatively spliced isoforms. *J. Biol. Chem.* **276,** 43818–43823 (2001).

107. Xie, J., Sun, M., Guo, L., Liu, W., Jiang, J., Chen, X., Zhou, L. & Gu, J. Human Dectin-1 isoform E is a cytoplasmic protein and interacts with RanBPM. *Biochem. Biophys. Res. Commun.* **347,** 1067–1073 (2006).

108. Brown, J., O'Callaghan, C. A., Marshall, A. S., Gilbert, R. J., Siebold, C., Gordon, S., Brown, G. D. & Jones, E. Y. Structure of the fungal beta-glucan-binding immune receptor dectin-1: implications for function. *Protein Sci.* **16,** 1042–1052 (2007).

109. Huysamen, C. & Brown, G. D. The fungal pattern recognition receptor, Dectin-1, and the associated cluster of C-type lectin-like receptors. *FEMS Microbiol. Lett.* **290,** 121–128 (2008).

110. Plato, A., Willment, J. A. & Brown, G. D. C-type lectin-like receptors of the dectin-1 cluster: ligands and signaling pathways. *Int Rev Immunol* **32,** 134–156 (2013).

111. Gringhuis, S. I., den Dunnen, J., Litjens, M., van der Vlist, M., Wevers, B., Bruijns, S. C. M. & Geijtenbeek, T. B. H. Dectin-1 directs T helper cell differentiation by controlling noncanonical NF-κB activation through Raf-1 and Syk. *Nat. Immunol.* **10,** 203–213 (2009).

112. Gringhuis, S. I., Wevers, B. A., Kaptein, T. M., van Capel, T. M. M., Theelen, B., Boekhout, T., de Jong, E. C. & Geijtenbeek, T. B. H. Selective C-Rel Activation via Malt1 Controls Anti-Fungal T-H-17 Immunity by Dectin-1 and Dectin-2. *PLoS Pathog.* **7,** e1001259 (2011).

113. Sancho, D. & Reis e Sousa, C. Signaling by Myeloid C-Type Lectin Receptors in Immunity and Homeostasis. *Annu. Rev. Immunol.* **30,** 491–529 (2012).

114. Adams, E. L., Rice, P. J., Graves, B., Ensley, H. E., Yu, H., Brown, G. D., Gordon, S., Monteiro, M. A., Papp-Szabo, E., Lowman, D. W., Power, T. D., Wempe, M. F. & Williams, D. L. Differential High-Affinity Interaction of Dectin-1 with Natural or Synthetic Glucans Is Dependent upon Primary Structure and Is Influenced by Polymer Chain Length and Side-Chain Branching. *J. Pharmacol. Exp. Ther.* **325,** 115–123 (2008).

115. Czop, J. K. & Austen, K. F. A beta-glucan inhibitable receptor on human monocytes: its identity with the phagocytic receptor for particulate activators of the alternative complement pathway. *J. Immunol.* **134,** 2588–2593 (1985).

116. Goodridge, H. S., Reyes, C. N., Becker, C. A., Katsumoto, T. R., Ma, J., Wolf, A. J., Bose, N., Chan, A. S. H., Magee, A. S., Danielson, M. E., Weiss, A., Vasilakos, J. P. & Underhill, D. M. Activation of the innate immune receptor Dectin-1 upon formation of a 'phagocytic synapse'. *Nature* **472,** 471–475 (2011).

117. Agarwal, S., Specht, C. A., Huang, H., Ostroff, G. R., Ram, S., Rice, P. A. & Levitz, S. M. Linkage specificity and role of properdin in activation of the alternative complement pathway by fungal glycans. *MBio* **2,** e00178-11 (2011).

118. Denning, D. W. & Bromley, M. J. How to bolster the antifungal pipeline. *Science.* **347,** 1414–1416 (2015).

119. Vallabhaneni, S., Cleveland, A. A., Farley, M. M., Harrison, L. H., Schaffner, W., Beldavs, Z. G., Derado, G., Pham, C. D., Lockhart, S. R. & Smith, R. M. Epidemiology and Risk Factors for Echinocandin Nonsusceptible *Candida glabrata* Bloodstream Infections: Data From a Large Multisite Population-Based Candidemia Surveillance Program, 2008–2014. *Open Forum Infect. Dis.* **2,** ofv163 (2015).

120. Lockhart, S. R., Iqbal, N., Cleveland, A. A., Farley, M. M., Harrison, L. H., Bolden, C. B., Baughman, W., Stein, B., Hollick, R., Park, B. J. & Chiller, T. Species Identification and Antifungal Susceptibility Testing of Candida Bloodstream Isolates from Population-Based Surveillance Studies in Two U.S. Cities from 2008 to 2011. *J. Clin. Microbiol.* **50,** 3435–3442 (2012).

121. Howse, G. L., Bovill, R. A., Stephens, P. J. & Osborn, H. M. I. Synthesis and antibacterial profiles of targeted triclosan derivatives. *Eur. J. Med. Chem.* **162,** 51–58 (2019).

122. Avery, O. T. & Goebel, W. F. Chemo-immunological studies on conjugated carbohydrate-proteins: II. Immunological specificity of synthetic sugar-protein antigens. *J. Exp. Med.* **50,** 533–50 (1929).

123. Berti, F. & Adamo, R. Antimicrobial glycoconjugate vaccines: an overview of classic and modern approaches for protein modification. *Chem. Soc. Rev* **47,** 9015–9025 (2018).

124. Campbell, H., Borrow, R., Salisbury, D. & Miller, E. Meningococcal C conjugate vaccine: The experience in England and Wales. *Vaccine* **27,** B20–B29 (2009).

125. Palucka, K. & Banchereau, J. Cancer immunotherapy via dendritic cells. *Nat. Rev. Cancer* **12,** 265–277 (2012).

126. Trumpfheller, C., Longhi, M. P., Caskey, M., Idoyaga, J., Bozzacco, L., Keler, T., Schlesinger, S. J. & Steinman, R. M. Dendritic cell-targeted protein vaccines: a novel approach to induce T-cell immunity. *J. Intern. Med.* **271,** 183–192 (2012).

127. Awate, S., Babiuk, L. A. & Mutwiri, G. Mechanisms of action of adjuvants. *Front. Immunol.* **4,** 114 (2013).

128. Lipinski, T., Fitieh, A., St Pierre, J. J., Ostergaard, H. L., Bundle, D. R., Touret, N., St. Pierre, J., Ostergaard, H. L., Bundle, D. R. & Touret, N. Enhanced Immunogenicity of a Tricomponent Mannan Tetanus Toxoid Conjugate Vaccine Targeted to Dendritic Cells via Dectin-1 by Incorporating beta-Glucan. *J. Immunol.* **190,** 4116–4128 (2013).

129. Pappas, P. G., Lionakis, M. S., Arendrup, M. C., Ostrosky-Zeichner, L. & Kullberg, B. J. Invasive candidiasis. *Nat. Rev. Dis. Prim.* **4,** 18026 (2018).

130. Kobayashi, H., Shibata, N. & Suzuki, S. Evidence for oligomannosyl residues containing both beta-1,2 and alpha-1,2 linkages as a serotype A-specific epitope(s) in mannans of Candida albicans. *Infect. Immun.* **60,** 2106–9 (1992).

131. Yu, R. J., Bishop, C. T., Cooper, F. P., Hasenclever, H. F. & Blank, F. Structural studies of mannans from Candida albicans (serotypes A and B), Candida parapsilosis, Candida stellatoidea , and Candida tropicalis. *Can. J. Chem.* **45,** 2205–2211 (1967).

132. Shibata, N., Arai, M., Haga, E., Kikuchi, T., Najima, M., Satoh, T., Kobayashi, H. & Suzuki, S. Structural Identification of an Epitope of Antigenic Factor 5 in Mannans of Candida albicans NIH B-792 (Serotype B) and J-1012 (Serotype A) as B-1,2-Linked Oligomannosyl Residues. *Infect. Immun.* **60,** 4100–4110 (1992).

133. Han, Y. & Cutler, J. E. Antibody response that protects against disseminated candidiasis. *Infect. Immun.* **63,** 2714–2719 (1995).

134. Faille, C., Wieruszeski, J.-M., Michalski, J.-C., Poulain, D. & Strecker, G. Complete 1H- and 13C-resonance assignments for d-mannooligosaccharides of the β-d-(1 → 2)-linked series released from the phosphopeptidomannan of Candida albicans VW.32 (serotype A). *Carbohydr. Res.* **236,** 17–27 (1992).

135. Poláková, M., Roslund, M. U., Ekholm, F. S., Saloranta, T. & Leino, R. Synthesis of β-(1→2)-Linked Oligomannosides. *European J. Org. Chem.* **2009,** 870–888 (2009).

136. Chiku, K., Nihira, T., Suzuki, E., Nishimoto, M., Kitaoka, M., Ohtsubo, K. & Nakai, H. Discovery of two β-1,2-mannoside phosphorylases showing different chain-length specificities from Thermoanaerobacter sp. X-514. *PLoS One* **9,** e114882 (2014).

137. Hirai, K. & To, H. Advances in the understanding of Coxiella burnetii infection in Japan. *J. Vet. Med. Sci.* **60,** 781–90 (1998).

138. Moodie, C., Thompson, H., Meltzer, M. & Swerdlow, D. Prophylaxis after Exposure to Coxiella burnetii. *Emerg. Infect. Dis.* **14,** 1558–1566 (2008).

139. Madariaga, M. G., Rezai, K., Trenholme, G. M. & Weinstein, R. A. Q fever: a biological weapon in your backyard. *Lancet Infect. Dis.* **3,** 709–721 (2003).

140. Ackland, J. R., Worswick, D. A. & Marmion, B. P. Vaccine prophylaxis of Q fever. A follow-up study of the efficacy of Q-Vax (CSL) 1985-1990. *Med. J. Aust.* **160,** 704–8 (1994).

141. Arricau-Bouvery, N., Souriau, A., Bodier, C., Dufour, P., Rousset, E. & Rodolakis, A. Effect of vaccination with phase I and phase II Coxiella burnetii vaccines in pregnant goats. *Vaccine* **23,** 4392–4402 (2005).

142. Fenollar, F., Fournier, P. E. & Raoult, D. Molecular detection of Coxiella burnetii in the sera of patients with Q fever endocarditis or vascular infection. *J. Clin. Microbiol.* **42,** 4919–24 (2004).

143. Zhi, Z. L., Laurent, N., Powell, A. K., Karamanska, R., Fais, M., Voglmeir, J., Wright, A., Blackburn, J. M., Crocker, P. R., Russell, D. A., Flitsch, S., Field, R. A. & Turnbull, J. E. A versatile gold surface approach for fabrication and interrogation of glycoarrays. *ChemBioChem* **9,** 1568–1575 (2008).

144. Flores-Ramirez, G., Janecek, S., Miernyk, J. A. & Skultety, L. In silico biosynthesis of virenose, a methylated deoxy-sugar unique to Coxiella burnetii lipopolysaccharide. *Proteome Sci.* **10,** 1–8 (2012).

145. Kharel, M. K., Nybo, S. E., Shepherd, M. D. & Rohr, J. Cloning and characterization of the ravidomycin and chrysomycin biosynthetic gene clusters. *ChemBioChem* **11,** 523–532 (2010).

146. Maes, E., Krzewinski, F., Garenaux, E., Lequette, Y., Coddeville, B., Trivelli, X., Ronse, A., Faille, C. & Guerardel, Y. Glycosylation of BclA glycoprotein from Bacillus cereus and Bacillus anthracis exosporium is domain-specific. *J. Biol. Chem.* **291,** 9666–9677 (2016).

147. Vadovic, P., Slaba, K., Fodorova, M., Skultety, L. & Toman, R. Structural and functional characterization of the glycan antigens involved in immunobiology of Q fever. *Ann. N. Y. Acad. Sci.* **1063,** 149–153 (2005).

148. La Scola, B. & Raoult, D. Serological cross-reactions between Bartonella quintana, Bartonella henselae, and Coxiella burnetii. *J. Clin. Microbiol.* **34,** 2270–4 (1996).

2. Chapter 2: Generation of β-(1-3)-glucan address tags and characterisation of their ability to interact with Dectin-1

2.1. Introduction

This chapter describes the process taken to generate β-(1-3)-glucan address tags and the analysis of their interaction with the C-type lectin receptor, Dectin-1. In brief, the aim was to use curdlan, a naturally occurring β-(1-3)-glucan produced by *Agrobacterium spp.*, to generate β-(1-3)-glucans of varying degrees of polymerisation by subjection to acid degradation. Coupling of β-(1-3)-glucan DP15 and laminarin to bovine serum albumin (BSA) via copper-free "click chemistry", as outlined in **Scheme 2. 1**, would allow analysis of their interactions with Dectin-1 through the use of a reporter cell line expressing the receptor in a plate-based assay.
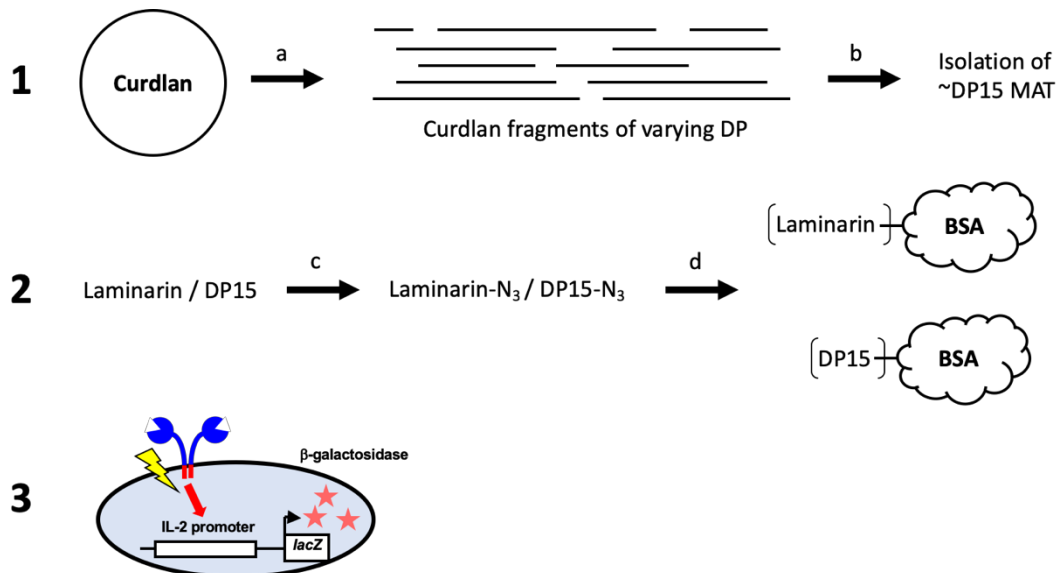
***Scheme 2. 1 - Schematic diagram of β-glucan glycoconjugate generation (1), conjugation (2), and reporter assay (3).** Curdlan was subjected to acetolysis (a) to produce acetylated curdlan fragments which were deprotected and fractionated (b) to yield a fraction containing predominantly DP15. Laminarin and β-(1-3)-glucan DP15 were functionalised with an anomeric azide (c) and coupled to BSA via click chemistry (d). The ability of these glycoconjugates to initiate a Dectin-1-mediated signalling response was determined using a Dectin-1 expressing reporter cell line.*

2.1.1. Generation of β-(1-3)-glucan molecular address tags

Beta-(1-3)-glucans are a naturally occurring group of oligo- and polysaccharides comprising of repeating D-glucose residues, joined by β-(1-3) glycosidic linkages[1]. As discussed previously in **Chapter 1**, these molecules have been chosen to act as molecular address tags for targeted vaccination therapies towards the Dectin-1 receptor on APCs due to the receptors unique ability to bind these molecules exclusively[2]. Producing β-(1-3)-glucan polysaccharides of defined chain lengths is an arduous task, with chemical synthesis limited to short hexasaccharides[3], and chemical[4] and enzymatic[5] degradation resulting in β-(1-3)-glucan fragments with a broad distribution of degrees of polymerisation[6]. Although large β-(1-3)-glucan particles exist in nature as storage polysaccharides, with DPs ranging from 35 for laminarin[7], to 3000 for paramylon[8,9], and as large as DP 5500 for the bacterial polysaccharide curdlan[10], at the time of commencing this work, the enzyme responsible for synthesis of these materials had not yet been identified[11]. Although chemical synthesis would allow more control over the chain length, the degree of polymerisation and quantities needed for this study would make chemical synthesis impractical. Therefore, chemical degradation was explored as a means of generating milligram quantities of β-(1-3)-glucan oligosaccharides of between DP10-25 in order to target the Dectin-1 receptor, which is known to bind β-(1-3)-glucans with a minimum DP of 12[12].

As described in **Chapter 1.1.1**, laminarin is a low molecular weight β-(1-3)-glucan with β-(1-3)-glucan side branches approximately every 3 residues along the backbone. This soluble β-(1-3)-glucan is able to act as a Dectin-1 antagonist, blocking the binding site and suppressing the immune response[13]. It is possible that laminarin is able to bind to Dectin-1 receptors, but the short chain lengths results in a small clustering effect of Dectin-1 receptors which is not sufficient for inducing a signalling response[14]. This thesis investigated the ability of laminarin to bind to Dectin-1, as both a free oligosaccharide and when conjugated to a BSA protein carrier, and trigger a Dectin-1-mediated signalling response.

2.1.2. Conjugation via "click chemistry"

The conjugation of carbohydrates to carrier proteins is essential for inducing a strong immune response (**Chapter 1.4.2**), as well as to allow efficient adhesion to surfaces in high-throughput assays. Recent advances in "click chemistry" have dramatically increased the potential for azide functionalised molecules in conjugation chemistry and microarrays. First coined by Sharpless and co-workers in 2001, the term "click" chemistry is traditionally a copper(I)-catalyzed azide-alkyne cycloaddition (CuAAC). These reactions have proven to be extremely versatile in conjugation chemistry, due to their chemoselectivity and ability to be performed in aqueous media and have transformed the trends in contemporary chemistry for its uses in biological and medicinal chemistry. Advances in click chemistry have quickly led to the development of copper-free, bioorthogonal click chemistry[15]. These strained-ring cyclooctynes are unstable and react spontaneously with azides and eliminate the need for a copper catalyst, the mechanism for which is outline in **Scheme 2. 2**, making the chemistry much safer for use *in vivo*.
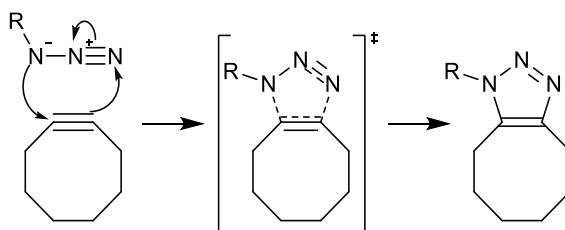
Scheme 2. 2 – Chemical mechanism for copper-free bioorthogonal click chemistry.

Research into incorporating bioorthogonal reagents into living systems in a targeted manner has led to advances in cancer diagnosis through the use of azide functionalised carbohydrates. Cancerous prostate tissues cultured in the presence of azide functionalised Ac4 ManNAz, the biosynthetic precursor for azide-functionalised sialic acid, was metabolised into azidosialic acid and incorporated into cell surface polysaccharides[16]. The introduction of cyclooctyne functionalised fluorophores was able to reveal the location of

cancerous prostate tissue. Such specific targeting of cancerous tissues would allow for targeted delivery of therapeutics[17].

The selective reactivity and biocompatibility of biorthogonal, copper-free click chemistry was chosen to couple β-(1-3)-glucan molecular address tags (MATs) to BSA as it offered a safe, quick and clean method of conjugation. (1*R*,8*S*,9*S*)-Bicyclo[6.1.0]non-4-yn-9-ylmethyl *N*-succinimidyl carbonate, an NHS-functionalised strained-ring cyclooctyne linker (BCN-NHS) was employed due to its dual reactivity, ideal for conjugation (**Scheme 2. 3**).
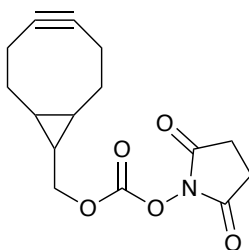
Scheme 2. 3 - Chemical structure of (1R,8S,9S)-bicyclo[6.1.0]non-4-yn-9-ylmethyl N-succinimidyl carbonate (BCN-NHS).

The incorporation of NHS-esters into linker molecules allow for reactivity with exposed amines, such as those found on surface lysines (**Scheme 2. 1a**), and strained-ring cyclooctynes allow for copper-free click chemistry with azide functionalised glycans (**Scheme 2. 1b and c**). These attributes make this linker a very attractive option for protein conjugation.

2.1.3. Ligand-lectin interactions

Dectin-1, a member of the C-type lectin family of receptors, has a high binding specificity for β-(1-3)-glucans, with a minimum chain length DP12 required to bind to this receptor[12], however, it is not known whether this chain length is sufficient for inducing a Dectin-1-mediated signalling response. As outlined in **Chapter 1.4**, it is proposed that clustering of Dectin-1 receptors to form a

phagocytic synapse triggers Src/Syk-dependent signalling in myeloid cells[14]. To determine if our β-(1-3)-glucan oligosaccharides and conjugates were able to induce such a response, our aim was to employ a murine Dectin-1 macrophage reporter cell assay (**Figure 2. 1**)[18], with a cell line expressing a murine Dectin-1 receptor-CD3ς fusion protein (**Figure 2. 1 A**). Upon successful binding of β-(1-3)-glucans, clustering of Dectin-1 receptors initiates CD3ς to stimulate the IL-2 promoter, leading to the transcription of β-galactosidase (LacZ) from the *lacZ* gene (**Figure 2. 1 B**). Addition of chlorophenol red β-D-galactopyranoside (1.5 mM CPRG) containing 100 mM 2-mercaptoethanol causes cell lysis and allows lacZ activity to be observed due to cleavage of the glycosidic linkage within CPRG, resulting in a visual colour change from yellow to red. If ligand-lectin binding is unsuccessful, β-galactosidase is not produced, and no colour change occurs. Mock cell lines, BWZ.36 cells lacking receptor expression act as a control to determine if *lacZ* responses are a result of ligand-lectin interactions. Use of this cell line provides a clear indication as to whether a signalling cascade has been initiated by ligand binding to Dectin-1.
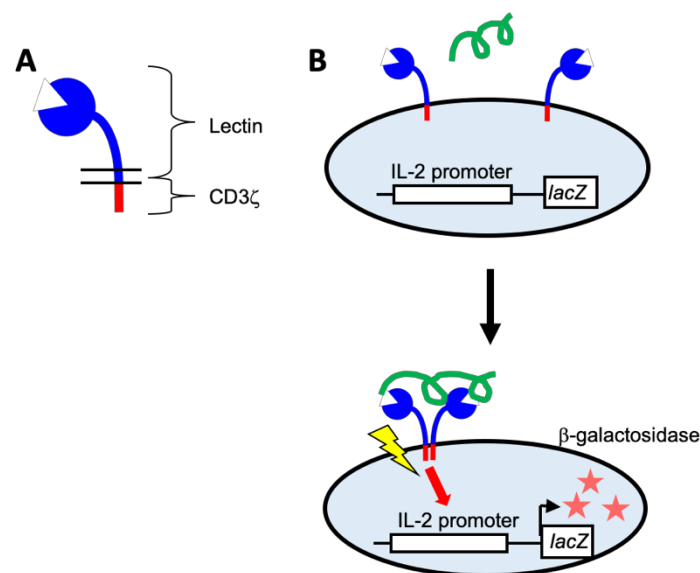
Figure 2. 1 – Schematic diagram of the Dectin-1 reporter cell assay*. (A) A Dectin-1-CD3ς-fusion protein is expressed on the surface of a BWZ.36 cell line. (B) Successful binding of β-(1-3)-glucan ligands to Dectin-1 receptors leads to stimulation of the IL-2 promoter to induce lacZ, resulting in the production of β-galactosidase allowing for colorimetric detection upon addition of CPRG. Green curly line represents carbohydrate ligands. Red stars represent β-galactosidase.*

2.2. Results and Discussion

2.2.1. Generation of β-(1-3)-glucan tags

2.2.1.1. Production of acetylated β-(1-3)-glucan fragments

Beta-(1-3)-glucan address tags were generated by partial acid degradation of curdlan, as outlined in **Chapter 5.2.1**. A handful of methods exist in the literature for generating β-(1-3)-glucan oligosaccharides via both top-down and bottom-up approaches, such as the degradation of curdlan to laminaribiose and peracetylated laminaribiose by enzymatic hydrolysis[5] and chemical degradation[4], respectively.

In this study, efforts were focused on the chemical degradation of a large β-(1-3)-glucan polysaccharide, curdlan, to achieve a series of β-(1-3)-glucan oligosaccharides with varying degrees of polymerisation. Initial attempts focused on the degradation of curdlan by treatment with neat trifluoracetic acid (TFA). Curdlan was mixed with TFA at 5 mg mL^{-1} and reacted in a Biotage Microwave Initiator at 80 °C with the frequency set to very high for 5, 10, 15, 20, and 30 minutes. To determine the chain length the resulting oligosaccharides were dried under compressed air and reacted with APTS via reductive amination. Briefly, 10 μL of each 10 mM 8-amino-1,3,6-pyrenetrisulfonic acid (APTS) and 1 M sodium cyanoborohydride (NaCNBH$_3$) was added to each dried oligosaccharide sample and the reaction incubated at 37 °C overnight. The labelled samples were then dried under nitrogen gas and resuspended in 50 μL of 6 M urea. Samples (5 μL were loaded) were loaded on to an acrylamide gel and run at 300 V for 30 minutes and visualised using a gel imager equipped with a 420 nm light source.

Whilst the degradation of curdlan was successful, as shown by the gel image in **Figure 2. 2**, large quantities of particulate material remained, suggesting the degradation was only effective at the terminal ends of the polysaccharide. After 5 minutes, the reaction had produced significant quantities of DP1-DP10, with larger chains also clearly present.

Figure 2. 2 – Gel analysis of TFA degraded Curdlan. *Curdlan in TFA (5 mg mL^{-1}) was degraded in a Biotage Microwave Initiator at 80 °C set to very high frequency for 5, 10, 15, 20 and 30 minutes. Degraded curdlan oligosaccharides were reacted with APTS via reductive amination and analysed on an acrylamide gel at 300 V for 30 minutes. The gel was visualised under a 420 nm wavelength light.*

The large presence of glucose, and the remaining particulate material, suggested this approach was not efficient at producing β-(1-3)-glucans of DP15. Further attempts were focused on the partial degradation of curdlan via acetolysis, as outlined in **Scheme 2. 4**.
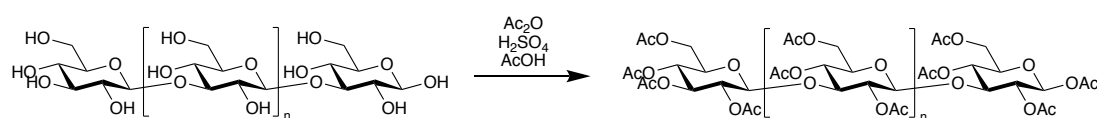
Scheme 2. 4 – Generation of acetylated β-(1-3)-glucan fragments by acetolysis of curdlan. *Reagents and conditions: curdlan, AcOH-Ac$_2$O (1:1), concentrated H$_2$SO$_4$), 30-40 °C for 30 mins, 28 °C for 24 hr, 20 °C, NaOAc. n = DP5500, x = DP12-24.*

Partial degradation of curdlan (10g scale) by acetolysis [acetic anhydride/acetic acid (1:1)], the mechanism for which is outlined in **Scheme 2. 5**.
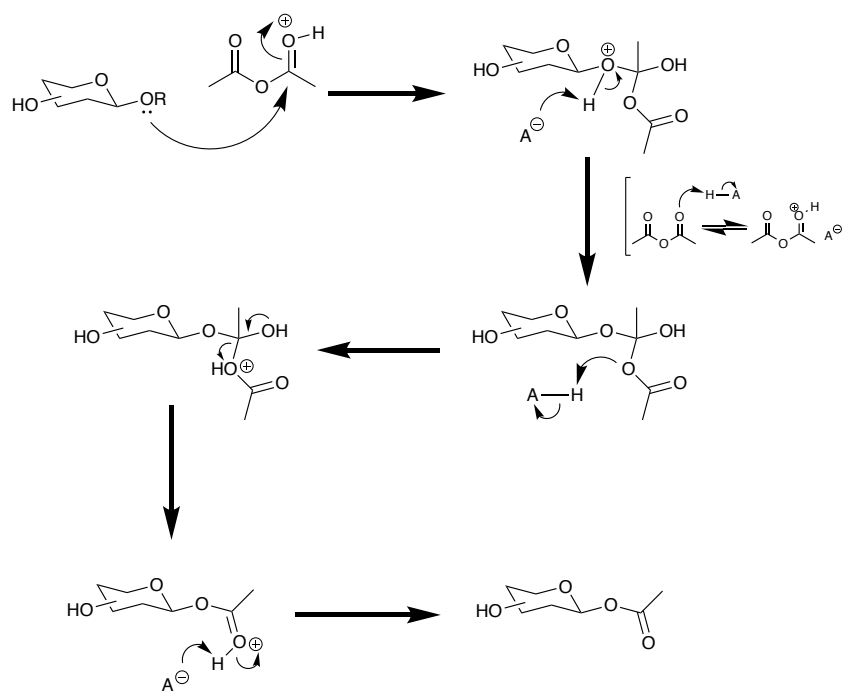
Scheme 2. 5 - Reaction mechanism for the acetolysis of curdlan.

The resulting acetylated curdlan fragments were subsequently fractionationated by flash chromatography on silica gel (300 g) to produce eleven 42 mL fractions of acetylated β-(1-3)-glucan fragments containing both individual oligosaccharides and their mixtures (**Figure 2. 3**).
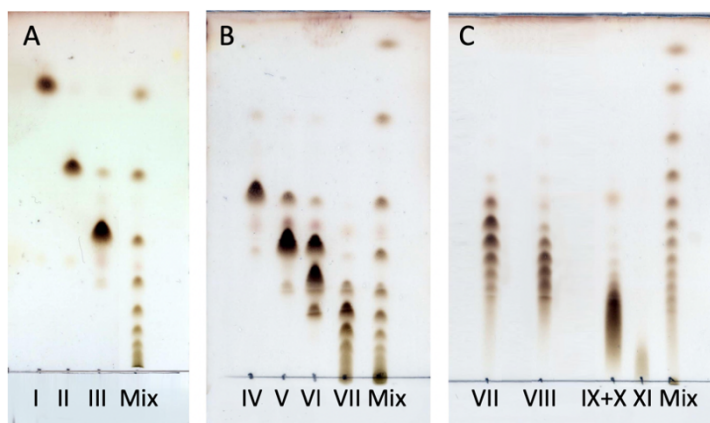
Figure 2. 3 – TLC of acetylated β-(1-3)-glucan fragments fractionated by flash chromatography.

Fractions containing acetylated β-(1-3)-glucan fragments of DP12-24 (fractions IX and X), as determined by MALDI-TOF/MS (**Figure 2. 4**), were combined and concentrated to yield 520 mg of product.
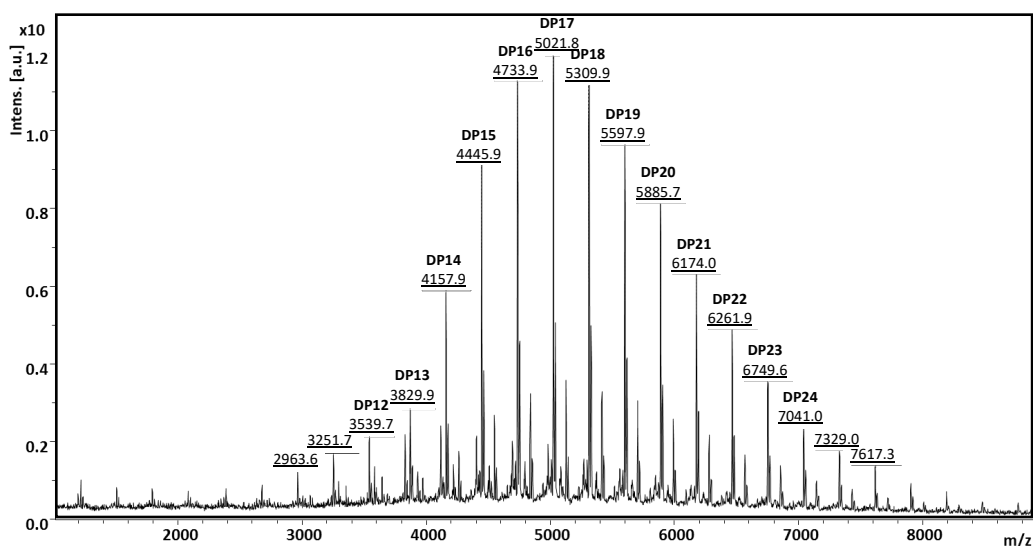
Figure 2. 4 – MALDI-TOF/MS analysis of acetylated curdlan fragments, fractions IX and X. *Mass analysis was performed on an MTP AnchorChip 384 target plate with DHB matrix (10 mg mL^{-1} in 30 % aq. MeCN) using a Bruker Daltronics Ultraflex ToF/ToF mass spectrometer. For calculated and found masses, see **Appendices 6. 1**.*

^{1}H and ^{13}C NMR spectroscopic analysis confirmed the presence of acetates by characteristic signals at 20.6 ppm and 2.22-1.94 ppm for ^{13}C and ^{1}H NMR, respectively (**Figure 2. 5**). Signal assignments for both ^{13}C and ^{1}H NMR, as shown in **Figure 2. 5**, were achieved as reported in the literature[19–21]. A signal at 53.5 ppm and 5.32 ppm for ^{13}C and ^{1}H NMR, respectively, confirms the presence of residual dichloromethane[22].
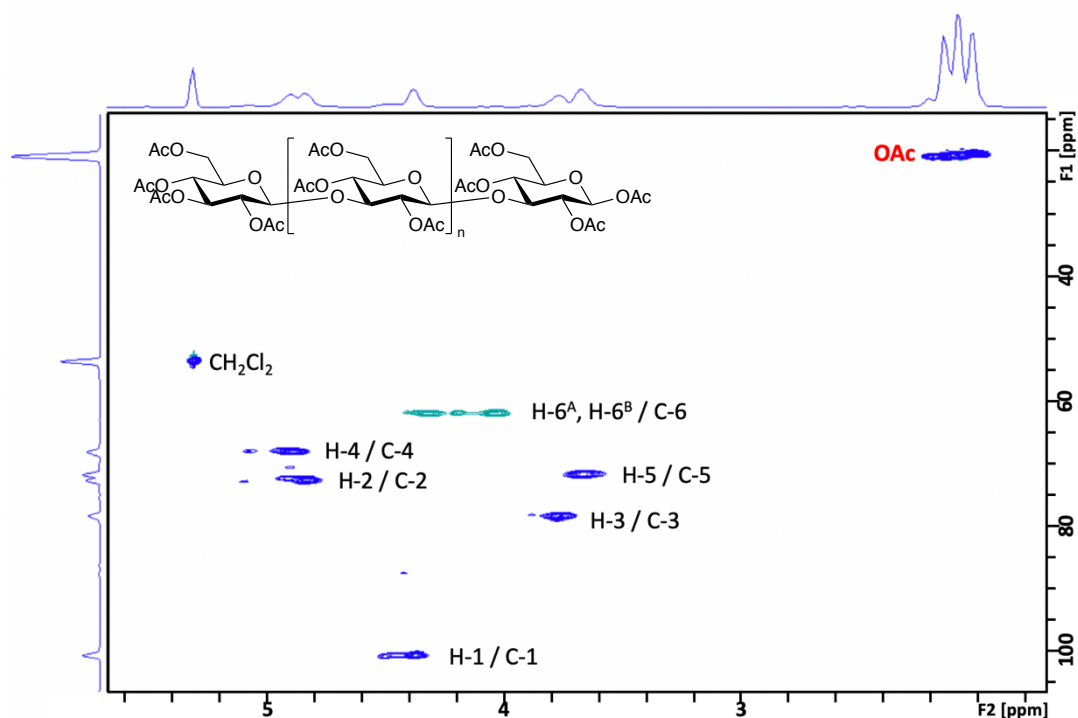
Figure 2. 5 – HSQCed NMR analysis (400 MHz, CDCl$_3$) of acetylated curdlan fragments. For chemical shift assignments, see Appendices 6. 2. Characteristic acetate signals are labelled in red.

2.2.1.2. Deprotection of acetylated β-(1-3)-glucan fragments

Prior to use as address tags, the acetylated curdlan oligosaccharides were deprotected to produce free sugars. A number of methods of deprotection are available for the removal of acetates, ranging from the mild conditions of triethylamine (TEA) in aqueous methanol[23], to the faster conditions of sodium methoxide (NaOMe) in methanol[24]. β-(1-3)-Glucans have been shown to be susceptible to 'chemical peeling' under basic conditions, the mechanism for which is shown in **Scheme 2. 6**, resulting in shortened β-(1-3)-glucan chains. To avoid compromising the degree of polymerisation of β-(1-3)-glucan address tags, harsh basic conditions should be avoided.
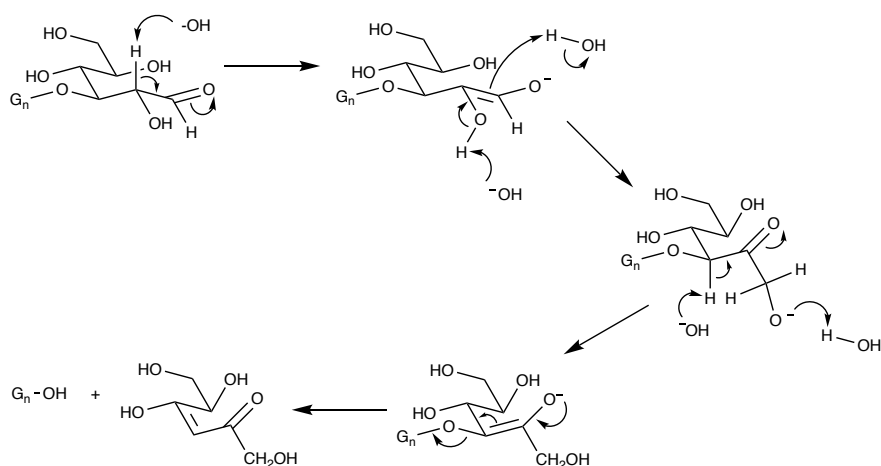
Scheme 2. 6 – The process of 'chemical peeling' of β-(1-3)-glucans under basic conditions. *Adapted from Zhang et al[25].*

To ensure the complete removal of acetates, deacetylation was performed using 1M NaOMe in dry MeOH and DCM (0.1:20:5) to aid the solubility of acetylated products, as outlined in **Scheme 2. 7**.
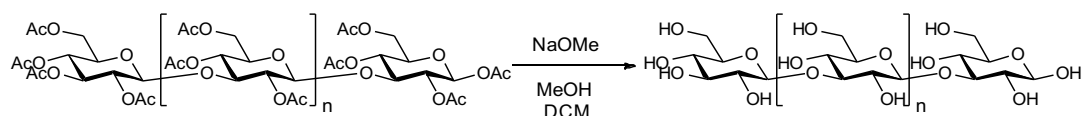
Scheme 2. 7 – Deprotection of acetylated β-(1-3)-glucan fragments. *Reagents and conditions: MeOH/DCM/1M NaOMe (20:5:0.1), 2h, RT, under nitrogen. n = DP1-23.*

From 260 mg of acetylated β-(1-3)-glucans DP13-24, deprotection with NaOMe yielded 115 mg of deacetylated product, which was subsequently analysed by ^{1}H and ^{13}C NMR (**Figure 2. 6**), MALDI-TOF/MS (**Figure 2. 7**) and high-performance anion-exchange chromatography with pulsed amperometric detection [HPAEC-PAD (**Figure 2. 8**)] to determine chain lengths.

^{1}H and ^{13}C NMR analysis (**Figure 2. 6**) clearly shows the removal of acetates, indicated by lack of a signal at 20.6 ppm and 1.94-2.22 ppm for ^{13}C and ^{1}H NMR, respectively, confirming that deprotection was successful. Signal

assignment (**Appendices 6. 3**) corresponds with literature reports for laminari-oligosaccharides[26–28].
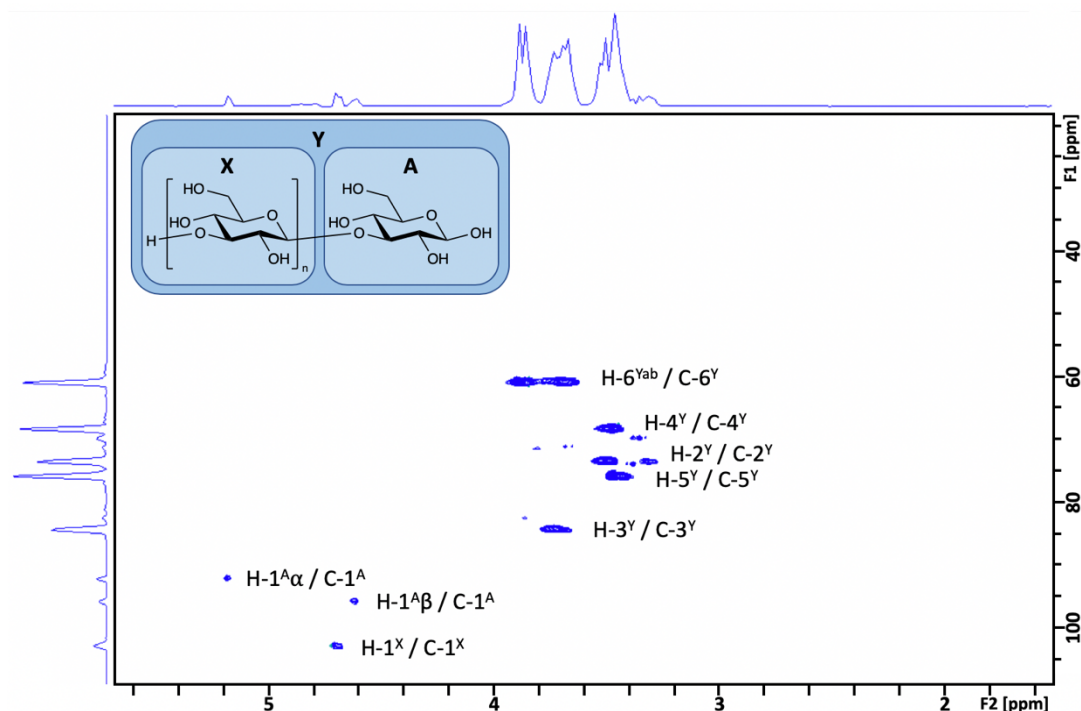

*Figure 2. 6 - HSQC NMR analysis (400 MHz, D₂O) of deacetylated β-(1-3)-glucan curdlan fragments. For chemical shift assignments, see **Appendices 6. 3**.*

Masses obtained from MALDI-TOF/MS (**Figure 2. 7**) indicate the complete deprotection of the β-(1-3)-glucans, with identified masses correlating with the calculated sodium adducts of DP5-23. It is possible that masses as low as DP1 exist, however strong matrix peaks below 500 Da did not allow adequate resolution. However, the distribution of masses has shifted towards the lower molecular weight range. As mentioned previously, β-(1-3)-glucans may be susceptible to 'chemical peeling' under basic conditions, and it is possible that a degree of peeling has occurred here. The ionizability of carbohydrates is much greater at short DPs, with increases in DP leading to a decrease in ionizability[29]. Removal of acetates from the polysaccharides significantly decreases the ionizability of the molecules[29]. Although MALDI-TOF/MS is able to provide m/z charge data of these compounds, it is not a method of quantification due to the reasons outlined previously and should not be considered so.
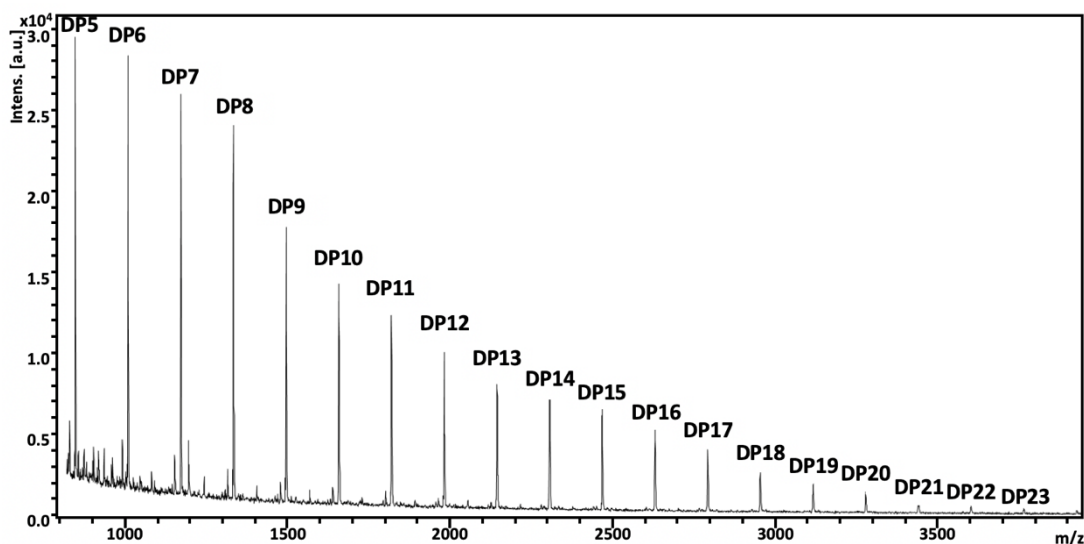
Figure 2. 7 – MALDI-TOF/MS analysis of deprotected β-(1-3)-glucan curdlan fragments. *Mass analysis was performed on an MTP AnchorChip 384 target plate with DHB matrix (10 mg mL^{-1} in 30 % aq. MeCN) using a Bruker Daltronics Ultraflex ToF/ToF mass spectrometer. For calculated and found masses, see* ***Appendices 6. 1****.*

HPAEC-PAD analysis of β-(1-3)-glucans was performed on a Dionex IC system equipped with a CarboPac PA100 (4 x 250 mm) anion exchange column coupled with an electrochemical detector, allowing the determination of retention times for the β-(1-3)-glucans. These analyses allowed for clear resolution of oligosaccharides in a single run, confirming the presences of DP1-23 (**Figure 2. 8**). Peak assignments were made following analysis of a laminarihexaose standard. The presence of β-(1-3)-glucan oligosaccharides below DP5 suggest a small degree of chemical peeling may have occurred during the deprotection stage. As the objective to generate β-(1-3)-glucan chains of DP10-25 was achieved in sufficient quantities for further investigation, the methods employed here were deemed successful and milder means of deprotection were not investigated.
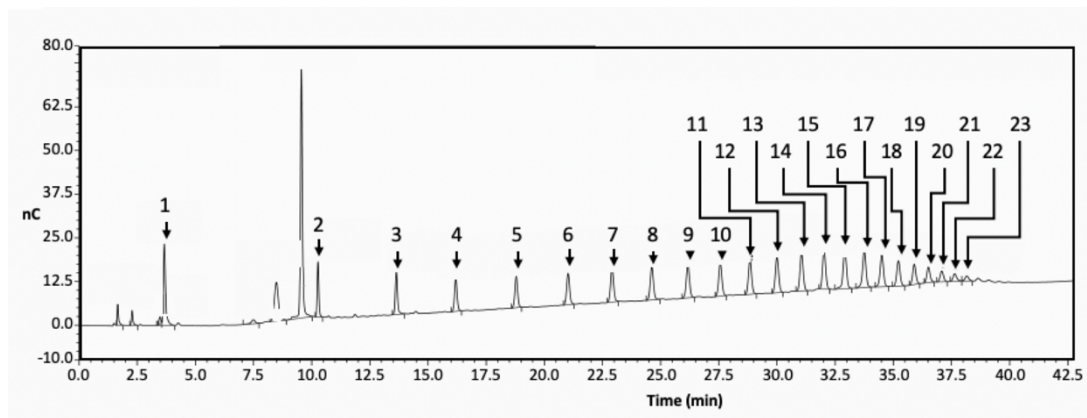
Figure 2. 8 – HPAEC-PAD analysis of deprotected β-(1-3)-glucan curdlan fragments. HPAEC-PAD analysis was performed using a CarboPac PA100 (4 x 250 mm) anion exchange column. Mobile phases (eluent A: 100 mM NaOH; eluent B: 100 mM NaOH with 500 mM NaOAc) were applied as a gradient to 100 % eluent B over 30 mins, isocratic eluent B for 10 mins and ending with isocratic 100 % eluent A for 0.1 mins. Flow rate remained constant at 0.25 mL min^{-1}. Numbers indicate the DP for each peak. For retention times, see **Appendices 6. 5**.

2.2.2. Fractionation of mixed β-(1-3)-glucan polysaccharides

It has been demonstrated that a minimum β-(1-3)-glucan length of DP12 is required for binding to Dectin-1. In order to achieve these chain lengths, fractionation of the deprotected β-(1-3)-glucan curdlan fragments was required. Although the solubility of β-(1-3)-glucan oligosaccharides decreases with increased chain length, it was found that they became soluble in aqueous solution with heating to 40 °C. This allowed fractionation to be achieved by GPC using a Biogel P2 chromatography column (26 x 900 mm) heated to 40 °C (**Figure 2. 9**). Large oligosaccharides of DP6-23 eluted as a broad peak between 190-240 mins, with smaller oligosaccharides eluting as individual peaks later on.
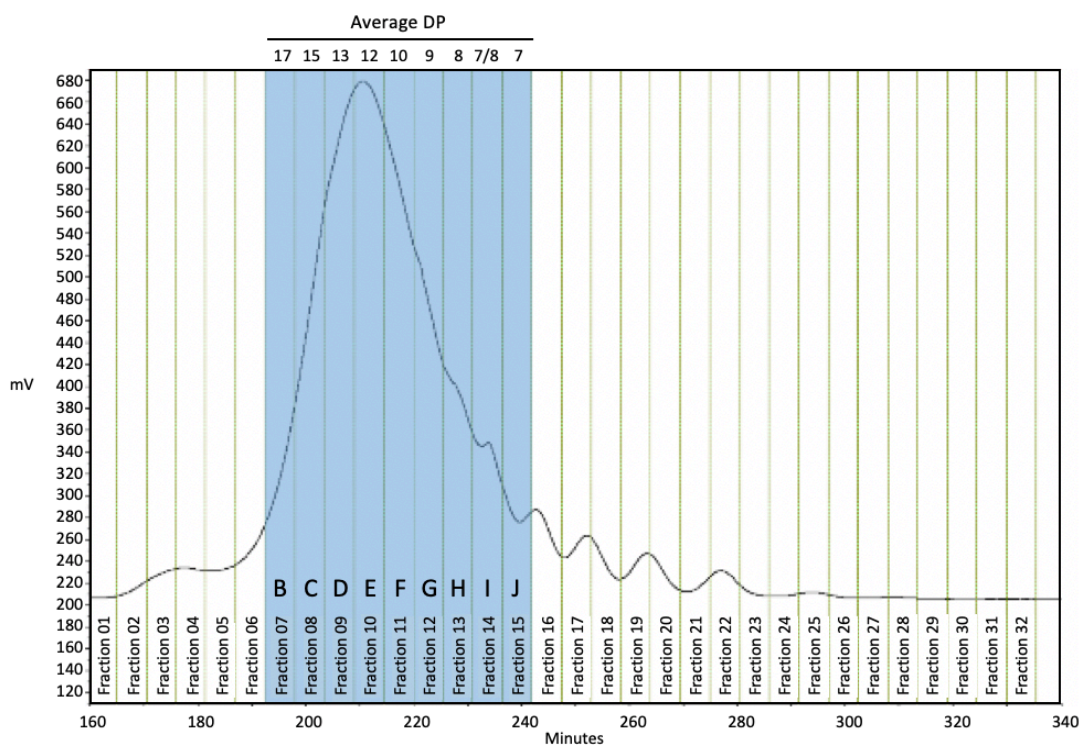
Figure 2. 9 – Seperation of β-(1-3)-glucans by gel permeation chromatography. *Mixed linear β-(1-3)-glucans were in injected into a Biogel P2 column (2.6 x 90 cm) at 40 °C in 30 mg batches with dH₂O at a 1 mL min⁻¹ flow rate. Fractions were collected between 160 and 600 mins at 5.5 mL intervals. Blue shading highlights fractions taken for further analysis.*

MALDI-TOF/MS analysis of fractions collected at 5.5 mL intervals between 190-240 mins reveal a narrower distribution of DPs within each fraction, with the average DP ranging from DP17 (**Figure 2. 10 B**) to DP7 (**Figure 2. 10 J**).
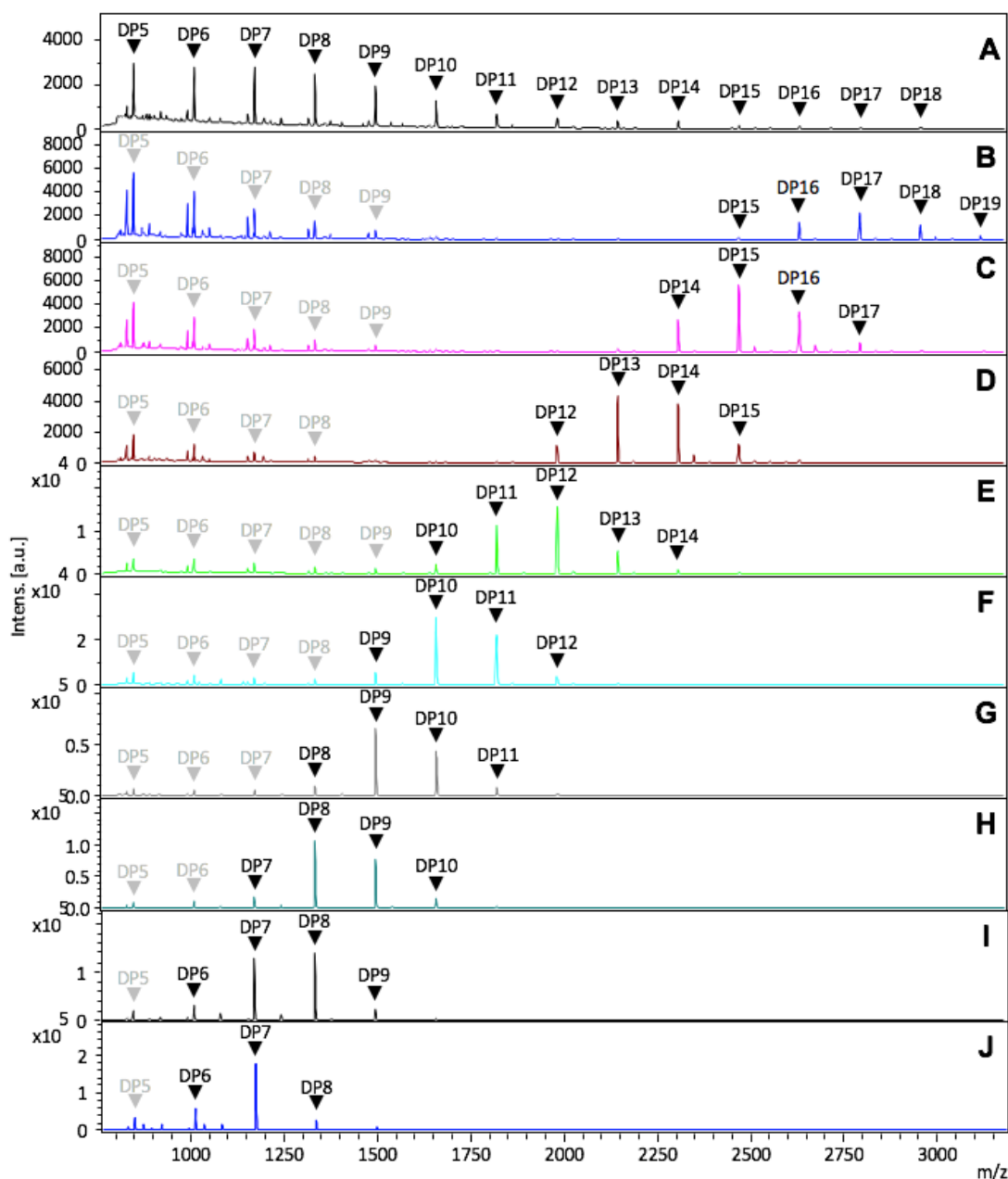
Figure 2. 10 – MALDI-TOF/MS analysis of deprotected β-(1-3)-glucans, prior to (A) and following fractionation by GPC (B-J). *MALDI-TOF/MS analysis performed on an MTP AnchorChip 384 target plate with DHB matrix. Grey labels represent minor peaks, black labels represent dominant peaks. A – Deprotected β-(1-3)-glucan curdlan fragments, B-J – GPC fractions. For calculated and found masses, see* ***Appendices 6. 1****.*

Low molecular weight peaks, corresponding to Na$^+$ and H$^+$ adducts of DP5-9 can been seen in fractions B-E (**Figure 2. 10 B-E**). As previously mentioned, low molecular weight oligosaccharides are more readily ionisable in comparison to medium-high molecular weight oligosaccharides, hence the strong signals seen here. Although MALDI-TOF/MS is able to provide the

masses of compounds present in these fractions, further analysis was required to determine the relative proportion of each oligosaccharides in these mixed fractions.

Chromatograms obtained for each β-(1-3)-glucan fraction show a narrower distribution of chain lengths with the average DP decreasing across fractions. **Figure 2. 11 B** shows an average chain length of DP17/18, with the average chain length decreasing in size to **Figure 2. 11 J** with an average DP of 7. This data is consistent with the data obtained my MALDI-TOF/MS (**Figure 2. 10**), allowing us to determine the average DP within each fraction with confidence. The absence of low molecular weight oligosaccharides (DP1-9) in fractions B-E (**Figure 2. 11 B-E**) by HPAEC-PAD analysis suggest the presence of these peaks by MALDI-TOF/MS (**Figure 2. 10 B-E**) is an artefact of the instrument, likely caused by the higher ionizability of short oligosaccharides.

In order to target the Dectin-1 receptor on APCs, a minimum chain length of DP12 is required, as determined by microarray data[30]. β-(1-3)-Glucan chains within fraction C comprise an average DP of 15, therefore this fraction was selected for further investigation for use as an address tag and will hereby be referred to as DP15.
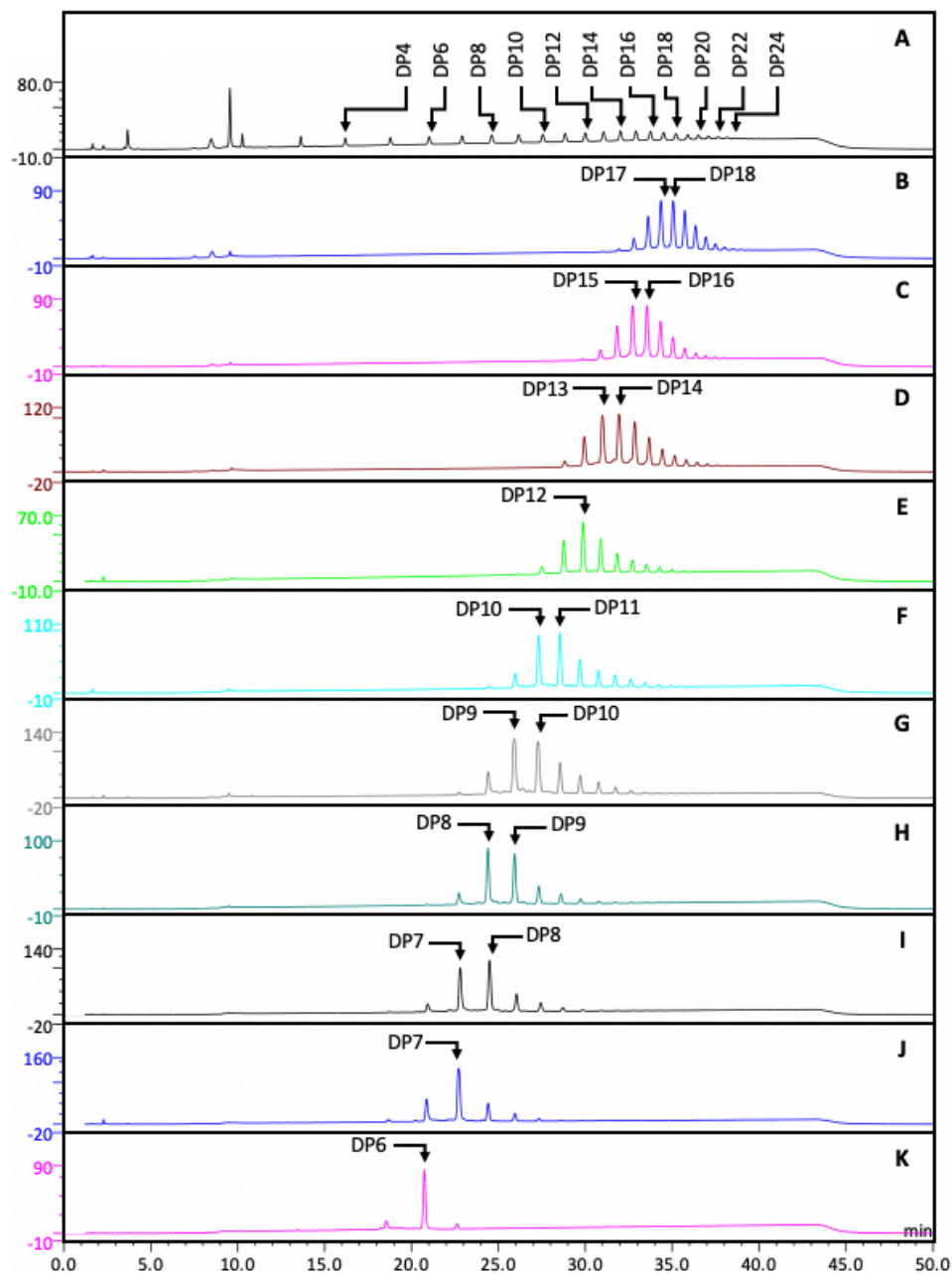
Figure 2. 11 – Analysis of GPC fractionated β-(1-3)-glucans by HPAEC-PAD. *Analysis was performed using a CarboPac PA100 (4 x 250 mm) anion exchange column. Mobile phases (eluent A: 100 mM NaOH; eluent B: 100 mM NaOH with 500 mM NaOAc) were applied as a gradient to 100 % eluent B over 30 mins, isocratic eluent B for 10 mins and ending with isocratic 100 % eluent A for 0.1 mins. Flow rate remained constant at 0.25 mL min^{-1}. A – Deprotected curdlan fragments, B-J – GPC fractions 7-15, K – Laminarihexaose standard. For retention times, see **Appendices 6. 5**.*

2.2.3. Characterisation of commercial laminarin

Laminarin, from *Laminaria digitata*, was purchased from Sigma (L9634) to investigate its use as an address tag to activate Dectin-1-mediated signalling. Characterisation was performed by HSQC NMR (**Figure 2. 1**).
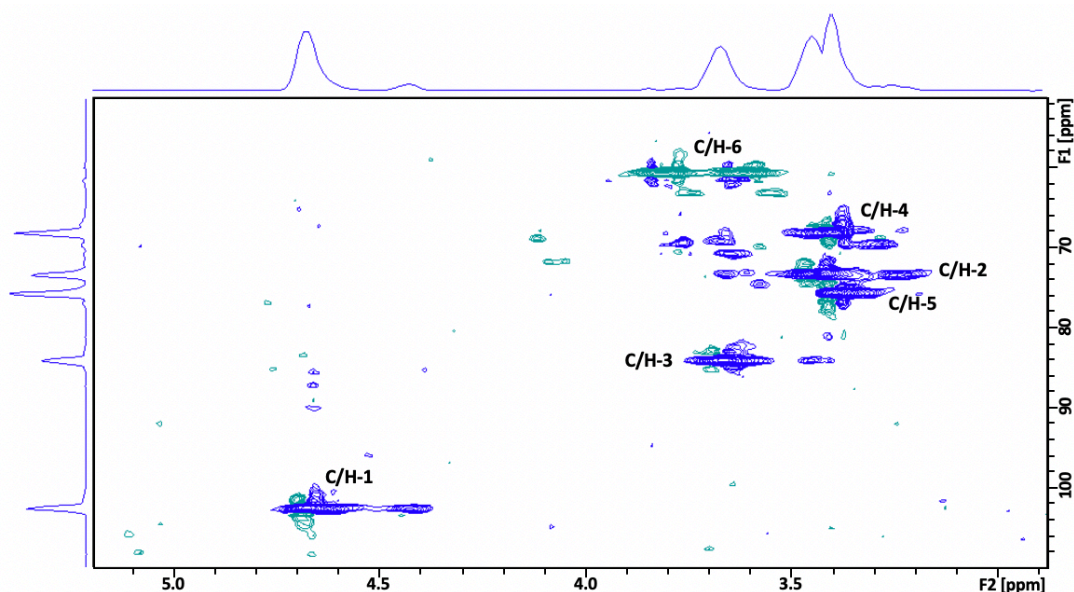
*Figure 2. 12 – HSQCed NMR analysis (400 MHz, D₂O) of commercial laminarin. For chemical shift assignments, see **Appendices 6. 6**.*

2.2.4. Azide functionalisation of β-(1-3)-glucan address tags

Alkyne-azide cycloaddition "click" reactions provide an efficient, highly selective and convenient method for producing stable covalent bonds, making this reaction popular for the coupling together of molecules[31–33]. In this study, copper-free click reactions between azides and a strained-ring alkyne[34] was utilised to conjugate β-(1-3)-glucan tags onto protein carriers.

Beta-(1-3)-glucan DP15 and laminarin were prepared for conjugation by introducing an azide at the anomeric position of the reducing terminus. Numerous reactions exist for introducing an anomeric azide onto carbohydrates, often requiring protecting group chemistry[35], or multiple step reactions[36–39]. In the case of higher oligosaccharides, neither of these approaches are suitable as they may result in cleavage of inner glycosidic bonds[38,40]. As a result, a one-pot method of introducing an anomeric azide was

selected (**Mechanism 2. 1**)[41], as outlined in **Scheme 2. 8**. 2-Chloro-1,3-dimethylimidazolinium chloride (DMC) activates the anomeric hydroxyl group to form a reactive intermediate. Nucleophilic attach by azide ions at the anomeric centre allows to the reaction to proceed to form azido sugars.
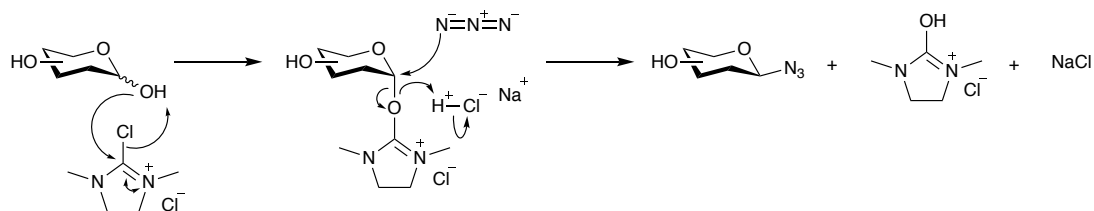
Mechanism 2. 1 – Reaction mechanism for the synthesis of sugar azides via DMC intermediate.
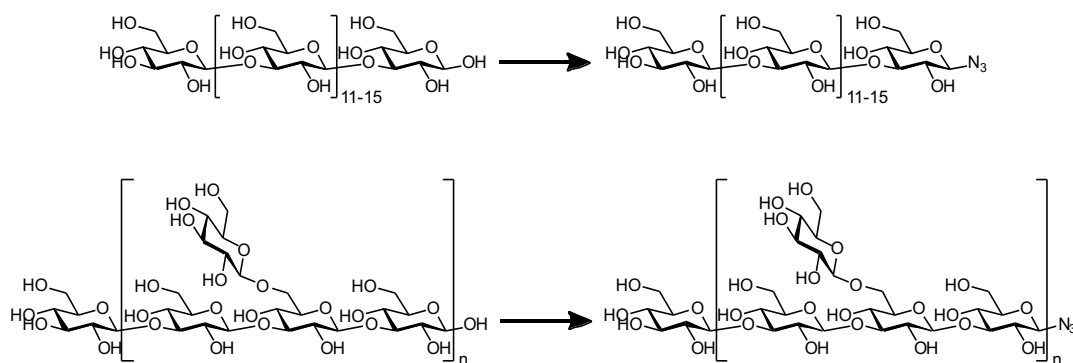
Scheme 2. 8 – Generation of β-glucosyl azides. Reagents and conditions: NaN$_3$ (2.5 M), DMC (5 eq), DIPEA (15 eq), D$_2$O, 18 hr, RT. n = 7-10.

The large size of these oligosaccharides, an average of DP15 for the linear curdlan fragments, makes it challenging to analyse their reducing terminal anomeric position. However, lengthy scan NMR analysis confirmed the introduction of a β-azide at the anomeric position of DP15 by the presence of a ^{13}C NMR signal at 89.9 ppm, which correlated to a ^{1}H NMR signal at 4.7 ppm by HSQCed (**Figure 2. 13**). This data is consistent with literature values reported for anomeric laminaritriosyl azide[42]. However, this reaction had not gone to completion with approximately 50 % of unreacted hemiacetal remaining, as is evident from ^{13}C NMR signals remaining at 92.1 and 95.8

ppm, correlating to ^{1}H NMR signals at 5.2 and 4.6 ppm, corresponding to unreacted α and β reducing termini, respectively.
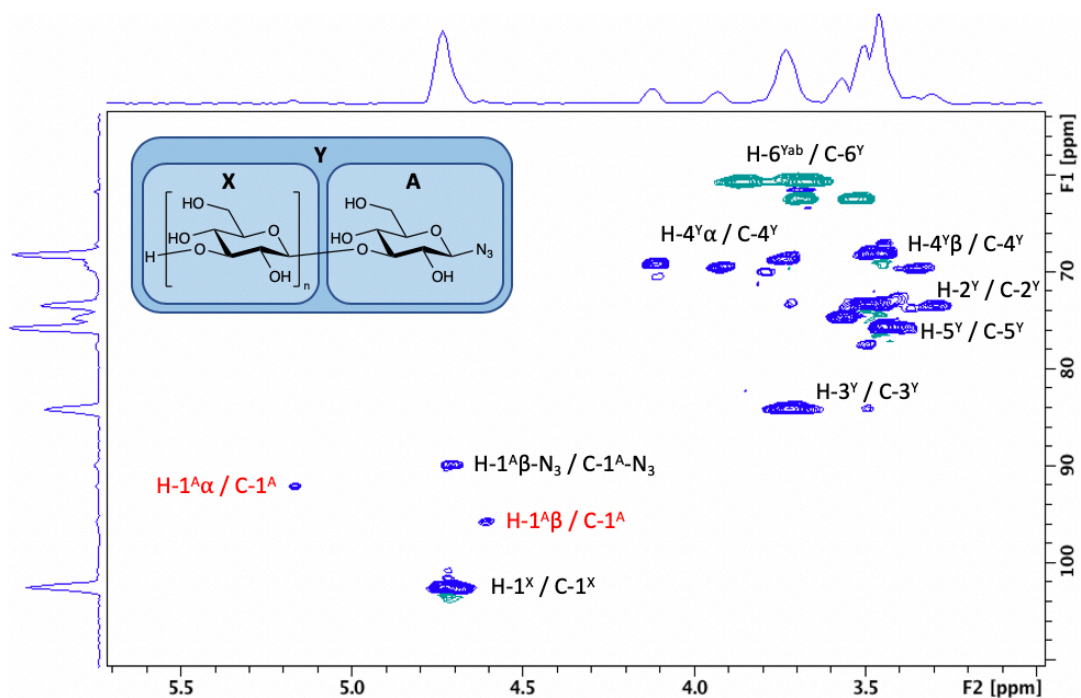
Figure 2. 13 – HSQCed NMR analysis of linear β-(1-3)-glucan DP15 azide. *Diagnostic signal at ^{1}H NMR 4.7 ppm and 13C NMR 89.9 ppm confirms the presence of an anomeric β-azide. ^{1}H NMR signals at 5.2 and 4.6 ppm, correlating to ^{13}C NMR signals at 92.1 and 95.8 ppm show unreacted anomeric α and β hydroxyl groups, respectively, indicating the reaction had not gone to completion. A – reducing glucose residue, X – remaining glucose residues of β-(1-3)-glucan chains, Y – complete β-(1-3)-glucan chains.*

The heterogeneity, average DP of 25-35, and the presence of both G- and M-series made laminarin more challenging to analyse. Although an anomeric β-azide was confirmed by correlating ^{13}C and ^{1}H NMR signals of 89.8 and 4.7 ppm, respectively, it was not possible to detect reducing C-1 position in either the starting material or the azide product, therefore the reaction efficiency could not be determined by NMR (**Figure 2. 14**).
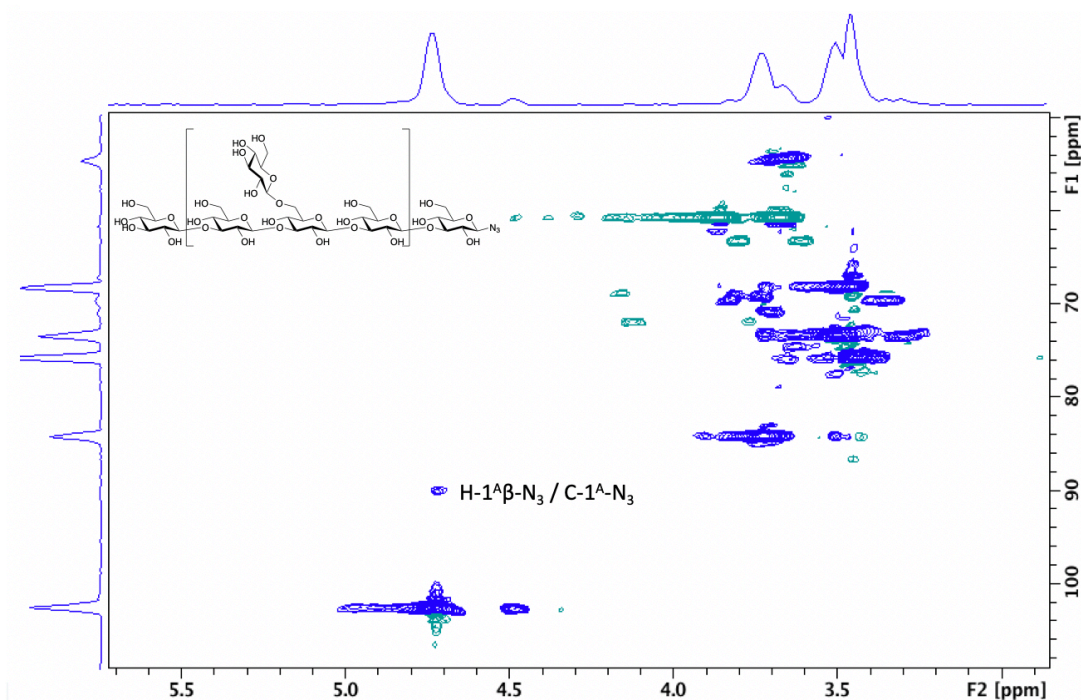
Figure 2. 14 – HSQCed NMR analysis of azide functionalised laminarin. Characteristic signals at ^1H NMR 4.7 ppm and ^{13}C NMR 89.8 ppm confirm the presence of an anomeric β-azide.

Mass spectrometry analysis was unsuccessful at identifying masses for β-(1-3)-glucan DP15 azide and laminarin azide due to the reduction of azide functional groups to amines under MALDI-TOF MS conditions[43].

FTIR analysis was also used as a means of detecting the presence of azide functional groups (**Figure 2. 15**). Characteristic azide shifts at 2122 and 2120 cm^{-1} can be seen in the spectra for DP15 azide (**Figure 2. 15 B**) and laminarin azide (**Figure 2. 15 C**), respectively, which are absent in the spectra for DP15 (**Figure 2. 15 A**) and laminarin (**Figure 2. 15 B**) starting materials.
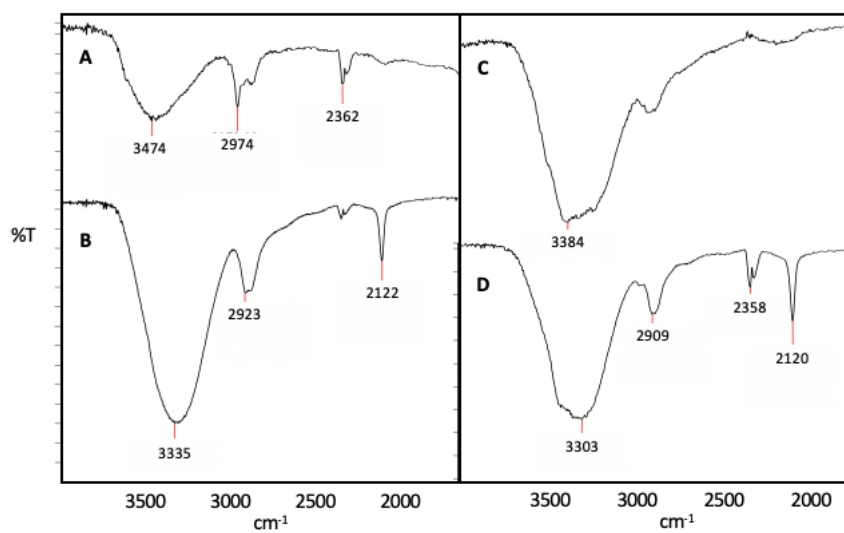
Figure 2. 15 – FTIR analysis of (A) DP15 linear β-(1-3)-glucans, (B) azide functionalised DP15, (C) laminarin, and (D) azide functionalised laminarin.

2.2.5. Alkyne functionalisation of BSA and conjugation of glucans via click chemistry

The amino acid sequence of BSA reveals the presence of 59 lysine residues, 30-35 of which are exposed for conjugation[44]. Introduction of a strained-ring bioorthogonal alkyne functionalised with an NHS-ester allows for selective reactivity to exposed amines to readily incorporate a reactive alkyne for conjugation through click chemistry, the mechanism for which is illustrated in **Scheme 2. 9**.
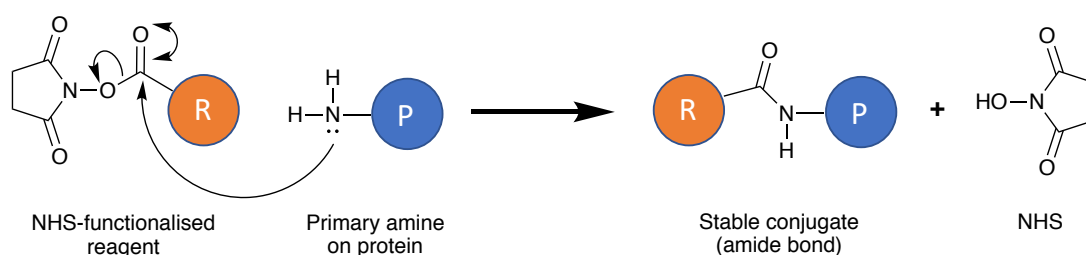
Scheme 2. 9 – Reaction mechanism for conjugation to primary amines via NHS-esters.

BSA was functionalised with (1*R*,8*S*,9*S*)-bicyclo[6.1.0]non-4-yn-9-ylmethyl *N*-succinimidyl carbonate (BCN-NHS), as outlined in **Scheme 2. 10a**.
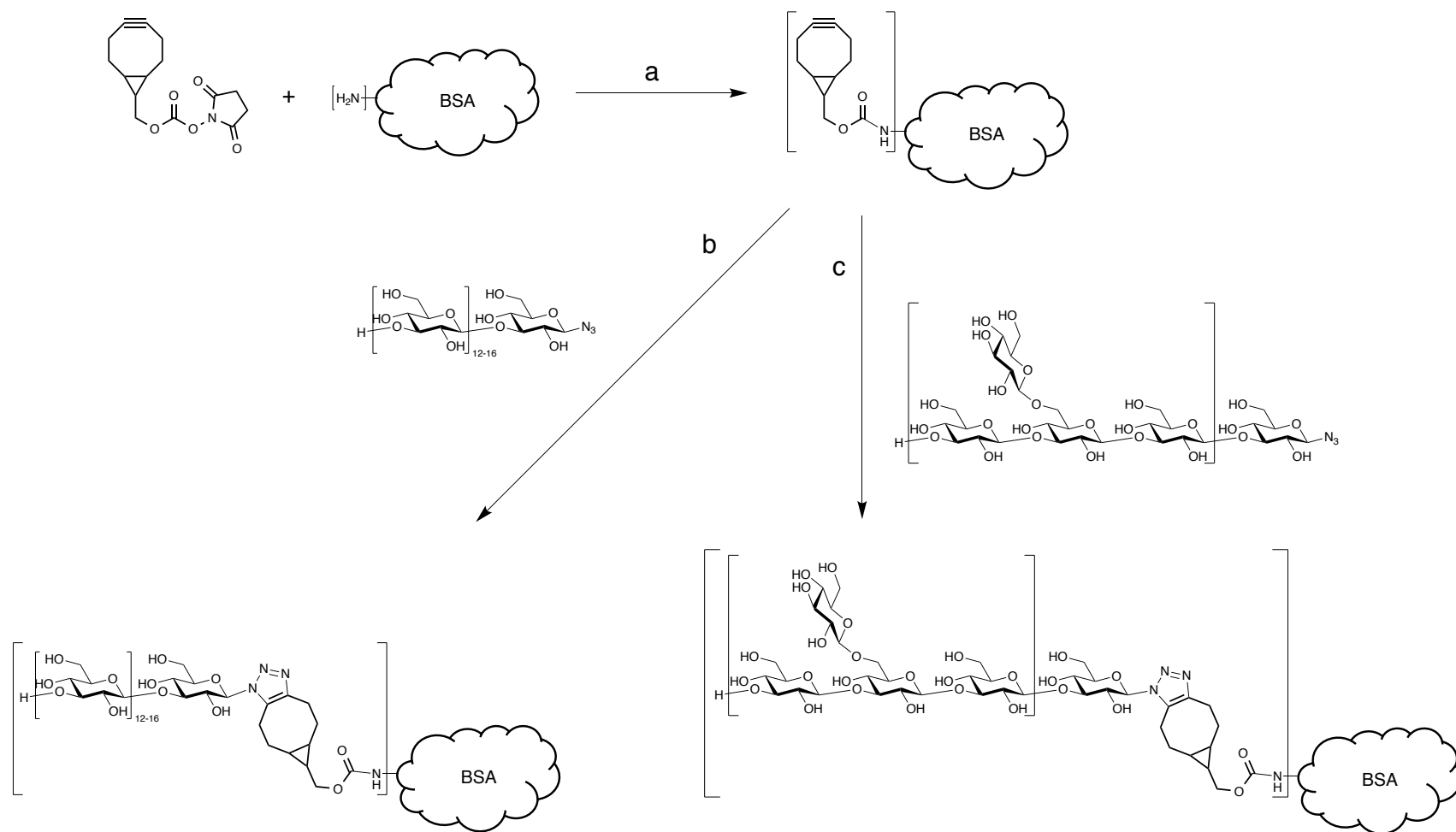
Scheme 2. 10 – Functionalisation of BSA with BCN-NHS and conjugation to β-(1-3)-glucan address tags. *Reagents and conditions: a) BSA (2 mg ml⁻¹), BCN-NHS (10 μL at 0.15 M in DMSO), PBS, 1 h, RT; b) DP15 azide/BCN-BSA (2:1) in PBS, 18 h, RT; c) laminarin azide / BCN-BSA (5:1) in PBS, 18 h, RT. n = 7-10.*

The dual functionality of the BCN-NHS linker allows for specific reactivity via both the strained-ring cyclooctyne to azides, and the NHS ester to exposed amines. The optimal degree of BCN loading on BSA was determined by reacting 5x, 10x, 20x and 30x molar excess of BCN-NHS to BSA. As shown in **Table 2. 1**, molar excess of BCN-NHS of 20x and greater resulted in protein precipitation due to changes to the isoelectric point of the protein. To maintain the solubility of BSA, a 10x molar excess of BCN-NHS to BSA was used.

Table 2. 1 – Table of BSA functionalisation optimisation. See Appendices 6. 7 for MALDI-TOF/MS spectra.

Conjugate		m/z (Da)	Degree of conjugation
BSA		66379	0
Molar excess of BCN-NHS to BSA	5x	67315	5.3
	10x	68304	10.8
	20x	Precipitate	ND
	30x	Precipitate	ND

Excess BCN-NHS reagent was quenched by the addition of Tris and removed by dialysis against PBS. BCN-functionalised BSA was analysed by SDS-PAGE (**Figure 2. 16**) and MALDI-TOF/MS (**Figure 2. 17**) to reveal an average of 9 linkers per protein (**Table 2. 2**).
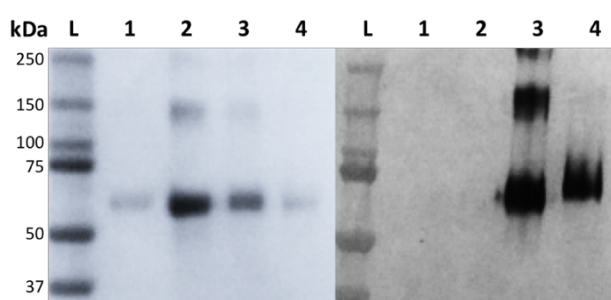
Figure 2. 16 – Characterisation of BSA conjugates by SDS-PAGE (left) and western blot (right). Lane L – ladder; lane 1 – BSA; lane 2 – BSA-linker; lane 3 – BSA-linker-DP15; lane 4 – BSA-linker-laminarin. SDS-PAGE (left) was run on a 12 % SDS gel at 200 V for 60 minutes at 4 ℃ before staining with Coomassie. Western blot (right) was transferred onto nitrocellulose membrane at 100 V for 1 hour at 4 ℃ before blocking with 1 % milk powder in PBST and probing with a mouse anti-β-(1-3)-glucan mAb and subsequent probing with a goat anti-mouse HRP secondary antibody.
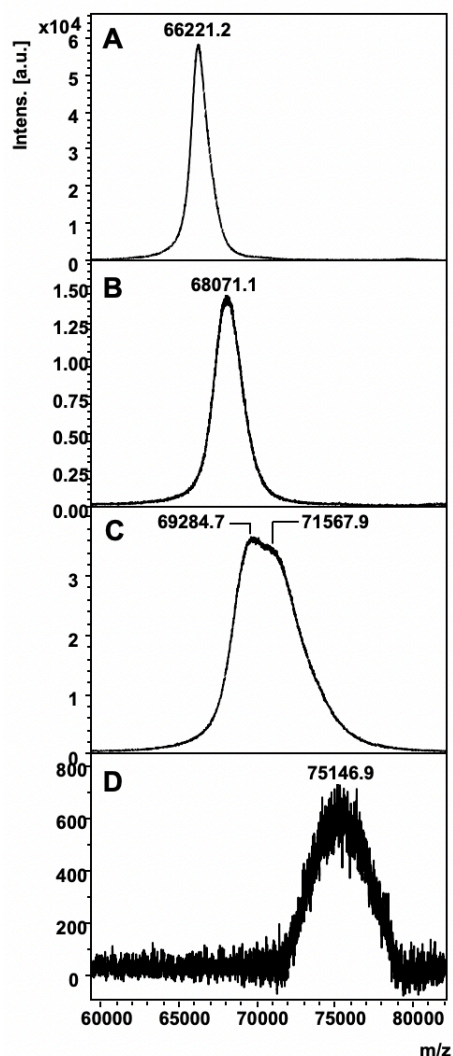
Figure 2. 17 – MALDI-TOF/MS analysis of BSA conjugates. A) Native BSA, m/z 66430 Da calculated, m/z 66221.2 Da found; B) BSA-BCN, m/z 68104 Da calculated, m/z 68071.1 Da found; C) BSA-BCN-DP15, m/z 71567 Da calculated, m/z 69284.7 Da and 71567.9 Da found; D) BSA-BCN-laminarin, m/z 75104 Da calculated, m/z 75146.9 Da found.

Copper-free click chemistry is an efficient and clean method for coupling molecules together. The lack of a copper catalyst not only allows for a faster and cleaner work up, but also makes the product safe for use in *in vivo* studies. Beta glucan address tags, DP15 azide and laminarin azide, were reacted with BCN-functionalised BSA using a 2x and 5x molar excess of glucan per mole of protein, respectively. Laminarin azide was reacted in a 5x molar excess to compensate for the mixed G- and M-series present. Analysis of the BSA conjugates by SDS-PAGE (**Figure 2. 16 left**) did not reveal whether successful conjugation has occurred, as the 12 % SDS gel used did not

provide adequate resolution. A gradient gel may have increased the resolution of conjugates, providing a clearer indication. However, analysis of the conjugates by Western blot revealed successful conjugation of DP15 azide and laminarin azide to BCN functionalised BSA when probed with a mouse anti-β-(1-3)-glucan mAb (**Figure 2. 16 right**).

Successful conjugation was further confirmed by MALDI-TOF/MS analysis (Figure 2. 17), revealing the introduction of an average of 1.4 and 2 glucan chains for DP15 azide and laminarin azide, a conjugation efficiency of 70 % and 40 % respectively (**Table 2. 2**), as determined by differences in mass between BSA-β-glucan conjugates and BCN functionalised BSA, divided by the mass of the corresponding β-glucan azide.

Table 2. 2 – Summary of β-(1-3)-glucan conjugation to BSA

Glycoconjugate	Molar excess*	Average conjugation per protein molecule	Conjugation efficiency (conjugate/molar excess) x100
BSA-BCN	10	9.4	94 %
BSA-BCN-DP15	2	1.4	70 %
BSA-BCN-Laminarin	5	2.0	40 %

*The top half of the table (above the double line) corresponds to the conjugation of BCN to BSA, below the double line corresponds to the conjugation of β-(1-3)-glucan DP15 and laminarin to BCN functionalised BSA. * = molar excess is the ratio between the moles of conjugate used per mole of protein.*

Although the efficiency of laminarin conjugation appears low at 40 %, this is in part due to the presence of M-series laminarin which lacks a reducing terminus. Peak broadening is characteristic for conjugations of this nature due to a number of factors, including the heterogenicity of chain lengths, the number of branch points (in the instance of laminarin)[45] along with the range of conjugated lysine residues.

Figure 2. 17 C shows splitting of the mass peak, suggesting the click reaction for DP15 azide was more efficient on a select portion of BCN-functionalised BSA. As the formation of DP15 azide did not go to completion (**Figure 2. 13**), DP15 azide consists of a mixture of reactive azide functionalised and unreactive hydroxyl groups at the reducing terminus, therefore only a portion (approximately 50 %) of this is able to react with the strained-ring alkynes on BCN-functionalised BSA. Conducting the click reaction prior to conjugation may have provided better control over the reaction and yielded a more uniform product. It was therefore concluded that the conjugation reaction was deemed sufficiently successful for this purpose, however, other conjugation techniques need to be explored for greater efficiency.

The BSA conjugates prepared herein were subsequently used to determine their ability to induce a Dectin-1-mediated signalling response, as discussed in **Section 2.2.6.**

2.2.6. The ability of β-(1-3)-glucans to induce a Dectin-1-mediated signalling response

The ability of β-(1-3)-glucan address tags to initiate a Dectin-1-mediated signalling response was determined by use of a Dectin-1 expressing reporter cell assay (**Figure 2. 1**). BSA conjugates were bound to the surface of 96-well ELISA plates and blocked with milk powder. The BWZ.36 reporter cell line[18], either Dectin-1 expressing, or a mock cell line which lacks expression of this receptor, were then applied. Upon successful binding to Dectin-1, β-galactosidase is produced as a result of CD3ς signalling inducing the IL-2 promoter leading to transcription of the *lacZ* gene and production of β-galactosidase. Addition of the substrate CPRG containing 2-mercaptoethanol causes cell lysis and allows binding efficiency to be determined via colorimetric detection as cleavage of the glycosidic linkage by β-galactosidase results in a colour change from yellow to red, as outlined in **Scheme 2. 11**.

Chlorophenol red β-D-galactopyranoside (CPRG)

β-galactosidase

Galactose   **Chlorophenol red**
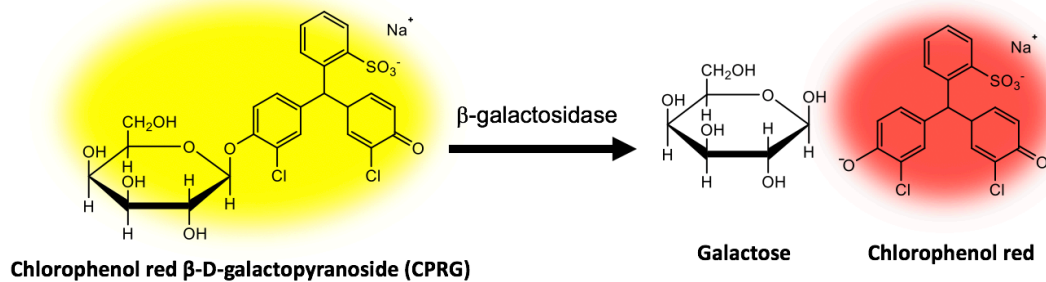
Scheme 2. 11 – Schematic representation of reporter assay detection method: β-galactosidase activity on CPRG leading to a colour change from yellow to red.

BSA conjugated with either β-(1-3)-glucans with an average DP of 15, or laminarin, allowed us to investigate whether the DP12 β-(1-3)-glucan ligand reported in the literature as being required for binding to Dectin-1 is able to initiate a Dectin-1-mediated signalling response. Curdlan, the parent molecule from which the linear β-(1-3)-glucans used in this study were derived, showed a strong binding response when treated with Dectin-1 expressing reporter cells (**Figure 2. 18**). In addition, laminarin, which has been reported to act as both a Dectin-1 agonist and antagonist[46], was also able to induce a significant signalling response of 0.25x the strength of that initiated by curdlan. Lack of a response from the mock cell line when exposed to all of the ligands tested in this assay demonstrates that the responses seen are a result of ligand-Dectin-1 interactions.
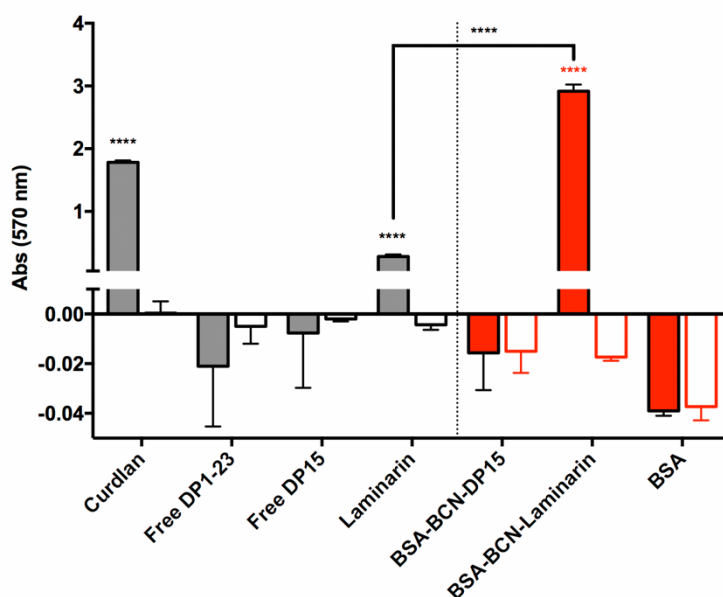
Figure 2. 18 - Dectin-1 reporter cell assay of free-sugars and glycoconjugates. *Filled bars represent Dectin-1 reporter cells, white bars represent mock reporter cells. Black borders represent free-sugar ligands, red borders represent BSA-conjugates. Error bars show standard deviation. Statistical analysis shows one-way ANOVA with post-hoc Sidak's multiple comparison test (P <0.0001 = ****).*

It is proposed that Dectin-1-mediated signalling responses occur as a result of receptor clustering on the cell surface to form a phagocytic synapse[14]. The insoluble, particulate nature of curdlan contributes to Dectin-1 clustering[14], leading to a strong binding response by the reporter cell assay. The ability of laminarin to initiate a signalling response suggests that branching and not just molecular size may play an important role in Dectin-1-mediated signalling. Studies have demonstrated that a single branch point inserted onto synthetic β-(1-3)-glucan nonasaccharide (29 μM) significantly enhanced the binding affinity to Dectin-1 in comparison to linear nona- (2.6 mM) and deca-saccharides (0.8 mM), with laminarin showing a strong binding capacity (22 nM)[47].

Interestingly, the linear β-(1-3)-glucan oligosaccharides derived from curdlan, both the mixed DP1-23 β-(1-3)-glucans prior to GPC fractionation and the DP15 dominant fraction, failed to elicit a Dectin-1-mediated signalling response. However, it is possible that these materials do not adhere well to the ELISA plate.

Conjugation of β-(1-3)-glucans to BSA, to ensure their binding to the ELISA plate, (shown by red bars in **Figure 2. 18**) led to a 2.5x increase in signal strength in the case of laminarin conjugates. However, it failed to elicit a response from the case of linear DP15 conjugates, suggesting that the simple linear β-(1-3)-glucan oligosaccharides of this size are not inducers of Dectin-1 signalling, even though they are able to bind to Dectin-1[48].

2.3. Conclusions

This chapter described efforts to generate and assess β-(1-3)-glucan molecular address tags by means of chemical degradation of curdlan. β-(1-3)-glucans of predominantly DP15, and low molecular weight, branched chain laminarin were functionalised with an anomeric azide and coupled to BCN-functionalised BSA via copper-free click chemistry to yield BSA-BCN-DP15 and BSA-BCN-laminarin glycoconjugates. Glycoconjugates were subsequently analysed for their ability to stimulate signalling in a Dectin-1-expressing reporter cell line.

Efforts to generate fragments of β-(1-3)-glucans by partial degradation of curdlan through acetolysis produced an array of acetylated β-(1-3)-glucan fragments. Deprotection with NaOMe yielded 115 mg of β-(1-3)-glucans of DP1-23. Separation of these chains into their individual counterparts is not possible with the technology available today; however, narrowing the average DP was achieved by fractionation using aqueous GPC at 40 °C (to aid solubility).

Utilising bioorthogonal click chemistry to conjugate β-(1-3)-glucan tags to BSA proved to be an efficient means of coupling. Functionalisation of β-(1-3)-glucans with anomeric azides using methodologies outlined by Tanaka and colleagues[41], was selective for the anomeric position in β-configuration. FTIR analysis of both DP15 azide and laminarin azide confirmed the introduction of an azide, with NMR analysis confirming the location at the anomeric position in β-configuration. NMR analysis also revealed the reaction had not gone to

completion for DP15 azide, and lack of adequate resolution of the reducing terminus meant the reaction efficiency for laminarin could not be determined, despite lengthy NMR scans. This one-pot approach of introducing an anomeric azide has many advantages over traditional azide introduction via glycosyl bromides, in that it does not require the use of protecting group chemistry, and does not necessitate the need for multi-stage synthesis. As the reaction is conducted in water, the workup can be carried out by aqueous gel permeation chromatography. However, this method has been optimised in the literature for low molecular weight oligosaccharides up to DP4[41]. In order to improve the efficiency of the reaction on large oligosaccharides of DP15+, further optimisation is required. In the case of this study, sufficient quantities of azide functionalised DP15 and laminarin were generated for further investigation, therefore optimisation was not continued further.

Copper-free click chemistry was employed to conjugate β-glucans to BSA. The use of a strained-ring cyclooctyne linkers allows a spontaneous click reaction to occur with azide-functionalised molecules, eliminating the need of a copper catalyst and making the reaction biocompatible as all by-products are biologically safe and easily removed by dialysis. NHS-functionalised cyclooctynes (BCN-NHS) allowed for convenient functionalisation of BSA via reaction with exposed amines on surface lysine residues. BCN-functionalisation was successful, with an average of 9.4 BCN moieties introduced per mole of BSA, as determined by MALDI-TOF/MS. Conjugation of laminarin azide to BCN-functionalised BSA resulted in average conjugation of 2 laminarin molecules per mole of BSA. Conjugation of DP15 azide to BCN-functionalised BSA appeared uneven, with peak splitting being observed by MALDI-TOF/MS. The reasons for this remains unclear, to ensure an even distribution of conjugation, it may be more efficient to click the azido sugars and linker together prior to coupling to protein. Alternatively, it is feasible to explore the multitude of conjugation methods available to find an alternative reaction allowing more control.

Linear β-glucans of DP12 have previously been shown to bind to Dectin-1[30]; however, the present study shows that a signalling response was not elicited

by β-(1-3)-glucans with an average of DP15, either unconjugated or coupled to BSA. Interestingly, laminarin and its BSA conjugate were able to induce a strong signalling response from the reporter cell line, as was curdlan. This is likely due to the large particles being able to induce Dectin-1 clustering, allowing a phagocytic synapse to be formed[14], as described in **Chapter 1.4.2**. Laminarin is a Dectin-1 antagonist[49], however, a recent report suggests that it is able to act as both a Dectin-1 agonist and antagonist depending on the source from which it is was aquired[46]. The laminarin used in this study was purchased from Sigma (L9634) and was identified as a Dectin-1 agonist by Smith *et al*[46] The ability of laminarin to act as a Dectin-1 agonist holds potential in targeted vaccination therapies and has been utilised in murine vaccines to protect against *C. albicans* and *A. fumigatus* in mouse models[6]. Microscopy studies have also shown co-localisation of fluorescently labelled laminarin-OVA conjugates with fluorescently labelled Dectin-1 expressed on CHO cells[45].

It is also worth noting that a common polymorphism in the human langerin receptor, which changes Lys-313 to isoleucine, abolishes recognition of oligosaccharides with terminal $6SO_4$-Gal residues and enhances binding to oligosaccharides with terminal GlcNAc residues, due to loss of Ca^{2+} ligation[51]. It is, therefore, possible that differences in nucleotide sequences for receptors may lead to differences in ligand recognition between species. In this study, murine Dectin-1 has been used as a model to test the ability of β-(1-3)-glucans to initiate a Dectin-1-mediated signalling response. Murine Dectin-1 shares 61 % sequence similarity with human Dectin-1, as outlined in **Chapter 1.4**, which is worth consideration if β-(1-3)-glucans are to be utilised in vaccines for humans. Expression of soluble murine and human Dectin-1 receptor proteins would allow for differences in binding specificities to be determined. This study has shown that binding is not always sufficient to initiate a signalling cascade, therefore, generation of a reporter cell line expressing human Dectin-1 would be advantageous. Alternatively, isolation of human and murine dendritic cells would allow for comparison of cytokine stimulations upon binding to β-glucan ligands. Future work in these areas would advance research into the use of β-

(1-3)-glucans as MATs and allow vaccination therapies to be tailored to each organism.

In conclusion, generation of linear β-(1-3)-glucan DP15 did not produce a signalling response when either unconjugated or conjugated to BSA, whereas conjugation of laminarin to BSA was able to significantly enhance Dectin-1-mediated signalling responses. The introduction of laminarin on to vaccine therapeutics would give rise to better presentation of antigens on the cell surface, resulting in an enhanced antibody response.

2.4. References

1. Stone, B. A. Chemistry, Biochemistry, and Biology of 1-3 Beta Glucans and Related Polysaccharides. *Academic Press*, 5-47 (2009). doi:10.1016/B978-0-12-373971-1.00002-9

2. Brown, G. D., Taylor, P. R., Reid, D. M., Willment, J. A., Williams, D. L., Martinez-Pomares, L., Wong, S. Y. C. & Gordon, S. Dectin-1 is a major beta-glucan receptor on macrophages. *J. Exp. Med.* **196,** 407–412 (2002).

3. Elsaidi, H. R. H., Paszkiewicz, E. & Bundle, D. R. Synthesis of a 1,3 β-glucan hexasaccharide designed to target vaccines to the dendritic cell receptor, Dectin-1. *Carbohydr. Res.* **408,** 96–106 (2015).

4. Wang, L.-X., Sakairi, N. & Kuzuhara, H. Peracetylated laminaribiose: preparation by specific degradation of curdlan and its chemical conversion into N-acetylhyalobiuronic acid. *Carbohydr. Res.* **219,** 133–148 (1991).

5. Kusama, S., Kusakabe, I., Zama, M., Murakami, K. & Yasui, T. Enzymatic Preparation of Crystalline Laminaribiose from Curdlan. *Agric. Biol. Chem.* **48,** 1433–1440 (1984).

6. Bromuro, C., Romano, M., Chiani, P., Berti, F., Tontini, M., Proietti, D., Mori, E., Torosantucci, A., Costantino, P., Rappuoli, R. & Cassone, A. Beta-glucan-CRM197 conjugates as candidates antifungal vaccines. *Vaccine* **28,** 2615–2623 (2010).

7. Nelson, T. E. & Lewis, B. A. Separation and characterization of the soluble and insoluble components of insoluble laminaran. *Carbohydr. Res.* **33,** 63–74 (1974).

8. Sonck, E., Stuyven, E., Goddeeris, B. & Cox, E. The effect of β-glucans on porcine leukocytes. *Vet. Immunol. Immunopathol.* **135,** 199–207 (2010).

9. Russo, R., Barsanti, L., Evangelista, V., Frassanito, A. M., Longo, V., Pucci, L., Penno, G. & Gualtieri, P. Euglena gracilis paramylon activates human lymphocytes by upregulating pro-inflammatory factors. *Food Sci. Nutr.* **5,** 205–214 (2017).

10. Shih, I.-L., Yu, J.-Y., Hsieh, C. & Wu, J.-Y. Production and characterization of curdlan by Agrobacterium sp. *Biochem. Eng. J.* **43,** 33–40 (2009).

11. Kuhaudomlarp, S., Patron, N. J., Henrissat, B., Rejzek, M., Saalbach, G. & Field, R. A. Identification of Euglena gracilis β-1,3-glucan phosphorylase and establishment of a new glycoside hydrolase (GH) family GH149. *J. Biol. Chem.* **293,** 2865–2876 (2018).

12. Palma, A. S., Feizi, T., Zhang, Y. B. & Stoll, M. S. Ligands for the beta-glucan receptor, Dectin-1, assigned using 'designer' microarrays of oligosaccharide probes (neoglycolipids) generated from glucan polysaccharides. (vol 281, pg 5771, 2006). *J. Biol. Chem.* **281,** 24999 (2006).

13. Huang, H., Ostroff, G. R., Lee, C. K., Wang, J. P., Specht, C. A. & Levitz, S. M. Distinct patterns of dendritic cell cytokine release stimulated by fungal β-glucans and toll-like receptor agonists. *Infect. Immun.* **77,** 1774–1781 (2009).

14. Goodridge, H. S., Reyes, C. N., Becker, C. A., Katsumoto, T. R., Ma, J., Wolf, A. J., Bose, N., Chan, A. S. H., Magee, A. S., Danielson, M. E., Weiss, A., Vasilakos, J. P. & Underhill, D. M. Activation of the innate immune receptor Dectin-1 upon formation of a 'phagocytic synapse'. *Nature* **472,** 471–475 (2011).

15. Jewett, J. C. & Bertozzi, C. R. Cu-free click cycloaddition reactions in chemical biology. *Chem. Soc. Rev.* **39,** 1272–1279 (2010).

16. Spiciarich, D. R., Nolley, R., Maund, S. L., Purcell, S. C., Herschel, J., Iavarone, A. T., Peehl, D. M. & Bertozzi, C. R. Bioorthogonal Labeling of Human Prostate Cancer Tissue Slice Cultures for Glycoproteomics. *Angew. Chem. Int. Ed. Engl.* **56,** 8992–8997 (2017).

17. Hapuarachchige, S., Kato, Y. & Artemov, D. Bioorthogonal two-component drug delivery in HER2(+) breast cancer mouse models. *Sci. Rep.* **6,** 1–10 (2016).

18. Sanderson, S. & Shastri, N. LacZ inducible, antigen/MHC-specific T cell hybrids. *Int. Immunol.* **6,** 369–376 (1994).

19. Lai, Y.-C., Luo, C.-H., Chou, H.-C., Yang, C.-J., Lu, L. & Chen, C.-S. Conversion of β-glycopyranoside to α-glycopyranoside by photo-activated radical reaction. *Tetrahedron Lett.* **57,** 2474–2477 (2016).

20. Ogawa, T. & Kasuragi, T. Synthesis of a branched d-glucotetraose, the repeating unit of the extracellular polysaccharides of Grifola umbellate, Sclerotinia libertiana, Porodisculus pendulus, and Schizophyllum commune fries. *Carbohydr. Res.* **103,** 53–64 (1982).

21. Rao, V. S. & Perlin, A. S. A reversal in the order of H-6R and H-6s chemical shifts of some aldohexopyranose derivatives, associated with the acetylation of OH-4 and OH-6 groups. A distinction between 3-and 4-linked D-glucose residues in disaccharides. *Can. J. Chem.* **61,** 2688–2694 (1983).

22. Gottlieb, H. E., Kotlyar, V. & Nudelman, A. *NMR Chemical Shifts of Common Laboratory Solvents as Trace Impurities.* (1997).

23. Meier, L., Monteiro, G. C., Baldissera, R. A. M. & Sá, M. M. Simple method for fast deprotection of nucleosides by triethylamine-catalyzed methanolysis of acetates in aqueous medium. *J. Braz. Chem. Soc.* **21,** 859–866 (2010).

24. Itoh, T., Takamura, H., Watanabe, K., Araki, Y. & Ishido, Y. A facile procedure for regioselective 1-O-deacylation of fully acylated sugars with sodium methoxide. *Carbohydr. Res.* **156,** 241–246 (1986).

25. Zhang, R. & Edgar, K. J. Properties, chemistry, and applications of the bioactive polysaccharide curdlan. *Biomacromolecules* **15,** 1079–1096 (2014).

26. Nanjo, F., Usui, T. & Suzuki, T. *Mode of Action of an exo-beta-(1-3)-D-Glucanase on the Laminaran from Eisenia bicyclis. Biol. Chem* **48,** (1984).

27. Roslund, M. U., Tähtinen, P., Niemitz, M. & Sjöholm, R. Complete assignments of the 1H and 13C chemical shifts and JH,H coupling constants in NMR spectra of d-glucopyranose and all d-glucopyranosyl-d-glucopyranosides. *Carbohydr. Res.* **343,** 101–112 (2008).

28. Kim, Y.-T., Kim, E.-H., Cheong, C., Williams, D. L., Kim, C.-W. & Lim, S.-T. Structural characterization of β-d-(1→3, 1→6)-linked glucans using NMR spectroscopy. *Carbohydr. Res.* **328,** 331–341 (2000).

29. Kailemia, M. J., Ruhaak, L. R., Lebrilla, C. B. & Amster, I. J. Oligosaccharide analysis by mass spectrometry: a review of recent developments. *Anal. Chem.* **86,** 196–212 (2014).

30. Palma, A. S., Feizi, T., Zhang, Y., Stoll, M. S., Lawson, A. M., Díaz-Rodríguez, E., Campanero-Rhodes, M. A., Costa, J., Gordon, S., Brown, G. D. & Chai, W. Ligands for the β-glucan receptor, dectin-1, assigned using 'designer' microarrays of oligosaccharide probes (neoglycolipids) generated from glucan polysaccharides. *J. Biol. Chem.* **281,** 5771–5779 (2006).

31. Hein, J. E. & Fokin, V. V. Copper-catalyzed azide–alkyne cycloaddition (CuAAC) and beyond: new reactivity of copper(i) acetylides. *Chem. Soc. Rev.* **39,** 1302 (2010).

32. Presolski, S. I., Hong, V. P. & Finn, M. G. Copper-Catalyzed Azide-Alkyne Click Chemistry for Bioconjugation. in *Current Protocols in Chemical Biology,* 153–162 (2011). doi:10.1002/9780470559277.ch110148

33. Meldal, M. & Tornøe, C. W. Cu-Catalyzed Azide−Alkyne Cycloaddition. *Chem. Rev.* **108,** 2952–3015 (2008).

34. Nicholas J. Agard, Jennifer A. Prescher, & Bertozzi, C. R. A Strain-Promoted [3 + 2] Azide−Alkyne Cycloaddition for Covalent Modification of Biomolecules in Living Systems. *J. Am. Chem. Soc.* **126**, 15046-15047 (2004).

35. Pintal, M., Charbonniere-Dumarcay, F., Marsura, A. & Porwański, S. Synthesis of new saccharide azacrown cryptands. *Carbohydr. Res.* **414,** 51–59 (2015).

36. El Meslouti, A., Beaupère, D., Demailly, G. & Uzan, R. One-pot stereoselective synthesis of glycosyl azides via 1,2-cyclic sulfite. *Tetrahedron Lett.* **35,** 3913–3916 (1994).

37. Williams, J. M. Tautomerism of saccharide hydrazones in solution and their reaction with nitrous acid. *Carbohydr. Res.* **117,** 89–94 (1983).

38. Gudmundsdottir, A. V. & Nitz, M. Protecting Group Free Glycosidations Using *p* -Toluenesulfonohydrazide Donors. *Org. Lett.* **10,** 3461–3463 (2008).

39. Banait, N. S. & Jencks, W. P. Reactions of anionic nucleophiles with .alpha.-D-glucopyranosyl fluoride in aqueous solution through a concerted, ANDN (SN2) mechanism. *J. Am. Chem. Soc.* **113,** 7951–7958 (1991).

40. Gouin, S. G. & Kovensky, J. Direct azidation of unprotected carbohydrates with PPh3/CBr4/NaN3. Modulation of the degree of substitution. *Tetrahedron Lett.* **48,** 2875–2879 (2007).

41. Tanaka, T., Nagai, H., Noguchi, M., Kobayashi, A. & Shoda, S. One-step conversion of unprotected sugars to beta-glycosyl azides using 2-chloroimidazolinium salt in aqueous solution. *Chem Commun* **23,** 3378–3379 (2009).

42. García-Viñuales, S., Delso, I., Merino, P. & Tejero, T. Stereoselective Ethynylation and Propargylation of Chiral Cyclic Nitrones: Application to the Synthesis of Glycomimetics. *Synthesis.* **48,** 3339–3351 (2016).

43. Li, Y., Hoskins, J. N., Sreerama, S. G. & Grayson, S. M. MALDI−TOF Mass Spectral Characterization of Polymers Containing an Azide Group: Evidence of Metastable Ions. *Macromolecules* **43,** 6225–6228 (2010).

44. Dammer, U., Hegner, M., Anselmetti, D., Wagner, P., Dreier, M., Huber, W. & Güntherodt, H. J. Specific antigen/antibody interactions measured by force microscopy. *Biophys. J.* **70,** 2437–2441 (1996).

45. Graiff, A., Ruth, W., Kragl, U. & Karsten, U. Chemical characterization and quantification of the brown algal storage compound laminarin — A new methodological approach. *J. Appl. Phycol.* **28,** 533–543 (2016).

46. Smith, A. J., Graves, B., Child, R., Rice, P. J., Ma, Z., Lowman, D. W., Ensley, H. E., Ryter, K. T., Evans, J. T. & Williams, D. L. Immunoregulatory Activity of the Natural Product Laminarin Varies Widely as a Result of Its Physical Properties. *J. Immunol.* **200,** 788–799 (2018).

47. Adams, E. L., Rice, P. J., Graves, B., Ensley, H. E., Yu, H., Brown, G. D., Gordon, S., Monteiro, M. A., Papp-Szabo, E., Lowman, D. W., Power, T. D., Wempe, M. F. & Williams, D. L. Differential High-Affinity Interaction of Dectin-1 with Natural or Synthetic Glucans Is Dependent upon Primary Structure and Is Influenced by Polymer Chain Length and Side-Chain Branching. *J. Pharmacol. Exp. Ther.* **325,** 115–123 (2008).

48. Palma, A. S., Zhang, Y., Childs, R. A., Campanero-Rhodes, M. A., Liu, Y., Feizi, T. & Chai, W. Neoglycolipid-based 'designer' oligosaccharide microarrays to define β-glucan ligands for dectin-1. *Methods Mol. Biol.* **808,** 337–359 (2012).

49. Tang, C., Kamiya, T., Liu, Y., Kadoki, M., Kakuta, S., Oshima, K., Hattori, M., Takeshita, K., Kanai, T., Saijo, S., Ohno, N. & Iwakura, Y. Inhibition of dectin-1 signaling ameliorates colitis by inducing lactobacillus-mediated regulatory T cell expansion in the intestine. *Cell Host Microbe* (2015).

50. Xie, J., Guo, L., Ruan, Y., Zhu, H., Wang, L., Zhou, L., Yun, X. & Gu, J. Laminarin-mediated targeting to Dectin-1 enhances antigen-specific immune responses. *Biochem. Biophys. Res. Commun.* **391,** 958–962 (2010).

51. Feinberg, H., Rowntree, T. J. W., Tan, S. L. W., Drickamer, K., Weis, W. I. & Taylor, M. E. Common polymorphisms in human langerin change specificity for glycan ligands. *J. Biol. Chem.* **288,** 36762–36771 (2013).

# 3. Chapter 3: Antigen generation and immunisation

This chapter discusses the efforts made to generate carbohydrate antigens, conjugation techniques used to generate glycoconjugate vaccines, and immunological assessment of sera by ELISA plate assays.

3.1. Mannose antigens

3.1.1. An introduction into β-(1-2)-mannans as antigens

As discussed in **Chapter 1.5.1**, β-(1-2)-mannosides are an uncommon PAMP present on the surface of pathogen *Candida albicans* and have been chosen as antigens in this chapter. Research suggests antibody recognition is dependent on mannans comprising of a high proportion of β-(1-2)-linkages which corresponding to the antigenic region[1]. Results indicate β-(1-2)-mannan trisaccharide antigens are optimal for antibody binding, with a significant decrease in activity reported for β-(1-2)-mannan tetra-, penta- and hexasaccharides[2], with internal residues proving to be immunodominant epitopes[3], implicating their viability for use as antigens in vaccine conjugates.

Until recently, β-(1-2)-mannoside antigens could only be obtained by isolation from microorganisms[4] or by lengthy protecting group chemistry, involving multiple steps, complex chemistry and toxic reagents[5–8]. Discovery of two β-(1-2)-mannoside phosphorylase enzymes, Teth514_1788 and Teth514_1789, has vastly improved the efficiency to synthesise these compounds[9]. In this thesis, Teth514_1788 was utilised to generate β-(1-2)-mannosides, with emphasis on the generation of tri- and tetra- saccharides (**Figure 3. 1**).

β-(1-2)-mannotriose   **β-(1-2)-mannotetraose**
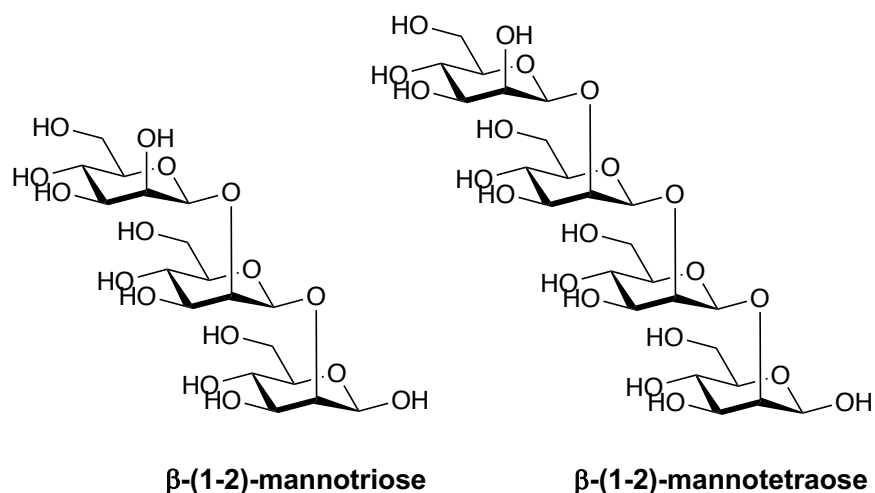
Figure 3. 1 – Structure of β-(1-2)-mannotriose and β-(1-2)-mannotetraose oligosaccharides.

Immunisation trials of glycoconjugate vaccines consisting of β-(1-2)-mannotriose antigens have reported a robust antibody response in immunised rabbits, with trisaccharide IgG ELISA titres in excess of 1:100,000[10]. Although it has been reported that antibody binding to β-(1-2)-mannotetraose is significantly weaker when compared with β-(1-2)-mannotriose[2], to the best of our knowledge, the immunological effects of β-(1-2)-mannotetraose in response to immunisation with β-(1-2)-mannotetraose have not yet been investigated. As previously mentioned, β-(1-2)-mannotriose has been shown to be optimal for antibody binding, with internal mannose residues proving to be the immunodominant epitopes. Using β-(1-2)-mannotetraose as an antigen in vaccination studies is a strong candidate for improved antibody responses due to an internal β-(1-2)-mannotriose epitope. In order to investigate the ability of β-(1-2)-mannotetraose as a carbohydrate antigens, this thesis set out to generate both β-(1-2)-mannotriose and -tetraose antigens for use in immunisation trials.

3.1.1.1. Tetanus toxoid as a protein carrier

Carbohydrates are often not immunogenic on their own, making them poor antigens. Their immunogenicity can be enhanced by coupling to an immunogenic carrier proteins, such as keyhole limpet haemocyanin (KLH)[11], non-toxic diphtheria toxin CRM197[12] and virus-like particles[13]. Tetanus Toxoid, a potent neurotoxin produced by *Clostridium tetani*, is also an effective carrier protein[14], consisting of both a heavy chain (100 kDa) and a light chain (50 kDa). Mild enzymatic cleavage with papain yields two major polypeptides, the smaller of which forming the carrier protein, TetHc. Conjugation of synthetic β-(1-2)-mannotriose to TetHc improved the immunogenicity compared with native *Candida* cell wall antigen, with average titres in excess of 180,000 and 40,000, respectively[10]. The high immunogenicity and low toxicity of TetHc make it an appealing option for a vaccine carrier[15]. Expression of TetHc at high levels in *E. coli* has been reported[16], allowing sufficient quantities to be generated with ease. The presence of 33 lysine (**Figure 3. 2**) residues allow for conjugation of antigens[17].
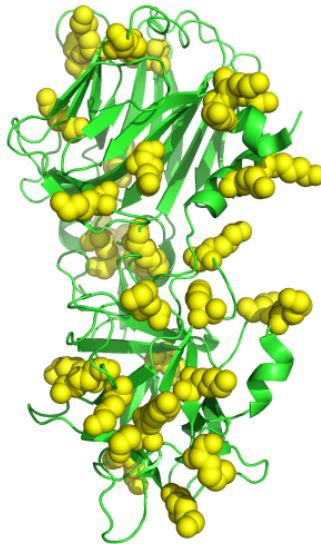
Figure 3. 2 – The structure of tetanus toxoid heavy chain fragment with lysine residues highlighted in yellow.

3.1.1.2. Conjugation chemistry

Conjugation chemistry is an extensive research area, with numerous methods available for a multitude of applications[18]. As previously discussed (**Chapter 2.1.2**), bifunctional linkers allow two different conjugation methods to be used, making them ideal for use in conjugate vaccines. In this chapter, methyl 5-hexynoate, was employed for conjugation (**Figure 3. 3**), allowing azide functionalised antigens to be reacted with the linker via click-chemistry prior to protein conjugation through derivatisation of the methyl ester.
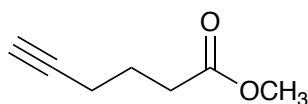
Figure 3. 3 – Structure of methyl 5-hexynoate linker.

β-(1-2)-Mannotriose and β-(-1-2)-mannotetraose oligosaccharides were functionalised with anomeric azides[19] and coupled to methyl 5-hexynoate via copper-catalysed click chemistry[20]. This methodical approach allows characterisation of the molecules at each step of the synthesis, and complete removal of excess reagents prior to exposure to the protein carrier. Conversion of the methyl ester to an acyl azide *in situ* allows conjugation to carrier proteins via the exposed amines on lysine residues[21,22], as outlined in **Scheme 3. 1**.
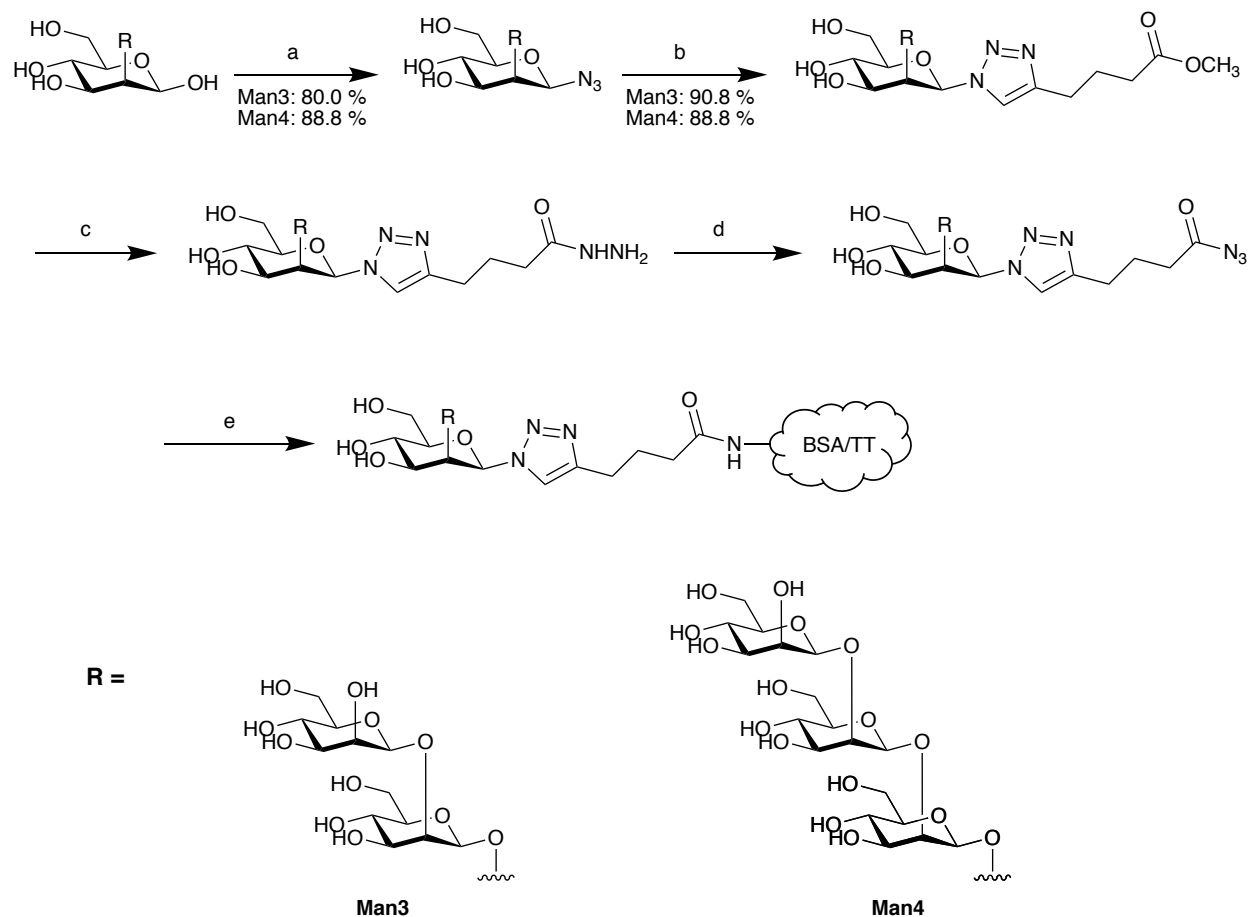
Scheme 3. 1 – Synthesis of β-(1-2)-mannan glycoconjugates via hydrazide chemistry. *Reagents and conditions: a) DMC (5 eq), DIPEA (15 eq), NaN$_3$ (2.5 M) in D$_2$O (0.5 mL) at RT for 3 hrs; b) methyl 5-hexynoate (5 eq), CuSO$_4$ (0.1 eq), NaASc (0.2 eq), THPTA (10 mM), water/t-butanol (1:10) at 50 °C for 16 hr; c) hydrazine monohydrate (1 mL), ethanol (2.5 mL) at 55 °C for 6 hr; d) DMF (1 mL), 4 M HCl in dioxane (9.5 μL), tert-butyl nitrite (1.6 μL) at -25 °C under nitrogen for 15 mins; e) Sulfamic acid (100 μL at 7.4 mg mL^{-1}), -25 °C – 0 °C, protein solution (2 mg mL^{-1} in Borax Buffer) at 4 °C for 36 hr.*

3.1.2. Results and Discussion

3.1.2.1. Expression of TETH514_1788, a β-(1,2)-mannose phosphorylase

Enzymatic synthesis of β-(1-2)-mannosides was performed with Teth514_1788, a β-(1,2)-mannoside phosphorylase enzyme capable of the synthesis and hydrolysis of β-(1,2)-mannosides[9]. *E. coli* Rosetta (DE3) cells transformed with pET24a (+) Teth514_1788 were a kind gift from Josef Voglmeir. Expression of the protein was carried out as outlined by Chiku *et al*[9], as described in **Chapter 5.3.1.** Analysis of Teth514_1788 performed by SDS-PAGE (**Figure 3. 4 A**) revealed the presence of a large band around 35 kDa in the induced soluble fraction (**Figure 3. 4 A - lane 4).** Affinity chromatography purification revealed the large band to be comprised of a band at 35 kDa and a marginally smaller band at 34 kDa (**Figure 3. 4 A – lanes 5-11)**, both corresponding with the Teth514_1788 control in lane 12.
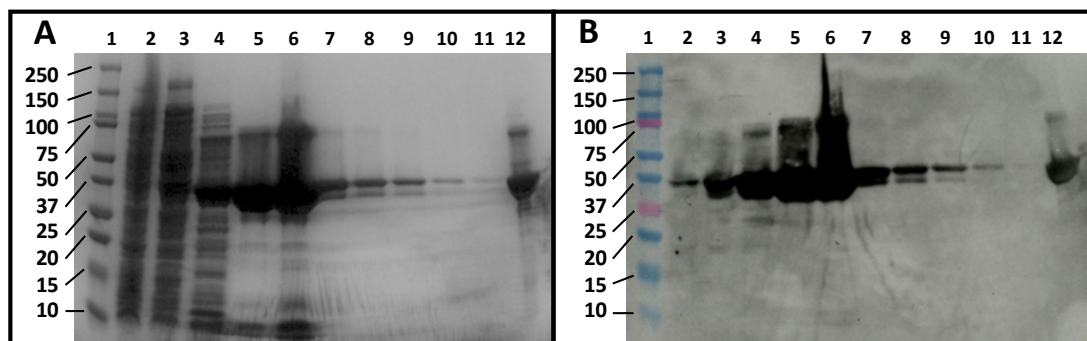
Figure 3. 4 – Characterisation of expressed Teth514_1788 by SDS-PAGE (A) and western blot (B). Gels were run at 200 V for 60 mins on a 12 % SDS-PAGE gel followed by staining with Coomassie to detect protein. Western blot was probed with a mouse anti-His primary antibody and a goat anti-mouse HRP conjugate secondary antibody. Lane 1 – Ladder; lane 2 – non-induced; lane 3 – induced, insoluble fraction; lane 4 – induced, soluble fraction; lanes 5-11 – AKTA fractions 1-7; lane 12 – Teth514_1788 standard.

Western blot analysis (**Figure 3. 4 B**) confirmed the expressed proteins contain a His-tag when probed with a mouse anti-His primary antibody and developed with a goat anti-mouse HRP conjugate secondary antibody. Expression of the His-tagged protein can be seen across all lanes of the blot,

including in a non-induced culture (**Figure 3. 4 B - lane 2**) and in the insoluble fraction of an induced culture (**Figure 3. 4 B - lane 3**), suggesting that 'leaky expression' of the protein is occurring. Intense bands can be seen in the induced soluble fraction (**Figure 3. 4 B - lane 4**) and across AKTA fractions 1-7 (**Figure 3. 4 B - lane 5-11**), with the bands corresponding to the Teth514_1788 control in lane 12. The data obtained by western blot is consistent with that of SDS-PAGE gel analysis (**Figure 3. 4 A**). A total of 124.5 mg of Teth514_1788 was produced from 2 L of culture, as determined by Bradford assay (**Appendices 6. 8**).

The theoretical mass of His-tagged Teth514_1788 was calculated as 35085.2 Da. MALDI-TOF/MS analysis of purified Teth514_1788 revealed a mass of 35003.3 Da (**Figure 3. 5**), confirming the expressed protein is the correct mass for His-tagged Teth514_1788.
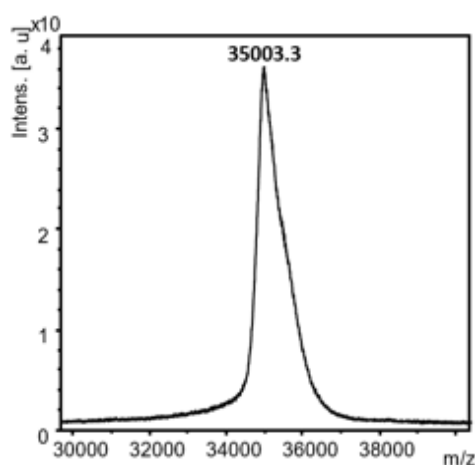
Figure 3. 5 – MALDI-TOF/MS of purified Teth514_1788. Calculated mass = 35085.2 Da, mass found = 35003.3 Da.

3.1.2.2. Synthesis of β-(1,2)-manno-oligosaccharides

Enzymatic synthesis of oligosaccharides allows fast, linkage specific generation of complex carbohydrates, a huge advantage over chemical synthesis. To date, access to β-(1-2)-manno-oligosaccharides has relied on either isolation from microorganisms, or multistep chemical synthesis[5,6,23,24].

Teth514_1788 was used to enzymatically synthesise β-(1-2)-manno-oligosaccharides, as shown in **Scheme 3. 2**.
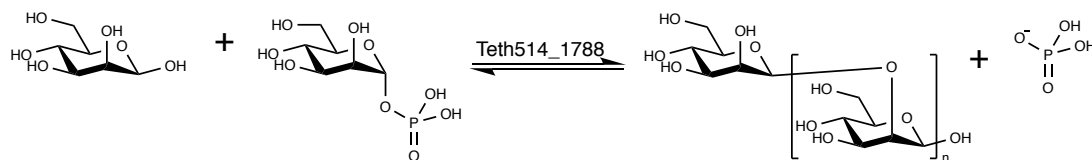
Scheme 3. 2 – Enzymatic synthesis of β-(1-2)-mannans catalysed by a β-(1-2)-mannose phosphorylase. Reagents and conditions: mannose, mannose-1-phosphate (4 eq), 0.1 M ammonium acetate (pH 5.0), 30 ℃, 6 hr.

Optimisation of the reaction revealed 2 mM mannose, 8 mM mannose-1-phosphate, Teth514_1788 (10 mg mL^{-1}) in 0.1 M ammonium acetate buffer (pH 5.0) at 30 °C for 6 hr was adequate to generate oligosaccharides, as confirmed by TLC (**Figure 3. 6**),
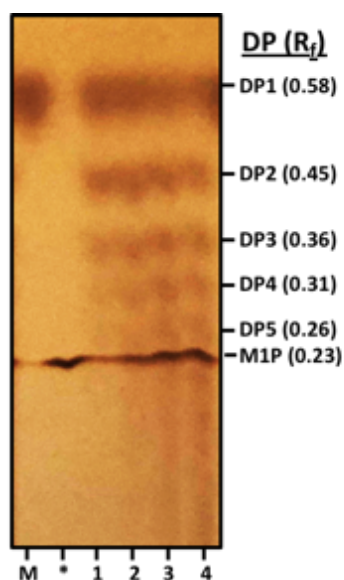
*Figure 3. 6 – Enzymatic synthesis of β-(1-2)-mannosides analysed by TLC. Solvent system: ButOH/EtOH/H$_2$O (10:8:7). M = mannose, * = mannose-1-phosphate, 1 = M:* (1:1), 2 = M:* (1:2), 3 = M:* (1:3), 4 = M:* (1:4). TLC developed using orcinol spray and charring.*

Teth514_1788 was removed from the reaction solution by heating, to precipitate proteins, and filtration through a 0.22 μm filter to remove protein precipitates. The resulting oligosaccharides were analysed by HPAEC-PAD, as outlined in **Chapter 5.1.3**. Injection of mannose on a CarboPac PA100 column revealed a retention time of 3.7 minutes (**Figure 3. 7 A**), which allowed for peak assignment of oligosaccharides from DP1 to DP8 at 15.9 min within the enzymatic reaction mixture (**Figure 3. 7 C**). Injection of a mannose-1-phosphate standard confirmed a retention time of 16.2 min (**Figure 3. 7 B**). Although further oligosaccharides were eluted after this time, peak assignment could not be clearly attributed. It is possible that Teth514_1788 is able to use M1P as an acceptor, and that these signals are a result of mannose oligosaccharides terminated with mannose-1-phosphate. It is also possible that Teth514_1788 is not as selective for the β-(1-2)-linkage as initially thought, and the unidentified peaks are mannose oligosaccharides with linkages other than β-(1-2).
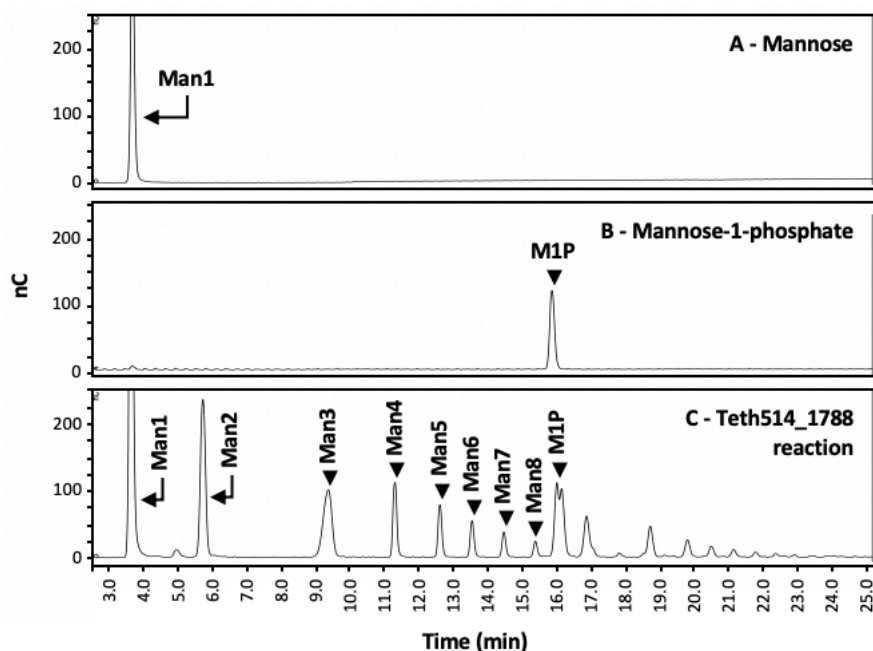
*Figure 3. 7 – HPAEC-PAD analysis of mannose (A), mannose-1-phosphate (B) and enzymatically synthesised β-(1-2)-mannosides (C). Analysis was performed as outlined in **Chapter 5.3.2**. For retention times, see **Appendices 6. 9**.*

Buffer salts and excess M1P were removed from solution by passing the oligosaccharide mixture through an activated charcoal/Celite (50:50) column. Carbohydrates are retained within the lattice structure of the charcoal column, allowing functionalised carbohydrates, such as M1P, and salts to pass straight through. Oligosaccharides are then eluted from the column by washing with 95 % ethanol. Concentration of the ethanol fraction yielded 45 mg of mixed oligosaccharides. Analysis by HPAEC-PAD confirmed the presence of DP1-8 with a small number of minor peaks eluting after Man8 (**Figure 3. 8**).
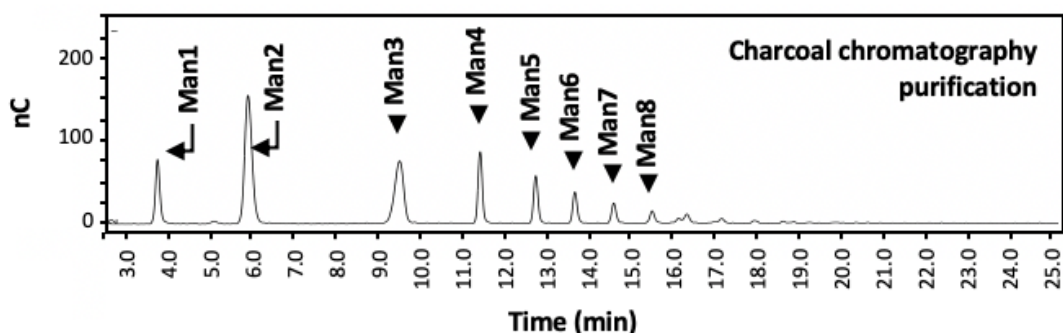
Figure 3. 8 – HPAEC-PAD analysis of β-(1-2)-mannosides purified on a charcoal/celite (1:1) chromatography column. For table of retention times, see Appendices 6. 9.

Oligosaccharide masses were determined by MALDI-TOF/MS and were consistent with the calculated masses for sodium adducts of DP3-12 (**Figure 3. 9**). Matrix interference up to 400 Da did not allow for adequate resolution of m/z signals within this region, therefore the presence of DP1 and DP2 could not be confidently determined by MALDI-TOF/MS.
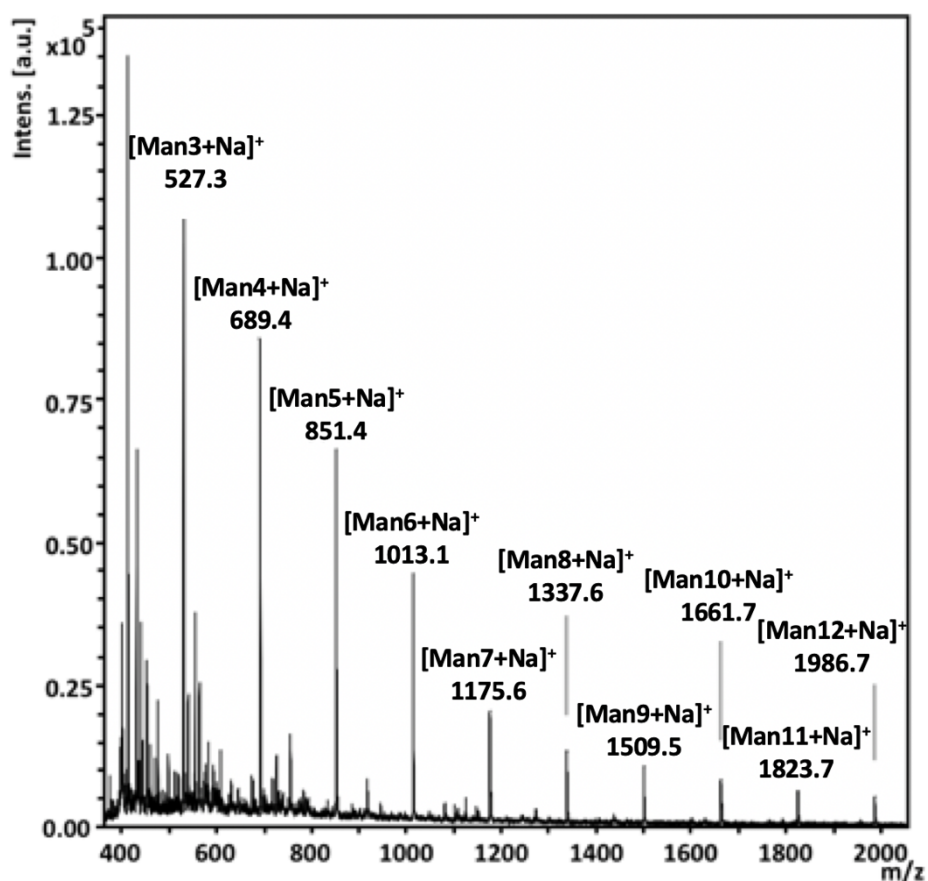
Figure 3. 9 – MALDI-TOF/MS analysis of enzymatically synthesised β-(1-2)-mannosides. *For table of masses, see **Appendices 6. 10**.*

3.1.2.3. Isolation of β-(1-2)-mannotriose and β-(1-2)-mannotetraose oligosaccharides

The solubility of β-(1-3)-glucans in water allowed β-(1-2)-mannotriose and β-(1-2)-mannotetraose to be isolated via gel permeation chromatography. A Biogel P2 column (2.5 x 90 cm) was used in water with a flow rate of 0.5 mL min^{-1}. Fractions were collected at 6 minutes intervals between 320 and 800 minutes (**Figure 3. 10**). Fractions were analysed by HPAEC-PAD (**Appendices 6. 11**) and TLC (**Appendices 6. 12**) to determine the oligosaccharides.
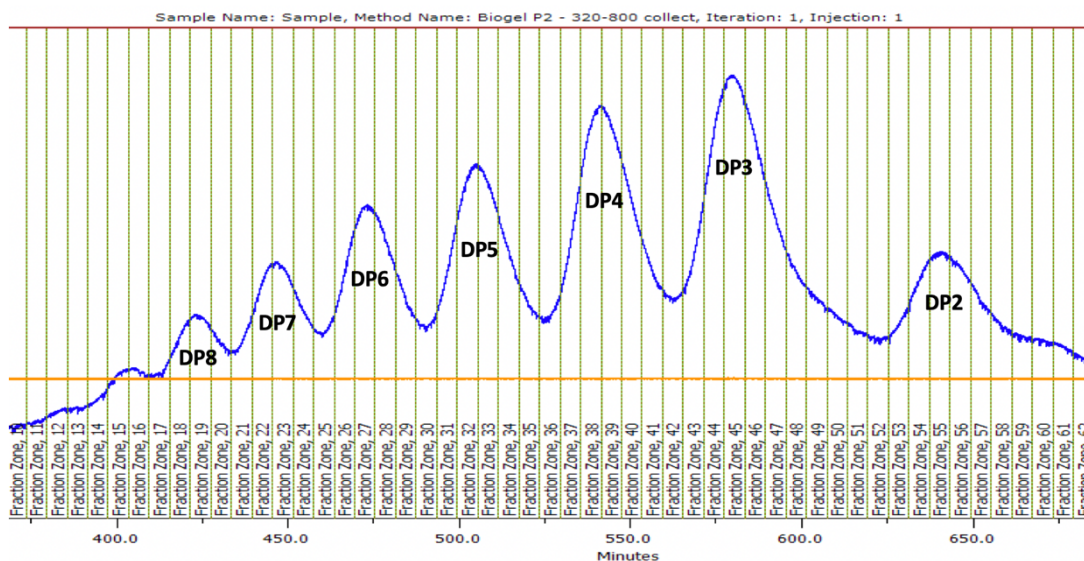
Figure 3. 10 – Seperation of β-(1-2)-mannosides (15) by gel permeation chromatography. GPC was performed using a Biogel P2 column (2.5 x 90 cm) with an aqueous mobile phase at 0.5 mL min⁻¹. Fractions were collected every 6 minutes from 320 to 800 mins.

Fractions containing exclusively β-(1-2)-mannotriose (fractions 43-49) were pooled together, as were fractions containing exclusively β-(1-2)-mannotetraose (fractions 36-41). Following lyophilisation, yields of 6.2 mg and 5.3 mg were recorded for β-(1-2)-mannotriose and β-(1-2)-mannotetraose, respectively. TLC analyses confirmed the samples contained exclusively either β-(1-2)-mannotriose (R_f 0.36) or β-(1-2)-mannotetraose (R_f 0.31), as shown in **Appendices 6. 13**.

HPAEC-PAD analysis also confirmed the homogeneity of the samples, with peaks at retention times 9.8 and 11.7 min for β-(1-2)-mannotriose and β-(1-2)-mannotetraose, respectively (**Figure 3. 11**).
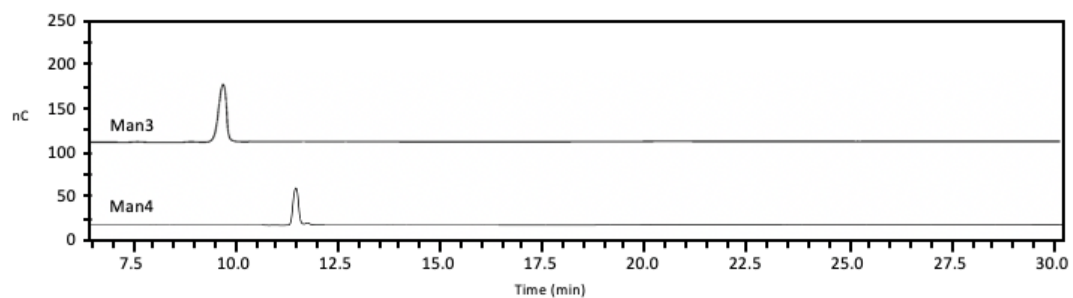
Figure 3. 11 – HPAEC-PAD analysis of β-(1-2)-mannose oligosaccharides. For table of retention times, see **Appendices 6. 11**.

Electrospray ionisation-mass spectrometry (ESI-MS) analysis was chosen to perform mass analysis of β-(1-2)-mannotriose and β-(1-2)-mannotetraose as oppose to MALDI-TOF/MS were matrix interference results in low mass resolution up to approximately 700 Da. ESI-MS confirmed the presences of a mass at 526.9 Da, consistent with the calculated mass for [β-(1-2)-mannotriose+Na]$^+$ (**Figure 3. 12 A**). The mass for β-(1-2)-mannotetraose was also confirmed by the presence of a masses at 688.8 and 689.5 Da, consistent with the calculated masses for Na adducts and ^{13}C Na adducts of β-(1-2)-mannotetraose and β-(1-2)-mannotetraose, respectively (**Figure 3. 12 B**).
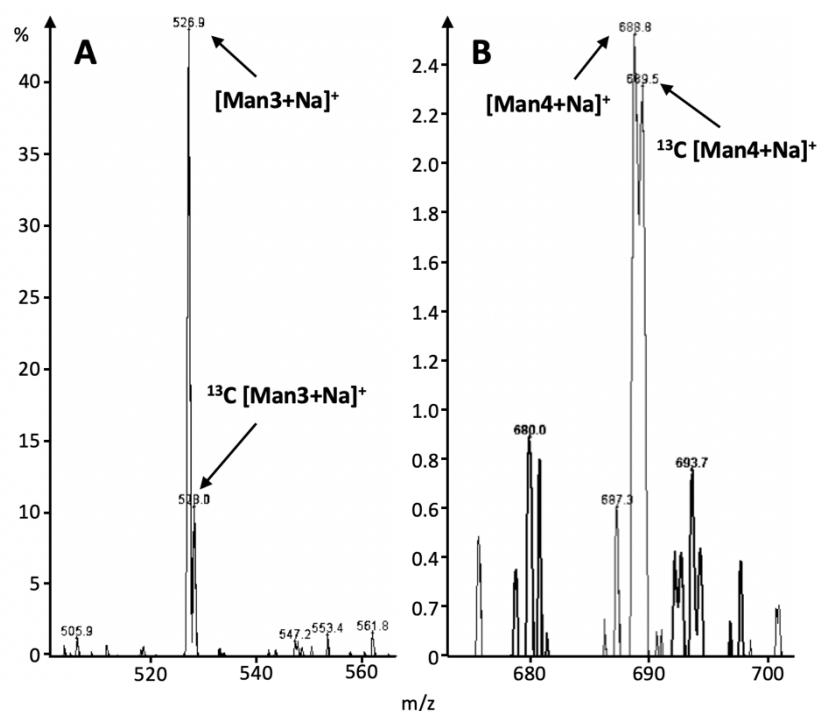
Figure 3. 12 – ESI-MS analysis of DP3 β-(1-2)-mannotriose (A) and β-(1-2)-mannotetraose (B).
Calculated mass [M+Na]⁺ = 527.2 Da and 689.2 Da, respectively. Masses found [M+Na]⁺ = 526.9 Da
and 688.8 Da, respectively, and ¹³C [M+Na]⁺ = 528.0 Da and 689.5 Da, respectively.

β-(1-2)-Mannotriose and β-(1-2)-mannotetraose were analysed by NMR. In particular, HSQCed 2D NMR spectra showed cross-peak patterns confirming the structures of mannose oligosaccharides with β-(1-2) linkages, as the values recorded were in line with those stated in the literature for both β-(1-2)-mannotriose (**Figure 3. 13**) and β-(1-2)-mannotetraose (**Figure 3. 14**)[4]. Clear resolution of the anomeric region in β-(1-2)-mannotriose HSQC spectrum allowed for assignment of the reducing end signals of H-1^{A}α and H-1^{A}β, identified by signals at 5.15 and 4.86 ppm, respectively, which correlated with ¹³C signals at 91.9 and 93.5 ppm for C-1^{A}α and C-1^{A}β hydroxyl groups, respectively. Very similar values of chemical shifts were observed for reducing end signals. NMR spectra of β-(1-2)-mannotetraose α-anomer can be identified by a ¹H NMR signal at 5.16 ppm, correlating with ¹³C NMR signal at 92.1 ppm; β-anomer was identified by a ¹H NMR signal at 4.86 ppm, correlating with a ¹³C NMR signal at 93.5 ppm. Clear identification of the anomeric signals of the reducing terminus is essential for these oligosaccharides required for subsequent conjugation.
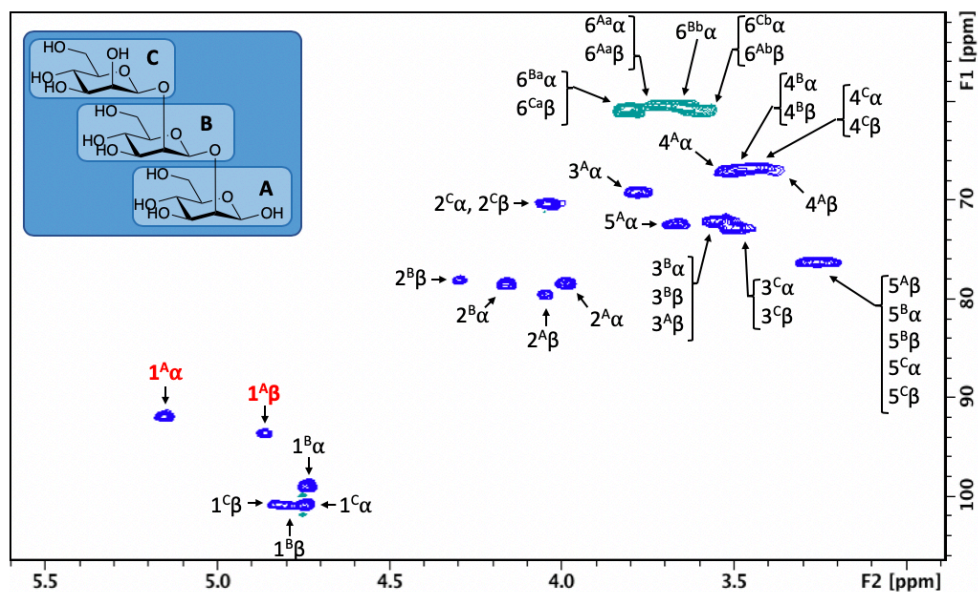
Figure 3. 13 – HSQC NMR analysis of β-(1-2)-mannotriose (400 MHz, D₂O). *Red labels represent the anomeric position. For a table of chemical shifts, see* **Appendices 6. 14**.
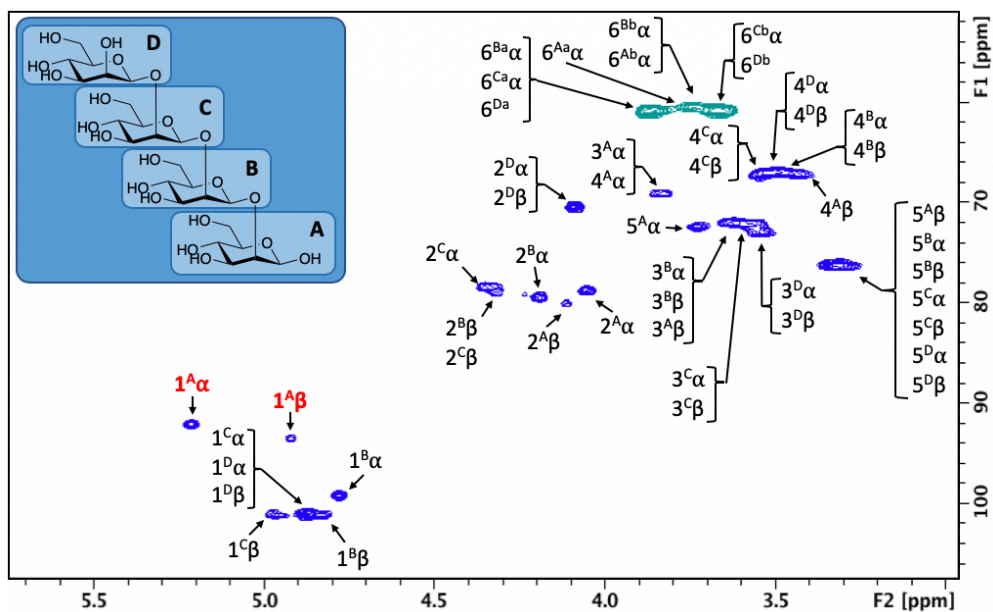
Figure 3. 14 – HSQC NMR analysis of β-(1-2)-mannotetraose (400 MHz, D₂O). *Red labels represent the anomeric position. For a table of chemical shifts, see* **Appendices 6. 15**.

3.1.2.4. Functionalisation of β-(1-2)-mannosides

3.1.2.4.1. Generation of methyl 5-hexynoate linker

By reacting the mannose oligosaccharides to a bifunctional linker prior to protein conjugation, it was anticipated that the conjugation efficiency to protein carriers would be improved.

Hexynoic acide was derivatised to methyl 5-hexynoate was generated as outlined by Cody et al (**Scheme 3. 3**)[25]. Briefly, hexynoic acid (1 g) was reacted with methyl iodide (MeI, 1.4 eq) in the presence of potassium carbonate (K_2CO_3, 1.2 eq) in dimethylformamide (DMF, 30 mL) at 0 °C. After 3 hours, the reaction was complete, yielding 630 mg of an oily product, with a reaction efficiency of 63 %. The complete removal of unreacted starting material was confirmed by TLC analysis on silica gel.
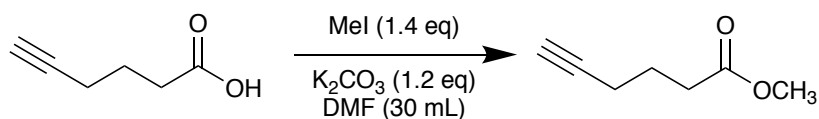
Scheme 3. 3 – Synthesis of methyl 5-hexynoate linker. *Reagents and conditions: Hexynoic acid, K_2CO_3 (1.2 eq), dry DMF, 0 °C. MeI (1.4 eq), 0 °C-RT over 3 hr.*

^{1}H NMR analysis of hexynoic acid (**Figure 3. 15 A**) and methyl 5-hexynoate (**Figure 3. 15 B**) confirmed the conversion of carboxylic acid to methyl ester by the appearance of a characteristic signal of the methyl group at 3.6 ppm.
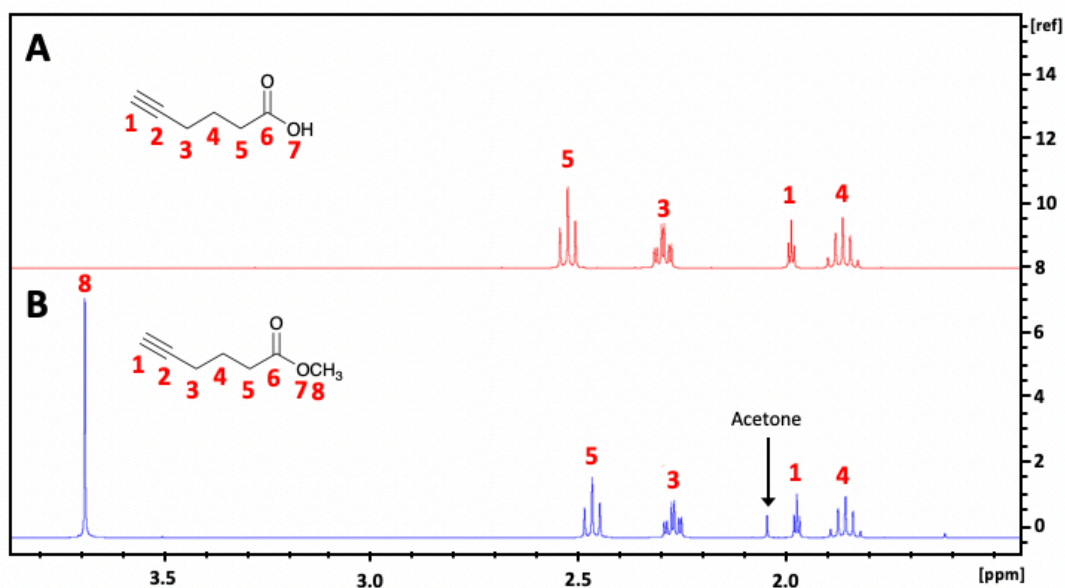
Figure 3. 15 – Analysis of hexynoic acid (A) and methyl 5-hexynoate (B) by ¹H NMR (400 MHz, CDCl₃).

^{13}C NMR analysis hexynoic acid (**Figure 3. 16 A**) and methyl 5-hexynoate (**Figure 3. 16 B**) also confirmed the introduction of a methyl ester by the presence of a signal at 51.6 ppm in the spectra for methyl 5-hexynoate.
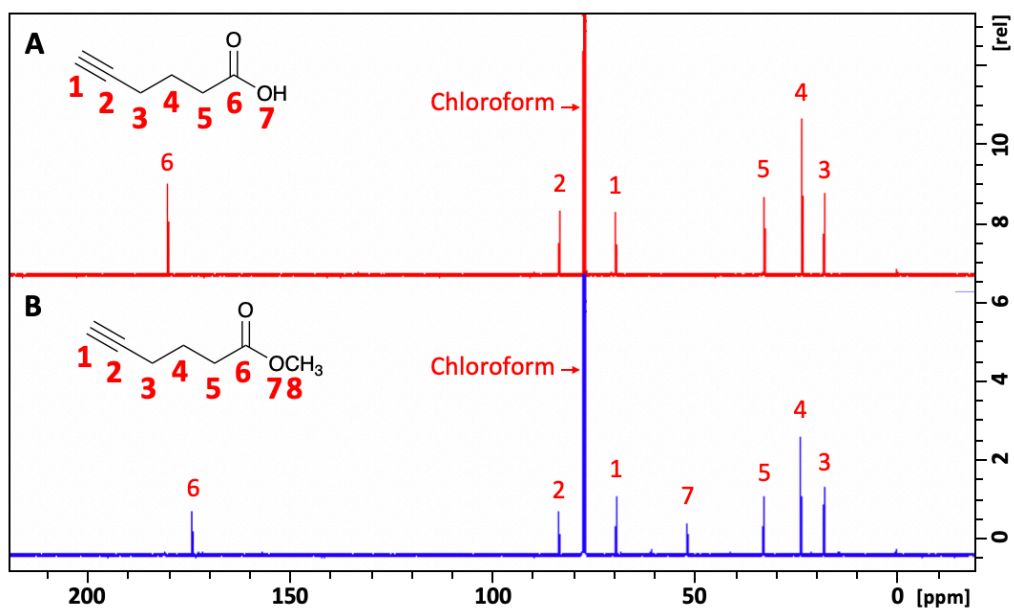
Figure 3. 16 – Analysis of hexynoic acid (A) and methyl 5-hexynoate (B) by ¹³C NMR (100 MHz, CDCl₃).

3.1.2.4.2. Azide functionalisation of β-(1-2)-manno-oligosaccharides

Introduction of an azide at the anomeric position of both β-(1-2)-mannotriose and β-(1-2)-mannotetraose would allow copper-catalysed click chemistry to be utilised for conjugation to the terminal alkyne of the methyl 5-hexynoate linker. Functionalisation of the anomeric position of the β-(1-2)-mannosides with an azide was achieved as outlined in **Scheme 3. 4**.

R =   β-(1-2)-mannotriose   β-(1-2)-man-β-(1-2)-man-
        β-(1-2)-mannotetraose   β-(1-2)-man-β-(1-2)-man-β-(1-2)-man-
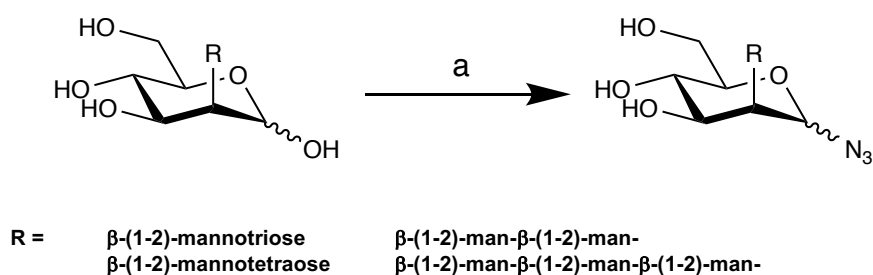
Scheme 3. 4 – Reaction scheme for azide functionalised mannose oligosaccharides. a) NaN$_3$ (2.5 M), DMC (5 eq), DIPEA (15 eq), D$_2$O, 18 hr, RT.

ESI-MS analysis confirmed the correct masses of β-(1-2)-mannotriosyl azide (**Figure 3. 17 A**) and β-(1-2)-mannotetraosyl azide, by [M+Na]$^+$ of 551.9 and 714.0 Da, respectively. Masses corresponding to unreacted β-(1-2)-mannotriose and β-(1-2)-mannotetraose were also identified by the presence of sodium adduct peaks at 526.9 and 689.1 Da, respectively.
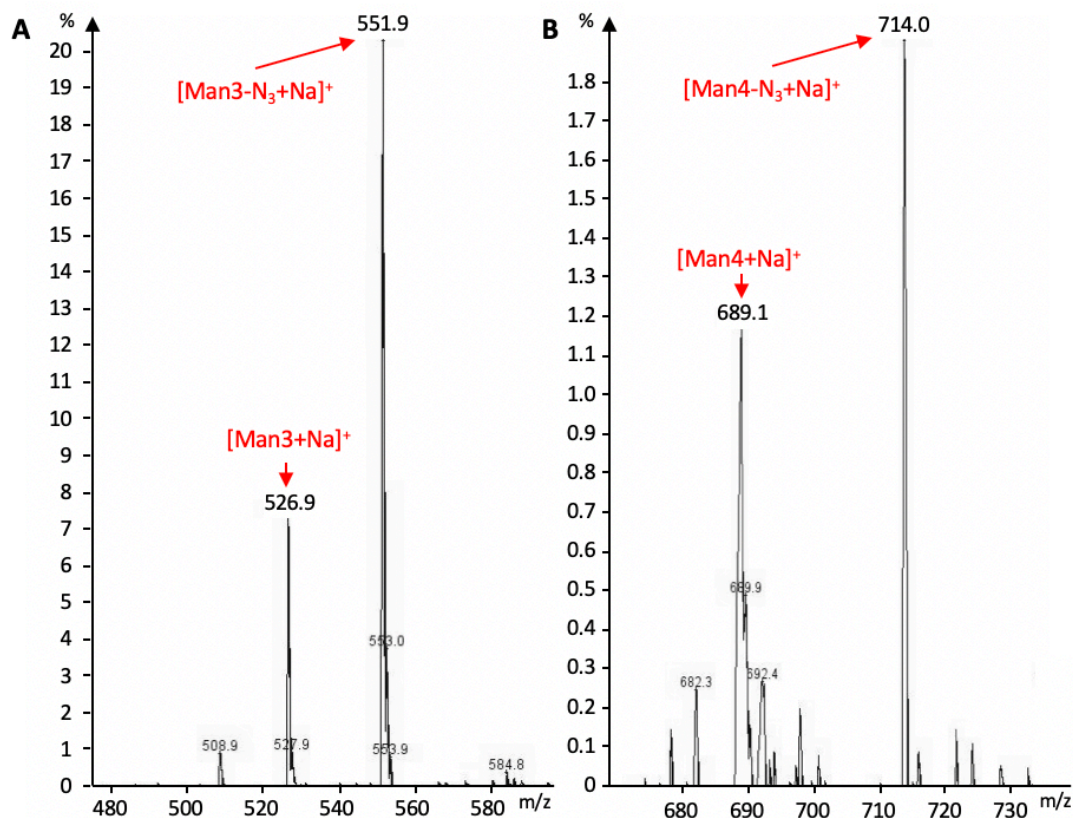
Figure 3. 17 – ESI-MS analysis of β-(1-2)-mannotriosyl azide (A) and β-(1-2)-mannotetraose-N_3 (B). *Calculated masses: [β-(1-2)-mannotriose-N_3+Na]$^+$ = 552.17, [β-(1-2)-mannotetraose-N_3+Na]$^+$ = 714.2. Masses found: [β-(1-2)-mannotriose-N_3+Na]$^+$ = 551.9, [β-(1-2)-mannotetraose-N_3+Na]$^+$ = 714.0. Some unreacted β-(1-2)-mannotriose and β-(1-2)-mannotetraose remains, as evident by masses at 526.9 [β-(1-2)-mannotriose+Na]$^+$ and 689.1 [β-(1-2)-mannotetraose+Na]$^+$.*

HSQCed NMR analysis allowed confirmation of the functionalisation on β-(1-2)-mannotriose with 1-azido group (**Figure 3. 18**). Chemical shifts at 5.0 ppm and 86.9 ppm for ^{1}H NMR and ^{13}C NMR spectra, respectively, are consistent with the presence of an anomeric β-azide. A smaller signal at 5.6 ppm in ^{1}H NMR spectra, correlating with 87.6 ppm in ^{13}C NMR spectra can be attributed to H-1$^A\alpha$ and C-1$^A\alpha$ azide.
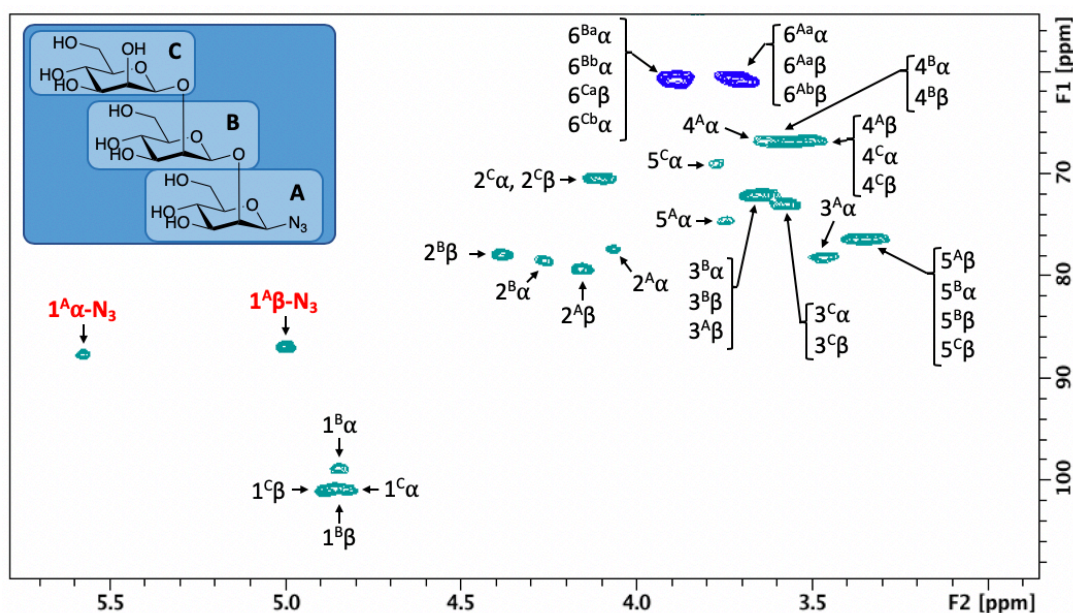
Figure 3. 18 – HSQCed NMR analysis of β-(1-2)-mannotriosyl azide (400 MHz, D_2O).

HSQCed NMR analysis of β-(1-2)-mannotetraosyl azide also confirmed formation of anomeric β-azide as followed from ^{1}H NMR chemical shift at 5.0 ppm, which correlated with a ^{13}C NMR chemical shift at 86.8 ppm (**Figure 3. 19**). Unreacted material was also identified by the presence of signals at 5.2 ppm and 4.9 ppm for H-1[A]α and H-1[B]β, respectively, which correlated with ^{13}C NMR chemical shifts at 92.0 ppm and 93.4 ppm, respectively.
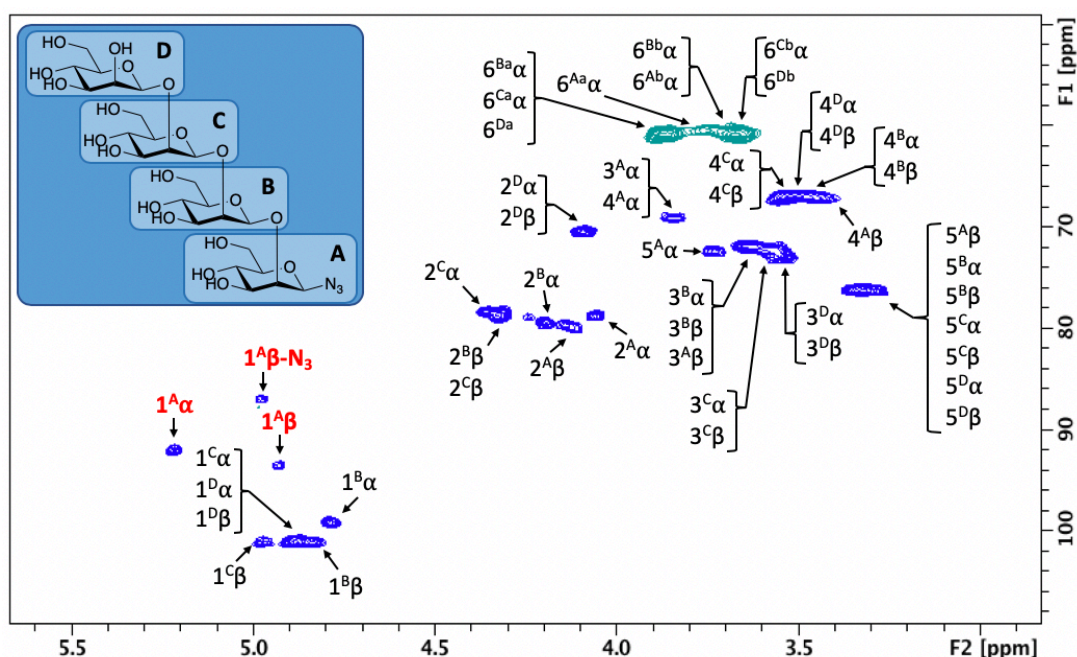
Figure 3. 19 – HSQCed NMR analysis of β-(1-2)-mannotetraosyl azide (400 MHz, D_2O).

Analysis of compounds by FTIR allows for clear distinction of azide by a strong signal within the region of 2160-2120 cm^{-1}. Analysis of β-(1-2)-mannotriosyl azide and β-(1-2)-tetraosyl azide confirmed the presence of an azide by a strong signal at 2118.5 cm^{-1} and 2122 cm^{-1}, respectively (**Appendices 6. 16**).

3.1.2.4.3. Coupling of azide functionalised β-(1-2)-mannosides to methyl 5-hexynoate via click chemistry

Traditional methods of copper-catalysed click chemistry[26] were employed to couple β-(1-2)-mannoside azides to methyl 5-hexynoate, with the addition of the accelerating ligand THPTA (tris-hydroxypropyltriazolylmethylamine)[27], as outlined in **Scheme 3. 5**.
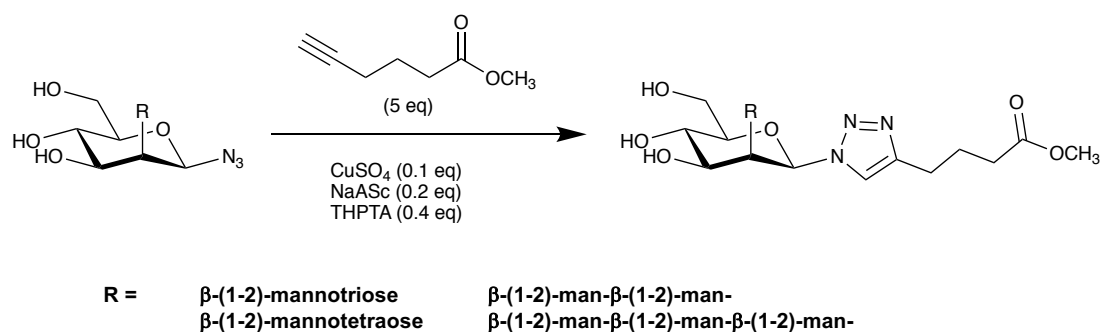
Scheme 3. 5 – Copper catalysed click reaction of azide functionalised β-(1-2)-mannosides with methyl 5-hexynoate[20].

Briefly, 5 mg of each β-(1-2)-mannotriosyl azide and β-(1-2)-mannotetraosyl azide were reacted with methyl 5-hexynoate (5 eq), $CuSO_4$ (0.1 eq), NaASc (0.2 eq) and THPTA (0.4 eq) in 300 μL of water/tert-butanol (1:1) at 50 °C for 16 hr. Extraction by EtOAc washes was used to remove excess reagents followed by GPC for further purification. Lyophilisation yielded 4.5 mg and 4.2 mg of β-(1-2)-mannotriose and β-(1-2)-mannotetraose clicked products, respectively.

Clicked products were analysed by ESI-MS to determine the molecular masses of clicked products. β-(1-2)-Mannotriose click product was confirmed by the presence of a mass at 678.5 Da, consistent with the calculated mass for sodium adducts, 678.2 Da (**Figure 3. 20 A**). The presence of β-(1-2)-mannotetraose click product was confirmed by the presence of a mass at 840.6 Da, consistent with that calculated for sodium adducts, 840.3 Da (**Figure 3. 20 B**).
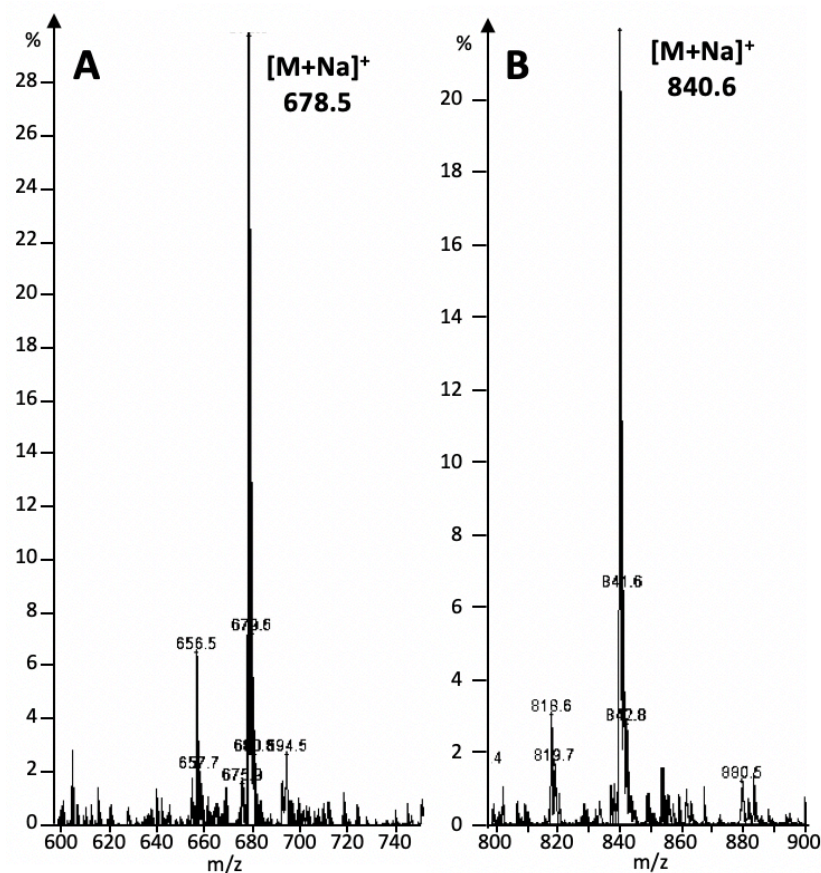
Figure 3. 20 – ESI-MS analysis of β-(1-2)-mannotriose (A) and β-(1-2)-mannotetraose (B) clicked products. *Calculated masses = [β-(1-2)-mannotriosyl click+Na]$^+$ = 678.2 Da, [β-(1-2)-mannotetraosyl click+Na]$^+$ = 840.3 Da. Masses found = [β-(1-2)-mannotriosyl click+Na]$^+$ = 678.5 Da, [β-(1-2)-mannotetraosyl click+Na]$^+$ = 840.6 Da.*

Successful click reactions were further confirmed by ^{1}H NMR analysis (**Figure 3. 21**) which revealed complete disappearance of signals of H-1^{A}α (5.6 ppm) and H-1^{A}β (5.0 ppm) corresponding to mannosyl azide residues, and the appearance of characteristic triazole signals at around 8 ppm[28]. More specifically, triazole signals in both β-(1-2-)mannotriose and β-(1-2)-mannotetraose click product ^{1}H NMR spectra appeared in pairs at 8.00 and 7.94 ppm, which can be attributed to β- and α-linked triazole rings, respectively. The α-/β-ratio was ca. 1:2 for mannotriose and ca. 1:2.5 for mannotetraose derivatives as followed from integration of these signals (**Appendices 6. 17** and **Appendices 6. 18**). The same α-/β-ratios were found for integrals measured for H-1^{A}α (6.06 ppm) and H-1^{A}β (6.14 ppm) signals of the reducing ends of triazole-linked β-(1-2)-mannotriose and β-(1-2)-

mannotetraose derivatives. Multiplets at 1.88-1.95, 2.34-2.39 and 2.70-2.76 ppm corresponded to protons at positions 3, 4 and 5, respectively, of the linker, as numbered in **Figure 3. 15**. A strong singlet at 3.6 ppm corresponds to the methyl group, whereas multiplets between 4.9-3.1 ppm compose the characteristic signature of H-2 – H-6 signals of carbohydrates.
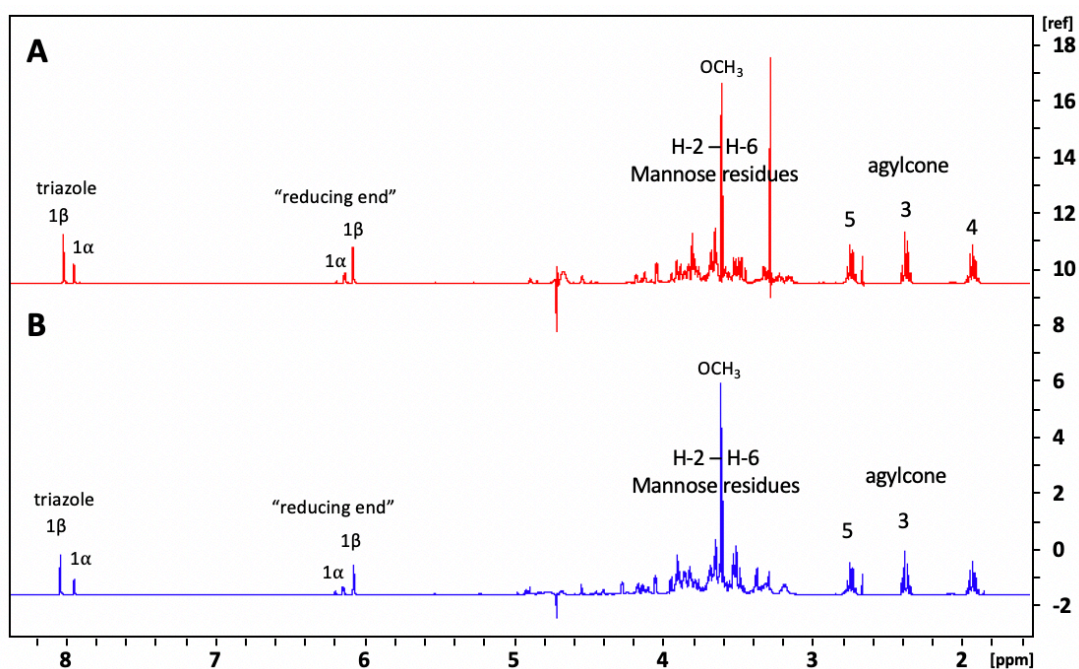
Figure 3. 21 – ^{1}H NMR analysis of β-(1-2)-mannotriose (A) and β-(1-2)-mannotetraose (B) click products (400 MHz, D$_2$O).

3.1.2.5.   Conjugation β-(1-2)-mannoside click products to protein carriers

Attempts were made to conjugate β-(1-2)-mannoside click products to TetHc and BSA carrier proteins, as outlined in **Scheme 3. 6**.

R = Man4: β-Man(1-2)-β-Man(1-2)-β-Man

Man3: β-Man(1-2)-β-Man
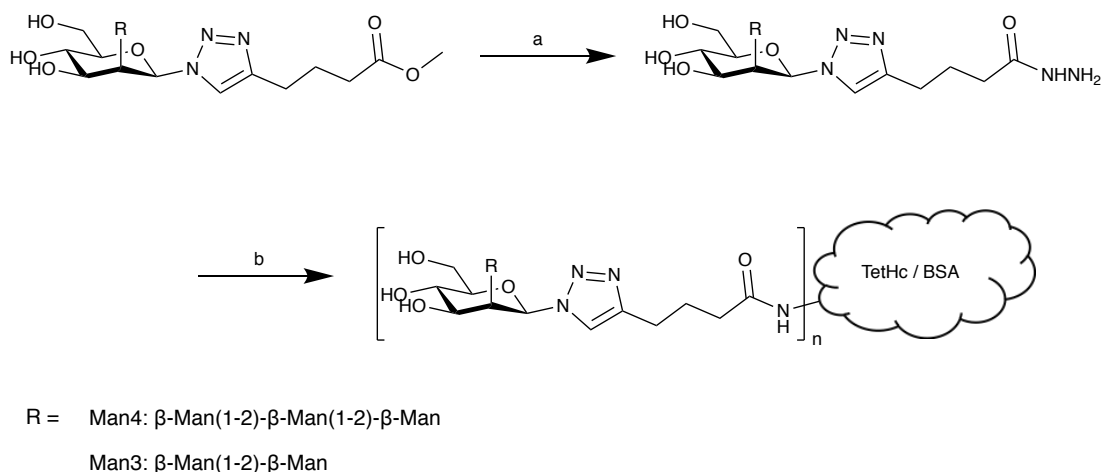
Scheme 3. 6 – General reaction scheme for conjugation of β-(1-2)-mannotriose and β-(1-2)-mannotetraosyl click products to carrier proteins. *Reagents and conditions: a) hydrazine monohydrate, EtOH, 6 hr, 55 °C; bi) tert-butyl nitrite, 4M HCl in dioxane, DMF, -20 °C 15 mins; bii) TetHc/BSA, 0.08 M Borax/0.35 M KHCO₃, pH 9.0, 18 h, 4 °C.*

3.1.2.5.1. Expression of soluble tetanus toxoid carrier protein

Expression of TetHc was performed by induction of *E.coli* pLysS-TetHc cells with IPTG, as described in **Chapter 5.3.12.** Cell lysate was purified on an AKTA prime system equipped with a 5 mL HisTrap HP column (**Appendices 6. 19**). Analysis of each stage of the expression process was performed by SDS-PAGE and Western blot (**Figure 3. 22**). A TetHc standard (**Figure 3. 22 – Lane 1**) allowed determination of the correct molecular mass by comparison. *E. coli* expression cells prior to IPTG lacked the presence of a 57 kDa His-tagged protein, as shown by lack of a band at the corresponding size in both SDS-PAGE (**Figure 3. 22 A – Lane 2**) and Western blot (**Figure 3. 22 B – Lane 2**). Following IPTG induction, proteins were isolated into insoluble and soluble fractions. SDS-PAGE analysed showed the presence of a large band at 57 kDa within the insoluble fraction (**Figure 3. 22 A – Lane 3**), which corresponded with the control band in lane 1. Western blot analysis confirmed this protein to contain a His-tag (**Figure 3. 22 B – Lane 3**). However, analysis of the soluble fraction confirmed the presence of a soluble His-tagged protein of the correct size (**Figure 3. 22 – Lane 4**). AKTA purification of His-tagged proteins was successful in removing the majority of contaminating proteins from the sample, however SDS-PAGE revealed some minor protein bands remained (**Figure 3. 22 A – Lanes 5-11**). Western blot confirmed the large

116

protein band present at 57 kDa was indeed His-tagged (**Figure 3. 22 B – Lane 5-11**).
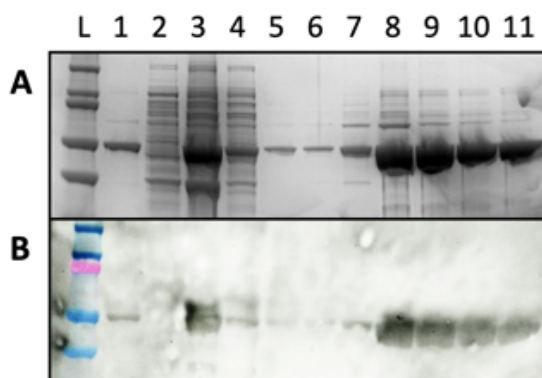
Figure 3. 22 – SDS-PAGE (A) and Western blot (B) analysis of TetHc expression. *A - 12 % SDS gels were run at 200 V for 50 mins. B – Western blot analysis was performed using a mouse anti-His primary antibody and a goat anti-mouse(HRP) secondary antibody. L – Ladder, 1 – TetHc standard, 2 – Non-induced E.coli cells, 3 – Induced insoluble fraction, 4 – Induced soluble fraction, 5-11 – AKTA fractions A1-A7.*

In an attempt to remove residual contamination proteins, TetHc was subjected to further purification by GPC, as described in **Chapter 5.3.12.** SDS-PAGE analysis confirmed that this purification was successful in removing residual proteins (**Figure 3. 23**). Protein yield was determined, by BCA assay, to be 55 mg from 1 L of culture.
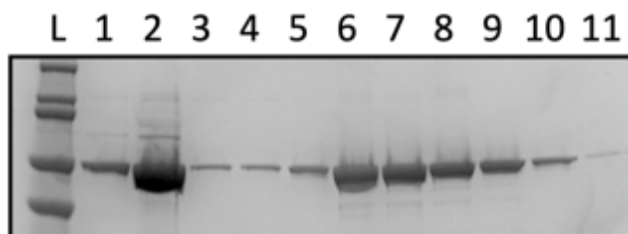
Figure 3. 23 – SDS-PAGE analysis of TetHc AKTA GPC fractions. *L – ladder, 1 – TetHc standard, 2 – AKTA fractions (pre GPC), 3-11 – AKTA GPC fractions C3-D7.*

MALDI-TOF/MS analysis revealed the molecular mass of the purified protein to be 56.4 kDa, consistent with the predicted mass of His-tagged TetHc (**Figure 3. 24**).
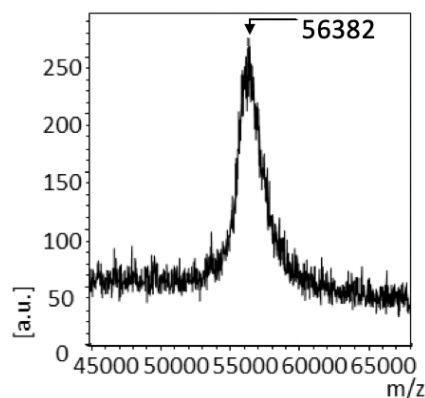
Figure 3. 24 - MALDI-TOF/MS of purified TetHc. Expected mass = 57 kDa. mass found = 56.4 kDa.

3.1.2.5.2. Conjugation of β-(1-2)-mannoside click products to TetHc and BSA carrier proteins

Conjugate β-(1-2)-mannoside click products was targeted towards exposed lysine residues on BSA and TetHc carrier proteins by conversion of the terminal methyl ester group to an acyl hydrazide. β-(1-2)-Mannotriosyl and β-(1-2)-mannotetraosyl click products (4 mg each) were reacted with hydrazine monohydrate in ethanol for 6 hr at 55 °C. Co-evaporation of excess reagents with toluene yielded 5 mg of β-(1-2)-mannotriose and β-(1-2)-mannotetraose acyl hydrazide products. Conversion of methyl ester to hydrazide was confirmed ^{1}H NMR analysis by the loss of a signal at δ 3.6 ppm for both β-(1-2)-mannotriosyl (**Appendices 6. 20 A**) and β-(1-2)-mannotetraosyl (**Appendices 6. 20 B**) acyl hydrazide products.

In order for conjugation of acyl hydrazide products to exposed lysine residues on BSA and TetHc carrier proteins, acyl hydrazides were converted to acyl azides[29]. The reaction conditions for this to occur are described in **Chapter 5.3.13**. Briefly, *tert*-butyl nitrite was reacted with 4 M HCl in DMF at -25 °C to produce nitrous acid, allowing *in situ* conversion of acyl hydrazide to acyl azide

via oxidation. Sulfamic acid (740 µg in DMF) was added to the acyl azide solutions, to prevent the build-up of nitrous oxide[30], and the reaction allowed to reach 0 °C before being added dropwise to a cooled solution of protein in Borax buffer, pH 9.0[31].

Successful conjugation of acyl azide functionalised β-(1-2)-mannotriose and β-(1-2)-mannotetraosyl click products is dependent on the primary amines of lysine residues being in the free base form (**Scheme 3. 7**)[22,32].
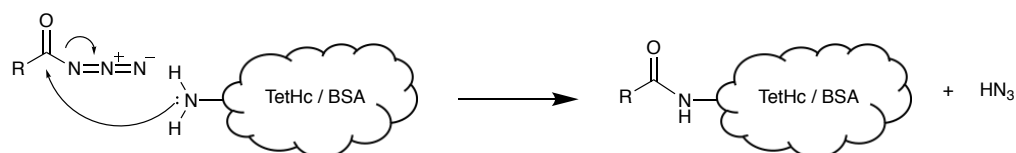
Scheme 3. 7 – Reaction mechanism for amide bond formation.

To ensure lysine residues were in the free base form, the conjugation reaction was performed in Borax buffer, pH 9.0. However, upon addition of the acyl azides to cooled protein solutions, protein precipitation occurred. Attempts to determine the degree of conjugation by MALDI-TOF/MS were unsuccessful (data not shown). SDS-PAGE analysis of TetHc conjugates did not reveal a band shift when compared to native TetHc (**Figure 3. 25 A**). Analysis of BSA conjugates, however, did reveal a slight band shift by SDS-PAGE (**Figure 3. 25 B**), although the presence of carbohydrates could not be detected when analysed by Invivogen^{TM} Pro-Q™ Emerald 300 Glycoprotein Gel and Blot Stain Kit (**Figure 3. 25 C**).
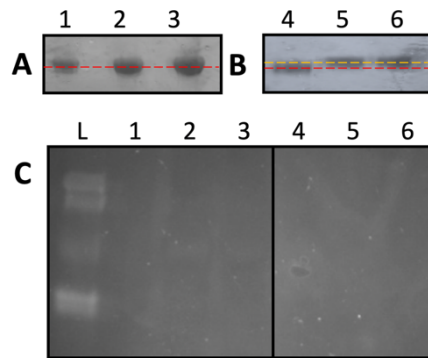
Figure 3. 25 – SDS-PAGE analysis of β-(1-2)-mannoside protein conjugates. Gel analysis was performed on 4-20 % SDS-PAGE gels at 200 V. A) SDS-PAGE analysis of TetHc conjugates; B) SDS-PAGE analysis of BSA conjugates; C) Invivogen^{TM} Pro-Q^{TM} Emerald 300 Glycoprotein Gel stain of TetHc and BSA conjugates. L = Precision Plus Protein Ladder, 1 = Native TetHc, 2 = TetHc-β-(1-2)-mannotriose conjugate, 3 = TetHc-β-(1-2)-mannotetraose conjugate, 4 = Native BSA, 5 = BSA-β-(1-2)-mannotriose conjugate, 6 = BSA-β-(1-2)-mannotetraose conjugate.

These conjugation efforts require further experimentation to optimise, however, time did not allow for this and conjugation efforts were not continued further. Future work should focus on optimising the conjugation technique for coupling to protein carriers. Direct conversion of hexynoic acid to the acyl azide would be a more direct approach for conjugation and is worth consideration.

3.2. Virenose antigens for a Q fever vaccine

3.2.1. An introduction to Virenose

To date vaccination therapies against Q fever have comprised of whole killed Phase I *Coxiella burnetii* cells, as described in **Chapter 1.5.2**[33–35]. *C. burnetii* exists in two LPS phases, the avirulent phase II, comprising of a lipid A moiety coupled to an inner core and an outer core, and the virulent phase I[34], which in addition to Phase LPS also contains an *O* antigen region (**Figure 3. 26**).
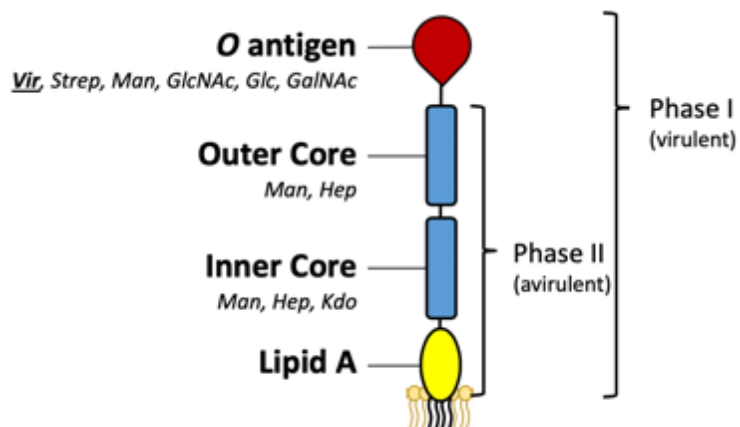
Figure 3. 26 – Tentative structure of C. burnetii Phase I and II LPS.

Research into the carbohydrate composition of the *O* antigen has revealed the presence of two unique sugars, virenose and dihydrohydroxystreptose [(DHHS) **Figure 3. 27**], accounting for 32.3 % and 6.7 % of the polysaccharide composition, respectively, although the exact position of the sugars within the *O* antigen is yet to be determined[36].
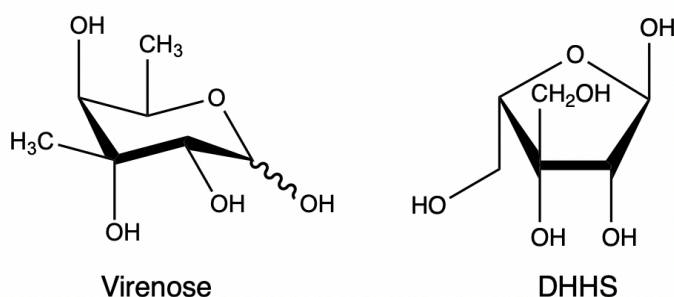
Figure 3. 27 – The chemical structure of virenose and dihydrohydroxystreptose (DHHS).

Given the uniqueness of virenose, and its presence within the *O* antigen of *C. burnetii*, it is reasonable to believe that vaccines containing virenose antigens would generate a potent enough Ab response to protect against Q fever infection. Presently, isolation of virenose from *C. burnetii* has only resulted in crude LPS mixtures which requires the use of category 2 growth facilities, and complex chemical synthesis is required to yield pure virenose antigens[37,38]. In

this study, disaccharide virenose antigens of α-Vir(1-4)-α-Vir-propyl azide and β-Vir(1-4)-β-Vir-propyl azide were chemically synthesised by Dr Irina Ivanova of the John Innes Centre.

3.2.1.1. Virus-like particle carrier protein in a Q fever vaccine

Virus-like particles are becoming an increasing popular candidate as a protein carrier in vaccination therapies[39,40] since their first use in the 1980s[41,42]. To date, 5 VLP vaccines are commercially available (**Table 3. 1**), with a number of others currently undergoing clinical trials[40].

Table 3. 1 - Commercial VLP vaccines

VLP	Vaccine name	Ref
Human Papilloma Virus (HPV)	Cervarix ®	43,44
	Gardasil ®	43–46
	Gardasil9 ®	47–49
Hepatitis B Virus (HBV)	3rd generation Sci-B-Vac™	50,51
Malaria	Mosquirix™	52–54

VLPs consist of the multi-protein shell of virus particles, spanning 20-200 nm in size, but lack a viral genome required for replication allowing them the ability to induce potent immune responses[55]. In this study Conjucore, a Hepatitis B VLP modified to contain a DKDKDK insert to enhance conjugation efficiency, was provided by Dr Lucy Beales of Mologic to act as a protein carrier, (**Figure 3. 28**).
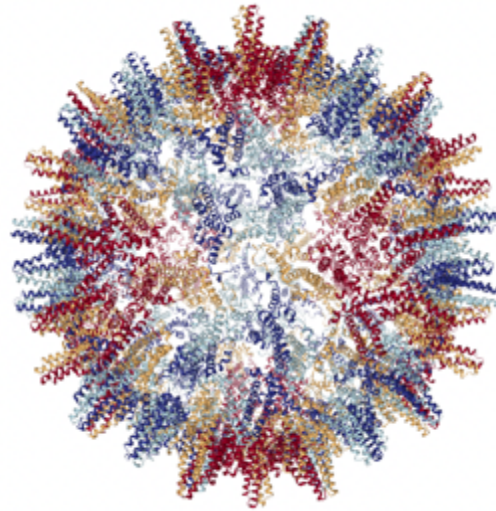
Figure 3. 28 – The crystal structure of Hepatitis B HBcAg virus-like particle containing a DKDKDK insert.

In this study, laminarin was chosen to act as a molecular address tag due to its ability to initiate a strong Dectin-1-mediated signalling response, as shown in **Chapter 2.2.6.** Literature reports have shown the addition of laminarin to vaccine conjugates can increase the antibody response towards the antigen[14] and laminarin itself is able to raise antibodies which are effective against murine vaginal candidiasis[56]. Laminarin azide was provided to Dr Simone Dedola of Iceni Diagnostics to generate a targeted virenose vaccines consisting of α-Vir(1-4)-α-Vir-propyl azide (**Figure 3. 29 A**) or β-Vir(1-4)-β-Vir-propyl azide (**Figure 3. 29 B**) and laminarin conjugated to Conjucore VLP via BCN-NHS linkers, as described in **Chapter 5.3.14.**
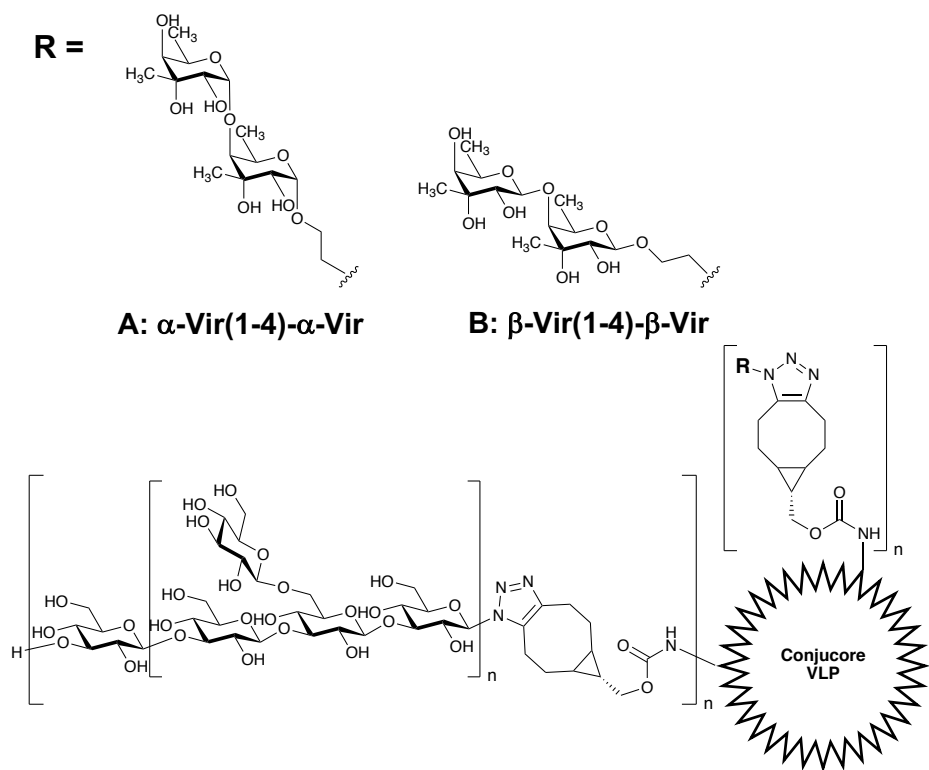
Figure 3. 29 – Structure of laminarin targeted α-Vir(1-4)-α-Vir (A) and β-Vir(1-4)-β-Vir (B) vaccine conjugates.

3.2.2. Results and Discussion

3.2.2.1. Immunisation trials of laminarin-VLP-virenose conjugates

In an attempt to generate an improved vaccination therapy to protect against Q fever, a tri-component vaccine was generated which consisted of a central VLP protein carrier (Conjucore), to which disaccharide virenose antigens and a laminarin address tag were coupled, as outlined in **Figure 3. 29**. Azide-functionalised laminarin was provided to Dr Simone Dedola of Iceni Diagnostics for generation of targeted Q fever vaccination. Vaccines comprising of α-Vir(1-4)-α-Vir and β-Vir(1-4)-β-Vir propyl azide constructs and azide functionalised laminarin conjugated to Conjucore VLP were prepared via copper-free click chemistry, as described in **Chapter 2.1.2**. Laminarin was chosen to act as a molecular address tag as Dectin-1 binding studies performed in **Chapter 2.2.6** showed laminarin was able to induce a strong Dectin-1-mediated signalling response when conjugated to a BSA carrier protein.

3.2.2.2. Immunisation of vaccine conjugates

Immunisation trials were performed by Mologic as outlined in **Chapter 5.3.15.**
Briefly, VLP conjugates were emulsified with Complete Freunds adjuvant for
immunisation which were administered to 2 rabbits at 10 µg as 4 x 0.25 mL
injection sites on days 0, 28, 56 and 84 (**Figure 3. 30**). Bleeds were taken on
days 0 (pre-immunisation), 35 (bleed 1), 63 (bleed 2) and 91 (bleed 3).
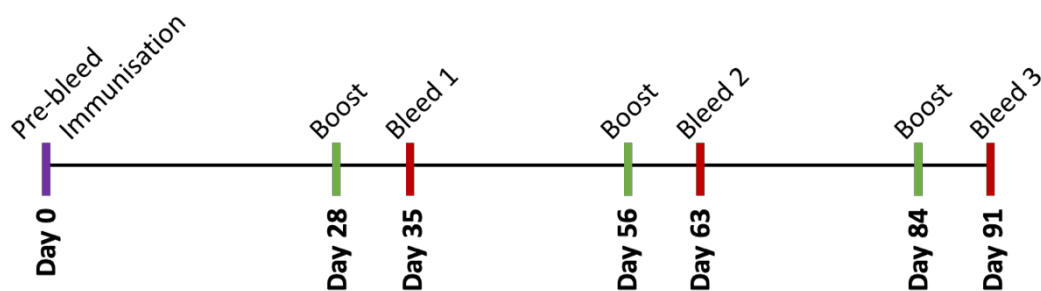
*Figure 3. 30 – Immunisation time line for virenose vaccination trials. Purple line represents Day 0
when a pre-bleed was taken, and the first immunisation was received. Green lines represent days when
boost immunisations were received. Red lines represent days when bleeds were taken.*

VLP conjugates were prepared for immunisation by emulsifying with adjuvant
to a final injection volume of 1 mL. Immunisation was performed with Complete
Freunds adjuvant and all boost injections were emulsified in Incomplete
Freunds adjuvant. VLP glycoconjugate were injected intramuscularly into 2
rabbits at 4 sites, 1 injection into each thigh muscle and subcutaneously into
2 sites on the back. A total of 0.25 mL of emulsion was injected at each site.
Rabbits were immunised with 10 µg of VLP glycoconjugate on day 0 with
boosts being provided on days 28, 56 and 84. A preimmune bleed was taken
on day 0, before immunisation, and test bleeds were taken on days 35, 63 and
91. Blood samples were collected from the marginal ear vein into a sterile vial.
For preimmune and test bleeds, 25 mL of whole blood was collected, and 50
mL of whole blood collected for all subsequent bleeds (dependent on body
weight).

3.2.2.3. Generation of BSA conjugates

To analyse the antibody response generated towards out VLP vaccine conjugates, a series of BSA-antigen conjugates were generated (**Figure 3. 31**).
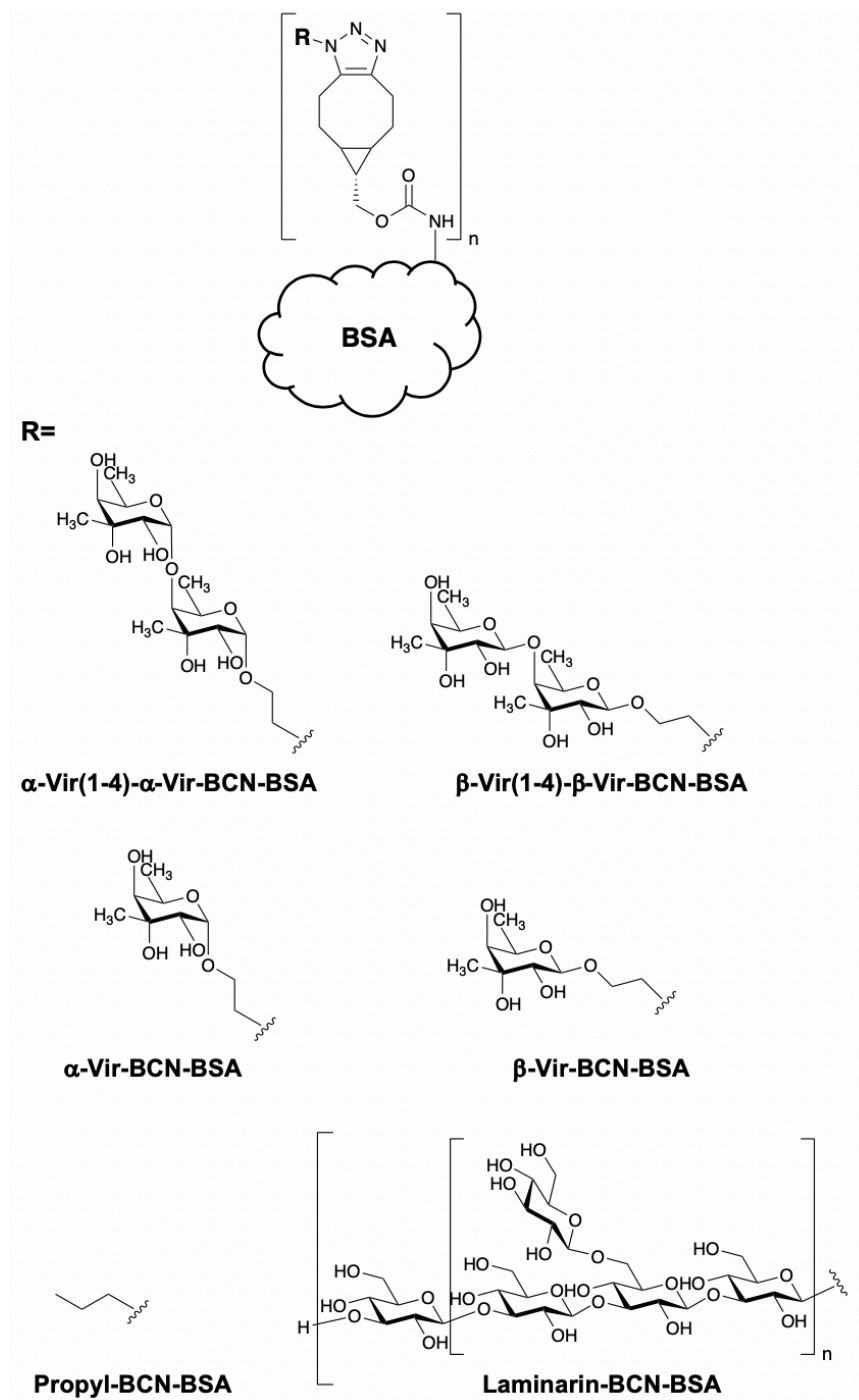
Figure 3. 31 – Summary of BSA conjugates generated for ELISA analysis.

Briefly, virenose mono- and disaccharide antigens were synthesised by Dr Irina Ivanova of the John Innes Centre. As well as the laminarin azide prepared in **Chapter 2.2.4** the antigens were reacted with BSA-BCN, prepared in **Chapter 2.2.5**. As a control, propyl azide was also reacted with BSA-BCN.

The presence of virenose on BSA conjugates was determined by SDS-PAGE and Western blot analysis. Following conjugation, all virenose conjugates show a shift in band size by SDS-PAGE, confirming that the molecular mass has increased following conjugation (**Figure 3. 32 A1, 2, 3 and 4**), in comparison to BCN-BSA controls (**Figure 3. 32 ***).
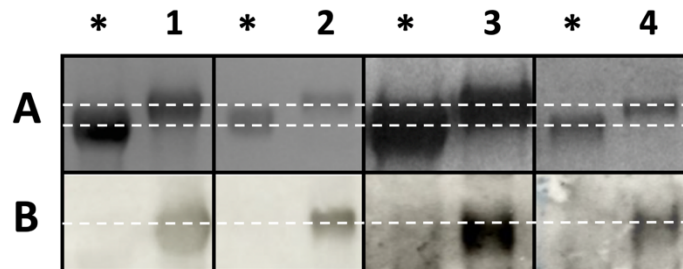
Figure 3. 32 – SDS-PAGE (A) and Western blot (B) analysis of BCN-BSA (*), α-Vir(1-4)-α-Vir-BCN-BSA (1), α-Vir-BCN-BSA (2), β-Vir(1-4)-β-Vir-BCN-BSA (3) and β-Vir-BCN-BSA (4). SDS-PAGE analysis was performed on pre-cast 4-20 % SDS-PAGE gels at 200 V for 60 mins. Western blot analysis was performed with blood serum from rabbits immunised with the corresponding virenose configuration and developed with a mouse anti-rabbit HRP secondary antibody.

Western blot analysis of the BSA conjugates was performed with serum obtained from the immunisation trials. Serum from rabbits immunised with α-Vir(1-4)-α-Vir-BCN-VLP-BCN-laminarin were used to probe for α-Vir(1-4)-α-Vir- and α-Vir- BSA conjugates, and similarly, serum from β-Vir(1-4)-β-Vir-BCN-VLP-BCN-laminarin immunised rabbits was used to probe for β-Vir(1-4)-β-Vir- and β-Vir- BSA conjugates. Blots were developed by probing with a secondary mouse anti-rabbit HRP antibody. Clear bands can be observed across all virenose conjugates (**Figure 3. 32 B1, 2, 3 and 4**), whereas no bands could be detected in BCN-BSA standard (**Figure 3. 32 B***). Therefore, it was deduced that virenose conjugation was successful.

Laminarin conjugation to BSA was also shown to be successful by the presence of a characteristic smear for laminarin-BCN-BSA conjugates by SDS-PAGE (**Figure 3. 33 A**), which was confirmed to contain β-(1-3)-glucans by Western blot analysis performed with an anti β-(1-3)-glucan primary antibody (**Figure 3. 33 B**).
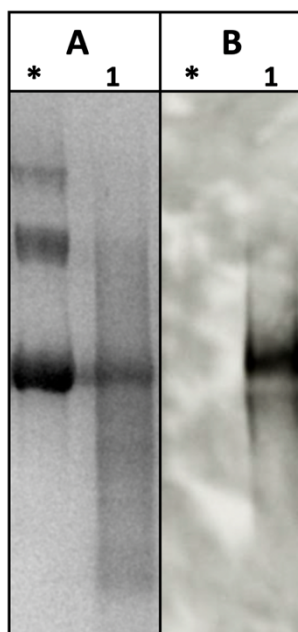
Figure 3. 33 – Analysis of BSA (*) and laminarin-BCN-BSA (1) conjugates by SDS-PAGE (A) and Western blot analysis (B).

3.2.2.4.   Immunological analysis of anti-virenose conjugate antibodies

Enzyme-linked immunosorbent assays were employed to determine the IgG antibody response generated as a result of immunisation with laminarin targeted α-Vir(1-4)-α-Vir and β-Vir(1-4)-β-Vir vaccine conjugates (**Scheme 3. 7**). Standard ELISA (**Scheme 3. 8A**) allowed detection of IgG responses directed towards specific antigens, whereas competitive ELISA allows the specificity of this interaction to be determined (**Scheme 3. 8B**). BSA conjugates described in **Figure 3. 31** were adhered to a 96-well ELISA plate and subjected to standard ELISA analysis as described in **Chapter 5.3.16.** Serum samples from all bleeds were analysed (**Appendices 6. 21**), with bleed

3 showing the strongest response, as expected due to the development of cellular memory by the immune system. As outlined in **Chapter 1.5**, after 3-4 weeks antibody generation ceased. Re-immunisation with the same antigen results in constant stimulation of the immune system and a stronger antibody response.
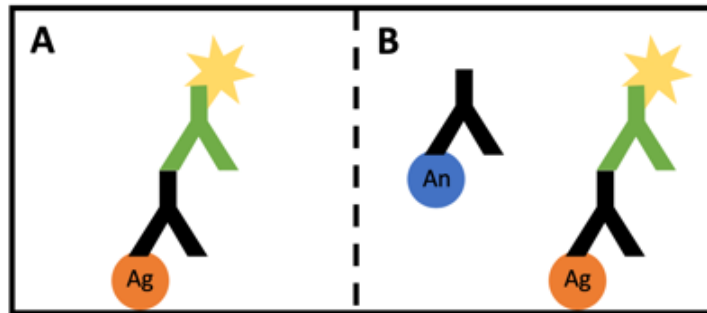
Scheme 3. 8 – Schematic representation of standard ELISA (A) and competitive ELISA (B). *Standard ELISA (A) is performed by adhering the target antigen (Ag) to an ELISA plate. Serum is then applied to the plate to allow antibody-antigen recognition to occur, any unbound antibodies are washed away. A secondary antibody is applied, which recognises the primary antibody and allows colourimetric detection. Competitive ELISA (B) differs from standard ELISA in that serum is pre-incubated with a target analyte prior to incubation with the target antigen. Specific antibody recognition is determined by a colourimetric response if towards the target antigen, or lack of a colourimetric response if antibody recognition is specific towards the target analyte.*

3.2.2.4.1. Analysis of antibody response towards disaccharide antigens

Serum derived from α-Vir(1-4)-α-Vir-BCN-VLP-BCN-laminarin-immunised rabbits was not able to recognise β-Vir(1,4)-β-Vir antigens (**Figure 3. 34 A**) but showed a strong response towards α-Vir(1-4)-α-Vir-, with a significant difference (P <0.05) when compared to the pre-immune serum of the same rabbits (**Figure 3. 34 B**). Interestingly, serum from β-Vir(1-4)-β-Vir-BCN-VLP-BCN-laminarin immunised rabbits was able to recognise β-Vir(1-4)-β-Vir-antigen with a P value of 0.002 (**Figure 3. 34 A**) but was also able to recognise α-Vir(1-4)-α-Vir- antigen (**Figure 3. 34 B**), although this response was not significant with a P value of 0.0514. The ability of serum from β-Vir(1-4)-β-Vir-BCN-VLP-BCN-laminarin immunised rabbits to recognise both disaccharide antigens posed the question of whether the antibody response was generated

towards the disaccharide antigen, or whether monosaccharide α or β virenose antigens are sufficient to see a response.

3.2.2.4.2. Analysis of antibody response towards monosaccharide antigens

Analysis of the serum towards monosaccharide antigens showed only β-Vir(1-4)-β-Vir-BCN-VLP-BCN-laminarin immunised was able to recognise β (**Figure 3. 34 C**) and α (**Figure 3. 34 D**) monosaccharide antigens, with P values of 0.0106 and 0.0280, respectively. Although the serum response from α-Vir(1-4)-α-Vir-BCN-VLP-BCN-laminarin immunised rabbits was slightly elevated above the response from pre-immune serum for both α and β monosaccharide virenose antigens, these responses were not significant.

3.2.2.4.3. Analysis of antibody response towards Conjucore VLP

The use of immunogenic carrier proteins is essential for generating a strong immune response towards carbohydrates, which are often not immunogenic on their own. Conjucore VLP comprised the carrier protein component of the vaccines used in these trials. ELISA analysis of serum derived from α-Vir(1-4)-α-Vir-BCN-VLP-BCN-laminarin and β-Vir(1-4)-β-Vir-BCN-VLP-BCN-laminarin immunised rabbits both showed a strong antibody response towards Conjucore, with no antibody responses detected prior to immunisation by either (**Figure 3. 34 E**).

3.2.2.4.4. Analysis of antibody response towards laminarin

Laminarin was incorporated into the vaccine conjugate to target the vaccine towards Dectin-1 expressed on APCs in an attempt to generate a more robust antibody response. Literature reports have shown increased antibody responses upon the addition of laminarin, with IgG antibodies also being

raised towards laminarin[14,57]. However, in this study, a laminarin antibody response could not be detected from either α-Vir(1-4)-α-Vir-BCN-VLP-BCN-laminarin or β-Vir(1-4)-β-Vir-BCN-VLP-BCN-laminarin immunisation serums (**Figure 3. 34 F**).

3.2.2.4.5. Analysis of antibody response towards triazoles

Reports in the literature raise concern over the immunogenicity of triazoles which are formed as a result of azide-alkyne click reactions[58]. To deduce whether an IgG antibody response had been generated towards the triazoles used in this study, BCN-BSA was reacted with azidopropanol to generate a triazole for use as an antigen in ELISA assay. However, triazole specific antibodies could not be detected in the serums of α-Vir(1-4)-α-Vir-BCN-VLP-BCN-laminarin or β-Vir(1-4)-β-Vir-BCN-VLP-BCN-laminarin immunised rabbits (**Figure 3. 34 G**).

3.2.2.4.6. Ability of antibodies to recognise *Coxiella burnetii*

Whole killed *C. burnetii* cells were kindly provided by DSTL in order to analyse the antibody response generated from our immunisation trials. Interestingly, serum from α-Vir(1-4)-α-Vir-BCN-VLP-BCN-laminarin and β-Vir(1-4)-β-Vir-BCN-VLP-BCN-laminarin immunised rabbits did not produce a significant response towards *C. burnetii* cells (**Figure 3. 34 H**). Similarly, a significant response was not detected in response to Coxevac®, a commercial vaccine administered to livestock to protect against Q fever composed of whole killed cells, by either serum (**Figure 3. 34 I**).
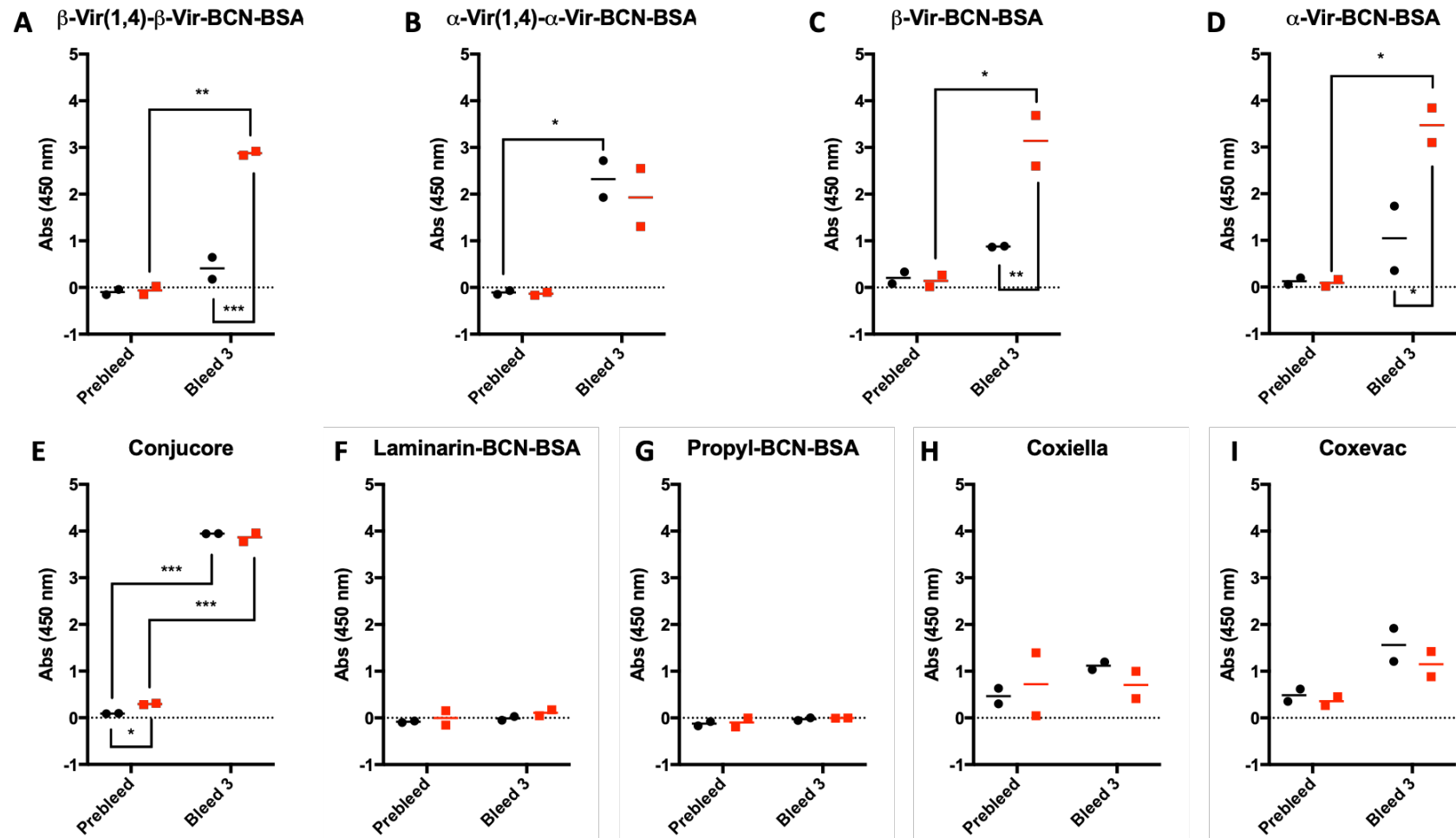
Figure 3. 34 – Comparison of prebleed and bleed 3 standard ELISA of α-Vir(1-4)-α-Vir- (black circles) and β-Vir(1-4)-β-Vir- (red squares) BCN-VLP-BCN-Laminarin immunised rabbits. *P values: * = 0.05, ** = 0.01, *** = 0.005.*

Competitive ELISA was performed to determine the binding preference of antibodies generated in response to α-Vir(1-4)-α-Vir-BCN-VLP-BCN-laminarin and β-Vir(1-4)-β-Vir-BCN-VLP-BCN-laminarin immunisation. Analysis of serum responses towards α-Vir(1-4)-α-Vir-BCN-BSA antigen were performed with and without pre-incubation with β-Vir(1-4)-β-Vir-BCN-BSA analyte (**Figure 3. 35 A**). No significant change in response was seen when α-Vir(1-4)-α-Vir-BCN-VLP-BCN-laminarin serum was incubated with analyte, however, β-Vir(1-4)-β-Vir-BCN-VLP-BCN-laminarin serum showed an almost complete loss of response when incubated with β-Vir(1-4)-β-Vir-BCN-BSA analyte when compared to the serum alone. Competitive ELISA analysis of serum responses towards β-Vir(1-4)-β-Vir-BCN-BSA antigen did not reveal any significant change in response when the serum was preincubated with an α-Vir(1-4)-α-Vir-BCN-BSA analyte compared to serum alone (**Figure 3. 35 B**).
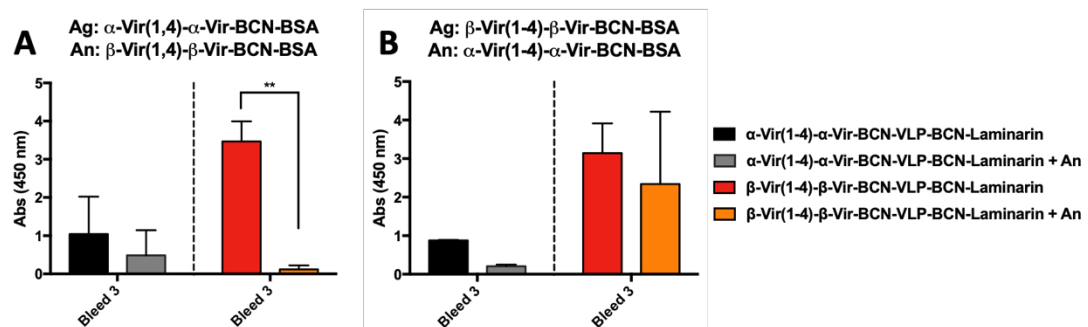
Figure 3. 35 – Competition ELISA of virenose disaccharide BSA conjugates. *A) α-Vir(1-4)-α-Vir-BCN-BSA antigen and β-Vir(1-4)-β-Vir-BCN-BSA analyte. B) β-Vir(1-4)-β-Vir-BCN-BSA antigen and α-Vir(1-4)-α-Vir-BCN-BSA analyte. Bar colours represent the following serum samples: black - α-Vir(1-4)-α-Vir-BCN-VLP-BCN-Laminarin, grey α-Vir(1-4)-α-Vir-BCN-VLP-BCN-Laminarin serum plus analyte, red - β-Vir(1-4)-β-Vir-BCN-VLP-BCN-Laminarin, β-Vir(1-4)-β-Vir-BCN-VLP-BCN-Laminarin serum plus analyte. P value: ** = 0.01.*

A standard ELISA was performed with a commercial *C. burnetii* monoclonal antibody, which was raised against the phase I LPS of *C. burnetii*. Virenose has been shown to be present within the *O* antigen section of phase I LPS[36] (**Chapter 1.5.2**), therefore a strong response towards virenose BSA conjugates was anticipated. Interestingly, none of the BSA conjugates were able to elicit a response with this antibody, however, Coxevac and whole killed *C. burnetii* cells were both able to elicit a strong response (**Figure 3. 36**).
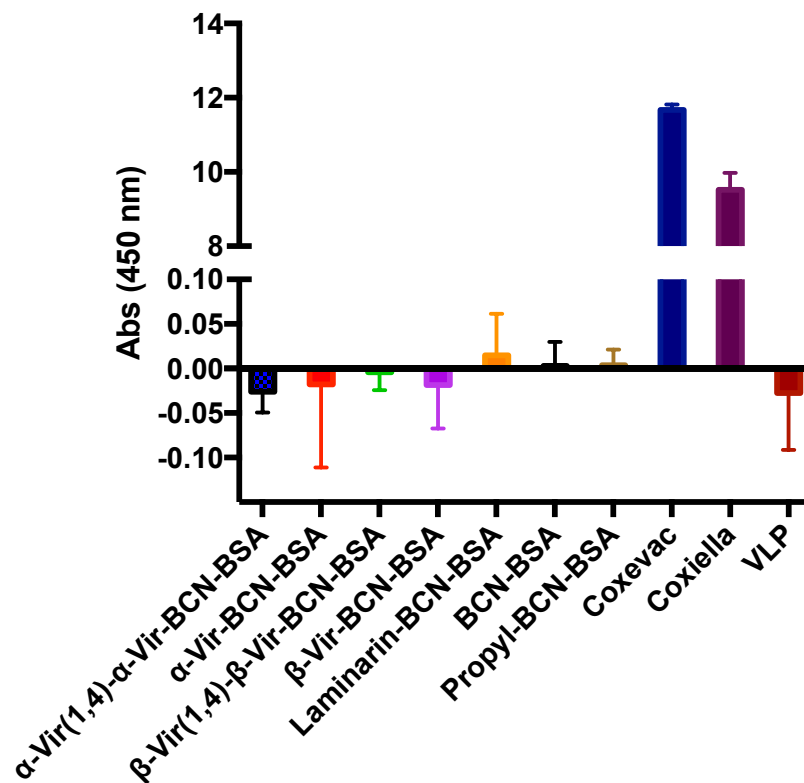
Figure 3. 36 – Standard ELISA of BSA conjugates, Coxevac vaccine, Coxiella and VLP probed with a commercial C. burnetii Phase I LPS pAb.

3.2.3. Conclusions

The initial work described in this chapter demonstrates the ability to yield β-(1-2)-mannan oligosaccharides in milligram quantities by enzymatic synthesis, with polymerisation ranging from DP1-8. β-(1-2)-Mannotriose and β-(1-2)-mannotetraose were successfully isolated by GPC, with yields of 6.2 mg and 5.3 mg, respectively. The isolated oligosaccharides were subsequently functionalised with anomeric azides using methodologies outlined by Tanaka *et al*[19], resulting in mixture of α and β anomeric azide for β-(1-2)-mannotriose, but only β-azides for β-(1-2)-mannotetraose, as determined by HSQCed NMR. Methyl 5-hexynoate was chosen to act as a bifunctional linker to allow conjugation of β-(1-2)-mannosides to TetHc and BSA carrier protein. Copper-catalysed click chemistry proved to be an efficient mechanism of conjugation of sugar azides to the linker. Although derivatisation of the methyl ester to an acyl hydrazide was successful, conjugation to BSA and TetHc carrier proteins resulted in protein precipitation. Conjugation by this method has proved successful in literature reports, and it is likely that optimisation of the reaction conditions would lead to successful conjugation in the future, however time restraints meant that these efforts could not be pursued.

The latter part of this chapter focuses on the immunisation efforts of a laminarin targeted vaccination therapy comprised of either α-Vir(1-4)-α-Vir-BCN-VLP-BCN-laminarin or β-Vir(1-4)-β-Vir-BCN-VLP-BCN-laminarin. Serum analysis by ELISA plate assays revealed antibodies were successfully raised against virenose antigens, although the specificity varied depending on linkage. Immunisation with α-Vir(1-4)-α-Vir-BCN-VLP-BCN-laminarin generated an antibody response specific towards the α-Vir(1-4)-α-Vir-disaccharide antigen. However, immunisation with β-Vir(1-4)-β-Vir-BCN-VLP-BCN-laminarin generated a strong response towards β-Vir(1-4)-β-Vir-disaccharide and β-Vir- monosaccharide antigens, but a significant response towards α-Vir(1-4)-α-Vir- disaccharide and α-Vir monosaccharide was also observed.

Interestingly, neither whole killed *C. burnetii* cells nor Coxevac® were recognised by antibodies present in the serum of either vaccination therapies. Literature reports have revealed a virenose content of 32.2 mol % within the *O* antigen of phase I LPS, although the sequence of *O* antigen carbohydrates is unknown. Although the virenose content is relatively high, it may be that it is submerged within the *O* antigen and not accessible to antibodies.

The implications of using laminarin to target vaccines towards DCs in immunisation trials remains unknown. Lack of rabbit availability meant test groups consisted of 2 rabbits for treatment without a non-laminarin control group. In this study, laminarin was not able to generate an IgG antibody response, contradictory to what is reported in the literature. β-(1-3)-glucans are present on the surface of many microbial species, therefore exposure to such species prior to commencement of the immunisation may result in a basal level anti-β-(1-3)-glucan antibody response. To determine whether the addition of laminarin to vaccine translates into a more robust antibody response, larger test groups are required.

In conclusion, β-(1-2)-mannose oligosaccharide antigens were successfully synthesised enzymatically, with β-(1-2)-mannotriose and β-(1-2)-mannotetraose isolated via gel permeation chromatography. Although conjugation efforts to BSA and TetHc carrier proteins resulted in protein precipitation, further optimisation is required to allow for successful conjugation. Although immunisation with virenose antigens were able to raise a significant virenose specific antibody response these were not able to recognise *C. burnetii*, the use of virenose antigens in immunisation should not be ruled out. The rare occurrence of virenose in nature provides a unique opportunity to generate a specific vaccination therapy against Q fever, with little cross-reactivity with other species. A better understanding of the sequence of carbohydrates within the *O* antigen of LPS would provide more insight into what is needed to generate a protective antibody response.

3.3. References

1. Shibata, N., Arai, M., Haga, E., Kikuchi, T., Najima, M., Satoh, T., Kobayashi, H. & Suzuki, S. Structural Identification of an Epitope of Antigenic Factor 5 in Mannans of Candida albicans NIH B-792 (Serotype B) and J-1012 (Serotype A) as B-1,2-Linked Oligomannosyl Residues. *Infect. Immun.* **60,** 4100–4110 (1992).

2. Nitz, M., Ling, C.-C., Otter, A., Cutler, J. E. & Bundle, D. R. The unique solution structure and immunochemistry of the Candida albicans beta - 1,2-mannopyranan cell wall antigens. *J. Biol. Chem.* **277,** 3440–3446 (2002).

3. Johnson, M. A., Cartmell, J., Weisser, N. E., Woods, R. J. & Bundle, D. R. Immunodominance of internal epitopes in Candida mannans 1 Molecular Recognition of Candida albicans (1→2)-β-Mannan Oligosaccharides by a Protective Monoclonal Antibody Reveals the Immunodominance of Internal Saccharide Residues. *J. Biol. Chem.* **287,** 18078–18090 (2012).

4. Faille, C., Wieruszeski, J.-M., Michalski, J.-C., Poulain, D. & Strecker, G. Complete 1H- and 13C-resonance assignments for d-mannooligosaccharides of the β-d-(1 → 2)-linked series released from the phosphopeptidomannan of Candida albicans VW.32 (serotype A). *Carbohydr. Res.* **236,** 17–27 (1992).

5. Poláková, M., Roslund, M. U., Ekholm, F. S., Saloranta, T. & Leino, R. Synthesis of β-(1→2)-Linked Oligomannosides. *European J. Org. Chem.* **2009,** 870–888 (2009).

6. Ekholm, F. S., Sinkkonen, J. & Leino, R. Fully deprotected β-(1→2)-mannotetraose forms a contorted α-helix in solution: convergent synthesis and conformational characterization by NMR and DFT. *New J. Chem.* **34,** 667–675 (2010).

7.   Tang, S.-L. & Pohl, N. L. B. Automated fluorous-assisted solution-phase synthesis of β-1,2-, 1,3-, and 1,6-mannan oligomers. *Carbohydr. Res.* **430,** 8–15 (2016).

8.   Crich, D., Banerjee, A. & Yao, Q. Direct Chemical Synthesis of the beta-D-Mannans: The beta-(1-2) and beta-(1-4) Series. *J. Am. Chem. Soc.* **126,** 14930–14934 (2004).

9.   Chiku, K., Nihira, T., Suzuki, E., Nishimoto, M., Kitaoka, M., Ohtsubo, K. & Nakai, H. Discovery of two β-1,2-mannoside phosphorylases showing different chain-length specificities from Thermoanaerobacter sp. X-514. *PLoS One* **9,** e114882 (2014).

10. Lipinski, T., Wu, X., Sadowska, J., Kreiter, E., Yasui, Y., Cheriaparambil, S., Rennie, R. & Bundle, D. R. A β-mannan trisaccharide conjugate vaccine aids clearance of Candida albicans in immunocompromised rabbits. *Vaccine* **30,** 6263–6269 (2012).

11. Harris, J. . & Markl∗, J. Keyhole limpet hemocyanin (KLH): a biomedical review. *Micron* **30,** 597–623 (1999).

12. Rennels, M. B., Edwards, K. M., Keyserling, H. L., Reisinger, K. S., Hogerman, D. A., Madore, D. V., Chang, I., Paradiso, P. R., Malinoski, F. J. & Kimura, A. Safety and Immunogenicity of Heptavalent Pneumococcal Vaccine Conjugated to CRM197 in United States Infants. *Pediatrics* **101,** 604–611 (1998).

13. Zeltins, A. Construction and Characterization of Virus-Like Particles: A Review. *Mol. Biotechnol.* **53,** 92–107 (2013).

14. Lipinski, T., Fitieh, A., St Pierre, J. J., Ostergaard, H. L., Bundle, D. R., Touret, N., St. Pierre, J., Ostergaard, H. L., Bundle, D. R. & Touret, N. Enhanced Immunogenicity of a Tricomponent Mannan Tetanus Toxoid Conjugate Vaccine Targeted to Dendritic Cells via Dectin-1 by Incorporating beta-Glucan. *J. Immunol.* **190,** 4116–4128 (2013).

15. Matsuda, M. & Yoneda, M. Antigenic substructure of tetanus neurotoxin. *Biochem. Biophys. Res. Commun.* **77,** 268–274 (1977).

16. Morelli, L., Poletti, L. & Lay, L. Carbohydrates and Immunology: Synthetic Oligosaccharide Antigens for Vaccine Formulation. *European J. Org. Chem.* **2011,** 5723–5777 (2011).

17. Umland, T. C., Wingert, L. M., Swaminathan, S., Furey, W. F., Schmidt, J. J. & Sax, M. Structure of the receptor binding fragment HC of tetanus neurotoxin. *Nat. Struct. Biol.* **4,** 788–792 (1997).

18. Hermanson, G. T. & Preceded by: Hermanson, G. T. Bioconjugate techniques. *Academic Press*, 229-258 (1996). doi:doi.org/10.1016/C2009-0-64240-9

19. Tanaka, T., Nagai, H., Noguchi, M., Kobayashi, A. & Shoda, S. One-step conversion of unprotected sugars to beta-glycosyl azides using 2-chloroimidazolinium salt in aqueous solution. *Chem Commun* **23,** 3378–3379 (2009).

20. Presolski, S. I., Hong, V. P. & Finn, M. G. Copper-Catalyzed Azide-Alkyne Click Chemistry for Bioconjugation. in *Current Protocols in Chemical Biology* **3**, 153–162 (2011). doi:10.1002/9780470559277.ch110148

21. van Dongen, S. F., Teeuwen, R. L., Nallani, M., van Berkel, S. S., Cornelissen, J. J., Nolte, R. J. & van Hest, J. C. Single-step azide introduction in proteins via an aqueous diazo transfer. *Bioconjug. Chem.* **20,** 20–23 (2009).

22. Cuadros, J., Aldega, L., Vetterlein, J., Drickamer, K. & Dubbin, W. Reactions of lysine with montmorillonite at 80 °C: Implications for optical activity, H+ transfer and lysine–montmorillonite binding. *J. Colloid Interface Sci.* **333,** 78–84 (2009).

23. Paszkiewicz, E., Sarkar, S., Tam, P.-H., Luu, T., Bundle, D. R., Lipinski, T., Cartmell, J. & Dziadek, S. Synthesis of antifungal vaccines by conjugation of β-1,2 trimannosides with T-cell peptides and covalent anchoring of neoglycopeptide to tetanus toxoid. *Carbohydr. Res.* **403,** 123–134 (2014).

24. Bundle, D., Paszkiewicz, E., Elsaidi, H., Mandal, S., Sarkar, S., Bundle, D. R., Paszkiewicz, E., Elsaidi, H. R. H., Mandal, S. S. & Sarkar, S. A Three Component Synthetic Vaccine Containing a β-Mannan T-Cell Peptide Epitope and a β-Glucan Dendritic Cell Ligand. *Molecules* **23,** 1–17 (2018).

25. Cody, J. A., Ahmed, I. & Tusch, D. J. Studies toward the total synthesis of eletefine: An efficient construction of the AB ring system. *Tetrahedron Lett.* **51,** 5585–5587 (2010).

26. Meldal, M. & Tornøe, C. W. Cu-Catalyzed Azide−Alkyne Cycloaddition. *Chem. Rev.* **108,** 2952–3015 (2008).

27. Hong, V., Steinmetz, N. F., Manchester, M. & Finn, M. G. Labeling Live Cells by Copper-Catalyzed Alkyne−Azide Click Chemistry. *Bioconjug. Chem.* **21,** 1912–1916 (2010).

28. Hua, Y. & Flood, A. H. Click chemistry generates privileged CH hydrogen-bonding triazoles: the latest addition to anion supramolecular chemistry. *Chem. Soc. Rev.* **39,** 1262–1271 (2010).

29. Kim, K. & Kim, Y. H. Preparation of azides from hydrazines by using dinitrogen tetroxide as nitrosonium ion source. *Arch. Pharm. Res.* **16,** 94–98 (1993).

30. Dzelzkalns, L. S. & Bonner, F. T. Reaction between nitric and sulfamic acids in aqueous solution. *Inorg. Chem.* **17,** 3710–3711 (1978).

31. Lemieux, R. U., Bundle, D. R. & Baker, D. A. Properties of a synthetic antigen related to the human blood-group Lewis a. *J. Am. Chem. Soc.* **97,** 4076–4083 (1975).

32. Ingemar André, Sara Linse, & Frans A. A. Mulder. Residue-Specific pKa Determination of Lysine and Arginine Side Chains by Indirect 15N and 13C NMR Spectroscopy: Application to apo Calmodulin. *J. Am. Chem. Soc.* **129,** 15805–15813 (2007).

33. Lackman, D. B., Bell, E. J., Frederick Bell, J. & Pickens, E. G. Intradermal Sensitivity Texting in Man with a Purified Vaccine for Q Fever. *Am J Public Health Nations Health*, **52**, 87-93 (1962).

34. Ormsbee, R. A., Bell, E. J., Lackman, D. B. & Tallent, G. The Influence of Phase on the Protective Potency of Q Fever Vaccine. *J. Immunol.* **92,** 404–12 (1964).

35. Chiu, C. K. & Durrheim, D. N. A review of the efficacy of human Q fever vaccine registered in Australia. *N. S. W. Public Health Bull.* **18,** 133–136 (2007).

36. Vadovic, P., Slaba, K., Fodorova, M., Skultety, L. & Toman, R. Structural and functional characterization of the glycan antigens involved in immunobiology of Q fever. *Ann. N. Y. Acad. Sci.* **1063,** 149–153 (2005).

37. Brimacombe, J. S., Hanna, R. & Tucker, L. C. N. A synthesis of methyl 6-deoxy-3-C-methyl-α-d-gulopyranoside (methyl α-virenoside). *Carbohydr. Res.* **112,** 320–323 (1983).

38. Hong, N., Sato, K. & Yoshimura, J. Synthesis of Methyl 6-Deoxy-3-C-methyl-β-D-gulopyranoside (Methyl β-Virenoside). *Bull. Chem. Soc. Jpn.* **54,** 2379–2382 (1981).

39. Michel, M.-L. & Tiollais, P. Hepatitis B vaccines: Protective efficacy and therapeutic potential. *Pathol. Biol.* **58,** 288–295 (2010).

40. Mohsen, M. O., Zha, L., Cabral-Miranda, G. & Bachmann, M. F. Major findings and recent advances in virus–like particle (VLP)-based vaccines. *Semin. Immunol.* **34,** 123–132 (2017).

41. Szmuness, W., Stevens, C. E., Harley, E. J., Zang, E. A., Oleszko, W. R., William, D. C., Sadovsky, R., Morrison, J. M. & Kellner, A. Hepatitis B Vaccine: demonstration of efficacy in a controlled clinical trial in a high-risk population in the United States. *N. Engl. J. Med.* **303,** 833–841 (1980).

42. Maupas, P., Goudeau, A., Coursaget, P., Drucker, J. & Bagros, P. Immunisation against hepatitis B in man. *Lancet.* **1,** 1367–1370 (1976).

43. Haskins-Coulter, T., Southern, J., Andrews, N. & Miller, E. Reactogenicity of Cervarix and Gardasil human papillomavirus (HPV) vaccines in a randomized single blind trial in healthy UK adolescent females. *Hum. Vaccin. Immunother.* **13,** 1412–1420 (2017).

44. Haghshenas, M., Mousavi, T., Kheradmand, M., Afshari, M. & Moosazadeh, M. Efficacy of human papillomavirus l1 protein vaccines (cervarix and gardasil) in reducing the risk of cervical intraepithelial neoplasia: A meta-analysis. *Int. J. Prev. Med.* **8,** 44–49 (2017).

45. Makiyama, K., Hirai, R. & Matsuzaki, H. Gardasil Vaccination for Recurrent Laryngeal Papillomatosis in Adult Men. *J. Voice* **31,** 104–106 (2017).

46. Inbar, R., Weiss, R., Tomljenovic, L., Arango, M.-T., Deri, Y., Shaw, C. A., Chapman, J., Blank, M. & Shoenfeld, Y. Behavioral abnormalities in female mice following administration of aluminum adjuvants and the human papillomavirus (HPV) vaccine Gardasil. *Immunol. Res.* **65,** 136–149 (2017).

47. Zhai, L. & Tumban, E. Gardasil-9: A global survey of projected efficacy. *Antiviral Res.* **130,** 101–109 (2016).

48. Gupta, A. K., MacLeod, M. A. & Abramovits, W. GARDASIL 9 (Human Papillomavirus 9-Valent Vaccine, Recombinant). *Skinmed* **14,** 33–7

49. Cuzick, J. Gardasil 9 joins the fight against cervix cancer. *Expert Rev. Vaccines* **14,** 1047–1049 (2015).

50. Alon, D., Stein, G. Y., Hadas-Golan, V., Tau, L., Brosh, T. & Turner, D. Immunogenicity of Sci-B-Vac (a Third-Generation Hepatitis B Vaccine) in HIV-Positive Adults. *Isr. Med. Assoc. J.* **19,** 143–146 (2017).

51. Elhanan, E., Boaz, M., Schwartz, I., Schwartz, D., Chernin, G., Soetendorp, H., Gal Oz, A., Agbaria, A. & Weinstein, T. A randomized, controlled clinical trial to evaluate the immunogenicity of a PreS/S hepatitis B vaccine Sci-B-Vac™, as compared to Engerix B®, among vaccine naïve and vaccine non-responder dialysis patients. *Clin. Exp. Nephrol.* **22,** 151–158 (2018).

52. Regules, J. A., Cummings, J. F. & Ockenhouse, C. F. The RTS,S vaccine candidate for malaria. *Expert Rev. Vaccines* **10,** 589–599 (2011).

53. Olotu, A., Moris, P., Mwacharo, J., Vekemans, J., Kimani, D., Janssens, M., Kai, O., Jongert, E., Lievens, M., Leach, A., Villafana, T., Savarese, B., Marsh, K., Cohen, J. & Bejon, P. Circumsporozoite-Specific T Cell Responses in Children Vaccinated with RTS,S/AS01E and Protection against P falciparum Clinical Malaria. *PLoS One* **6,** e25786 (2011).

54. Moorthy, V. S. & Ballou, W. R. Immunological mechanisms underlying protection mediated by RTS,S: a review of the available data. *Malar. J.* **8,** 312 (2009).

55. Oropesa, R., Ramos, J. R., Falcón, V., -, A., Yan Ling, T., Zuo, Z., H Pui, D. Y., Lopez, M., Nelson Rodriguez, E., Lobaina, Y., Musacchio, A., Falcon, V., Guillen, G. & Aguilar, J. C. Characterization of the size distribution and aggregation of virus-like nanoparticles used as active ingredients of the HeberNasvac therapeutic vaccine against chronic hepatitis B. *Adv. Nat. Sci Nanosci. Nanotechnol* **8,** 1–6 (2017).

56. Pietrella, D., Rachini, A., Torosantucci, A., Chiani, P., Brown, A. J. P., Bistoni, F., Costantino, P., Mosci, P., d'Enfert, C., Rappuoli, R., Cassone, A. & Vecchiarelli, A. A beta-glucan-conjugate vaccine and anti-beta-glucan antibodies are effective against murine vaginal candidiasis as assessed by a novel in vivo imaging technique. *Vaccine* **28,** 1717–1725 (2010).

57. Bromuro, C., Romano, M., Chiani, P., Berti, F., Tontini, M., Proietti, D., Mori, E., Torosantucci, A., Costantino, P., Rappuoli, R. & Cassone, A. Beta-glucan-CRM197 conjugates as candidates antifungal vaccines. *Vaccine* **28,** 2615–2623 (2010).

58. Yin, Z., Chowdhury, S., McKay, C., Baniel, C., Wright, W. S., Bentley, P., Kaczanowska, K., Gildersleeve, J. C., Finn, M. G., BenMohamed, L. & Huang, X. Significant Impact of Immunogen Design on the Diversity of Antibodies Generated by Carbohydrate-Based Anticancer Vaccine. *Acs Chem. Biol.* **10,** 2364–2372 (2015).

4. Chapter 4: Conclusions and Future Outlook

Targeting vaccines towards receptors of the immune system holds great potential in improving vaccination therapies and diagnostics. The use of molecular address tags with high affinities for immune receptors holds the prospect of better presentation of antigen epitopes by antigen presenting cells (APCs), leading to enhanced antibody responses with greater specificity towards the antigen (**Figure 4. 1**). As discussed in **Chapter 1.4**, Dectin-1, a member of the C-type lectin family of receptors, is an appealing candidate for targeted therapies due to its high specificity for β-(1-3)-glucan oligosaccharides of at least DP12[1]. This thesis set out to exploit the Dectin-1 receptor, in order to achieve enhanced antibody responses towards antigens, by generating β-(1-3)-glucan address tags for incorporation into vaccination therapies.
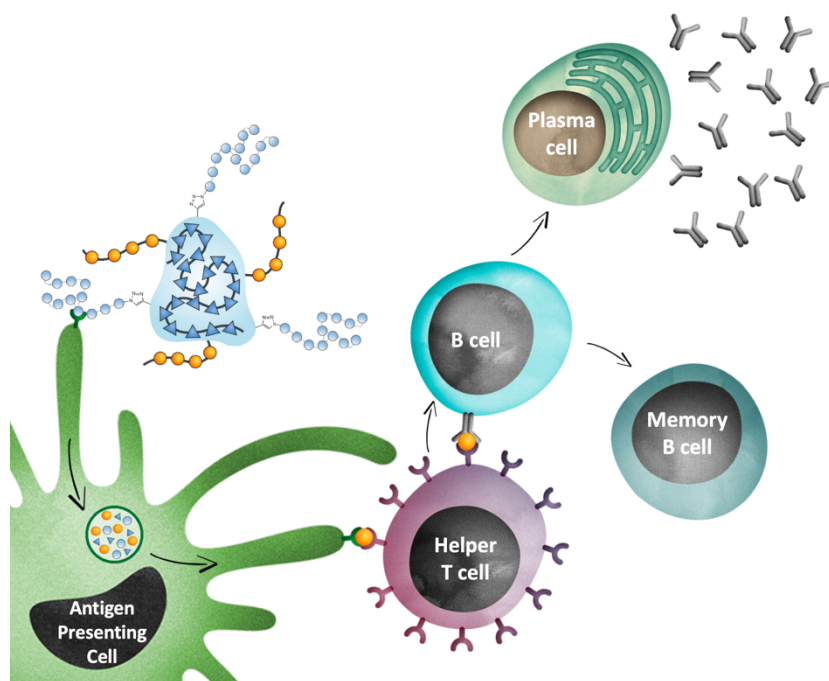
Figure 4. 1 – Schematic representation of targeted vaccines reading to presentation of antigen and generation of a specific antibody response.

This final chapter summarises the progress made during this thesis and the implications this research has for future vaccine designs.

4.1. β-Glucan address tags and their ability to bind to Dectin-1

Generation of β-(1-3)-glucan address tags was performed using naturally occurring sources of β-(1-3)-glucans, curdlan and laminarin. Curdlan, an easily accessible particulate form of β-(1-3)-glucan produced by *Agrobacterium spp.*, was subjected to chemical degradation by acetolysis [acetic anhydride/acetic acid (1:1)], to afford a range of linear acetylated β-(1-3)-glucan fragments of varying chain lengths. Initial fractionation was performed using flash chromatograph to isolate a series of acetylated oligosaccharides ranging from DP1-DP25. Following deacetylation using sodium methoxide (NaOMe), β-(1-3)-glucans were further fractionated by gel permeation chromatography to yield a fraction of β-(1-3)-glucans with an average DP of 15 which was chosen to act as an address tag based on literature reports suggesting a minimum of DP12 is required for binding to the Dectin-1 carbohydrate recognition domain (CRD)[1]. Laminarin, a naturally occurring β-(1-3)-glucan with occasional β-(1-6)-side chains, was also chosen for use as an MAT due to its known interactions with Dectin-1[2].

Many methods of conjugation exist for coupling carbohydrates to proteins. In this thesis, biorthogonal copper-free click chemistry was employed to conjugate β-(1-3)-glucan tags to BSA due to the biocompatibility of the reaction making it a safe option for use in vaccination therapies. A bifunctional linker, BCN-NHS, was used to pre-functionalised BSA with strained-ring cyclooctynes, which are able to react specifically and spontaneously with azide-functionalised molecules. Azides were introduced at the anomeric C-1 position of both β-(1-3)-glucan DP15 and laminarin using the methodology outlined by Tanaka *et al*[3], allowing the molecules to be conjugated by simply mixing together. Successful conjugation was confirmed by SDS-PAGE analysis, and Western Blot performed with an anti-β-(1-3)-glucan monoclonal antibody (mAb).

The ability of β-(1-3)-glucans to interact with Dectin-1 was analysed using a reporter cell line expressing murine Dectin-1. Whilst linear β-(1-3)-glucans of DP12 are able to bind to Dectin-1, DP15 was unable to induce a Dectin-1-

mediated signalling response, either as free oligosaccharides or conjugated to BSA. It was established that curdlan, a particulate β-(1-3)-glucan, was able to induce a strong Dectin-1-mediated signalling response, suggesting the dimerisation of Decitn-1 receptors, as described by Goodridge *et al*[4]. The ability of curdlan to initiate a Dectin-1-mediated signalling response highlights its potential use as an address tag. Conjugation of antigens directly on to the surface curdlan particles, as outlined in **Figure 4. 2**, possess an interesting prospect for a vaccine candidate. Further work is needed to verify this potential, but a two-component vaccine could simplify the process for generating glycoconjugate vaccines which are able to target to immune receptors and provide immunological protection. As carbohydrates are poorly immunogenic on their own, the choice of antigen would need careful consideration to ensure a robust immune response is achieved.
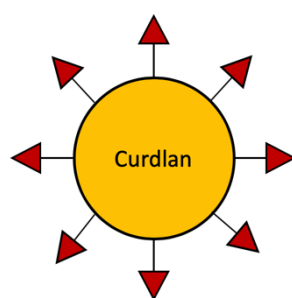
Figure 4. 2 – Schematic representation of a curdlan vaccine.

Laminarin was able to initiate a small signalling response when subjected to the reporter cell assay as a free oligosaccharide, suggest β-(1-6)-side branches, which are present in laminarin and possibly within curdlan[5], play a crucial role in Dectin-1 signalling. Interestingly, conjugation of laminarin to BSA enhanced the signalling response by 2.5x orders of magnitude. It is likely that the multimeric display of laminarin on the surface of BSA was able to induce Dectin-1 clustering, leading to initiation of a signalling cascade. It is possible that laminarin could also be implemented into a dual component vaccine, with antigens conjugated directly on to laminarin. However, the antagonistic propertis of laminarin towards Dectin-1 may hinder its use as an address tag.

In order to induce a strong signalling response, formation of laminarin glycoclusters is worth consideration. Multimeric presentation of laminarin on dendrimers to form glycoclusters, as outlined in **Figure 4. 3**, may allow for larger clustering of Dectin-1 receptors. With the development of new, multivalent scaffolds, this may prove a good candidate for targeted vaccines[6].
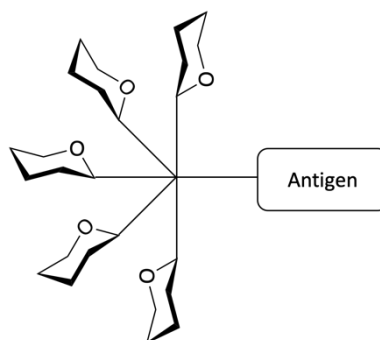
Figure 4. 3 – Schematic representation of β-glucan glycoclusters targeted antigens.

4.2. β-(1-2)-Mannan antigens

β-(1-2)-Mannotriose has previously been used in glycoconjugate vaccines due to its well characterised immunogenic effects[7], to the best of our knowledge, the immunological effects of β-(1-2)-mannotetraose remain unknown. Generation of β-(1-2)-mannose antigens has previously relied on complex chemical synthesis, making it difficult to generate scalable quantities for use in immunological assays. Enzymatic synthesis of β-(1-2)-mannose oligosaccharides offers a reliable route of generating scalable quantities of β-(1-2)-mannose antigens. It was anticipated, based on internal β-(1-2)-mannose trisaccharide residues being immunogenic epitopes[8], that DP4 could prove to be a good antigen for use in vaccines. In this research project, Teth514_1788 – a β-(1-2)-mannose phosphorylase enzyme[9], was utilised to generate β-(1-2)-mannose antigens, followed by isolation of β-(1-2)-mannotriose and β-(1-2)-mannotetraose by aqueous gel permeation chromatography.

β-(1-2)-Mannotriose and β-(1-2)-mannotetraose were functionalised with an anomic azide[3], and coupled to a methyl 5-hexynoate linker via copper-catalysed click chemistry. Attempts were made to conjugate the clicked products to BSA and TetHc via derivatisation of the methyl ester. Initially, the terminal methyl ester was successfully converted to an acyl hydrazide, however attempts to conjugate to carrier proteins TetHc and BSA resulted in protein precipitation. It is possible that changes to the isoelectric point of protein carriers resulted from over-conjugation of antigens, or the use of too large an excess of organic solvent. Further optimisation of the reaction conditions could result in successful conjugation of antigens to protein carriers, such as direct conversion of the methyl ester to an acyl azide, eliminating the need for the methyl ester to be converted to a hydrazine intermediate. Whilst these conjugation efforts were not successful, attempts to optimise this approach is ongoing and should focus on streamlining the conjugation efforts.

4.3. Virenose antigens in a vaccine towards Q fever

Despite being on the Centre for Disease Controls (CDC) list of potential biowarfare agents[10], there is not yet a human vaccine approved for protection against the causative agent of Q fever, *Coxiella burnetii*. Vaccines which have been licensed for use in livestock comprise whole-cell killed *C. burnetii*. This thesis set out to generate a Q fever vaccine with specificity towards unique carbohydrates antigens found within the LPS of the bacterium, in collaboration with JIC spin out Iceni Diagnostics, and Mologic Ltd.

Two Q fever vaccines were generated, both with Conjucore VLP, a proteinaceous carrier provided by Mologic Ltd, and laminarin address tags conjugated via a BCN linker. One vaccine candidate contained α-Vir(1-4)-α-Vir-propyl antigens, and the other β-Vir(1-4)-β-Vir-propyl antigen, both conjugated via BCN linkers. Immunisation trials were performed in collaboration with Mologic Ltd. Two rabbits per vaccine candidate type were immunised, with boosters administered at 28-day intervals and bleeds taken one-week post injection, until the final bleed at day 91.

Serum analysis by ELISA revealed a strong antibody reactivity towards α-Vir(1-4)-α-Vir- disaccharide when rabbits were immunised with α-Vir(1-4)-α-Vir-BCN-VLP-BCN-Laminarin. Immunisation with β-Vir(1-4)-β-Vir-BCN-VLP-BCN-Laminarin revealed a reactivity towards all virenose antigens, regardless of their linkage confirmation or chain length. The ability of antibodies within the serum to recognise monosaccharide α and β virenose antigens suggests it may be possible to immunise with monosaccharide virenose antigens. If so, this would have significant beneficial impact on the synthesis of virenose antigens which currently depend on complex chemical synthesis[11,12].

Although antibodies raised in this trial were unable to recognise *C. burnetii* whole killed cells, the use of virenose as an antigen should not be ruled out. Although the carbohydrates within the *O* antigen have been identified[13], the sequence in which they occur has yet to be elucidated. It may be that the location of virenose within the *O* antigen is not accessible to antibodies, or the antibodies present in the serum are located terminally within *O* antigen. Further work is required to identify the sequence of carbohydrates would help to better inform the optimal carbohydrate sequence to be used as antigens for Q fever vaccination.

4.4. Summary

There is still a long way to go before the research conducted in this thesis can be developed into a viable targeted vaccination therapy. The results obtained underpin on-going research into the development of monoclonal antibodies, currently being conducted by JIC and Iceni Diagnostics. Beyond vaccination therapies, the ability to generate antibodies with a strong specificity towards antigens has broad potential in the development in diagnostics, such as their use in lateral flow devices. Carbohydrates play an important role in disease development, prevention and cure, and further research is required to fully exploit their potential uses within therapeutics and diagnostics.

4.5. References

1. Palma, A. S., Feizi, T., Zhang, Y., Stoll, M. S., Lawson, A. M., Díaz-Rodríguez, E., Campanero-Rhodes, M. A., Costa, J., Gordon, S., Brown, G. D. & Chai, W. Ligands for the β-glucan receptor, dectin-1, assigned using 'designer' microarrays of oligosaccharide probes (neoglycolipids) generated from glucan polysaccharides. *J. Biol. Chem.* **281,** 5771–5779 (2006).

2. Smith, A. J., Graves, B., Child, R., Rice, P. J., Ma, Z., Lowman, D. W., Ensley, H. E., Ryter, K. T., Evans, J. T. & Williams, D. L. Immunoregulatory Activity of the Natural Product Laminarin Varies Widely as a Result of Its Physical Properties. *J. Immunol.* **200,** 788–799 (2018).

3. Tanaka, T., Nagai, H., Noguchi, M., Kobayashi, A. & Shoda, S. One-step conversion of unprotected sugars to beta-glycosyl azides using 2-chloroimidazolinium salt in aqueous solution. *Chem Commun* **23,** 3378–3379 (2009).

4. Goodridge, H. S., Reyes, C. N., Becker, C. A., Katsumoto, T. R., Ma, J., Wolf, A. J., Bose, N., Chan, A. S. H., Magee, A. S., Danielson, M. E., Weiss, A., Vasilakos, J. P. & Underhill, D. M. Activation of the innate immune receptor Dectin-1 upon formation of a 'phagocytic synapse'. *Nature* **472,** 471–475 (2011).

5. Saito, H., Misaki, A. & Harada, T. A Comparison of the Structure of Curdlan and Pachyman. *Agric. Biol. Chem.* **32,** 1261–1269 (1968).

6. Cominetti, M. M. D., Hughes, D. L. & Matthews, S. E. Open-resorcinarenes, a new family of multivalent scaffolds. *Org. Biomol. Chem.* **14,** 10161–10164 (2016).

7.   Lipinski, T., Fitieh, A., St Pierre, J. J., Ostergaard, H. L., Bundle, D. R., Touret, N., St. Pierre, J., Ostergaard, H. L., Bundle, D. R. & Touret, N. Enhanced Immunogenicity of a Tricomponent Mannan Tetanus Toxoid Conjugate Vaccine Targeted to Dendritic Cells via Dectin-1 by Incorporating beta-Glucan. *J. Immunol.* **190,** 4116–4128 (2013).

8.   Johnson, M. A., Cartmell, J., Weisser, N. E., Woods, R. J. & Bundle, D. R. Immunodominance of internal epitopes in Candida mannans 1 Molecular Recognition of Candida albicans (1→2)-β-Mannan Oligosaccharides by a Protective Monoclonal Antibody Reveals the Immunodominance of Internal Saccharide Residues. *J. Biol. Chem.* **287,** 18078–18090 (2012).

9.   Chiku, K., Nihira, T., Suzuki, E., Nishimoto, M., Kitaoka, M., Ohtsubo, K. & Nakai, H. Discovery of two β-1,2-mannoside phosphorylases showing different chain-length specificities from Thermoanaerobacter sp. X-514. *PLoS One.* **9,** e114882 (2014).

10.   Moodie, C., Thompson, H., Meltzer, M. & Swerdlow, D. Prophylaxis after Exposure to Coxiella burnetii. *Emerg. Infect. Dis.* **14,** 1558–1566 (2008).

11.   Brimacombe, J. S., Hanna, R. & Tucker, L. C. N. A synthesis of methyl 6-deoxy-3-C-methyl-α-d-gulopyranoside   (methyl   α-virenoside). *Carbohydr. Res.* **112,** 320–323 (1983).

12.   Hong, N., Sato, K. & Yoshimura, J. Synthesis of Methyl 6-Deoxy-3-C-methyl-β-D-gulopyranoside (Methyl β-Virenoside). *Bull. Chem. Soc. Jpn.* **54,** 2379–2382 (1981).

13.   Vadovic, P., Slaba, K., Fodorova, M., Skultety, L. & Toman, R. Structural and functional characterization of the glycan antigens involved in immunobiology of Q fever. *Ann. N. Y. Acad. Sci.* **1063,** 149–153 (2005).

5. Chapter 5: Materials and Methods

5.1. General Methods

All reagents were purchased from commercial suppliers (Sigma Aldrich, Pierce, Fisher Scientific Ltd), unless otherwise stated, and used without further purification.

5.1.1. Thin-Layer Chromatography

Thin layer chromatography (TLC) was performed on silica gel 60 F_{254} aluminium backed sheets (Merck). Carbohydrates were detected by staining with orcinol spray [2 % (w/v) in ethanol/sulfuric acid/water (8.3:1.1:0.6)] and developed by charring.

5.1.2. Mass Spectrometry

MALDI-TOF MS analysis was conducted on a Bruker Daltonics autoflex speed ToF/ToF mass spectrometer with a N_2 laser in linear 50 shot mode. A total of 500 shots were collected per sample with 60-90 % laser intensity and 32× gain, dependent on signal intensity. Mass data were analysed using Bruker Daltronics Flexanalysis software. Samples for MALDI-TOF MS analyses were prepared by mixing 0.5 μL of sample (1 mg mL^{-1}) with 0.5 μL matrix [DHB matrix for carbohydrate analysis (10 mg mL^{-1} in 30 % aq. MeCN), SA matrix for protein analysis (0.4 mg/mL in 70 % aq. MeCN, 0.1% TFA)], loading 1 μL of mixture onto an MTP AnchorChip 384 target plate and allowed to air dry and crystallise.

Low resolution electrospray ionisation mass spectrometry (ESI MS) was performed using an Advion expression^{L} Compact Mass Spectrometer Prior to injection, samples were filtered through a 0.22 μm membrane disk filters. Data was recorded in both positive and negative ionisation modes and processed using Advion Mass Express software.

5.1.3. HPAEC-PAD Analysis

High-performance anion-exchange chromatography coupled with pulsed electrochemical detection (HPAEC-PAD) analysis was performed on a Dionex IC system equipped with a CarboPac PA100 (4 x 250 mm) anion exchange column and guard cartridge, and an electrochemical detector to register peaks and determine their retention times. Mobile phase was composed of various combinations of 100 mM NaOH (eluent A) and 100 mM NaOH with 500 mM NaOAc (eluent B). For β-D-(1-3)-glucan and its fragments, the elution profile was as follows: 100 % A to 100 % B in 30 min then isocratic 100 % B for 10 min and finally 100 % A for 0.1 min. (1-2)-β-D-Mannooligosaccharides were analysed using 100 % A to 100 % B in 40 min then isocratic 100 % B for 10 min and finally 100 % A for 0.1 min.

β-D-(1-2)-Mannose oligosaccharides were analysed using mobile phases eluent A (100 mM NaOH) and eluent B (100 mM NaOH with 400 mM NaOAc) applied as a gradient to 100 % eluent B over 40 minutes, isocratic eluent B for 10 mins and ending with isocratic 100 % eluent A over 0.1 mins. Flow rates remained constant as 0.25 mL min^{-1} for all analysis.

5.1.4. Nuclear Magnetic Resonance Spectroscopy

NMR spectra were recorded on a Bruker Avange III HD 400 MHz spectrometer equipped with a broadband BBFO probe at 400 MHz (^{1}H) and 100 MHz (^{13}C) in deuterated solvents at 298 °C. Chemical shifts (δ) are reported in parts per million (ppm) using residual solvent signal for referencing. Spectra assignments were carried out with the aid of HSQCed two-dimensional correlation spectroscopy.

5.1.5. FTIR

Fourier transform infrared (FTIR) spectra were recorded on Perkin Elmer Spectrum BX II system equipped with MIRacle single-reflection horizontal Zn/Se ATR accessory.

5.1.6. SDS-PAGE analysis

Proteins were analysed by SDS-PAGE using RunBlue precast 4-20 % gradient or 8% gels (Expedeon). Before analysis, protein samples (10 μL) were mixed with laemmli buffer [10 μL (Biorad)] and boiled at 95 °C for 10 mins. Samples were allowed to cool, centrifuged briefly and then loaded on to SDS-PAGE gels as 10 μL samples. All SDS-PAGE analysis was performed alongside a Precision Plus Protein^{TM} Dual Color Ladder [5 μL (Biorad)] and run at 200 V for 50 mins in 1x RunBlue running buffer (Expedeon). Gels were stained with Coomassie Brilliant Blue Protein Stain (Sigma) for a minimum of 2 hrs to visualise proteins. Gels were imaged on a Syngene G:Box.

5.1.7. Western blot analysis

Unless otherwise stated, Western blot analysis was performed as follows. SDS-PAGE gels were carried out as outlined in Section 5.1.6 without protein staining. Proteins were transferred to nitrocellulose membrane, pre-wetted with water, in a cassette packed with blotting paper on both sides. Protein transfer was carried out in transfer buffer [25 mM tris, 192 mM glycine, 20 % aqueous methanol (1 L), pH 8.6] at 100 V for 1 hr at 4 °C. Following transfer, the membrane was washed with PBS (3x) and blocked with 5 % milk powder in PBS$_T$ (30 mL) for 2 hr at room temperature (RT). The membrane was again washed with PBS (3x) before applying the primary antibody, prepared in 1.4 % milk powder in PBS$_T$ (30 mL), for 2 hr at RT. After washing again with PBS (3x), a secondary antibody containing a horse radish peroxidase (HRP) conjugate was applied, prepared as per the primary antibody. The membrane was incubated for a further 1 hr at RT before washing a final time with PBS

(3x), briefly drip drying to remove excess PBS and developing with Chemiluminescence HRP substrate (Clontech) according the manufacturers instructions[1]. Membranes were imaged using an ImageQuant LAS 500 chemiluminescence CCD camera.

5.2. Chapter 2 experimental

5.2.1. Generation of acetylated laminarioligosaccharides by acetolysis of curdlan
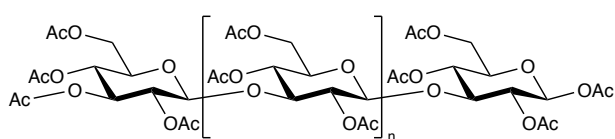
A suspension of curdlan [(10 g) Wako Chemicals] was vigorously stirred in AcOH-Ac$_2$O (1:1, 65 mL), and concentrated H$_2$SO$_4$ (10 mL) was added in a dropwise manner at 30-40 °C for 30 mins. The mixture was stirred for 24 hr at 28 °C before being brought to 20 °C and treated with NaOAc (30 g). Water (100 mL) was added and the mixture was stirred overnight. The precipitate was separated from the supernatant and dissolved in CH$_2$Cl$_2$ (400 mL), washed with H$_2$O and saturated aq. NaHCO$_3$ solution. Solvents were removed by evaporation and the products were purified by flash chromatography on silica gel (300 g) using gradient elution with toluene-acetone (90:10 to 40:60) to give twelve fractions containing both individual oligosaccharides and their mixtures. High molecular weight fraction 11 was selected. MALDI-TOF MS *m/z* 3869.86 [DP13+Na]$^+$, 4157.88 [DP14+Na]$^+$, 4445.90 [DP15+Na]$^+$, 4733.93 [DP16+Na]$^+$, 5021.83 [DP17+Na]$^+$, 5309.91 [DP18+Na]$^+$, 5597.94 [DP19+Na]$^+$, 5885.69 [DP20+Na]$^+$, 6173.98 [DP21+Na]$^+$, 6461.89 [DP22+Na]$^+$, 6749.63 [DP23+Na]$^+$, 7040.99 [DP24+Na]$^+$, calculated m/z 3870.12 [DP13+Na]$^+$, 4158.20 [DP14+Na]$^+$, 4446.29 [DP15+Na]$^+$, 4734.37 [DP16+Na]$^+$, 5022.46 [DP17+Na]$^+$, 5310.54 [DP18+Na]$^+$, 5598.63 [DP19+Na]$^+$, 5886.71 [DP20+Na]$^+$, 6174.80 [DP21+Na]$^+$, 6462.88 [DP22+Na]$^+$, 6750.97 [DP23+Na]$^+$, 7039.05 [DP24+Na]$^+$; ^{1}H NMR (400 MHz, CDCl$_3$), δ 5.10-4.80 (m, H-4), 5.10-4.75 (m, H-2), 4.50-4.30 (m, H-1), 4.40-

3.95 (m, H-6), 3.90-3.70 (m, H-3), 3.75-3.55 (m, H-5), 2.20-1.95 (m, OAc); ^{13}C NMR (100 MHz, CDCl$_3$) δ 100.7 (C-1), 78.2 (C-3), 72.5 (C-2), 71.7 (C-5), 68.0 (C-4), 61.8 (C-6), 20.6 (OAc).

5.2.2. Deacetylation of fraction 11 of curdlan acetolysis.
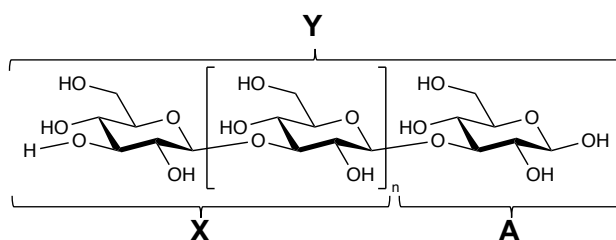
Fraction 11 of acetylated curdlan (260 mg) was dissolved in a mixture of dry methanol (20 mL) and dry CH$_2$Cl$_2$ (5 mL), 1 M NaOMe (100 µL) was added and the mixture was stirred at room temperature for 2 hrs. Solvents were removed under vacuum to leave a white powder which was dissolved in water (20 mL) and neutralised by Amberlite IR120 (H$^+$) resin until the pH became neutral as indicated by litmus paper.   The resin was filtered off and the water was removed by freeze-drying to give 115 mg of a white powder. Deacetylated products were analysed as unpurified mixture, MALDI-TOF MS, *m/z* 1013.17 [DP6+Na]$^+$, 1175.21 [DP7+Na]$^+$, 1337.24 [DP8+Na]$^+$, 1499.27 [DP9+Na]$^+$, 1661.30 [DP10+Na]$^+$, 1823.33 [DP11+Na]$^+$, 1985.37 [DP12+Na]$^+$, 2147.38 [DP13+Na]$^+$,   2309.40   [DP14+Na]$^+$,   2472.41   [DP15+Na]$^+$,   2633.45 [DP16+Na]$^+$,   2795.47   [DP17+Na]$^+$,   2957.48   [DP18+Na]$^+$,   3119.48 [DP19+Na]$^+$, 3281.46 [DP20+Na]$^+$, 3443.48 [DP21+Na]$^+$, calculated m/z 1013.32 [DP6+Na]$^+$, 1175.37 [DP7+Na]$^+$, 1337.42 [DP8+Na]$^+$, 1509.48 [DP9+Na]$^+$, 1661.53 [DP10+Na]$^+$, 1823.58 [DP11+Na]$^+$, 1985.63 [DP12+Na]$^+$, 2147.69 [DP13+Na]$^+$, 2309.74 [DP14+Na]$^+$, 2471.79 [DP15+Na]$^+$, 2633.85 [DP16+Na]$^+$,   2795.90   [DP17+Na]$^+$,   2957.95   [DP18+Na]$^+$,   3120.00 [DP19+Na]$^+$, 3282.06 [DP20+Na]$^+$, 3444.11 [DP21+Na]$^+$; HPAEC-PAD, retention time (min): 3.7 (DP1), 10.3 (DP2), 13.6 (DP3), 16.2 (DP4), 18.9 (DP5), 21.0 (DP6), 22.9 (DP7), 24.6 (DP8), 26.2 (DP9), 27.6 (DP10), 28.8 (DP11), 30.0 (DP12), 31.1 (DP13), 32.0 (DP14), 32.9 (DP15), 33.8 (DP16), 34.5 (DP17), 35.2 (DP18), 35.9 (DP19), 36.5 (DP20), 37.1 (DP21), 37.7

(DP22), 38.2 (DP23); ^{1}H NMR (400 MHz, D$_2$O), δ 5.15 (s, H-1^{A}α), 4.70-4.65 (m, H-1^X), 4.60 (s, H-1^{A}β), 3.90-3.60 (m, H-6^{Yab}), 3.75-3.65 (m, H-3^Y), 3.50-3.45 (m, H-2^Y), 3.50-3.40 (m, H-4^Y), 3.45-3.40 (m, H-5^Y), ^{13}C NMR (100 MHz, D$_2$O) δ 102.6 (C-1^X), 95.7 (C-1^{A}β), 92.0 (C-1^{A}α), 84.1 (C-3^Y), 75.7 (C-5^Y), 73.1 (C-2^Y), 67.9 (C-4^Y), 60.6 (C-6^Y).

5.2.3. β-D-(1-3)-Glucan DP 15 by fractionation using GPC

To produce β-D-(1-3)-glucan fractions with a narrower molecular weight distribution, the deprotected product described in 5.2.2 was fractionated by GPC on a Biogel P2 column (2.6 cm x 90 cm) heated to 40 °C and eluted with water at a 1 ml min^{-1} flow rate. Batches of 30 mg of 5.2.2 product were used for each run and 5.5 ml fractions were collected between 160 and 600 mins. Congruent fractions from each run were pooled and analysed by MALDI-TOF MS and HPAEC-PAD to allow selection a fraction with average DP 15. Lyophilisation yielded 16.7 mg of a white powder product. MALDI-TOF MS, *m/z* 2309.37 [DP14+Na]$^+$, 2471.38 [DP15+Na]$^+$, 2633.47 [DP16+Na]$^+$, 2795.47 [DP17+Na]$^+$, calculated *m/z* 2309.74 [DP14+Na]$^+$, 2471.79 [DP15+Na]$^+$, 2633.85 [DP16+Na]$^+$, 2795.90 [DP17+Na]$^+$; HPAEC-PAD retention time (min): 30.9 (DP13), 31.8 (DP14), 32.7 (DP15), 33.6 (DP16), 34.3 (DP17), 35.1 (DP18), 35.7 (DP19), 36.3 (DP20), 36.9 (DP21).

5.2.4. Anomeric azide of β-D-(1-3)-glucan DP15
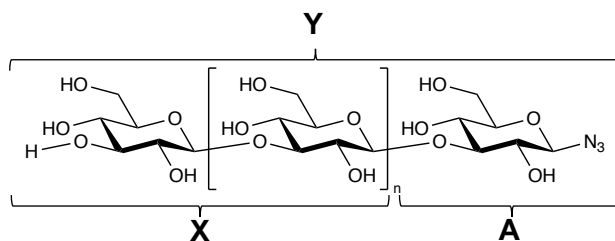
Anomeric azide was introduced following *Shoda*'s methodology[2]. 2-Chloro-1,3-Dimethylimidazolinium chloride [DMC (3.5 mg, 20 μmol, 5 eq)] was added to a mixture of β-(1-3)-glucan DP15 (10 mg, 4 μmole), DIPEA (10.7 μL, 61

158

µmol, 15 eq) and NaN_3 (81.3 mg, 2.5 M) in D_2O (0.5 mL), and the reaction mixture was stirred for 36 hrs at RT. The reaction mixture was then passed through a TSK HW40S GPC column (1.6 cm x 90 cm) in water at 0.5 ml min^{-1} for purification. Fractions containing carbohydrates were identified by TLC and staining with orcinol and then pooled. Lyophilisation yielded 8.7 mg of a white powder. ^1H NMR (400 MHz, D_2O), δ 5.15 (s, H-1^{A}α), 4.75-4.65 (m, H-1^X), 4.70 (s, H-1^{A}β-N_3), 4.60 (s, H-1^{A}β), 4.10-3.75 (m, H-4^{Y}α), 3.90-3.60 (m, H-6^{Yab}), 3.80-3.65 (m, H-3^Y), 3.60-3.35 (m, H-5^Y), 3.50-3.25 (m, H-2^Y), 3.50-3.30 (m, H-4^{Y}β); ^{13}C NMR (100 MHz, D_2O) δ 60.6 (C-6^Y), 68.8 (C-4^Y), 73.2 (C-2^Y), 75.6 (C-5^Y), 84.1 (C-3^Y), 89.9 (C-1^{A}β-N_3), 92.1 (C-1^{A}α), 95.6 (C-1^{A}β), 102.4 (C-1^X); FTIR ν_{max}/cm^{-1} 2122 (s, N_3).

5.2.5. Functionalised laminarin with anomeric azide group

R = -OH
    -Glc
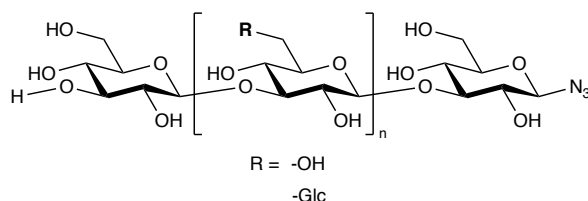
Laminarin was functionalised with an anomeric azide as described in **Section 5.2.4**. Briefly, DMC (12.1 mg, 71.4 µmol, 5 eq) was added to a mixture of laminarin [(50 mg, 14.3 µmol) Sigma], DIPEA (37.3 µL, 214.3 µmol, 15 eq) and NaN_3 (2.5 M) in D_2O (2 mL), and the reaction mixture was stirred for 36 hrs at RT. The reaction was then passed through a TSK HW40S GPC column (1.6 cm x 90 cm) in water at 0.5 ml min^{-1} for purification. Fractions containing carbohydrates were identified by TLC plate and staining with orcinol and then pooled. Lypholisation yielded 46.3 mg of white powder product. ^1H NMR (400 MHz, D_2O) δ 5.15 (s, H-1^{A}α), 4.75-4.65 (m, H-1^X), 4.70 (s, H-1^{A}β-N_3), 4.60 (s, H-1^{A}β), 4.10-3.75 (m, H-4^{Y}α), 3.90-3.60 (m, H-6^{Yab}), 3.80-3.65 (m, H-3^Y), 3.60-3.35 (m, H-5^Y), 3.50-3.25 (m, H-2^Y), 3.50-3.30 (m, H-4^{Y}β); ^{13}C NMR (100 MHz, D_2O) δ 60.6 (C-6^Y), 68.8 (C-4^Y), 73.2 (C-2^Y), 75.6 (C-5^Y), 84.1 (C-3^Y), 89.9 (C-1^{A}β-N_3), 92.1 (C-1^{A}α), 95.6 (C-1^{A}β), 102.4 (C-1^X); FTIR ν_{max}/cm^{-1} 2120 (s, N_3).

5.2.6. Preparation of BCN-functionalised BSA

BSA (2 mg mL^{-1} in PBS 5 mL) was reacted with (1R,8S,9s)-bicyclo[6.1.0]non-4-yn-9-ylmethyl N-succinimidyl carbonate (Sigma), hereafter referred to as BCN-NHS (10 µL of 0.15 M in DMSO), for 1 h before quenching with the addition of 1 M Tris-HCl (50 µl). Dialysis with 6-8 K MWCO Spectra/Por® dialysis membrane against dH$_2$O was used to remove small molecules and excess reagents. Final purification was via GPC using a TSK-HW40S column (26 mm × 900 mm) in water with a 0.5 mL min^{-1} flow rate. Refractive index and UV detectors were used to determine fractions containing protein conjugates, which were subsequently pooled. Lyophilisation yielded 9.1 mg of white powder. MALDI-TOF MS, m/z 68104, calculated m/z 68071. For SDS-PAGE analysis, see **Chapter 2.2.5.**

5.2.7. Coupling of BCN-functionalised protein to β-ᴅ-(1,3)-glucan DP15 azide and laminarin azide

Copper-free click reaction was employed to couple azide-functionalised β-glucans to BSA-BCN. BSA-BCN (2 mg mL^{-1} in 1x PBS) was mixed with β-ᴅ-(1-3)-glucan DP15 azide (0.8 mg, two times molar excess per mole of protein) and laminarin azide (2.6 mg, five times molar excess per mole of protein), respectively. The reaction mixtures were incubated at RT for 18 hours with gentle agitation followed by removal of unreacted β-glucans via dialysis against 1x PBS, using a 10 K MWCO SnakeSkin dialysis membrane tubing at room temperature. Successful conjugation was confirmed by MALDI-TOF/MS (**Figure 2. 17**), SDS-PAGE (**Figure 2. 16 A**) and Western blot analysis using a mouse anti-β-(1-3)-glucan mAb [Biosupplies Australia PTY LTD (**Figure 2. 16 B**)]. Protein concentration was determined to be 1.6 mg mL^{-1} and 1.7 mg mL^{-1} by Bradford assay for β-(1-3)-glucan DP15 and laminarin conjugates, respectively.

5.2.8. Reporter assay

Reporter cells were used to test the ability of β-D-(1-3)-glucan-containing glycoconjugates to initiate a signalling response through Dectin-1. Proteins, protein-glycan conjugates and glycans (2 μg in 100 μl) in coating buffer (Na_2CO_3-$NaHCO_3$, pH 9.5) was loaded onto a 96-well Nunc^{TM} MaxiSorp plate and incubated at 4 °C overnight. Supernatants were then discarded, and the plate was washed with PBS (200 μl). BWZ.36 cells expressing Dectin-1 provided by Dr N. Kawasaki of Quadrum Institute Biosciences-NBI, and were maintained on R10 [RPMI 1640 (Sigma) with 25 mM HEPES, FBS (10 % v/v), 2-mercaptoethanol (50 μM), streptomycin (100 U/ml) and L-glutamine (2 mM)]. Cells were washed with PBS and pelleted by gentle centrifugation at 270 x g for 5 mins before resuspending in R10 media. Cell density was determined by haemocytometer and adjusted to 0.5 x 106 cells/μl in R10. To each sample coated well 200 μl of cell suspension was added, and the plate incubated at 37 °C for 18 h. Following brief centrifugation at 270 x g for 5 mins, the supernatant was discarded, and cells were lysed by the addition of 100 μl Z buffer (100 mM 2-mercaptoethanol, 9 mM $MgCl_2$, 0.125 % NP-40 in PBS) containing chlorophenol red β-D-galactopyranoside (CPRG, 1.5 mM) to each well. The plate was again incubated at 37 °C for 1 h, until colour change was detected by absorbance measurement at 570 nm with 630 nm as a reference wavelength.

5.3. Chapter 3 experimental

### 5.3.1. Expression of Teth514_1788, a β-D-(1-2)-mannoside phosphorylase

Teth_1788, the β-D-(1-2)-mannoside phosphorylase used in this study was a kind gift from Josef Voglmeir[3]. Rosetta 2 (DE3) (Novagen) strains containing the expression plasmid were grown in LB broth [1000 mL (1 % tryptone, 1 % NaCl, 0.5 % yeast extract) containing carbenicillin (50 µg mL^{-1})] at 37 °C with 200 rpm agitation until an absorbance of 0.6 at 600 nm was reached. Expression was then induced by the addition of 0.1 mM IPTG (final concentration) and growth continued at 18 °C with 200 rpm agitation for 24 hr. Cells were harvested by centrifugation at 10,000 x g for 20 min, followed by suspension in Buffer A [50 mM HEPES-NaOH buffer (pH 7.0), 0.5 M NaCl]. Cells were disrupted by sonication a Sonics Vibra Cell^{TM} probe sonicator at 70 % intensity and the supernatant collected by centrifugation at 20,000 x g for 20 mins at 4 °C. The His-tagged protein was isolated by affinity chromatography on an AKTA prime system equipped with a 1 mL HisTrap HP column equilibrated in Buffer A. Fractions collected were analysed by SDS-PAGE (**Figure 3. 22 A**) and Western blot (**Figure 3. 22 B**) to determine the estimated molecular mass. Fractions containing the correct mass were pooled and the buffer exchanged to Tris buffer (50 mM Tris-HCl, 0.5 M NaCl) using an AMICON Ultra-15 10 K MWCO filter and washing three times at 4,000 x g for 15 mins. Protein concentration was determined be 26 mg mL^{-1} in 5 mL by BCA assay from 2 L of culture, and the molecular mass determined by MALDI-TOF MS (**Figure 3. 24**).

5.3.2. Synthesis of β-D-(1-2)-mannan oligosaccharides

A reaction mixture (30 mL) containing mannose (10 mg, 2 mM), mannose-1-phosphate [(M1P) 62.4. mg, 8 mM] and Teth514_1788 (0.5 mg mL^{-1} final concentration in 0.2 M ammonium acetate buffer, pH 5) at 30 °C for 6 hr. The reaction was terminated by boiling at 95 °C for 15 mins, the mixture was briefly centrifuged to pellet the denatured protein and the supernatant filtered through

a 0.22 μm membrane filter. Salts and excess M1P were removed by passing through a charcoal/celite (50:50) Biotage® 10g column prepared in water. Mannose oligosaccharides were eluted off the column in 95 % aqueous ethanol and the solvent was removed by evaporation *in vacuo* to yield mannooligosaccharides (45 mg). TLC [butanol/ethanol/water (10:8:7)] R_f 0.58 (DP1), 0.45 (DP2), 0.36 (DP3), 0.31 (DP4), 0.26 (DP5); MALDI-TOF MS *m/z* 527.3 [DP3+Na]$^+$, 689.4 [DP4+Na]$^+$, 851.4 [DP5+Na]$^+$, 1013.1 [DP6+Na]$^+$, 1175.6 [DP7+Na]$^+$, 1337.6 [DP8+Na]$^+$, 1509.7 [DP9+Na]$^+$, 1661.7 [DP11+Na]$^+$, 1823.7 [DP12+Na]$^+$, 1986.7 [DP13+Na]$^+$; calculated *m/z* 527.2 [DP3+Na]$^+$, 689.2 [DP4+Na]$^+$, 851.4 [DP5+Na]$^+$, 1013.1 [DP6+Na]$^+$, 1175.6 [DP7+Na]$^+$, 1337.6 [DP8+Na]$^+$, 1509.7 [DP9+Na]$^+$, 1661.7 [DP11+Na]$^+$, 1823.7 [DP12+Na]$^+$, 1986.7 [DP13+Na]$^+$; HPAEC-PAD retention time (min): 3.7 (DP1), 5.9 (DP2), 9.8 (DP3), 11.7 (DP4), 13.1 (DP5), 14.1 (DP6), 15.0 (DP7), 16.0 (DP8), 16.1 (M1P).

5.3.3. β-D-(1-2)-Mannotriose
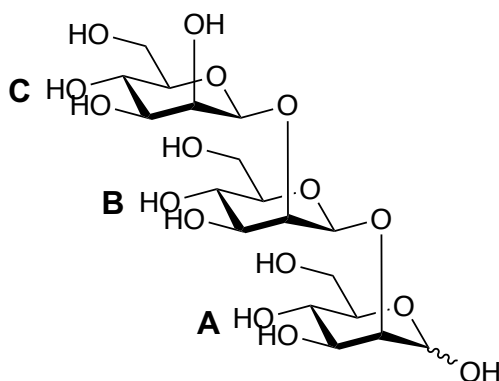
Purification of β-D-(1-2)-mannotriose was performed by GPC using a Biogel P2 chromatography column (2.5 x 90 cm) in water with a flow rate of 0.5 mL min^{-1}. Fractions were collected at 6 min intervals from 320 to 800 mins. On the basis of TLC [butanol/ethanol/water (10:8:7) R_f 0.36 **Appendices 6. 12**] and HPAEC-PAD (**Appendices 6. 11**), fractions 43-47, containing exclusively β-D-(1-2)-mannotriose, were pooled. Lyophilisation yielded white powder (6.2 mg). ESI-MS *m/z* 526.9 [M+Na]$^+$, calculated *m/z* 527.2 [M+Na]$^+$; HPAEC-PAD retention time = 9.76 min; ^{1}H NMR (600 MHz, D$_2$O) δ 5.10 (1H, d, $J_{1,2}$ = 1.68

Hz, H-1^{A}α), 4.85 (1H, d, $J_{1,2}$ = 2.07 Hz, H-1^{A}β), 4.85-4.70 (3H, m, H-1^{C}β, H-1^{B}β, H-1^{C}α), 4.70 (1H, s, H-1^{B}α), 4.30 (1H, d, $J_{1,2}$ = 3.12 Hz, H-2^{B}β), 4.15 (1H, d, $J_{1,2}$ = 3.24 Hz, H-2^{B}α), 4.00 (1H, d, $J_{1,2}$ = 3.2 Hz, H-2^{A}β), 4.10-4.00 (2H, m, H-2^{C}α, H-2^{C}β), 3.95 (1H, dd, $J_{1,2}$ = 2.04 Hz, $J_{2,3}$ = 3.24 Hz, H-2^{A}α), 3.85-3.75 (2H, m, H-6^{Ba}α, H-6^{Ca}β), 3.80 (1H, d, $J_{1,2}$ = 3.04, H-3^{A}α), 3.75-3.70 (2H, m, H-6^{Aa}α, H-6^{Aa}β), 3.65-3.60 (2H, m, H-5^{A}α, H-6^{Bb}α), 3.60-3.55 (2H, m, H-6^{Cb}α, H-6^{Ab}β), 3.60-3.50 (3H, m, H-3^{B}α, H-3^{B}β, H-3^{A}β), 3.55-3.45 (2H, m, H-3^{C}α, H-3^{C}β), 3.55-3.45 (3H, m, H-4^{A}α, H-4^{B}α, H-4^{B}β), 3.40-3.35 (3H, m, H-4^{C}α, H-4^{C}β, H-4^{A}β), 3.30-3.20 (5H, m, H-5^{A}β, H-5^{B}α, H-5^{B}β, H-5^{C}α, H-5^{C}β); ^{13}C NMR (151 MHz, D$_2$O) δ 100.9 (C-1^{B}β), 100.8 (C-1^{C}α), 100.7 (C-1^{C}β), 98.8 (C-1^{B}α), 93.5 (C-1^{A}β), 91.8 (C-1^{A}α), 79.5 (C-2^{A}β), 78.4 (C-2^{B}α, C-2^{A}α), 77.9 (C-2^{B}β), 76.2 (C-5^{A}β, C-5^{B}α, C-5^{B}β, C-5^{C}α, C-5^{C}β), 72.7 (C-3^{C}α, C-3^{C}β), 72.3 (C-5^{A}α), 72.0 (C-3^{B}α, C-3^{B}β, C-3^{A}β), 70.2 (C-2^{C}α, C-2^{C}β), 69.1 (C-3^{A}α), 67.1 (C-4^{A}β, C-4^{A}α), 66.8 (C-4^{B}α, C-4^{B}β), 66.6 (C-4^{C}α, C-4^{C}β), 60.9 (C-6^{C}α), 60.5 (C-6^{A}α), 60.3 (C-6^{B}α).

5.3.4. β-D-(1-2)-Mannotetraose
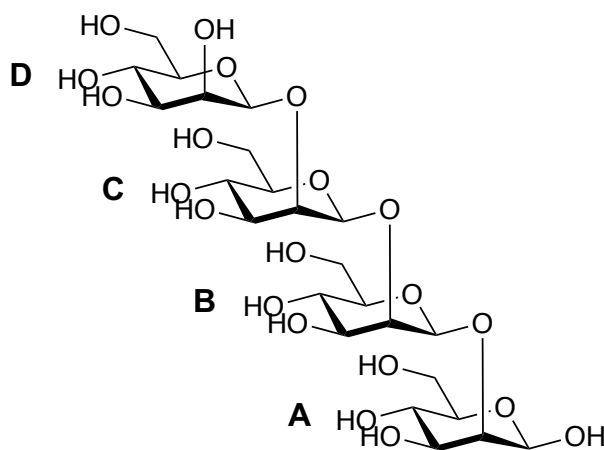
Purification of the title compound was carried out as described in **Section 5.3.2**. Fractions 36-40, identified by TLC [butanol/ethanol/water (10:8:7) R$_f$ 0.31 (**Appendices 6. 12**)] and HPAEC PAD (**Appendices 6. 11**) as containing exclusively β-D-(1-2)-mannotetraose, were pooled and lyophilised to yield white powder (5.3 mg). ESI-MS m/z 689.0 [M+Na]$^+$, calculated m/z 689.2

[M+Na]$^+$; HPAEC-PAD retention time = 11.58 min; ^{1}H NMR (600 MHz, D$_2$O) δ 5.10 (1H, d, $J_{1,2}$ = 1.5 Hz, H-1^{A}α), 4.90 (1H, s, H-1^{C}β), 4.85 (1H, s, H-1^{A}β), 4.80-4.75 (3H, m, H-1^{C}α, H-1^{D}α, H-1^{D}β), 4.70 (1H, s, H-1^{B}β), 4.65 (1H, s, H-1^{B}α), 4.25 (1H, d, $J_{1,2}$ = 3.24 Hz, H-2^{C}α), 4.25-4.20 (2H, m, H-2^{B}β, H-2^{C}β), 4.10 (1H, d, $J_{1,2}$ = 3.24 Hz, H-2^{B}α), 4.00 (1H, d, $J_{1,2}$ = 2.99 Hz, H-2^{A}β), 4.00-3.95 (2H, m, H-2^{D}α, H-2^{D}β), 3.95 (1H, dd, $J_{1,2}$ = 1.97 Hz, $J_{2,3}$ = 2.99 Hz, H-2^{A}α), 3.80-3.70 (3H, m, H-6Da, H-6^{Ba}α, H-6^{Ca}α), 3.75-3.70 (2H, m, H-3^{A}α, H-4^{A}α), 3.70 (1H, s, H-6^{Aa}α), 3.65-3.60 (2H, m, H-6^{Bb}α, H-6^{Ab}α), 3.65-3.60 (1H, m, H-5^{A}α), 3.60-3.50 (2H, m, H-6^{Cb}α, H-6^{Db}), 3.55-3.50 (3H, m, H-3^{B}α, H-3^{B}β, H-3^{A}β), 3.50-3.40 (2H, m, H-3^{C}α, H-3^{C}β), 3.45-3.40 (2H, m, H-4^{C}α, H-4^{C}β), 3.45-3.40 (2H, m, H-3^{D}α, H-3^{D}β), 3.40-3.35 (2H, m, H-4^{D}α, H-4^{D}β), 3.40-3.35 (2H, m, H-4^{B}α, H-4^{B}β), 3.25 (1H, s, H-4^{A}β), 3.25-3.15 (7H, m, H-5^{A}β, H-5^{B}α, H-5^{D}β, H-5^{C}α, H-5^{C}β, H-5^{D}α, H-5^{D}β); ^{13}C NMR (151 MHz, D$_2$O) δ 101.2-100.9 (m, C-1^{C}α, C-1^{B}β, C-1^{C}β, C-1^{D}α, C-1^{D}β), 99.2 (s, C-1^{B}α), 93.5 (s, C-1^{A}β), 92.1 (s, C-1^{A}α), 80.0 (s, C-2^{A}β), 79.4 (s, C-2^{B}α), 79.0 (s, C-2^{B}β), 78.7 (s, C-2^{A}α), 78.4 (s, C-2^{C}α), 78.3 (s, C-2^{C}β), 76.3-76.1 (m, C-5^{C}α, C-5^{D}α, C-5^{A}β, C-5^{B}α), 72.9 (d, C-3^{D}α, C-3^{D}α), 72.4 (s, C-5^{A}α), 72.2-72.2 (d, C-3^{C}α, C-3^{C}β), 71.9-71.9 (t, C-3^{A}α, C-3^{B}β, C-3^{B}α), 70.4 (s, C-2^{D}α, C-2^{D}β), 69.1 (s, C-3^{A}α), 67.4 (s, C-4^{A}α, C-4^{A}β), 67.2-67.1 (d, C-4^{C}β, C-4^{C}α), 70.0-66.9 (d, C-4^{B}α, C-4^{B}β), 66.8-66.8 (d, C-4^{D}β, C-4^{D}α), 61.2-61.2 (d, C-6^{C}α), 60.8 (s, C-6^{D}α), 60.7-60.6 (m, C-6^{B}α), 60.4 (s, C-6^{A}α).

5.3.5. Methyl 5-hexynoate
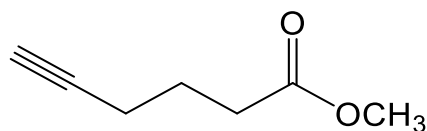
Methyl hexynoate was synthesised as described by *Cody et al*[4]. Hexynoic acid (1 g, 15.9 mmol, 1 eq) was mixed with K$_2$CO$_3$ (1.3 g, 19.0 mmol, 1.2 eq) in DMF (30 mL) and cooled to 0 °C with stirring. Iodomethane (1.575 g, 22.2 mmol, 1.4 eq) was added to the reaction mixture dropwise and the solution was allowed to warm to room temperature over 3 hours. After 3 hours, the

reaction was diluted with water (30 mL), extracted twice with EtOAc (20 mL), and washed 3 times with water (20 mL) and 3 times with 50 % brine (20 mL) before being dried over magnesium sulfate, filtered and concentrated to afford an oily product (620 mg, 62 %); TLC [hexane/ethyl acetate (8:2)] R_f 0.64; ESI-MS m/z 149.2 [M+Na]$^+$, calculated m/z 149.06 [M+Na]$^+$; ^{1}H NMR (400 MHz, CDCl$_3$) δ 3.68 (3H, s, CH$_3$), 2.46 (2H, t, J = 7.5 Hz, CH$_2$), 2.26 (2H, td, J = 6.9, 2.7 Hz, CH$_2$), 1.97 (1H, t, J = 2.6 Hz, CH), 1.85 (2H, q, J = 7.2 Hz, CH$_2$); ^{13}C NMR (100 MHz, CDCl$_3$) δ 179.6 (COOCH$_3$), 83.2 (CCH$_2$), 69.5 (HC), 51.6 (OCH$_3$), 32.6 (CH$_2$COOCH$_3$), 23.3 (CH$_2$), 17.7 (CCH$_2$).

5.3.6. β-D-(1-2)-Mannotriosyl azide
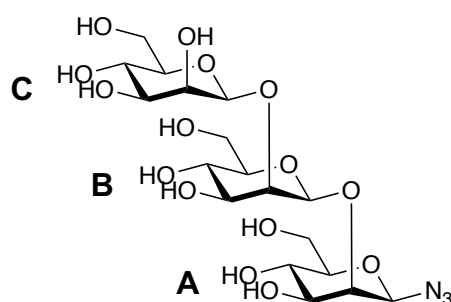
Anomeric azide was introduced following *Shoda*'s methodology[2]. DMC (8.4 mg, 49.6 μmol, 5 eq) was added to a mixture of β-D-(1-2)-mannotriose (5 mg, 9.9 μmol), DIPEA (25.9 mL, 148.8 μmol, 15 eq) and NaN$_3$ (81.3 mg, 1.25 mmol, 2.5 M) in D$_2$O (0.5 mL), and the reaction mixture was stirred for 3 hrs at RT. The reaction mixture was then passed through a TSK HW40S GPC column (1.6 × 90 cm) in water at 0.5 ml min^{-1}, fractions containing carbohydrates were identified by TLC and staining with orcinol and then pooled to yield white powder (4.2 mg, 80 %). ESI-MS m/z 552.1 [M+Na]$^+$, calculated m/z 552.2 [M+Na]$^+$; ^{1}H NMR (400 MHz, D$_2$O) δ 5.60 (1H, d, $J_{1,2}$ = 1.86 Hz, H-1^{A}α-N$_3$), 5.00 (1H, d, $J_{1,2}$ = 1.71 Hz, H-1^{A}β-N$_3$), 4.90-4.80 (4H, m, H-1^{C}β, H-1^{B}β, H-1^{C}α, H-1^{B}α), 4.40 (1H, d, $J_{1,2}$ = 3.18 Hz, H-2^{B}β), 4.25 (1H, t, $J_{1,2}$ = 3.66 Hz, H-2^{B}α) 4.15 (1H, d, $J_{1,2}$ = 2.99 Hz, H-2^{A}β), 4.15-4.05 (2H, m, (H-2^{C}α, H-2^{C}β), 4.05 (1H, m, H-2^{A}α), 3.95-3.85 (4H, m, H-6^{Ba}α, H-6^{Bb}α, H-6^{Ca}β, H-6^{Cb}α), 3.75 (2H, m, H-5^{A}α, H-5^{C}α), 3.75-3.65 (3H, m, H-6^{Aa}α, H-6^{Aa}β,

H-6$^{Ab}\beta$), 3.70-3.60 (3H, m, H-3$^B\alpha$, H-3$^B\beta$, H-3$^A\beta$), 3.65 (1H, m, H-4$^A\alpha$), 3.60-3.55 (4H, m, H-4$^B\alpha$, H-4$^B\beta$, H-3$^C\alpha$, H-3$^C\beta$), 3.55-3.45 (3H, m, H-4$^A\beta$, H-4$^C\alpha$, H-4$^C\beta$), 3.45 (1H, m, H-3$^A\alpha$), 3.40-3.30 (4H, m, H-5$^A\beta$, H-5$^B\alpha$, H-5$^B\beta$, H-5$^C\beta$); ^{13}C NMR (100 MHz, D$_2$O) δ 100.9 (C-1$^B\beta$, C-1$^C\alpha$, C-1$^C\beta$), 98.8 (C-1$^B\alpha$), 87.6 (C-1$^A\alpha$-N$_3$), 86.9 (C-1$^A\beta$-N$_3$), 79.3 (C-2$^A\beta$), 78.5 (C-2$^B\alpha$), 78.3 (C-3$^A\alpha$), 77.9 (C-2$^B\beta$), 77.3 (C-2$^A\alpha$), 76.4 (C-5$^A\beta$, C-5$^B\alpha$, C-5$^B\beta$, C-5$^C\beta$), 74.6 (C-5$^A\alpha$), 73.0 (C-3$^C\alpha$, C-3$^C\beta$), 72.1 (C-3$^B\alpha$, C-3$^B\beta$, C-3$^A\beta$), 70.5 (C-2$^C\alpha$, C-2$^C\beta$), 69.0 (C-5$^C\alpha$), 66.8 (C-4), 60.8 (C-6); FTIR ν_{max}/cm^{-1} 2118.5 (s, N$_3$).

5.3.7. β-D-(1-2)-Mannotetraosyl azide
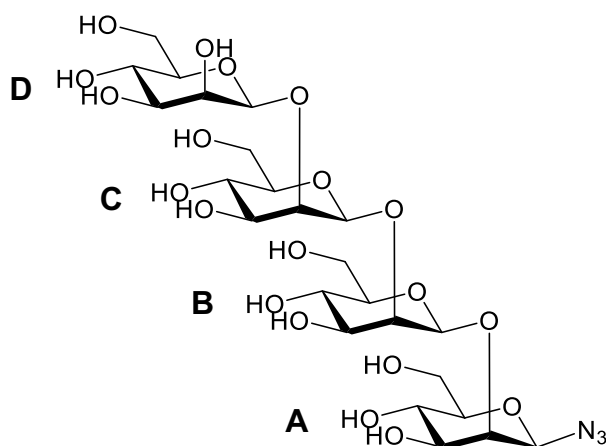
Anomeric azide was introduced as described in **Chapter 2.2.4.** Briefly, DMC (6.3 mg, 37.5 μmol, 5 eq) was added to a mixture of β-D-(1-2)-mannotetraose (5 mg, 7.5 μmol), DIPEA (19.6 μL, 112.6 μmol, 15 eq) and NaN$_3$ (81.3 mg, 1.25 mmol, 2.5 M) in D$_2$O (0.5 mL), and the reaction mixture was stirred for 3 hrs at RT. The reaction mixture was then passed through a TSK HW40S GPC column (1.6cm x 90 cm) in water at 0.5 ml min^{-1} for purification. Fractions containing carbohydrates were monitored by spotting on a TLC plate and staining with orcinol and then pooled to yield a white powder product (4.5 mg, 86.7 %). The introduction of an anomeric azide was confirmed by ESI-MS, HSCQed NMR and FTIR. ESI-MS m/z 714.1 [M+Na]$^+$, calculated m/z 714.2 [M+Na]$^+$; ^{1}H NMR (400 MHz, D$_2$O) δ 5.25 (1H, d, $J_{1,2}$ = 1.81 Hz, H-1$^A\alpha$), 5.10 (1H, d, $J_{1,2}$ = 1.66 Hz, H-1$^A\beta$-N$_3$), 5.00 (1H, d, $J_{1,2}$ = 2.33 Hz, H-1$^C\beta$), 4.95 (1H,

s, H-1^{A}β), 4.95-4.80 (4H, m, H-1^{B}β, H-1^{C}α, H-1^{D}α, H-1^{D}β), 4.80 (1H, s, H-1^{B}α), 4.40-4.30 (3H, m, H-2^{B}β, H-2^{C}α, H-2^{C}β), 4.20-4.10 (2H, m, H-2^{A}β, H-2^{B}α), 4.10-4.05 (2H, m, H-2^{D}α, H-2^{D}β), 4.05 (1H, t, $J_{1,2}$ = 2.54 Hz, H-2^{A}α), 3.95-3.85 (3H, m, H-6^{Ba}α, H-6^{Ca}α, H-6Da), 3.90-3.85 (3H, m, H-3^{A}α, H-4^{A}α, H-6^{Aa}α), 3.75 (1H, m, H-5^{A}α), 3.80-3.65 (4H, m, H-6^{Bb}α, H-6^{Ab}α, H-6^{Cb}α, H-6^{Db}), 3.70-3.65 (3H, m, H-3^{B}α, H-3^{B}β, H-3^{A}β), 3.65-3.55 (4H, m, H-3^{C}α, H-3^{C}β, H-3^{D}α, H-3^{D}β), 3.60-3.40 (7H, m, H-4^{C}α, H-4^{C}β, H-4^{D}α, H-4^{D}β, H-4^{B}α, H-4^{B}β, H-4^{A}β), 3.40-3.30 (7H, m, H-5^{A}β, H-5^{B}α, H-5^{B}β, H-5^{C}α, H-5^{C}β, H-5^{D}α, H-5^{D}β); ^{13}C NMR (100 MHz, D$_2$O) δ 101.1 (C-1^{B}β, C-1^{C}α, C-1^{C}β, C-1^{D}α, C-1^{D}β), 99.1 (C-1^{B}α), 93.4 (C-1^{A}β), 92.0 (C-1^{A}α), 86.8 (C-1^{A}β-N$_3$), 79.1 (C-2^{A}α, C-2^{A}β, C-2^{B}β, C-2^{B}β, C-2^{C}α, C-2^{C}β), 76.2 (C-5^{A}β, C-5^{B}α, C-5^{B}β, C-5^{C}α, C-5^{C}β, C-5^{D}α, C-5^{D}β), 72.3 (C-3^{A}β, C-3^{B}α, C-3^{B}β, C-3^{C}α, C-3^{C}β, C-3^{D}α, C-3^{D}β, C-5^{A}α), 70.4 (C-2^{D}α, C-2^{D}β), 69.0 (C-3^{A}α, C-4^{A}α), 66.9 (C-4^{A}β, C-4^{B}α, C-4^{B}β, C-4^{C}α, C-4^{C}β, C-4^{D}α, C-4^{D}β), 60.6 (C-6); FTIR ν$_{max}$/cm^{-1} 2122.8 (s, N$_3$).

5.3.8. 1-(2-*O*-(2-*O*-β-D-mannopyranosyl-β-D-mannopyranosyl)-β-D-mannopyranosyl)-4-(3-methoxycarbonylpropyl) [1,2,3]-triazole

A mixture of β-D-(1-2)-mannotriosyl azide (4 mg, 7.6 μmol), methyl 5-hexynoate (4.5 mL, 37.8 μmol, 5 eq), CuSO$_4$ (120 μg, 0.76 μmol, 0.1 eq), NaASc (299.5 mg, 1.51 μmol, 0.2 eq) and tris(3-hydroxypropyltriazolylmethyl)amine [THPTA (1.3 mg, 10 mM)] was stirred in a

mixture of water/*t*-butanol (1:10) at 50 °C for 16 hours. Excess of methyl 5-hexynoate was removed by extraction with EtOAc and the aqueous fractions were purified by GPC using a TSK HW40S column (1.6 x 90 cm) in water at 0.5 mL min^{-1} to afford a white powder, yield 4.5 mg (90.8 %), ESI-MS, *m/z* 678.5 [M+Na]$^+$, calculated m/z 678.2 [M+Na]$^+$; ^{1}H NMR (400 MHz, D$_2$O) δ 8.00 (1H, s, H-1^{A}β-triazole), 7.95 (1H, s, H-1^{A}α-triazole), 6.15 (1H, d, $J_{1,2}$ = 2.87 Hz, H-1^{A}α), 6.05 (1H, s, H-1^{A}β), 4.90-3.15 (36H, m, H-2, H-3, H-4, H-5, H-6), 3.60 (OC*H$_3$*), 2.74 (C*H$_2$*C(O)OCH$_3$), 2.37 (CH$_2$C*H$_2$*CH$_2$), 1.92 (CHC*H$_2$*CH$_2$).

5.3.9. 1-(2-*O*-(2-*O*-(2-*O*-β-D-mannopyranosyl-β-D-mannopyranosyl)-β-D-mannopyranosyl)β-D-mannopyranosyl)-4-(3-methoxycarbonylpropyl) [1,2,3]-triazole
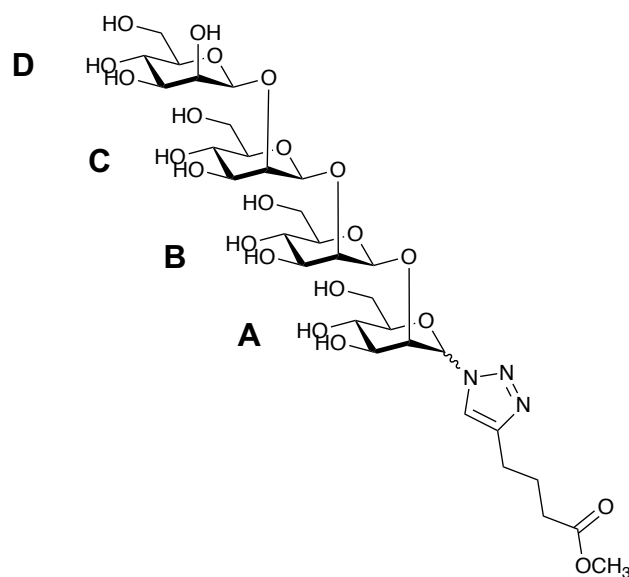
β-D-(1-2)-mannotetraosyl azide (4 mg, 5.79 μmol) was reacted with methyl 5-hexynoate (3.4 μL, 28.93 μmol, 5 eq), CuSO$_4$ (92.4 μg, 0.58 μmoles, 0.1 eq), NaASc (229.3 μg, 1.16 μmol, 0.2 eq) and tris(3-hydroxypropyltriazolylmethyl)amine [THPTA (1.3 mg, 10 mM)] in 300 μL of water/*t*-butanol (1:10) at 50 °C for 16 hours. Excess linker was removed by washing with EtOAc and the aqueous fractions purified by GPC, using a TSK

HW40S (1.6 x 90 cm) column in water at 0.5 mL min^{-1}, to afford a white powder product (4.2 mg, 88.8 %). Product analysis was performed by ESI-MS **Section 5.1.2** and ^{1}H NMR **Section 5.1.4**. ESI-MS m/z 840.6 [M+Na]$^+$ found, calculated m/z 840.3 [M+Na]$^+$; ^{1}H NMR (400 MHz, D$_2$O) δ 8.00 (1H, s, H-1^{A}β-triazole), 7.95 (1H, s, H-1^{A}α-triazole), 6.15 (1H, d, $J_{1,2}$ = 2.87 Hz, H-1^{A}α), 6.10 (1H, s, H-1^{A}β), 4.95-3.15 (48H, m, H-2, H-3, H-4, H-5, H-6), 3.60 (OC$\underline{H_3}$), 2.74 (C$\underline{H_2}$C(O)OCH$_3$), 2.37 (CH$_2$C$\underline{H_2}$CH$_2$), 1.92 (CHC$\underline{H_2}$CH$_2$).

5.3.10. 1-(2-*O*-(2-*O*-β-D-mannopyranosyl-β-D-mannopyranosyl)-β-D-mannopyranosyl)-4-(3-hydrazinocarbonylpropyl) [1,2,3]-triazole

A mixture of β-D-(1-2)-mannotriosyl clicked product 5.3.8 (4.5 mg, 7.63 μmol) was incubated with hydrazine monohydrate (1 mL) and ethanol (2.5 mL) at 55 °C for 6 hr. Excess reagents and by-products were removed by co-evaporation with toluene (3 x 10 mL). Completion of the conversion of methyl ester into acyl hydrozide was confirmed by disappearance of methyl ester a signal at δ 3.6 ppm in ^{1}H NMR spectrum (**Appendices 6. 20 A**).
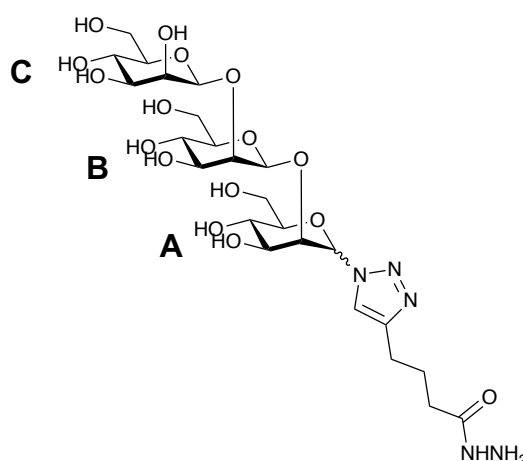
5.3.11. 1-(2-*O*-(2-*O*-(2-*O*-β-D-mannopyranosyl-β-D-mannopyranosyl)-β-D-mannopyranosyl)β-D-mannopyranosyl)-4-(3-hydrazinocarbonylpropyl) [1,2,3]-triazole
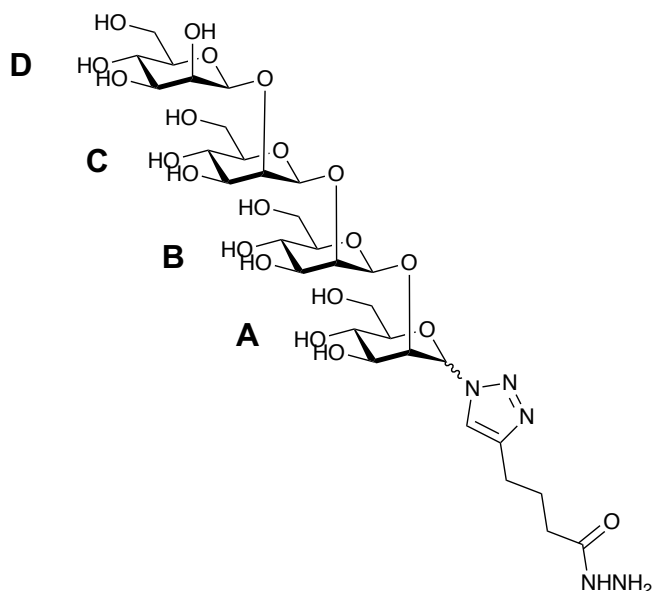
A mixture of β-D-(1-2)-mannotetraosyl clicked product 5.3.9 (4.2 mg, 6.1 μmol) was incubated at 55 °C for 6 hr with hydrazine monohydrate (1 mL) and ethanol (2.5 mL). Excess reagents and by-products were removed by co-evaporation with toluene (3 x 10 mL). Complete conversion of acyl hydrazine was confirmed by loss of a signal at δ 3.6 ppm by ^{1}H NMR spectrum (**Appendices 6. 20 B**).

5.3.12. Expression of TetHc from *E.coli* pSK1-TetHc

The heavy chain of tetanus toxoid was expressed for use as a carrier protein. Briefly, cultures of E. coli pSK1-TetHc, provided by Dr A. Scott of DSTL-Porton Down, were grown in 1 L culture flasks of LB containing 50 μg/ml kanamycin overnight at 37 °C with shaking. After 16 h the cultures were induced by the addition of isopropyl β-D-1-thiogalactopyranoside (IPTG, 1 mM final concentration), and incubated for a further 4 hours. Cells were pelleted by centrifugation and lysed in cell lysis buffer (20 mL: HEPES 100 mM, NaCl 500

mM, EDTA 1 mM, TCEP 5 mM, protease inhibitor 10 μL/ml and lysozyme 0.25 mg/ml), followed by sonication of 3 x 20 seconds with 20 second intervals. Benzonase nuclease (1 μL) was added and incubated at room temperature for 30 mins. Cellular debris was pelleted by centrifugation for 15 mins at 10,000 x g. His-tagged TetHc was isolated from the supernatant on AKTA by passing through a HisTrapHP MT (GE Healthcare) 5 mL purification column (wash buffer: 50 mM Tris-HCl pH 8, 0.5 M NaCl, 30 mM imidazole; elution buffer: 50 mM Tris-HCl pH 8, 0.5 M NaCl, 0.5 M imidazole), followed by further purification on a HiLoad 16/600 Superdex 200 pg GPC column (GPC Buffer: 50 mM HEPES pH 7.5, 100 mM NaCl). Isolated TetHc protein was quantified by Bradford assay and analysed by MALDI-TOF/MS (**Figure 3. 24**), SDS-PAGE (**Figure 3. 22 A**) and Western blot with a mouse anti-His monoclonal primary antibody (**Figure 3. 22 B**).

5.3.13.   Generation   of   β-D-(1-2)-mannoligosaccharide glycoconjugates

Conjugation of β-D-(1-2)-mannotriosyl and β-D-(1-2)-mannotetraosyl acyl hydrazides (Sections 5.3.10 and 5.3.11 respectively) to BSA and TetHc carrier proteins was carried out as outlined by Kim *et al*[5]. Acyl hydrazides (4 mg) were dissolved in dry DMF (1 mL) and cooled to -25 °C. The reaction was initiated by the addition of 4 M HCl in dioxane (9.5 μL) and *tert*-butyl nitrite (1.6 μL) and the mixture allowed to stir under nitrogen for 15 mins at -25 °C. Sulfamic acid (100 μL at 7.4 mg mL^{-1} in dry DMF) was added to prevent the build-up of nitrous oxide[6]. The reaction was allowed to reach 0 °C before being added dropwise to a cooled protein solution (2 mg mL^{-1} in Borax buffer) and left at 4 °C for 36 hr. Analysis of protein conjugates was performed by SDS-PAGE using a 4-20 % gradient SDS-PAGE gel (**Figure 3. 25 A and B**), and Invivogen™ Pro-Q™ Emerald 300 Glycoprotein Gel and Blot Stain Kit as per the manufacturer's instructions (**Figure 3. 25 C**)[7].

5.3.14. Generation of virenose BSA glycoconjugates

All virenose antigens used in this study were synthesised by Dr Irina Ivanova of the John Innes Centre. Conjucore VLP was used as a protein carrier in this study, and was provided by Dr Lucy Beales of Mologic Ltd. Laminarin azide described in **Chapter 5.2.5** was provided to Dr Simone Dedola of Iceni Diagnostics who assembled the vaccine conjugates α-Vir-(1-4)-α-Vir-BCN-VLP-BCN-laminarin and β-Vir-(1-4)-β-Vir-BCN-VLP-BCN-laminarin which were used for immunisation trials.

BSA antigen conjugates incorporating α-Vir-(1-4)-α-Vir, β-Vir-(1-4)-β-Vir, α-Vir, β-Vir and laminarin and azido propyl were generated by reacting corresponding azido-functionalised derivatives (**Figure 3. 31**) with BSA-BCN according to the protocol described in **Chapter 5.2.6**). Azides were used at a 2 × molar excess per alkyne, except laminarin azide which was used in 5 × molar excess. Successful conjugation was confirmed by SDS-PAGE using a 4-20 % gradient SDS-PAGE gel**,** and Western blot analysis**.** Sera from the corresponding virenose vaccine conjugate were used to probe for α and β mono and disaccharide virenose antigens, and a mouse anti-β-(1-3)-glucan monoclonal antibody, used in **Chapter 5.2.7**, was used to probe for laminarin.

5.3.15. Immunisation trials

Immunisation trials were performed by Mologic using the following procedures. VLP conjugates were prepared for immunisation by emulsifying with adjuvant to a final injection volume of 1 mL. Immunisation was performed with complete Freunds adjuvant and all boost injections were emulsified in incomplete Freunds adjuvant. VLP glycoconjugate were injected intramuscularly into 2 rabbits at 4 sites, 1 injection into each thigh muscle and subcutaneously into 2 sites on the back. A total of 0.25 mL of emulsion was injected at each site. Rabbits were immunised with 10 μg of VLP glycoconjugate on day 0 with boosts being provided on days 28, 56 and 84. A preimmune bleed was taken on day 0, before immunisation, and test bleeds were taken on days 35, 63 and

91. Blood samples were collected from the marginal ear vein into a sterile vial. For preimmune and test bleeds, 25 mL of whole blood was collected, and 50 mL of whole blood collected for all subsequent bleeds (dependent on body weight).

5.3.16. ELISA Protocols

ELISA assays were performed using Nunc™ MaxiSorp™ 96-well ELISA plates (BioLegend 423501). Unless otherwise stated, all dilutions were made in PBS$_T$ made from PBS (Sigma P4417) and Tween20 (Sigma P1379). Blocking steps were performed using milk powder (Marvel). Goat anti-rabbit IgG (whole molecule)-HRP was ordered from Sigma A6154. ELISA assays were developed using TMB substrate (Thermo Scientific N301) and quenched with HCl (Fisher 10294190). Absorbance readings were recorded using a FLUOstar Omega (BMG labtech) plate reader with absorbance at wavelength 450 nm. All samples were analysed in triplicate with each serum also being analysed against a PBS control. Each ELISA was performed in triplicate with average result and standard error used for data analysis. Data analysis was performed using GraphPad Prism 7.2 software with statistical analysis performed by two-way ANOVA with post-hoc Fisher's LSD.

5.3.16.1. Serum analysis by standard ELISA

BSA-antigen conjugates (200 µL at 200 ng ml^{-1} in PBS) were coated on a 96-well Maxisorb ELISA plate at 4 °C overnight. Each well was washed 3 times with PBS and then blocked for 1 hour with blocking buffer (1 % milk powder protein in PBST) at room temperature. Plates were again washed 3 times with PBS and 200 µL of serum dilutions (1:1000 diluted in 0.1 % milk powder protein in PBST) were applied to each well at room temperature for 3 hrs. Plates were washed 3 times with PBST before the addition of a secondary antibody (Sigma A6154 at 1:10000 dilution in 0.1 % milk powder protein in PBST) at room temperature for 1 hr. Plates were washed 3 times with PBST.

Stabilised chromogen [TMB substrate (Life technologies)] was added at 100 µL per well for 15 mins before the reaction was stopped by the addition of 1 M HCl (100 µL per well). Measurements were recorded as an absorbance reading at 450 nm.

5.3.16.2. Serum analysis by competitive ELISA

Competitive ELISA was performed similarly to standard ELISA (**Section 5.3.16.1**) with the following changes. Target analytes were prepared in PBS$_T$ and mixed 50:50 with a 1 in 800 dilution of serum in PBS$_T$ and incubated at 4 °C for 16 hours prior to applying to the ELISA plate.

5.4. References

1.   *Product Manual Western BLoT Chemiluminescence HRP Substrate Sample For Research Use v201211*.

2.   Tanaka, T., Nagai, H., Noguchi, M., Kobayashi, A. & Shoda, S. One-step conversion of unprotected sugars to beta-glycosyl azides using 2-chloroimidazolinium salt in aqueous solution. *Chem Commun* **23,** 3378–3379 (2009).

3.   Chiku, K. *et al.* Discovery of two β-1,2-mannoside phosphorylases showing different chain-length specificities from Thermoanaerobacter sp. X-514. *PLoS One* **9,** e114882 (2014).

4.   Cody, J. A., Ahmed, I. & Tusch, D. J. Studies toward the total synthesis of eletefine: An efficient construction of the AB ring system. *Tetrahedron Lett.* **51,** 5585–5587 (2010).

5.   Kim, K. & Kim, Y. H. Preparation of azides from hydrazines by using dinitrogen tetroxide as nitrosonium ion source. *Arch. Pharm. Res.* **16,** 94–98 (1993).

6.   Dzelzkalns, L. S. & Bonner, F. T. Reaction between nitric and sulfamic acids in aqueous solution. *Inorg. Chem.* **17,** 3710–3711 (1978).

7.   Pro-Q Emerald 300 Glycoprotein Gel and Blot Stain Kit. Available at: https://www.thermofisher.com/document-connect/document-connect.html?url=https://assets.thermofisher.com/TFS-Assets/LSG/manuals/mp21857.pdf&title=Pro-Q   Emerald   300 Glycoprotein Gel and Blot Stain Kit. (Accessed: 1st December 2018)

6. Appendix

Chapter 2 appendices

The following table is split into **Calculated** masses (columns β-glucan (-OAc) [M], [M+Na]+; β-glucan (-OH) [M], [M+Na]+; β-glucan (-OAc)) and **Found [M+Na]+** per chromatographic **Fraction** (columns A β-glucan (-OH), B, C, D, E, F, G, H, I, J).

| DP	β-glucan (-OAc) [M]	β-glucan (-OAc) [M+Na]+	β-glucan (-OH) [M]	β-glucan (-OH) [M+Na]+	β-glucan (-OAc)	A β-glucan (-OH)	B	C	D	E	F	G	H	I	J
5	1542.45	1565.44	828.27	851.26	-	-	851.17	851.16	851.18	851.33	851.26	851.54	851.38	851.27	851.17
6	1830.54	1853.53	990.33	1013.32	-	1013.17	1013.24	1013.20	1013.20	1013.38	1013.32	1013.65	1013.33	1013.36	1013.26
7	2118.62	2141.61	1152.38	1175.37	-	1175.21	1175.27	1175.25	1175.27	1175.44	1175.40	1175.39	1175.41	1175.45	1175.41
8	2406.71	2429.70	1314.43	1337.42	-	1337.24	1337.32	1337.34	1337.32	1337.52	1337.48	1337.87	1337.54	1337.51	1337.52
9	2694.79	2717.78	1486.49	1509.48	-	1509.27	1509.38	1509.36	-	1509.58	1509.52	1509.99	1509.62	1509.56	-
10	2982.88	3005.87	1638.54	1661.53	2963.60	1661.30	-	-	-	1661.64	1661.54	1662.10	1661.66	-	-
11	3270.96	3293.95	1800.59	1823.58	3251.69	1823.33	-	-	-	1823.76	1823.59	1824.21	-	-	-
12	3559.05	3582.04	1962.64	1985.63	3539.73	1985.37	-	-	1985.39	1985.82	1985.66	-	-	-	-
13	3847.13	3870.12	2124.70	2147.69	3869.86	2147.38	-	-	2147.39	2147.86	-	-	-	-	-
14	4135.21	4158.20	2286.75	2309.74	4157.88	2309.40	-	2309.37	2309.41	2309.90	-	-	-	-	-
15	4423.30	4446.29	2448.80	2471.79	4445.90	2472.41	2471.55	2471.38	2471.51	-	-	-	-	-	-
16	4711.38	4734.37	2610.86	2633.85	4733.93	2633.45	2633.58	2633.47	-	-	-	-	-	-	-
17	4999.47	5022.46	2772.91	2795.90	5021.83	2795.47	2795.62	2795.47	-	-	-	-	-	-	-
18	5287.55	5310.54	2934.96	2957.95	5309.91	2957.48	2957.66	-	-	-	-	-	-	-	-
19	5575.64	5598.63	3097.01	3120.00	5597.94	3119.48	3119.71	-	-	-	-	-	-	-	-
20	5863.72	5886.71	3259.07	3282.06	5885.69	3281.46	-	-	-	-	-	-	-	-	-
21	6151.81	6174.80	3421.12	3444.11	6173.98	3443.48	-	-	-	-	-	-	-	-	-
22	6439.89	6462.88	3583.17	3606.16	6461.89	-	-	-	-	-	-	-	-	-	-
23	6727.98	6750.97	3745.23	3768.22	6749.63	-	-	-	-	-	-	-	-	-	-
24	7016.06	7039.05	3907.28	3930.27	7040.99	-	-	-	-	-	-	-	-	-	-
25	7304.14	7327.13	4069.33	4092.32	7328.96	-	-	-	-	-	-	-	-	-	-
26	7592.23	7615.22	4231.38	4254.37	7617.31	-	-	-	-	-	-	-	-	-	-

Appendices 6. 1 – Table of masses for acetylated and deprotected β-(1-3)-glucans. Grey shading represents dominant peaks.

Appendices 6. 2 – HSQCed NMR (400 MHz, CDCl₃) assignment of acetylated curdlan fragments.

Chemical shifts (δ) ppm								
¹³C NMR	CH₂Cl₂	**C-1**	**C-2**	**C-3**	**C-4**	**C-5**	**C-6**	O$\underline{C}$O$\underline{C}$H₃ (OAc)
	53.5	100.7	72.5	78.2	68.0	71.7	61.8	20.6
¹H NMR	C$\underline{H_2}$Cl₂	**H-1**	**H-2**	**H-3**	**H-4**	**H-5**	**H-6**	OCOC$\underline{H_3}$ (OAc)
	5.29-5.35	4.32-4.51	4.77-5.11	3.69-3.91	4.82-5.09	3.55-3.76	3.97-4.42	1.94-2.22

Appendices 6. 3 - HSQCed NMR (400 MHz, CDCl₃) assignment of deacetylated β-(1-3)-glucan curdlan fragments

	Chemical shifts (δ) ppm							
¹³C NMR	**C-1^{A}α**	**C-1^{A}β**	**C-1^X**	**C-2^Y**	**C-3^Y**	**C-4^Y**	**C-5^Y**	**C-6^Y**
	92.1	95.6	102.7	73.3	84.2	68.1	75.7	60.8
¹H NMR	**H-1^{A}α**	**H-1^{A}β**	**H-1^X**	**H-2^Y**	**H-3^Y**	**H-4^Y**	**H-5^Y**	**H-6^{Yab}**
	5.19	4.62	4.70	3.30-3.56	3.67-3.79	3.44-3.55	3.40-3.49	3.65-3.92
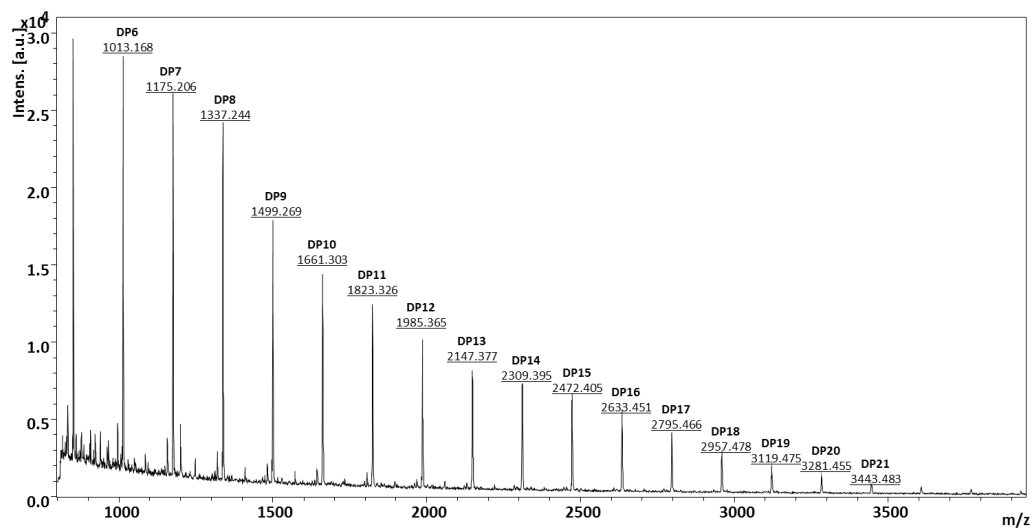
**Appendices 6. 4 – MALDI-TOF analysis of deacetylated curdlan fragments.**

Appendices 6. 5 – Table of HPAEC-PAD retention times (mins) for linear β-(1-3)-glucans prior to (A) and following (B-J) GPC fractionation and laminarihexaose (LHX) standard (K).

DP	A	Curdlan Fractions									LHX
		B	C	D	E	F	G	H	I	J	K
1	3.7	-	-	-	-	-	-	-	-	-	-
2	10.3	-	-	-	-	-	-	-	-	-	-
3	13.6	-	-	-	-	-	-	-	-	-	-
4	16.2	-	-	-	-	-	-	-	-	-	-
5	18.9	-	-	-	-	-	-	-	18.7	18.7	-
6	21.0	-	-	-	-	-	-	20.9	20.9	20.9	20.7
7	22.9	-	-	-	-	-	22.8	22.7	22.8	22.7	-
8	24.6	-	-	-	-	24.4	24.4	24.4	24.5	24.4	-
9	26.2	-	-	-	-	26.0	25.9	25.9	26.1	26.0	-
10	27.6	-	-	-	27.5	27.3	27.3	27.3	27.4	27.3	-
11	28.8	-	-	28.8	28.8	28.5	28.6	28.6	28.7	-	-
12	30.0	-	-	30.0	29.9	29.7	29.7	29.7	29.9	-	-
13	31.1	-	30.9	31.0	30.9	30.8	30.8	30.8	-	-	-
14	32.0	31.9	31.8	31.9	31.8	31.7	31.7	-	-	-	-
15	32.9	32.8	32.7	32.8	32.7	32.6	32.6	-	-	-	-
16	33.8	33.6	33.6	33.7	33.5	33.5	-	-	-	-	-
17	34.5	34.4	34.3	34.4	34.3	34.2	-	-	-	-	-
18	35.2	35.1	35.1	35.2	35.0	-	-	-	-	-	-
19	35.9	35.7	35.7	35.8	-	-	-	-	-	-	-
20	36.5	36.4	36.3	36.4	-	-	-	-	-	-	-
21	37.1	36.9	36.9	-	-	-	-	-	-	-	-
22	37.7	37.5	-	-	-	-	-	-	-	-	-
23	38.2	38.0	-	-	-	-	-	-	-	-	-

Appendices 6. 6 – HSQCed NMR (400 MHz, CDCl₃) assignment of commercial laminarin.

	Chemical shifts (δ) ppm					
¹³C NMR	**C-1**	**C-2**	**C-3**	**C-4**	**C-5**	**C-6**
	102.4	73.3	84.1	68.2	75.7	60.5
¹H NMR	**H-1**	**H-2**	**H-3**	**H-4**	**H-5**	**H-6**
	4.38-4.72	3.18-3.51	3.56-3.73	3.35-3.50	3.29-3.43	3.54-3.89

Appendices 6. 7 – MALDI-TOF analysis of BSA-BCN conjugation optimisation. A – BSA, B – BSA reacted with 5x molar excess of BCN-NHS, C – BSA reacted with 5x molar excess of BCN-NHS.
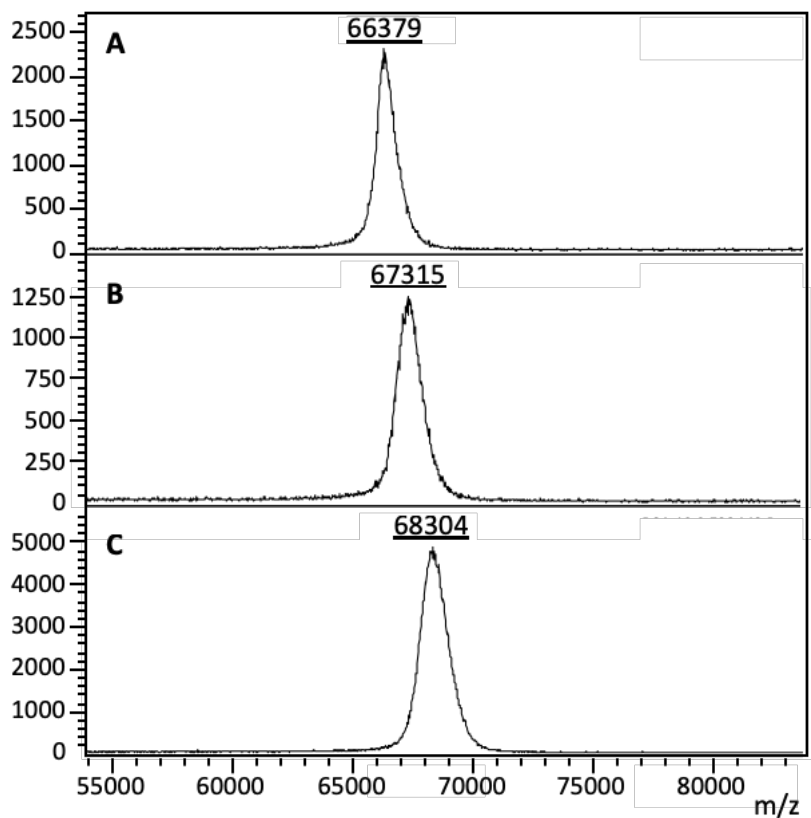
Chapter 3 appendices
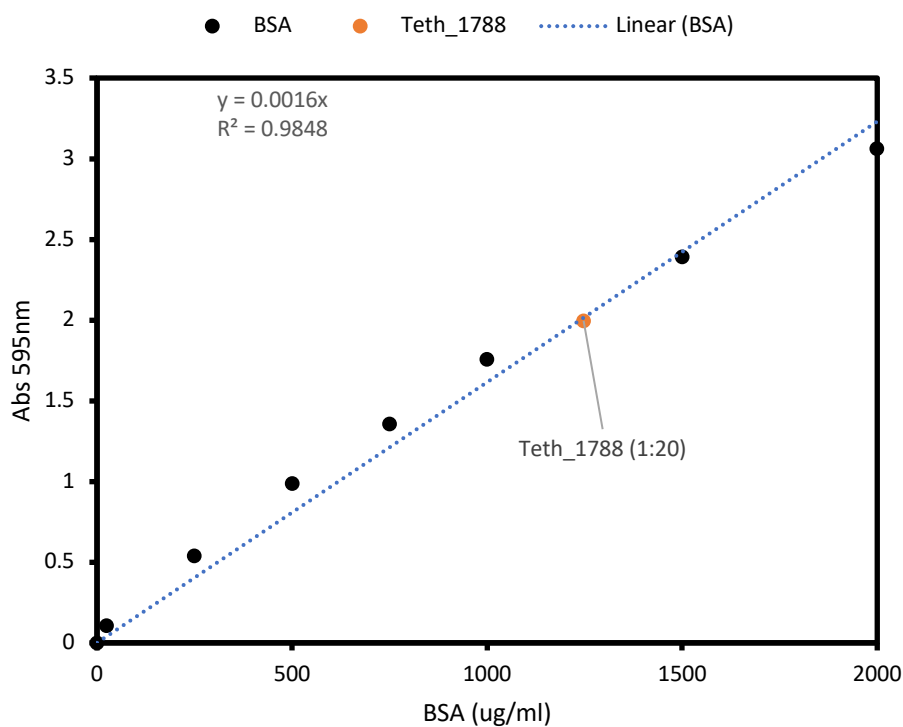
Appendices 6. 8 – BCA protein concentration analysis of Teth514_1788.

Appendices 6. 9 – Table of HPAEC-PAD retention times (mins) for β-(1-2)-mannan oligosaccharides.

DP	HPAEC-PAD β-(1-2)-mannoside retention times (min)						
	Ladder	Mannose	M1P	Enzymatic reaction	95% EtOH elution	Man3	Man4
1	3.7	3.7	-	3.7	3.7	-	-
2	5.9	-	-	5.9	5.9	-	-
3	9.7	-	-	9.8	9.7	9.8	-
4	11.6	-	-	11.7	11.5	-	11.6
5	13.0	-	-	13.1	12.9	-	-
6	14.0	-	-	14.1	13.9	-	-
7	14.9	-	-	15.0	14.9	-	-
8	15.9	-	-	16.0	15.8	-	-
M1P	16.2	-	16.1	16.1	16.3	-	-

Appendices 6. 10 – Table of masses for β-(1-2)-mannan oligosaccharides.

DP	Calculated		Found
	$[M]^+$	$[M+Na]^+$	$[M+Na]^+$
1	180.1	203.1	ND
2	342.1	365.1	ND
3	504.2	527.2	527.3
4	666.2	689.2	689.4
5	1542.5	851.3	851.4
6	1830.5	1013.3	1013.1
7	2118.6	1175.4	1175.6
8	2406.7	1337.4	1337.6
9	2694.8	1509.5	1509.5
10	2982.9	1661.5	1661.7
11	3271.0	1823.6	1823.7
12	3559.1	1985.6	1986.7
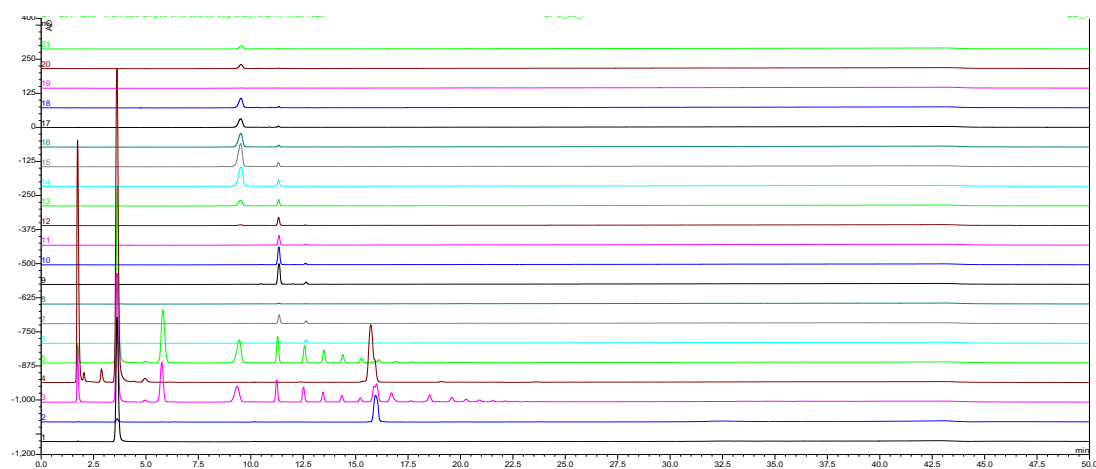
Appendices 6. 11 – HPAEC-PAD analysis of β-(1-2)-mannan oligosaccharides separated by gel permeation chromatography.

183
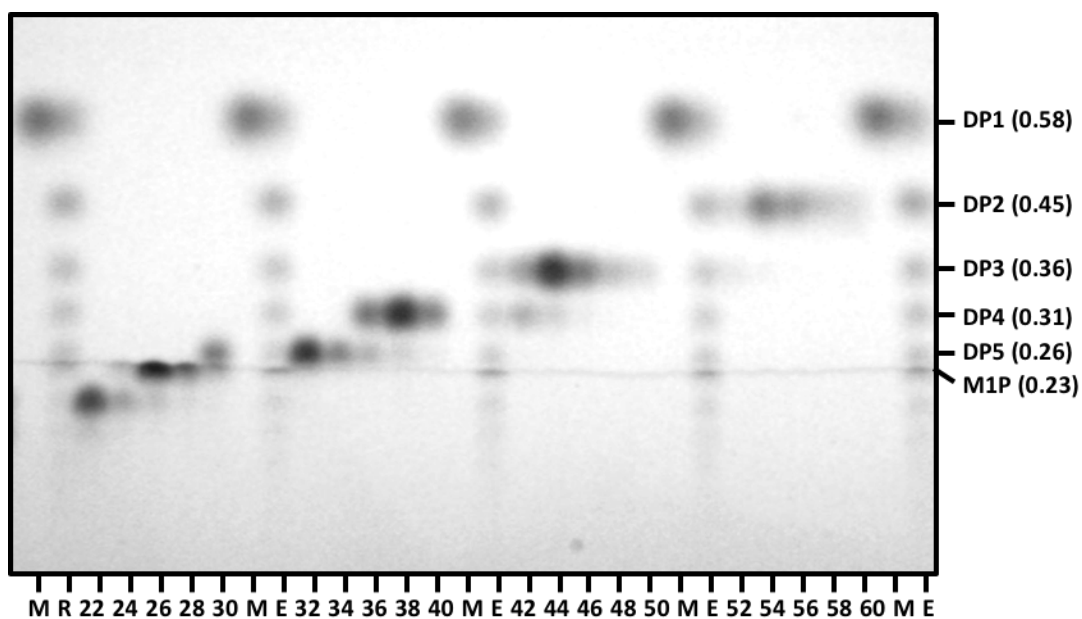
Appendices 6. 12 – TLC analysis of β-(1-2)-mannan oligosaccharides separated by gel permeation chromatography. Solvent system: BuOH/EtOH/H$_2$O (10:8:7).

Appendices 6. 13 – TLC analysis of β-(1-2)-mannotriose and β-(1-2)-mannotetraose β-(1-2)-mannosides. Solvent system - BuOH/EtOH/H$_2$O (10:8:7).

**Appendices 6. 14 – ^{1}H and ^{13}C NMR chemical shifts of β-(1-2)-mannotriose.**

| Units and anomers		Chemical shifts (δ)						
		H-1	**H-2**	**H-3**	**H-4**	**H-5**	**H-6a**	**H-6b**
C	α	4.74	4.04	3.50	3.38	3.26	3.82	3.59
	β	4.83	4.03	3.50	3.38	3.26	*a*	*a*
B	α	4.74	4.16	3.53	3.50	3.26	3.82	3.64
	β	4.80	4.29	3.53	3.50	3.26	*a*	*a*
A	α	5.15	3.99	3.78	3.54	3.66	3.72	3.59
	β	4.86	4.05	3.56	3.41	3.26	3.72	*a*
		C-1	**C-2**	**C-3**	**C-4**	**C-5**	**C-6**	
C	α	100.9	70.2	72.7	67.0	76.2	60.8	
	β	100.8	70.5	72.7	67.0	76.2	*a*	
B	α	98.9	78.5	72.0	66.9	76.2	60.8	
	β	101.0	78.0	72.0	66.9	76.2	*a*	
A	α	91.9	78.4	69.1	67.0	72.3	60.2	
	β	93.5	79.6	72.1	66.6	76.2	60.2	

a Not determined

Appendices 6. 15 – ^{1}H and ^{13}C NMR chemical shifts of β-(1-2)-mannotetraose.

| Units and anomers		Chemical shifts (δ)						
		H-1	**H-2**	**H-3**	**H-4**	**H-5**	**H-6a**	**H-6b**
D		4.83	4.05	3.51	3.46	3.28	3.83	3.63
C	α	4.83	4.3	3.52	3.51	3.28	3.83	3.63
	β	4.91	4.26	3.52	3.51	3.28	*a*	*a*
B	α	4.72	4.13	3.59	3.41	3.28	3.83	3.7
	β	4.77	4.26	3.59	3.41	3.28	*a*	*a*
A	α	5.16	4.01	3.8	3.8	3.69	3.71	3.7
	β	4.86	4.05	3.59	3.37	3.28	*a*	*a*
		C-1	**C-2**	**C-3**	**C-4**	**C-5**	**C-6**	
D		101	70.3	72.9	66.9	76.2	60.8	
C	α	101	78.3	72.1	67.2	76.2	60.8	
	β	101	78.5	72.1	67.2	76.2	*a*	
B	α	99.2	79.5	71.9	67	76.2	60.8	
	β	101.1	78.5	71.9	67	76.2	*a*	
A	α	92.1	78.8	69.1	69.1	72.3	60.4	
	β	93.5	80	71.9	67.1	76.2	*a*	
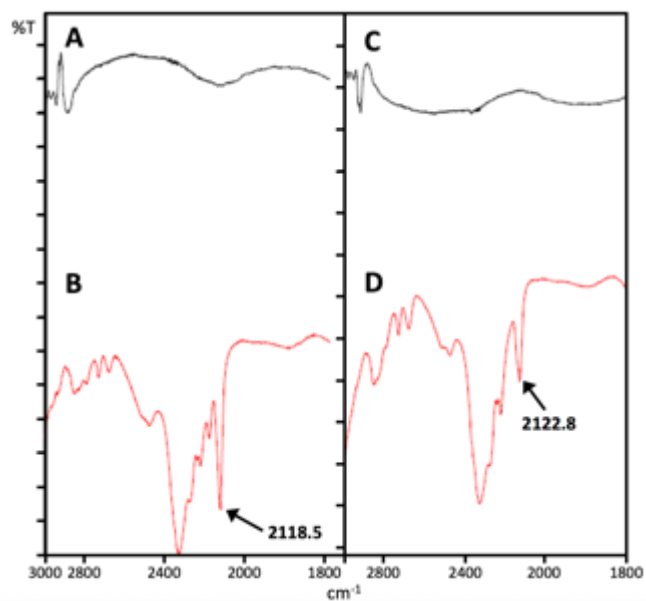
Appendices 6. 16 – FTIR analysis of β-(1-2)-mannotriose (A), β-(1-2)-mannotriosyl azide (B), β-(1-2)-mannotetraose (C) and β-(1-2)-mannotetraosyl azide (D).
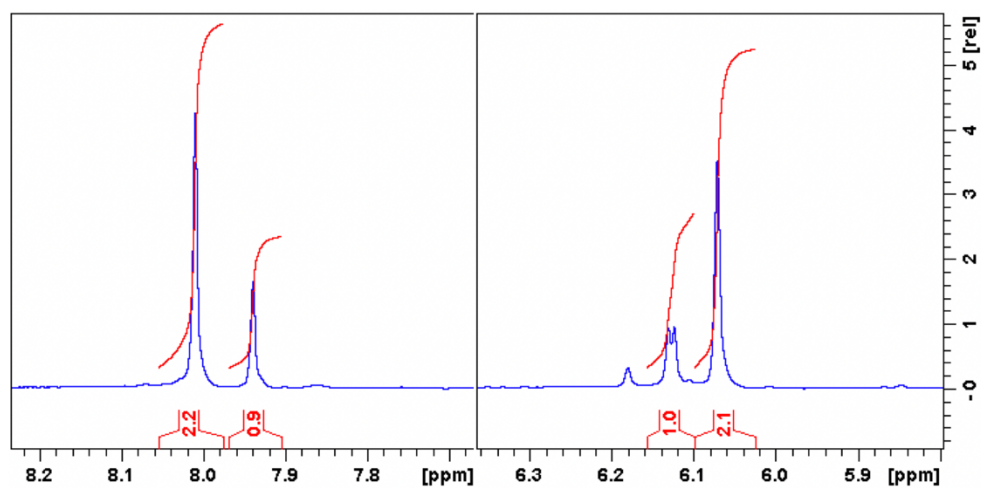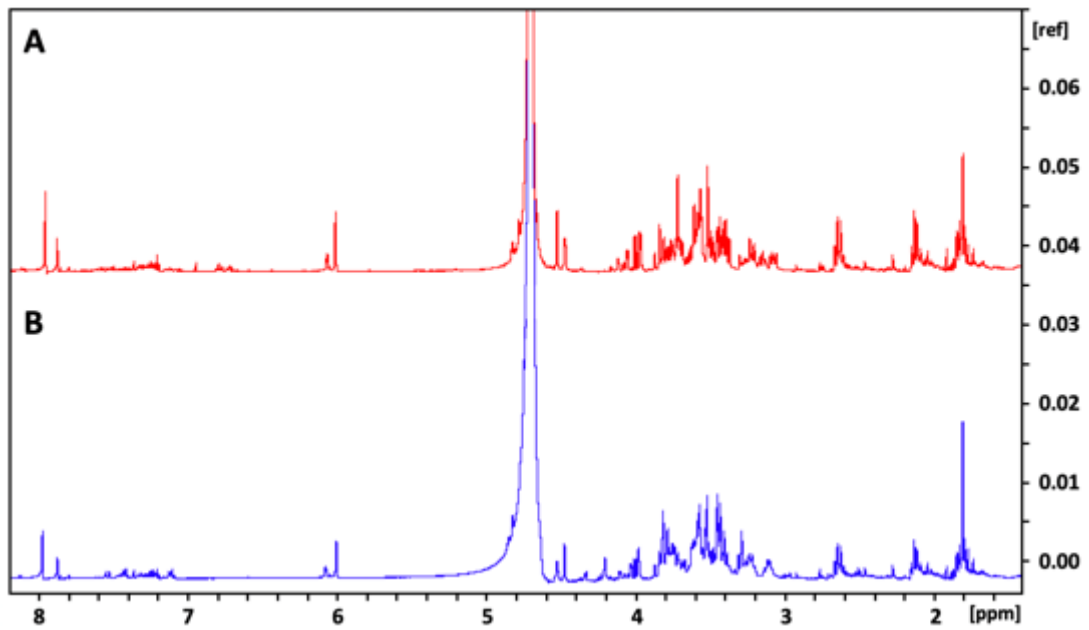

**Appendices 6. 17 – ¹H NMR integration of β-(1-2)-mannotriosyl clicked products.**
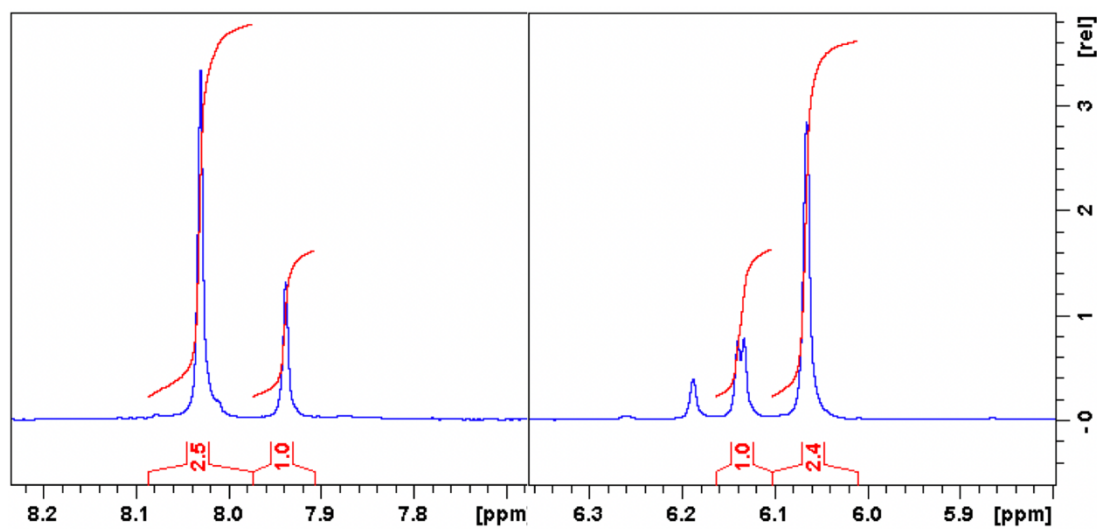
Appendices 6. 18 – ¹H NMR integration of β-(1-2)-mannotetraosyl clicked product.
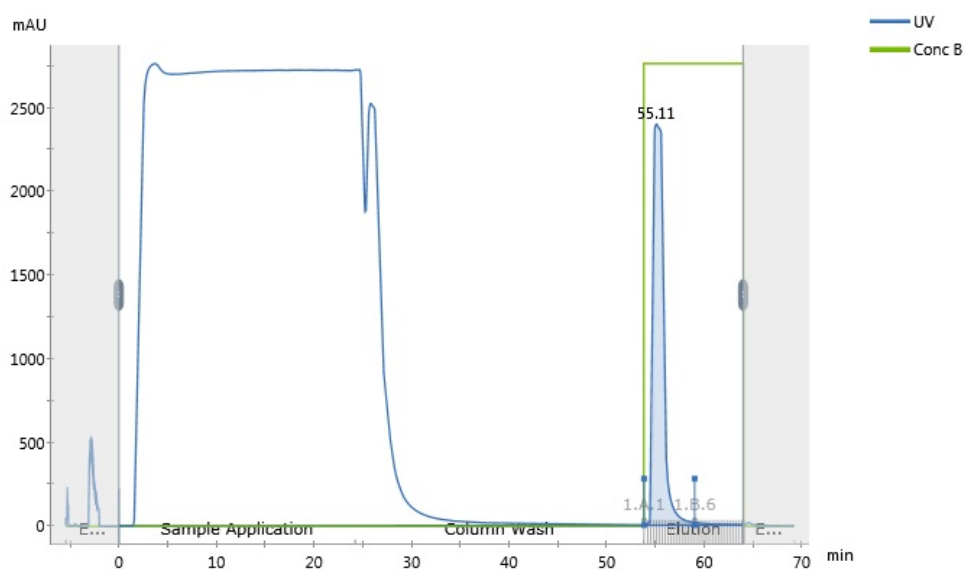
Appendices 6. 19 – Chromatogram of TetHc purification by affinity chromatography.

Appendices 6. 20 – 1H NMR analysis of hydrazide functionalised β-(1-2)-mannotriosyl (A) and β-(1-2)-mannotetraosyl (B) click products (400 MHz, D$_2$O).
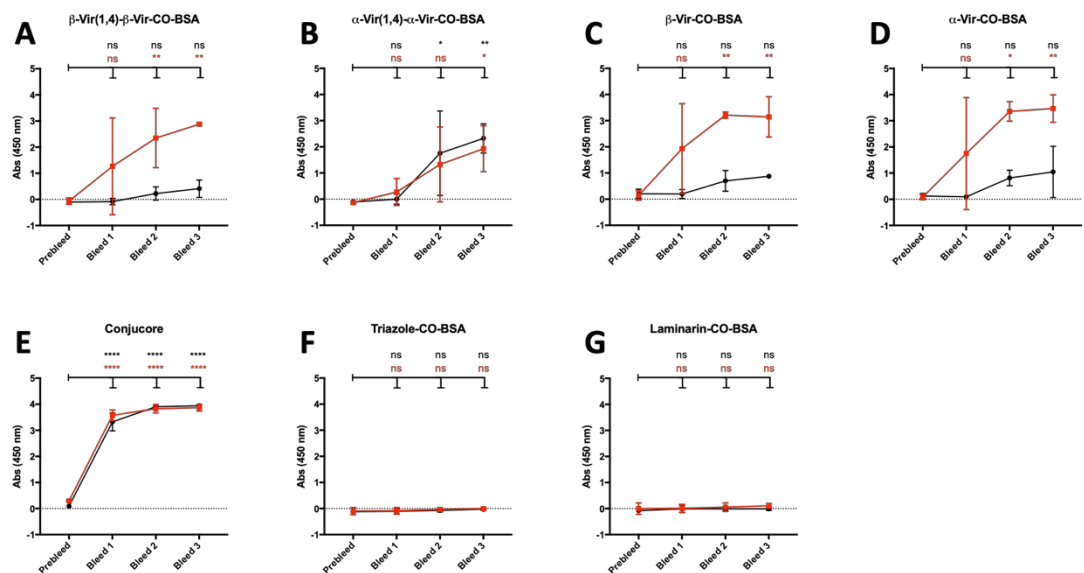
Appendices 6. 21 – Comparison of prebleed, bleed 1, bleed 2 and bleed 3 standard ELISA of α-Vir(1-4)-α-Vir-BCN-VLP-BCN-Laminarin (black), and β-Vir(1-4)-β-Vir-BCN-VLP-BCN-Laminarin (red). P values: * = 0.05, ** = 0.01, *** = 0.005.